Nagra
Nationale
Genossenschaft
für die Lagerung
radioaktiver Abfälle

Cédra
Société coopérative
nationale
pour l'entreposage
de déchets radioactifs

Cisra
Società cooperativa
nazionale
per l'immagazzinamento
di scorie radioattive

TECHNICAL REPORT 85-56

HYDROGEOLOGICAL AND HYDROGEOCHEMICAL INVESTIGATIONS IN BOREHOLES
Final Report of the Phase I Geochemical Investigations of the Stripa Groundwaters

D. K. Nordstrom (Ed., US Geological Survey)
J. N. Andrews (University of Bath, U.K.)
L. Carlsson (Swedish Geological Co, Göteborg)
J.-C. Fontes (Université Paris-Sud, France)
P. Fritz (University of Waterloo, Canada)
H. Moser (GSF-München, BRD)
T. Olsson (Uppsala Geosystem AB, Sweden)

July 1985

Parkstrasse 23 5401 Baden/Schweiz Telephon 056/20 55 11

Nagra
Nationale
Genossenschaft
für die Lagerung
radioaktiver Abfälle

Cédra
Société coopérative
nationale
pour l'entreposage
de déchets radioactifs

Cisra
Società cooperativa
nazionale
per l'immagazzinamento
di scorie radioattive

TECHNICAL REPORT 85-56

HYDROGEOLOGICAL AND HYDROGEOCHEMICAL INVESTIGATIONS IN BOREHOLES
Final Report of the Phase I Geochemical Investigations of the Stripa Groundwaters

D. K. Nordstrom (Ed., US Geological Survey)
J. N. Andrews (University of Bath, U.K.)
L. Carlsson (Swedish Geological Co, Göteborg)
J.-C. Fontes (Université Paris-Sud, France)
P. Fritz (University of Waterloo, Canada)
H. Moser (GSF-München, BRD)
T. Olsson (Uppsala Geosystem AB, Sweden)

July 1985

Parkstrasse 23 5401 Baden/Schweiz Telephon 056/20 55 11

Der vorliegende Bericht betrifft eine Studie, die für das Stripa-Projekt ausgeführt wurde. Die Autoren haben ihre eigenen Ansichten und Schlussfolgerungen dargestellt. Diese müssen nicht unbedingt mit denjenigen des Auftraggebers übereinstimmen.

Le présent rapport a été préparé pour le projet de Stripa. Les opinions et conclusions présentées sont celles des auteurs et ne correspondent pas nécessairement à ceux du client.

This report concerns a study which was conducted for the Stripa Project. The conclusions and viewpoints presented in the report are those of the authors and do not necessarily coincide with those of the client.

Das Stripa-Projekt ist ein Projekt der Nuklearagentur der OECD. Unter internationaler Beteiligung werden von 1980-86 Forschungsarbeiten in einem unterirdischen Felslabor in Schweden durchgeführt. Diese sollen die Kenntnisse auf folgenden Gebieten erweitern:
- hydrogeologische und geochemische Messungen in Bohrlöchern
- Ausbreitung des Grundwassers und Transport von Radionukliden durch Klüfte im Gestein
- Verhalten von Materialien, welche zur Verfüllung und Versiegelung von Endlagern eingesetzt werden sollen
- Methoden zur zerstörungsfreien Ortung von Störzonen im Fels

Seitens der Schweiz beteiligt sich die Nagra an diesen Untersuchungen. Die technischen Berichte aus dem Stripa-Projekt erscheinen gleichzeitig in der NTB-Serie der Nagra.

The Stripa Project is organised as an autonomous project of the Nuclear Energy Agency of the OECD. In the period from 1980-86, an international cooperative programme of investigations is being carried out in an underground rock laboratory in Sweden. The aim of the work is to improve our knowledge in the following areas:
- hydrogeological and geochemical measurement methods in boreholes
- flow of groundwater and transport of radionuclides in fissured rock
- behaviour of backfilling and sealing materials in a real geological environment
- non-destructive methods for location of disturbed zones in the rock

Switzerland is represented in the Stripa Project by Nagra and the Stripa Project technical reports appear in the Nagra NTB series.

Le projet Stripa est un projet autonome de l'Agence de l'OCDE pour l'Energie Nucléaire. Il s'agit d'un programme de recherche avec participation internationale, qui sera réalisé entre 1980 et 1986 dans un laboratoire souterrain, en Suède. Le but de ces travaux est d'améliorer et d'étendre les connaissances dans les domaines suivants:
- mesures hydrogéologiques et géochimiques dans les puits de forage
- chimie des eaux souterraines à grande profondeur
- écoulement des eaux souterraines et transport des radionucléides dans les roches fracturées
- comportement des matériaux de colmatage et de scellement des dépôt finals
- méthodes de localisation non destructive des zones de perturbation de la roche

La Suisse est représentée dans le projet Stripa par la Cédra. Les rapports techniques du projet Stripa sont publiés dans la série des rapports techniques de la Cédra (NTB).

ABSTRACT

The hydrogeochemical investigations of Phase I of the Stripa Project (1980-84) have been completed, and the results are presented in this final report. All chemical and isotopic data on the groundwaters from the beginning of the Stripa Project to the present (1977-84) are tabulated and used in the final interpretations. The background geology and hydrology is summarized and updated along with new analyses of the Stripa granite. Water-rock interactions form a basic framework for the changes in major-element chemistry with depth, including carbonate geochemistry, the fluid-inclusion hypothesis, redox processes, and mineral precipitation. The irregular distribution of chloride suggests channelling is occurring and the effect of thermomechanical perturbations on the groundwater chemistry is documented. Stable and radioactive isotopes provide information on the origin and evolution of the groundwater itself and of several elements within the groundwater. Subsurface production of radionuclides is documented in these investigations, and a general picture of uranium transformations during weathering is presented. One of the primary conclusions reached in these studies is that different dissolved constituents will provide different residence times because they have different origins and different evolutionary histories that may or may not be related to the overall evolution of the groundwater itself.

RESUME

Les investigations géochimiques de la phase I du projet de Stripa (1980-1984) sont achevées et leurs résultats présentés dans ce rapport final. Toutes les données chimiques et isotopiques des eaux souterraines profondes, du début du projet à nos jours (1977-1984), sont exposées dans des tableaux et utilisées dans l'évaluation finale. Les informations géologiques et hydrogéologiques de base y sont récapitulées et actualisées grâce à de nouvelles analyses du granite de Stripa. Les interactions eau/roche forment un cadre de base pour les modifications, fonction de la profondeur, dans la chimie des éléments principaux, y compris la géochimie des carbonates, l'hypothèse de l'inclusion liquide, les processus rédox et la précipitation minérale. La diffusion irrégulière de chlorure traduit la présence d'effets de canalisation (channelling). L'effet de perturbations thermomécaniques sur la chimie des eaux souterraines est documenté. Des isotopes stables et radioactifs fournissent des informations sur l'origine et l'évolution des eaux souterraines et des éléments qui y sont dissouts. La production souterraine de radionucléides est étayée par ces investigations, et une présentation générale de la mobilisation de l'uranium et de ses produits de désintégration par transformation hydrolytique de la roche est donnée. Ces études montrent notamment que les éléments dissouts dans les eaux souterraines sont de différentes origines, et que par là, leur durée d'attardement dans ces eaux ne dépend, que dans certaines conditions, de l'évolution de ces eaux.

ZUSAMMENFASSUNG

Die hydrogeochemischen Untersuchungen der Phase 1 des Stripaprojekts (1980-84) sind abgeschlossen worden, die Ergebnisse werden in diesem Schlussbericht präsentiert. Alle chemischen- und Isotopen-Daten der Tiefenwässer, vom Anfang des Projekts an bis heute (1977-84), werden tabellarisch aufgeführt und in der Schlussauswertung benützt. Die geologische und hydrogeologische Hintergrundinformation wird zusammengefasst aufgeführt, zusammen mit neuen Analysen des Stripagranits. Wasser-Gestein Wechselwirkungen bilden einen grundsätzlichen Rahmen für tiefenabhängige Aenderungen innerhalb der Hauptelementchemie, einschliesslich der Carbonatgeochemie, der Flüssigkeitseinschluss-Hypothese (fluid inclusion), Redoxprozesse und Mineralausfällung. Die unregelmässige Chloridausbreitung deutet auf Kanalisierungseffekte (channelling) hin. Die Auswirkung thermomechanischer Störungen der Grundwasserchemie wird dokumentiert. Stabile und radioaktive Isotopen liefern Informationen zur Herkunft der Wässer und der darin gelösten Bestandteile. Die unterirdische Radionuklidproduktion wird in diesen Untersuchungen dokumentiert und eine generelle Darstellung der Mobilisierung des Urans und dessen Zerfallstöchter durch die hydrolytische Gesteinsumwandlung wird präsentiert. Diese Studien zeigen insbesondere, dass die gelösten Bestandteile der Tiefenwässer unterschiedlichen Ursprungs sind und dadurch deren Verweilzeiten in den Tiefenwässern nur bedingt mit der Geschichte dieser Wässer zusammenhängen.

CONTENTS

SUMMARY

The geochemistry of the groundwaters, bedrock and fracture mineralogy at the Stripa test site is being investigated to understand the origin and evolution of groundwaters in a granitic bedrock. Geochemical parameters provide an important constraint to the hydrogeologic properties of groundwater flow and complement physical investigations such as geophysical measurements of fractures, hydraulic testing and tracer migration studies. Geochemical studies provide the only measure of long-term migration of solutes and water in the subsurface environment. These investigations have contributed substantially to our understanding of geologically both old and modern water-rock-gas interactions occurring within crystalline bedrock.

Several lines of evidence strongly suggest that the groundwater system at Stripa has evolved from fresh meteoric waters, typical of central Sweden, interacting with the Proterozoic crystalline bedrock composed dominantly of feldspars and quartz and fracture-fill minerals, such as calcite, chlorite, epidote, sericite, pyrite, fluorite, and hematite. Several hypotheses may account for the source of the Na-Ca-Cl type water found at depth, (a) salt associated with the crystalline rock itself, i.e., fluid inclusions and associated grain boundary salts or salty fluids, (b) intrusion of old seawater and (c) leaching of salts of sedimentary origin. All of these hypotheses are given careful consideration. Many of the water-rock interactions can be related to weathering processes and solubility equilibria such that a firm basis for predicting the effect of perturbations, like radioactive waste storage, can be made with greater reliability. For example, thermal stress will clearly affect the water chemistry and could actually increase chloride concentrations significantly in the near-field by extruding saline fluids from the micropores and/or microfracturing fluid inclusions. Increased salt concentrations can both increase and decrease the solubility of various minerals, depending on the mineral, the temperature, and the composition of the salt components. Changes in solubility can, in turn, affect the permeability of the bedrock.

Identification of active processes, such as calcite, fluorite, ferric hydroxide, and possibly barite precipitation, provides favorable conditions for radionuclide retardation in the far-field by coprecipitation or adsorption. When these processes are linked to other processes, such as silica dissolution and reprecipitation through a temperature gradient in the near-field, possible clay mineral formation, and the absorbing properties of the backfill, then the outlook for long-term radioactive waste storage looks even more favorable.

1 INTRODUCTION

1.1 General

The program "Hydrogeological and Hydrogeochemical Investigations in Boreholes" within the Stripa Project has the following objectives

- Methodology development for hydrogeological and hydrogeochemical investigations in subsurface horizontal and vertical boreholes.
- Instrumentation and equipment development in subsurface horizontal and vertical boreholes.
- Hydraulic, chemical and isotopic characterization of the Stripa granite and groundwaters.

The work was carried out according to a defined program (Carlsson and Olsson, 1981) which was slightly revised during its performance. The program included several activities that described the hydrogeological characteristics of the Stripa granite and the hydrogeochemical properties of the Stripa groundwaters. These activities included

- Drilling of two vertical boreholes (V1 and V2) and two horizontal boreholes (N1 and E1).
- Core logging with respect to rock type, fracturing, fracture minerals and fracture orientation.
- Core investigation for porosity and density.
- Geophysical logging for deviation, radiation, temperature, normal and lateral resistivity, differential resistance, caliper and density.
- Geophysical cross-hole measurements for fracture zone tracing.
- Hydraulic pressure build-up and fall-off-tests.
- Water injections tests.
- Hydraulic interference tests.
- Hydraulic head monitoring.

- Hydrogeochemical sampling and analysis with respect to major and minor constituents, trace elements, stable and unstable isotopes and noble gases.

In the vertical holes, priority was given to the hydrogeochemical studies and only a minor program for the hydraulic testing was carried out. The program for hydrogeochemical sampling, analyses and evaluation was slightly revised as a second deep borehole was included. The Hydrogeochemical Advisory Group (HAG), consisting of experts in several areas of hydrogeochemistry, was formed to advise and to make analyses and interpretations on the hydrogeochemistry. The members in this group are

John Andrews	UK
Erik Eriksson	Sweden
Tad Florkowski	IAEA
Jean-Charles Fontes	France
Peter Fritz	Canada
Heinz Loosli	Switzerland
Heribert Moser	West Germany
Kirk Nordstrom	USA, chairman

This document is the final report of the hydrogeochemical investigations carried out within the Stripa Project during 1980-84. All analytical data collected during the previous investigations (under the auspices of the Swedish-American Cooperative Program, SAC, 1977-80) have also been included so that all the data and interpretations could be found in a single document.

1.2 Test sites

Boreholes at two selected sites in the Stripa mine have been used to make measurements and collect water samples for the program. At the SGU-site, which is the main site located at the 360 m mine level, three boreholes were drilled, one vertical (V1) and two subhorizontal boreholes (N1 and E1). The fourth borehole (V2) is an extension of the old borehole Dbh V1 that was made during the SAC program. It was deepened by drilling to a total depth of 822 m (1230 m below ground surface). The location of the sites and the boreholes are shown in Figure 1-1. Data on the boreholes are given in Table 1-1. In addition to these boreholes, a number of other holes in the SAC-area were used for minor tests and water sampling. Water sampling was also conducted in private wells at the surface and from surface water schemes.

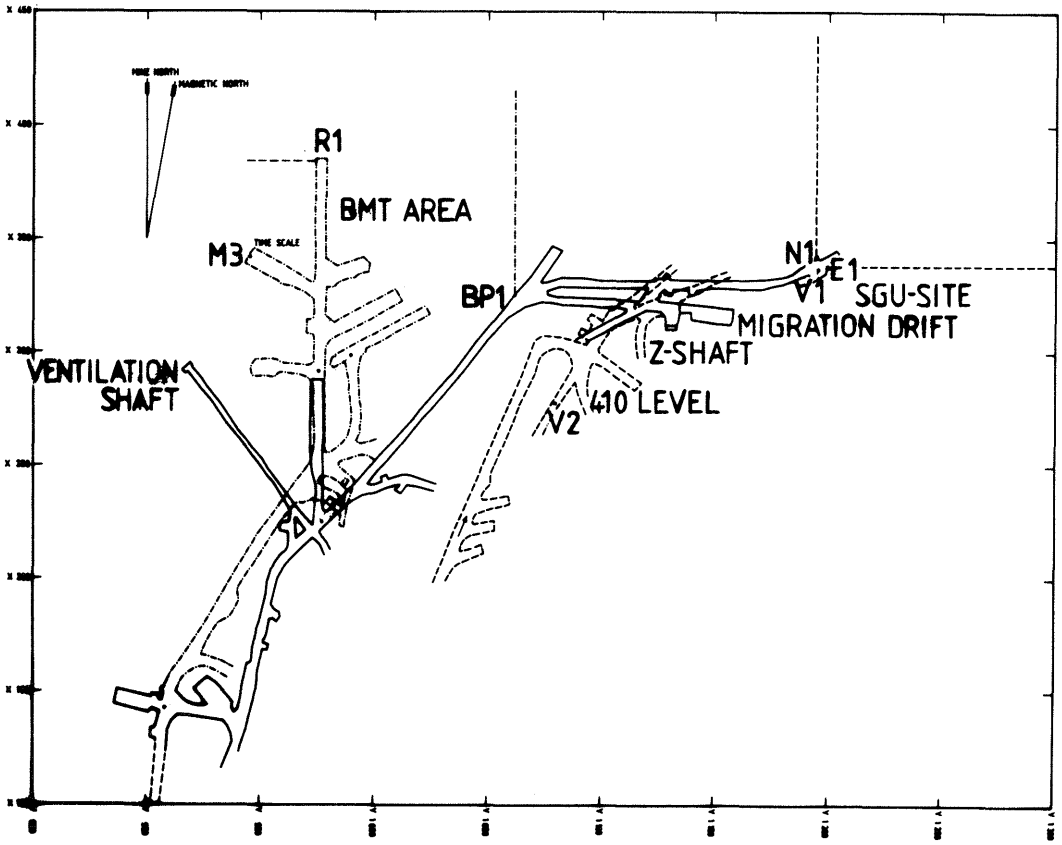

Figure 1-1. The investigation areas in the Stripa Mine with the boreholes used for water sampling.

Table 1-1. Data on the main boreholes included in the hydrogeological program.

Bh no	Diameter	Collar coordinates			Length
	mm	X	Y	Z	m
V1	76	336.8	1195.7	356.7	505.9
V2	56	270	1075	407.7	822.0
N1	76	342.2	1194.6	355.5	300
E1	76	338.4	1199.7	355.7	300

2 GEOLOGY

2.1 Introduction

Field investigations for the International Stripa Project are carried out at the Stripa Mine, located in Örebro County, south-central Sweden, (59°43'N, 15°5'30"W), 250 km west-northwest of Stockholm. The Stripa Mine lies within the Central Swedish Ore Province ("Mellansverige") consisting of more than a hundred iron-manganese and copper-zinc-lead mines. Mining at Stripa began around the year 1450 for iron ore (mostly specular hematite). The mining was intermittent but continued until 1976 when negotiations were made to keep the mine open as a research site.

The topography is hilly with the elevation at Stripa about 140 m above sea level. The Stripa area was slightly inundated by seawater during the Holocene since the highest paleo-shoreline is found at 170 m above sea level. Glacial sediments and tills cover most of the region but bedrock is exposed on the tops of hills. To the northwest, the elevation increases steadily by several hundred meters. Maps of the bedrock geology, structural geology, and a magnetic survey have been published on a scale of 1:50,000 (Koark and Lundström, 1979). Recent geological investigations have been reported by Olkiewicz, et al. (1978, 1979) and Wollenberg, et al. (1980). This section summarizes these previous studies and contains some additional geological data obtained in the course of the hydrogeochemical investigations.

2.2 Major lithologic units

The bedrock geology in the Stripa region consists of highly folded and deformed Precambrian rocks; primarily metasediments and metavolcanics intruded by several granitic bodies. The metamorphic rocks occur in a northeast-southwest-trending direction and are dominated by high-grade, silica-rich schists and gneisses (Figure 2-1). They also include a metamorphosed carbonate section (calcareous and dolomitic marble) occurring about 3 km from the Stripa site and varying in outcrop width from 50 m up to 1.7 km. Granitic intrusions range in size from less than 100 m to several tens of kilometers. Their compositions range from a true granite to granodiorite, although aplites, pegmatites, small gabbroic and amphibolite dikes all occur in the region (Koark and Lundström, 1979). Their occurrence is somewhat erratic and irregular. The granitic bodies appear greyish white, grey, reddish-grey, and red in color, and are commonly medium grained in texture.

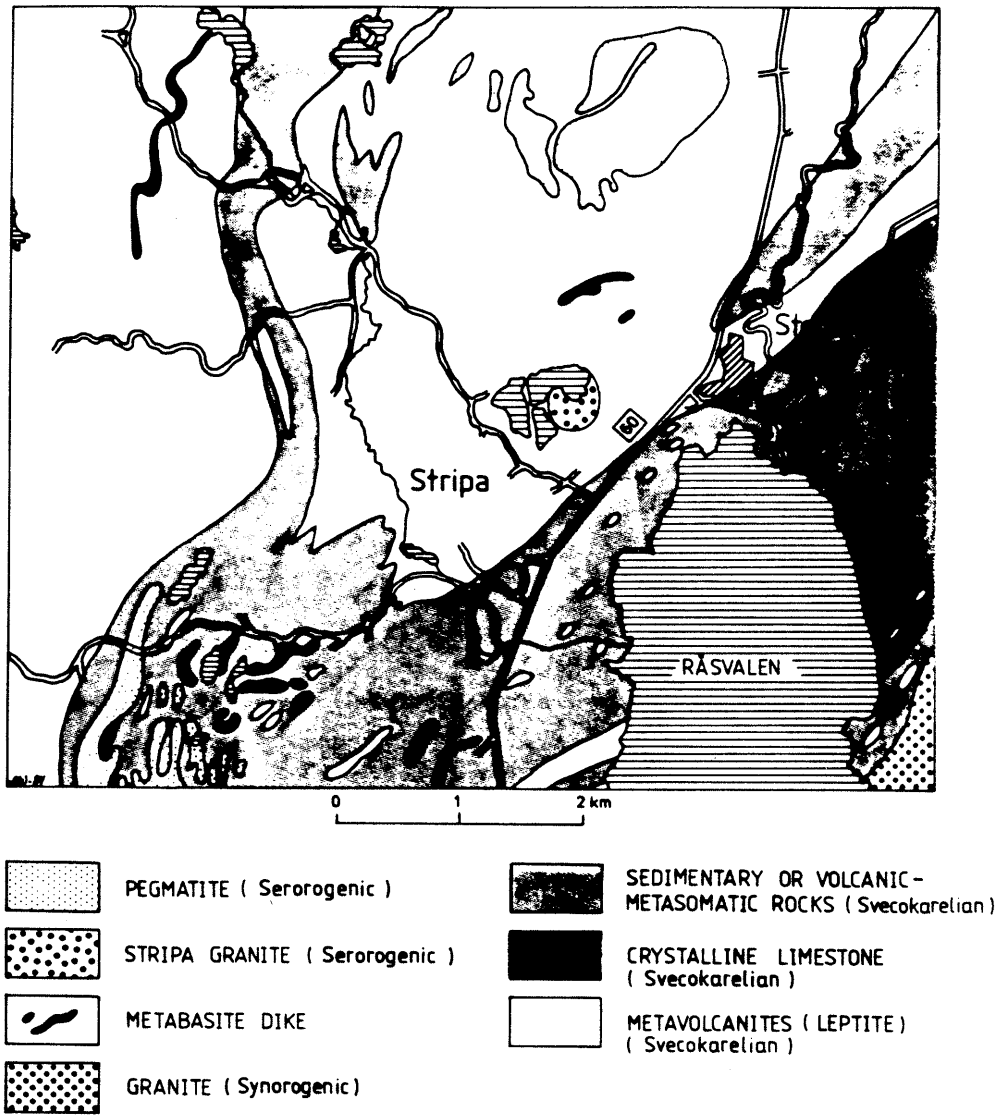

Figure 2-1. Geologic features of the Stripa area.

2.3 The Stripa ore

Stripa ore was, according to old registrations, first mined during 1448-1470 and 1551-1578. After years of no activity mining was again reestablished 1634-1771 (Paulsryd, 1941). In the 1780s mining started in larger scale, but it was first during the present century that the mining went deep underground and as late as 1930-1960 the deeper parts were mined.

The ore deposits occured mainly as two bodies called the Main and the Parallel ore body, respectively. The Main body with a maximum thickness of 16 to 17 meters was folded into a syncline with an undulating eastward pitch. Both the ore bodies were surrounded by leptite.

The iron ore is mainly a quartz-banded hematite, but magnetite occurs also. The skarn minerals associated with the ore are mainly actinolite, diopside and epidote. Pyrite occurs locally and is evidently of secondary origin (Geijer, 1938). The iron-ore in the Main ore body has a higher content of Fe than the ore in the Parallel body. In Table 2-1 the general composition of the two ore bodies is given.

Table 2-1. General composition of the two ore bodies at Stripa (Paulsryd, 1941).

Body	Fe %	P %	S %
Main	50	0.007	0.016
Parallel	41	0.009	0.037

The hematite of the ore bands developed as grains of 0.2 - 0.6 mm diameter, slightly elongated in the plane of bedding. The porphyroblastic magnetite can reach up to 15 mm, but the normal size is from 0.5 to 5 mm. Most of the magnetite ore in Stripa seems to have occured in connection with a secondary enrichment process that resulted in a very rich, coarsely crystalline magnetite ore (Geijer, 1938). Most of the high-grade magnetite occurs within a marked syncline, from which fault zones diverge striking ENE.

The type of folding and associated faulting movements that is represented by the Stripa deposit is typical of what could be encountered in large portions of the ore-bearing region of Central Sweden. On the whole the folding of the Stripa deposit has been comparatively small. There was little interior deformation within the ores, in spite of the normally incompetent character of the quartz-banded ores.

The faulting movements that apparently accompanied the folding exhibited a variety of types. One type appeared to be accentuations of folds, through slipping along contact planes. Echelon displacements in the different ore bodies belonged to this type also. Usually these displacement zones striked E, that is in slight angle to the fold-axis. Another related type is interpre-

ted as due to shearing movements. Movements along well-defined, steeply dipping fault planes were represented by most disturbances of this group in the main ore body. They usually were parallel to the fold axis. Movements along these faults appeared to have been in the form of overthrusts and there were, in some cases, indications that the horizontal component was greater than the vertical one (Geijer, 1938).

Later sets of faults, separated in age from those described, are associated by such geological events as the intrusions of basic rocks and of granite aplite. These faults were usually steep dipping and their orientations differed. However, the most common orientation was almost perpendicular to the fold axis and also towards NE. Usually the displacements had a larger vertical than horizontal component. According to Geijer (1938), the vertical component was usually not exceeding a few meters.

2.4 Petrology

The target rock for the investigations in the Stripa Mine is a small intrusive body of granite - Stripa granite, that predominantly is a grey to reddish, medium-grained rock of Precambrian age. The Stripa Granite occurs at the surface in a belt of older supracrustal metamorphic rocks. The largely concordant nature of the granite is not uncommon. Many postorogenetic granites in the Stripa region have been mapped as elongated intrusions parallel to the structures of the supracrustal belts (Koark and Lundström, 1979).

Leptite, a strongly metamorphosed sedimentary rock, normally of volcanic origin, is the dominant rock type in the supracrustal formation. The regional distribution of the rock types is shown in Figure 2-1.

The main features of the configuration of the contact between the leptite syncline and the granite is illustrated in Figure 2-2, based on the data obtained from the mine workings and investigations in the SAC-program. The contact between the leptites and the granite is transected by the access drift to the hydrogeological test site at the 360 m level, approximately 300 m SSE from the ventilation shaft. The granite at the contact occurs partly as inclusions or dikes in the leptite. The granite surrounds the leptites in the Stripa syncline in the northeastern part of the mine. The limits of the subsurface extension of the granite to the SE is partly shown by the prospecting boreholes Pjt 3 and Pjt 3B as shown in the vertical section in Figure 2-2. This section is taken perpendicular to the contact, i.e. in a northwest-southeast direction. The location of the section is indicated in Figure 2-3.

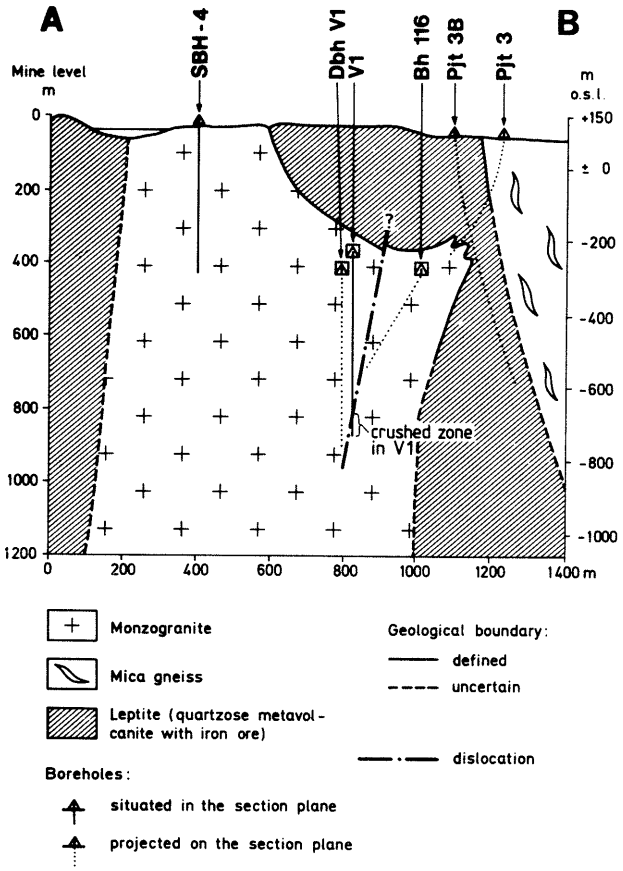

Figure 2-2. Vertical section through the investigation area. The location of the section is shown in Figure 2-3.

The petrology of the Stripa granite was studied by Olkiewicz, et al. (1978, 1979), Koark and Lundström (1979) and Wollenberg et al. (1980). In these reports the granitic intrusion is named quartz monzonite, monzogranite or granite. The technically correct name for this intrusion is "granite" based on both the mineralogy and the chemical composition.

Igneous rocks are classified petrographically where possible and chemically where not possible by petrographic techniques. Classification of high-silica, wholly-crystalline igneous rocks is based on the proportions of the three essential minerals: quartz, alkali feldspar and plagioclase feldspar. The Stripa granite contains 30-40% quartz, 25-35% plagioclase and 18-34% microcline. An additional 5-10% is muscovite and chlorite (altered biotite). The average of 6 modal analyses from Wollenberg, et al. (1980) and one sample by R Donahoe, US Geological Survey, is shown in Table 2-2. Plotting this data on the ternary diagram in Figure 2-4 shows that the rock falls well within the granite field according to the Streckeisen classification system which has been adopted by the International Union of Geological Sciences (Streckeisen, 1973, 1976). It has been adopted also by most modern workers in igneous petrology (Barker, 1981). Further

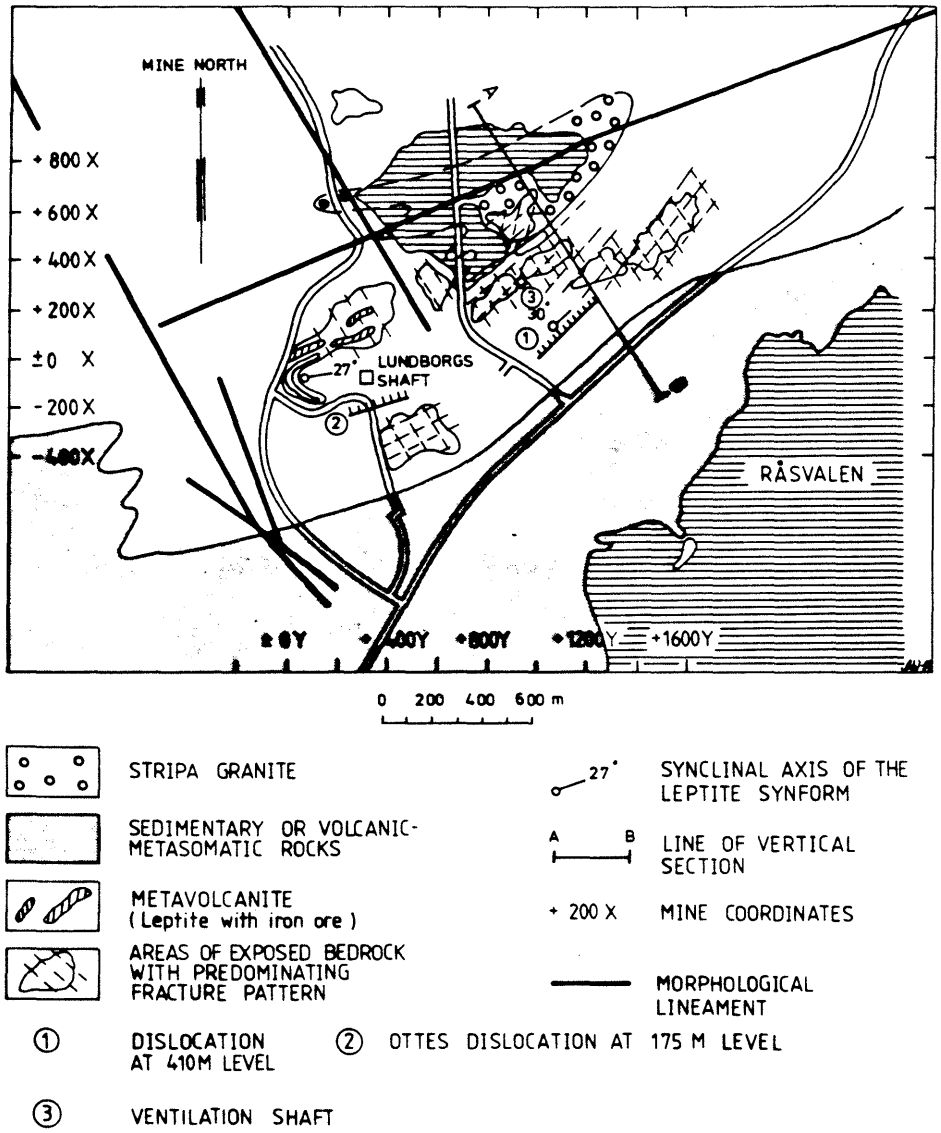

Figure 2-3. Major structures in the Stripa area.

chemical evidence for this classification is given in the next section.

Optical and X-ray studies by R Donahoe (pers. comm.) and Wollenberg, et al. (1980) indicate that the plagioclase is oligoclase (An_{27}) in composition. The plagioclase grains are sericitized and the microcline grains are frequently perthitic or microperthitic. The microcline is commonly interstitial to the quartz and plagioclase. The quartz appears optically biaxial due to strain and are highly fractured. Hematite is in some places dispersed as fine dust within the feldspar grains, particularly plagiocla-

Table 2-2. Analyses from 7 samples of Stripa granite*.

	A %	B %
Quartz	35.4	35
Plagioclase feldspar	30.0	32
K-feldspar	25.7	25
Muscovite/sericite	5.0	4
Chlorite	3.0	3

*Accessory minerals (opaques, carbonates, epidote, fluorite, zircon, garnet and apatite) are typically <1%. Biotite has mostly been altered to chlorite. Column A is the average of 6 modal analyses from the data of Wollenberg, et al. (1980). Column B is a single modal analysis of V1 core, interval 149.2 - 149.5 m obtained by R. Donahoe, US Geological Survey.

se, or along grain boundaries and cracks within grains. The red color in many of the granite samples is due to the occurrence of hematite (Wollenberg, et al., 1980).

The chlorite appears in two varieties - one is strongly pleochroic, dark green-black to light brown and the other is weakly pleochroic, light to dark green. The former variety appears to be incompletely chloritized biotite whereas the other occurs along grain boundaries and as microfracture veinlets, suggesting more complete alteration.

Fluid inclusion measurements are discussed in Section 2.7.

The Stripa granite typically shows an abundance of fractures, both continous and discontinous on a microscopic scale. Even in relatively unfractured rock samples fine, discontinuous cracks within primary grains or along grain boundaries are common. These cracks are filled with intergrown chlorite and sericite or by quartz and feldspars and they frequently originate among primary grains of the same minerals as those filling the cracks. This suggests that the crack fillings have not crystallized from fluids introduced from extraneous sources, but are due rather to remobilization and redeposition of primary components of the rock matrix (Wollenberg, et al., 1980). Veins or dikes of pegmatites and aplites are common in the granite.

Another distinctive feature of the Stripa granite is the prevalence of cataclastic textures. There are evidences of movements along fracture surfaces or breccia zones. Slickensides and fractures are filled with a microscopically irresolvable clay-rich fault gouge and contain rounded fragments of granitic rock (Wollenberg, et al., 1980).

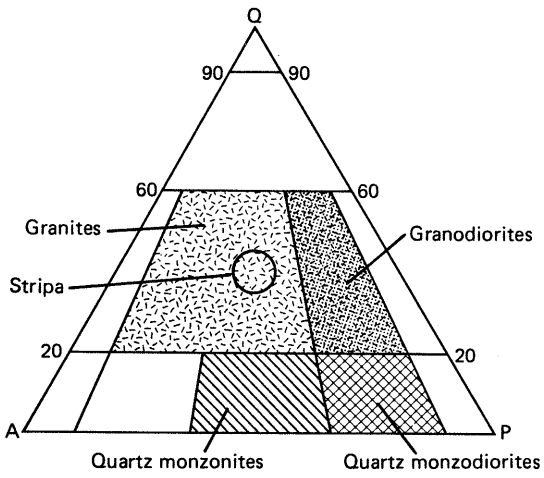

Figure 2-4. Classification of silica rich plutonic rocks according to the Streckeisen system. Compositions are normalized to A (alkali-feldspar) + P (plagioclase) + Q (quartz) = 100% by volume assuming that mafic minerals are less than 90%. The range of the modal analyses of the Stripa pluton fall within the range for granites.

Samples of Stripa granite and neighboring granitic rocks (Gusselby and Kloten massifs) were dated by the potassium-argon method at the University of California, Berkeley (Wollenberg, et al., 1980). The dates obtained were in millions of years 1691±16, 1604±14 and 1640±44 for Stripa, Gusselby and Kloten respectively. The leptite is considered to have a similar origin and is believed to be slightly older than the granite but no dates have been obtained.

The leptite is usually a gray, red or grey-green to black, fine-grained foliated metamorphic rock (microschist) cut by white or light green fractures. Mineralogically it is similar to the Stripa granite. Texturally, however, it does not resemble the granite, as it is finer, more even-grained and homogeneous. In detail, the leptite generally consists of a fine, even-grained mosaic of equant quartz with fewer plagioclase and microcline grains. Darker leptites generally contain more chlorite, at the expense of muscovite, than the lighter leptites, or they contain fewer porphyroblasts.

The contacts of leptite with Stripa granite was studied by Wollenberg, et al. (1980), in thin sections. The contacts are generally sharp, possibly fault contacts. They show little sign of alteration such as might be expected if the granite had intruded the leptite. The growths of sericite, or epidote-chlorite-filled fractures occur at the contact, in some places also opaque grains rich in uranium are associated with the contact.

Another variety of metamorphic rock at Stripa is a dark green fine-grained foliated rock rich in blue-green prismatic amphibole, usually logged as greenstone in core-logs. Texturally, it is a microschist like the more abundant leptite. However, its foliation is determined by amphibole prisms instead of chlorite and muscovite laths.

2.5 Chemical composition of the Stripa granite

Three samples were analyzed (one in duplicate) by X-ray fluorescence and reported by Wollenberg, et al. (1980). Seven samples were analyzed (all in duplicate) at the U.S. Geological Survey using X-ray fluorescence, emission spectroscopy and ion-selective electrodes depending on the constituent. Of the latter seven samples, four were taken from the VI borehole at depths of 107, 408 and 445 m from the borehole origin (355 m below surface) and three were taken from the V2 borehole at depths of 456, 471 and 760 m. The chemical analyses of the seven borehole samples are for fresh unfractured rock and are reported in Table 2-3. They are in excellent agreement with those reported by Wollenberg, et al. (1980), except for silica which is about 3% higher. Since the total sum of all constituents is also 3% higher (102%) than the sum in Wollenberg's report (99%) then it is likely that the silica values reported in Table 2-3 are biased a bit too high. In any case, silica is always greater than 72% and with K_2O falling in the range of 4-5%, the rock must be classified as a granite (Barker, 1981). The CIPW normative calculation used by Wollenberg, et al. (1980), is useful for basalts and experimental systems but not for natural granites.

Based on the chemical data given in Table 2-3 the Stripa granite can be further classified as a peraluminous granite by the criteria $Al_2O_3 > Na_2O + K_2O + CaO$ (Barker, 1981). In an effort to correlate the composition of granites to their mode of origin, recent emphasis has been placed on those derived by partial melting of sedimentary rocks, the S type, versus those derived from pre-existing igneous rocks, the I type. The S types are biotite-muscovite-bearing and strongly peraluminous whereas I types are biotite or biotite-hornblende bearing and metaluminous (Barker, 1981). The Stripa granite is clearly an S type which is consistent with the concept of partial melting of volcanic sediments in the leptite.

Certain minor and trace elements (Cl, F, S, Li and B) were determined to assist in the interpretation of fluid inclusion measurements, sources of sulfur and neutron flux studies. There is nothing unusual in the concentrations of these elements compared to most granites.

Table 2-3 U.S.G.S. Analyses of Stripa Granite.*

		V2-456	V2-471	V2-760	V1-107	V1-408	V1-408.03	V1-445	Average
SiO_2	%	76.3	76.9	76.3	75.9	76.6	78.1	77.5	76.8 ± .75
Al_2O_3	%	14.0	13.7	14.0	14.0	13.9	14.0	14.2	14.0 ± .21
Fe_2O_3	%	1.5	1.2	1.4	1.2	1.2	1.4	1.4	1.33 ± .18
MgO	%	.24	.26	.25	.26	.24	.28	.30	.26 ± .02
CaO	%	1.0	.72	.87	.80	.40	.43	.76	.72 ± .22
Na_2O	%	4.1	3.9	4.0	4.0	4.0	4.0	4.4	4.07 ± .22
K_2O	%	4.9	5.0	4.6	4.6	4.6	4.7	4.1	4.62 ± .29
TiO_2	%	.08	.08	.09	.08	.09	.08	.09	.08 ± .01
P_2O_5	%	.09	.09	.09	.08	.09	.10	.10	.09 ± .01
MnO	%	.05	.05	.05	.07	.05	.05	.06	.06 ± .01
Cl	%	.018	.013	.018	.015	.012	.020	.018	.016 ±.004
F	%	.052	.074	.061	.056	.019	.023	.024	.044 ±.021
S(total)	%	.03	.02	<.01	<.01	<.01	<.01	<.01	≤.03
Li(ppm)		1.8	2.8	28	8.4	4.5	4.6	5.5	7.9 ± 8.7
B(ppm)		3	3	3.5	5	4	4	4	3.8 ± 0.9

* Analysts: J Gillison, N. Rait, J. Fletcher, R. Johnson. Results from 7 samples done in duplicate. Averages are for 14 determinations of each constituent with one standard deviation. Note that rock samples are from clean, unfractured sections of core, and the analyses represent fresh granite. Higher concentrations of some constituents will be encountered in highly fractured rocks, especially where fracture-fill minerals occur.

Rare earth elements were determined on eight granite samples at Pierre Süe Laboratory in Saclay, France, by instrumental neutron activation analysis (NAA). The countings were performed using high resolution Ge-Li detectors, and low energy photon activities were measured by an intrinsic germanium detector, especially used for the Gd determination. The data are reported in Table 2-4 with duplicate analyses for each depth in V1 and V2 boreholes. Analytical precision is about 5% for each measurement.

Table 2-4 Rare earth element concentrations (ppm) in Stripa granite.

Sample	La	Ce	Nd	Sm	Eu	Gd	Tb	Yb	Lu	Total
V1 259.4 m	29.5	72.0	49.5	14.5	0.39	11.8	2.0	7.0	1.2	188
	25.0	58.0	35.5	11.5	0.25	9.5	1.8	6.5	1.1	149
V1 318.4 m	34.5	70.0	47.0	15.2	0.23	11.5	2.0	7.5	1.3	189
	33.5	69.0	48.0	14.5	0.39	13.5	2.5	8.0	1.4	190
V1 373.3 m	25.5	56.5	38.5	11.5	0.30	9.5	1.5	5.6	1.0	150
	38.0	81.0	57.5	17.5	0.59	11.5	2.0	7.5	1.3	215
V2 804.6 m	35.5	72.8	49.7	15.9	0.45	13.5	3.0	8.5	1.3	200
	34.5	71.0	48.5	16.2	0.25	12.0	2.5	8.0	1.4	194

Rare earth elements plus Ba, Co, Cr, Cs, Hf, Rb, Sb, Ta, Th, U, Zn, Zr and Sc were determined on 14 granite samples by NAA at the U.S. Geological Survey. These results are shown in Table 2-5.

Table 2-5 NAA Analyses of Stripa Granite

Element (ppm)	V2-456	V2-471	V2-760	V1-107	V1-408	V1-408.03	V1-445	Average
Ba	511	659	571	513	474	525	565	545±60
Co	0.67	0.64	0.76	0.71	0.64	0.73	0.81	0.71±0.06
Cr	<1	1.8	1.0	1.6	1.2	2.7	1.7	1.7±0.6
Cs	4.3	4.3	9.1	3.1	2.6	3.1	3.4	4.3±2.2
Hf	3.7	3.7	4.0	3.7	3.8	3.8	3.9	3.8±0.12
Rb	261	307	282	271	245	249	265	269±21
Sb	0.17	0.13	0.23	0.27	0.12	0.17	0.22	0.19±.05
Ta	7.9	8.0	6.8	8.8	7.8	7.9	7.8	7.9±0.6
Th	31	31	36	32	34	34	34	33±1.9
U	31	33	35	32	26	31	33	32±2.8
Zn	19	11	22	23	16	21	19	19±4.1
Sc	4.5	4.5	5.5	4.4	4.7	5.2	4.9	4.8±0.4
La	27	26	31	26	28	29	32	28±2.4
Ce	70	66	80	67	73	75	80	73±5.7
Nd	35	35	42	33	36	39	44	38±4.1
Sm	7.8	7.4	9.1	7.6	8.4	9.1	9.4	8.4±0.8
Eu	0.45	0.41	0.50	0.42	0.44	0.46	0.47	0.45±0.03
Gd	13	13	14	13	12	14	15	13±1.0
Tb	2.1	2.1	2.4	2.1	2.1	2.3	2.3	2.2±0.13
Tm	1.1	1.0	1.0	1.0	1.0	1.0	1.2	1.0±0.08
Yb	8.0	8.2	9.1	8.1	8.3	8.8	8.6	8.4±0.4
Lu	1.2	1.2	1.4	1.2	1.2	1.2	1.3	1.2±0.08

Rare earth elements distributions in geological samples are often described by normalized patterns. In igneous rocks, the reference sample is a chondritic ratio. The chondritic-normalized pattern of the granite is characterized by a light-REE enrichment, and by a strong Eu depletion (Figure 2-5). According to the alkali content of the granite (Wollenberg et al., 1980), these REE distribution curves are characteristic of similar granites (Henderson, 1984).

2.6 Fracture minerals

All boreholes within the program show similar characteristics regarding the existing fractures. Detailed fracture logs are given in previous reports on the core logs (Carlsson, et al., 1981; Carlsson, et al., 1982a and 1982b). The recorded fractures may be classified into one of five different groups;

1 Fractures with fresh, uneven surfaces

2 Open or sealed fractures

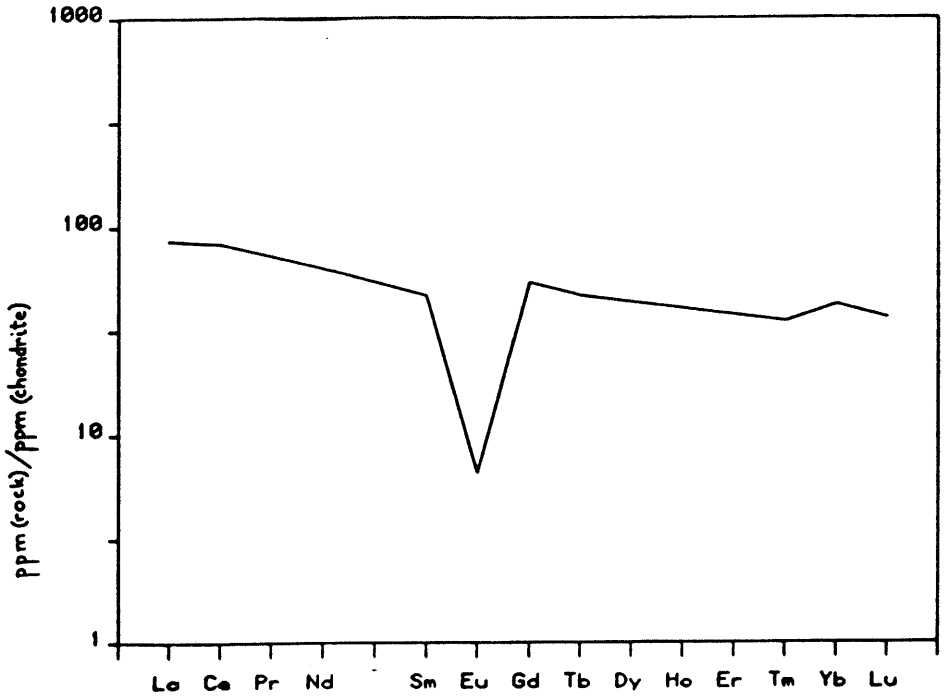

Figure 2-5. Rare earth abundance of the Stripa granite relative to the normalized chondrite values (see Haskin and Haskin, 1968; Haskin et al., 1966).

3 Small-scale shear zones

4 Brecciation and granulation of the granitic matrix

5 Quartz veins

Except for the fractures included in the first group, all others are characterized by the existence of coating minerals or weathering indications on the fracture surfaces. The fracture filling minerals were megascopically classified on the basis of colour, hardness and appearence of carbonates. As pointed out by Wollenberg, et al. (1980), it is normal that different fracture filling minerals are intergrown in varying combinations which makes the megascopical classification somewhat uncertain. An extra check was therefore made by using X-ray diffraction on five samples taken from the V2 core.

The result of this test showed that the plagioclase mixing with epidote was much more common than expected. The conclusion which may be drawn from the result is that plagioclase in general have been underestimated.

Chlorite, which is the most common fracture filling mineral, is very dark, almost black, and much harder than normal due to mixing with epidote and plagioclase. Also, the epidote shows many types of colour variations in the green colour spectrum when mixed with plagioclase.

Sericite, commonly intergrown with chlorite, is nearly as common as chlorite. Next to chlorite and sericite, calcite is the most common fracture filling mineral. Its occurrence ranges from fillings of hairline cracks and thin coatings and intergrowns with other minerals to coarse crystals grown in the spacings of large fractures.

Epidote occurs commonly in fractures, veins and shear zones, which are sealed in the core, associated with quartz, chlorite and sericite. Other fracture filling minerals identified in the cores include pyrite, chalcopyrite, fluorite, iron oxides and zinc sulphide. The great majority of the fracture infillings are less than 1 mm in width.

Borehole V2 penetrates the most deep-seated rock mass and it was therefore of interest to study the variation in mineral coatings versus depth. The result of this study is summarized in Figure 2-6, where it is seen that the coating of chlorite and chlorite/calcite-mixing are about constant throughout the full length of the borehole. The most striking change with depth is that the calcite shows a marked decrease at 250 - 450 m depth with a simultaneous increase in epidote. Each of the chlorite, calcite and epidote coatings make up about 25 - 30 per cent of all coated surfaces. The group of other minerals form a complex group with great variety. Pyrite, fluorite, iron oxides, zinc sulphide and clay are examples of coatings within this group.

The mentioned conditions are generally in agreement with the results reported by Wollenberg, et al. (1980), which is based on megascopical classifications, X-ray diffraction analyses and analyses of thin sections. An additional observation is the rare but noteworthy occurrence of asphaltite as fracture fill in the Stripa granite (Wollenberg, et al., 1980). Nothing is known about the origin of this organic material and it was found to contain high concentrations of uranium.

Additional studies on fracture minerals were reported by T. D. Reimer as part of the geochemical investigations during the SAC program (Fritz, et al., 1980). Chalcopyrite was found in one sample and some analyses of muscovite, sericite, Ca-mica, chlorite, feldspar, pyrite, chalcopyrite, calcite and dolomite (?) are reported. The compositional data for chlorites indicate that there are two varieties: an iron-rich member ($FeO/MgO = 7$) and a magnesium-rich member ($FeO/MgO = 0.9$). This observation is consistent with the optical information on chlorites in the rock matrix that indicates two species of different composition.

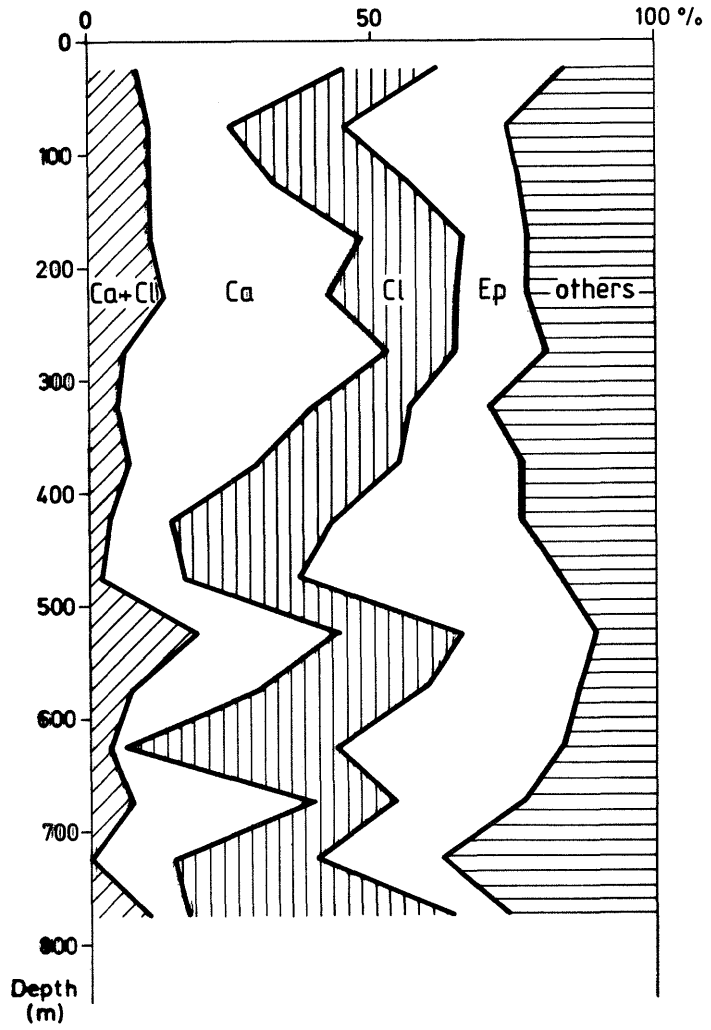

Figure 2-6. Distribution of coating minerals in V2 versus depth.

2.7 Fluid inclusions

Fluid inclusions are microscopic droplets of aqueous solution, silicate or sulfide melt, gas or organic material, that occur in most rocks and minerals. They commonly range in size between 1 and 10 micrometers (observed range is 20 nanometers up to a volume of 100 milliliters). The number of inclusions per unit volume varies inversely with the size of the inclusion, but commonly lies in the range of 10^8 inclusion/cm^3 (maximum observed is 10^{14} in a sample of white quartz). They typically contain 10 wt. % dissolved salts with NaCl being most abundant, although concentrations range from 0 to 50%. Many careful and detailed measurements have been made on fluid inclusions in the last several decades because of their usefulness in interpreting the origin of ore deposits. Most measurements are made on quartz, fluorite, calcite and sulfide ore minerals. Freezing point, melting point, and homogenization temperatures can be measured on the inclusion fluids, and, under the appropriate conditions, these can indicate the composition and temperature of the fluid in contact with the rock when it was formed (Roedder, 1984).

Fluid inclusions may affect the deep groundwater chemistry of crystalline rocks (Garrels, 1967; Gambell and Fisher, 1966; Jacks, 1978; Nordstrom, 1983), and this suggestion, supported by groundwater chemistry data, prompted an investigation of fluid inclusions in the Stripa granite.

Lindblom (1984) completed a study of fluid inclusions on both fractured and megascopically unfractured rocks from V1 and V2 cores. Freezing point, melting point, homogenization point temperatures were measured, and the population density of inclusions in quartz grains were measured. The main conclusions are:

1 The number of inclusions per cm^3 varies from 0.5 - 9 x 10^8.

2 The total volume of inclusions averages 14 µL per cm^3 of quartz in unfractured rock and 20 µL/cm^3 (20 L/m^3) in fractured rock.

3 The salinity of the fluid inclusions in the unfractured rock sections gives a mode of 4 wt. % NaCl and in the fractured rock sections, 1.7 wt. % NaCl. Unfractured rocks have a slightly lower volume of more saline inclusion fluid than the fractured rocks.

4 Homogenization temperatures vary between 90°C and 270°C and represent the temperatures of rehealing of fractures in quartz.

5 A modal homogenization temperature of 130°C represents an earlier event in unfractured rock sections. A later rehealing event is represented by another modal homogenization temperature at 190°C in fractured rock sections.

6 The rock may have been flushed by deep-circulating meteoric waters at a possible late date (something younger than several million years).

7 Total salt content in quartz inclusion fluids is 5.6 x 10^{-4} g/cm^3 for unfractured rocks and 3.4 x 10^{-4} g/cm^3 (340 g/m^3) for fractured rocks.

8 If the same fluid-inclusion content for the whole rock is assumed, then the percentage of fluid inclusions needed to mix with fresh groundwater to achieve 650 mg/L is only 1-2%, assuming static, or closed system, conditions. If the worst assumptions are made (e.g., that inclusions only occur in quartz, etc.), then the maximum of fluid inclusions needed might be as high as 10%.

9 The concentration of water-soluble chloride is estimated to be .0132 wt. % for unfractured rock sections, and .0078 wt. % for fractured rock sections, assuming that feldspars have the same number and type of inclusions as the quartz grains.

From the total Cl analyses shown, this represents 50 - 80% of the total Cl (although the uncertainty is high on the estimates of water-soluble chloride because the measurement gives "equivalent wt. % NaCl" not a direct reading).

Fluid inclusions in the Stripa granite appear to be dominantly or completely secondary and cover a wide range of temperature and compositional conditions. These data indicate that numerous thermal and tectonic events took place since the original emplacement of the granite.

The results of Lindblom's study shows that there is more than sufficient fluid-inclusion salt in the Stripa granite to account for the salinity of the groundwater, assuming static or near-static groundwater conditions and a porosity of 1%.

An independent measurement of chloride concentrations in the inclusion fluids was made by a published procedure for extracting fluid inclusions (Roedder, 1958; Roedder, et al., 1963). Samples were fragmented, cleaned, evacuated in a vacuum line for several days and then crushed under vacuum. The extracted water was measured and its ^{2}H content analyzed (see Table 2-6). Then the samples were sequentially extracted with a small volume of distilled water for 5 or 6 times until the Cl concentration was no longer detectable. The calculated Cl concentrations in the inclusion fluids are shown in Table 2-7. The average value of 41 g/L Cl is greater than the estimate made by measuring freezing/melting temperatures, but the range of values overlaps. If the rock leaching value is taken for the average Cl concentration of the fluid inclusions in quartz only, then the water-soluble Cl becomes 50 - 77% of the total. The leaching estimate of fluid-inclusion chloride is suspected of being biased too high because fluid inclusions are likely to occur in the feldspars (Roedder, 1972), and because some of the values give a higher rock chloride concentration than found by total rock analysis (Table 2-3). Therefore, the estimate of fluid-inclusion chloride taken from the freezing/melting temperatures is considered more reliable.

Table 2-6. ^{2}H data on fluid inclusions from the Stripa granite.

Drillhole	Depth (meters)	^{2}H °/oo, SMOW
V1	408	-58.8
V1	445	-68.5
V1	445	-86.5
V2	363	-79.8
V2	404	-73.7
V2	455	-52.5
V2	471	-74.5

Table 2-7. Chloride concentrations of fluid inclusions by direct analysis of leachates.

	Cl(g/L)
V1(445)	44
V1(445)	54
V2(404)	47
V1(505)	34
V1(408)	16
V2(455)	46
V2(363)	67
V2(471)	18
Average	41

2.8 Radiogeology

The abundance of radioelements in the rocks was measured by Wollenberg, et al. (1980). The fission-track radiographic method was used to determine the location and abundance of uranium in uncovered thin sections.

The Stripa granite is rather unique in its radioelement content, both in the abundance of elements and their ratios. Table 2-8 indicates the relatively high uranium and thorium contents of the granite, compared with other plutons in the region.

The measurements indicate that uranium is depleted in surface exposures of granite and leptite at Stripa, relative to its abundances in the same rock units underground.

In the Stripa granite, uranium is most highly concentrated in tiny opaque grains on the order of 50 micrometer in diameter, generally euhedral and in some places square in cross-section. These grains are usually found in chlorite, but also in muscovite-chlorite-sericite filled fractures, and even in cracks within quartz or feldspar. Usually the grains contain up to 5% uranium, but concentrations up to 10-15% have been observed (Wollenberg, et al., 1980). Another locus of uranium concentration was observed in opaque grains with both a quartz-epidote-sericite-filled fracture on a contact between granite and leptite, and with fine carbonate-sericite stringers intersecting that contact on the granite side. Although the concentration of uranium is lower in these grains, on the order of 2% U, the absolute abundance of uranium contained in them is greater.

Uranium is also found, in lower concentrations, dispersed along chlorite-filled fractures without associated discrete grains.

Table 2-8 Radioelement contents (after Wollenberg et al., 1980).

Rock type	No.	Uranium ppm	Thorium ppm	Potassium %	Th/U
Stripa granite					
Surface	9	26.9±5.5	33.0±5.7	4.6±0.7	1.1±0.1
Underground	34	37.4±6.2	29.2±3.8	3.9±0.3	0.8±0.1
Leptite					
Surface	5	3.3±0.7	11.9±2.9	3.1±0.6	3.6±0.4
Underground	9	5.4±3.1	17.9±1.4	2.8±0.5	3.9±1.2
Regional rocks					
Granites	7	17.6±15.4	26.6±6.6	5.2±1.5	2.4±1.2
Metamorphic	5	6.1±1.5	14.6±8.7	2.5±1.1	2.6±1.9

Table 2-9. Radiogenic heat production of the rock in the Stripa region (Wollenberg, et al., 1980).

Rock type	No.	Heat production $\mu W/m^3$
Stripa granite		
Surface	9	9.5
Underground	34	11.9
Leptite		
Surface	5	2.0
Underground	9	2.9
Regional rocks		
Granites	7	6.8 to 7.1
Metamorphic	5	2.8

Concentrations are generally about 0.5% or lower, but occasionally range up to 1.0% uranium.

The Stripa leptite contains no appreciable discrete concentration of uranium either in the matrix or in a coarse epidote-filled fracture cutting it (Wollenberg, et al., 1980). Uranium minerals were observed in chlorite-filled fractures cutting the iron ore at Stripa (Welin, 1964).

The heat production was calculated from the radioelements of the Stripa pluton by Wollenberg, et al. (1980). In Table 2-9 the radiogenic heat production of the various rocks in the Stripa region are listed.

The Stripa granite averages 11.9 microWatts per cubic meter. This should be compared with 2.8, considered to be the mean for granitic rocks (Heier and Rogers 1963), 6.9 $\mu W/m^3$ for the Bohus granite of southwestern Sweden (Landström, et al., in prep) and 7.1 $\mu W/m^3$ for the Malingsbo granite just north of Stripa (Malmqvist, et al., 1983). The radiogenic heat production of the Stripa granite is four times that of the neighboring leptite and nearly twice the heat production of other plutons in the region.

Geophysical well logging played an important part in the current program for hydraulic, structural, stability and chemical purposes. A standard geophysical well-logging program was set up and performed in the four main boreholes. This program compiled the following logs:

Type of log	Purpose
Deviation log	Direction and deviation of the borehole
Natural gamma	Rock type, dykes, veins and fracture indications
Single point resistivity	Resistivity of the rock in the borehole wall i.e. conducting minerals and fractures
Resistivity logs	Fracture indications
Temperature log	In- and outflow zones in the hole
Drillhole fluid	In- and outflow zones in the hole resistivity
Self potential log	Measures anomalies which indicate fracture zones

Table 2-10. Radiation level in the boreholes E1, N1, V1 and V2.

	Average	Peak
V1	65 microR/h	406 microR/h
V2	100 microR/h	250 microR/h
E1	117 microR/h	
N1	250 microR/h	430 microR/h

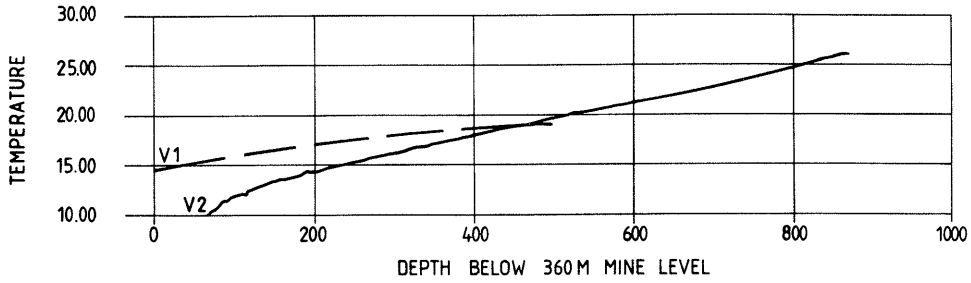

Figure 2-7. Temperature versus depth in boreholes V1 and V2.

The results of natural gamma logs presented in Table 2-10 show large differences between the holes. The high level in N1 is due to the radon content in combination with the very low water outflow. The radiation level in the granite is most accurately given by the values from V1 where the water outflow is high.

The temperature of the water in the boreholes V1 and V2 is given in Figure 2-7. The influence on the temperature from the drift can be seen down about 100 m in V2. From there the temperature gradient is about 17 degreesC/km down 480 m where it decreases to around 15 degreesC/km. From 610 m the gradient increases to 18 degreesC/km down to the bottom of the hole. In V1 the influence of the drift is not recognized. Instead there is a higher temperature than in V2 due to the outflowing water emanating from the borehole below 460 m depth. At the bottom of V1 the temperature is 19.1 degreesC and at the corresponding level in V2 the temperature is 19.6 degreesC.

2.9 Structure

In Figure 2-3, the major structures in the Stripa area are visualized. The location of the section (Figure 2-2 above) is also included together with existing boreholes made from the ground surface. As regards the lineaments in the granite, it is seen that their direction generally is parallel to the syncline axis of the supracrustal formation.

The greater morphological lineaments diverges in direction from the syncline geometry, but may, however, also be governed by the configuration of the supracrustal rocks. Two dominant directions occur for the lineaments, i.e. ENE-WSW and NW-SE.

Based on both surface boreholes (SBH1 and SBH2) and subsurface holes (V1 and V2), the variation in fracture frequency versus depth was studied. The variation with depth is shown in Figure 2-8. It must be noted that since V1 and V2 both are vertical, me-

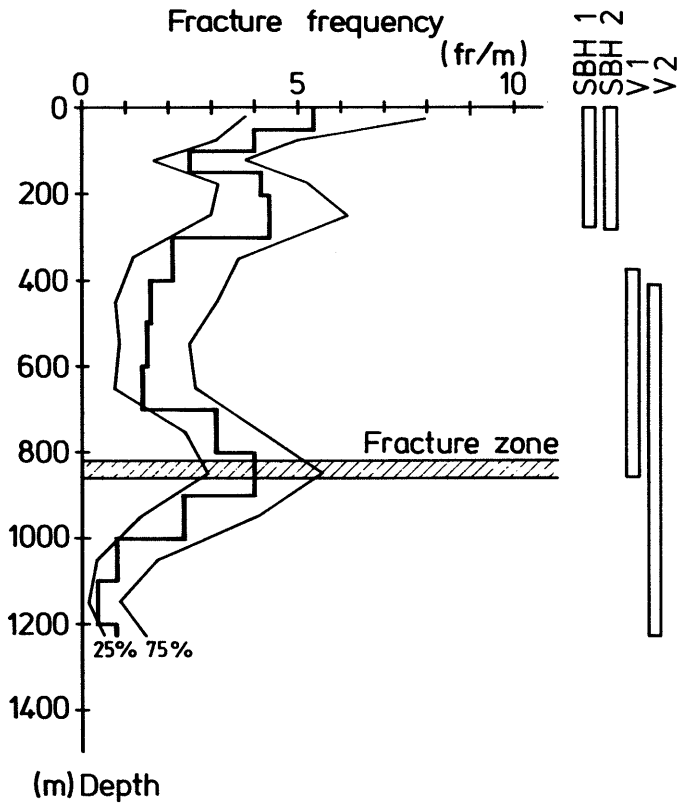

Figure 2-8. Fracture frequency versus depth based on core-logs from SBH1, SBH2, V1 and V2. The frequency is assumed to be log-normally distributed.

dium-steep and steep fractures will be underestimated. The fracture frequencies obtained in N1 and E1 are also included in the figure. These boreholes are more accurate measures of the steeply dipping fractures at the 360 m level.

A number of zones of fractured or crushed rock also exists in the granite. Normally these zones are thin, not exceeding 1 m in the cores, but a few zones are of several meters in thickness. A more extensive zone was found in the lowermost part of V1. Tectonically less disturbed granite in the upper part of the borehole extends down to the 466 m depth and contains more widely spaced fracture zones and crushed zones usually less than 1 m in width. Fracturing tends to be more intense towards the bottom of this section, with a prominent increase in number of subvertical fractures.

A detailed compilation of fracturing is impractical for the strongly crushed part of the borehole (466 m down to the bottom of the borehole at 505 m). Totally 7.7 m of this section is disconnected or crushed to rubbles. The number of the fractures in the crushed zone is partly based on an estimation (38 per cent from totally 510 fractures within this 40 m wide zone) and their dipping were not possible to establish. The fracture frequency

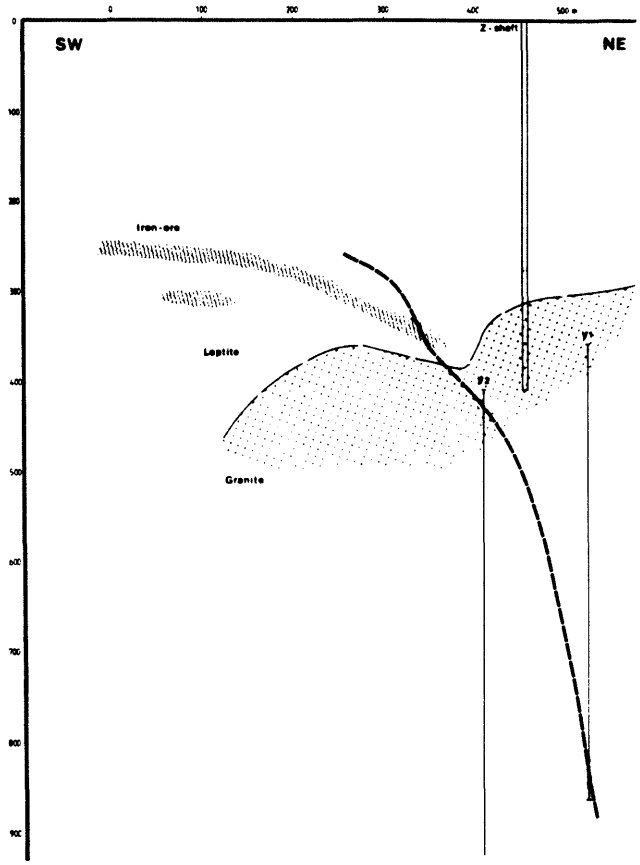

Figure 2-9. Vertical section through the investigation area.

was 12.9 fr/m in the zone to be compared to 1.5 fr/m for the rock mass above the zone.

The fracture zone in V1 has a high water inflow. The hydraulic conductivity is high in comparison to the rock mass and the zone is assumed to be of crucial importance for the groundwater system in the granite. However, the extension and orientation of the zone could be interpreted according to different possibilities.

One of the possible interpretations of this zone is indicated in Figure 2-2. However, the zone was not found in V2 when this borehole was deepened down to a final depth of 820 m (1 230 m below ground surface). A cross-hole electrical measurement was made between V1 and V2 and the result indicated that the major zone found in V1 was connected through three (possible four) minor zones intersected by V2. None of these zones showed, however, a fracturing in accordance with that found in V1.

Figure 2-9 shows a profile through the rock mass with the boreholes V1 and V2 in relation to the ore body. In this section a fracture zone found during the ore mapping is included. Its orientation is well defined in and around the ore body while its extension through V1 and V2 is hypothetical. The assumed exten-

Table 2-11. Fracture frequency in V1, V2, N1 and E1.

Borehole	Fracture frequency
V1 (above the crushed zone)	1.5
V1 (crushed zone)	12.9
V2	2.1
N1	1.6
E1	4.7

sion is, however, indicated by the intense fracturing in the lowermost part of V1, but also of a somewhat more intense fracturing in the uppermost part of V2.

This gives three probable explanations of the geometry of the fracture zone found in V1, none of which is more reliable than the others.

1 A zone striking N70E and dipping 60SE as indicated in Figure 2-2.

2 A zone striking NW-SE steeply dipping to NE as indicated in Figure 2-9.

3 The major zone is connected to V2 by a number of minor zones as indicated by geophysical measurements.

The actual interpretation may also be a combination between any of the mentioned possibilities.

The mean fracture frequencies for the boreholes included in the hydrogeological program are given in Table 2-11.

Figure 2-10 shows a cumulative fracture diagram for V2 with regard to the dipping of the fractures. It is seen that medium steep fractures dominate while steeply dipping fractures have a low fracture frequency. Flat-lying fractures are in an intermediate position. This is in full agreement with the result obtained in V1 (Carlsson, et al., 1981). It must be stressed that the vertical borehole V2 tends to underestimate vertical or steeply dipping fractures while sub-horizontal or flat-lying fractures are recorded with their actual frequency. With this in mind, it is clearly seen from Figure 2-10 that the steeply dipping fractures dominate and the relative frequency of these fractures increases with depth with a simultaneous decrease in flat-lying fractures. This is even more pronounced than illustrated in the

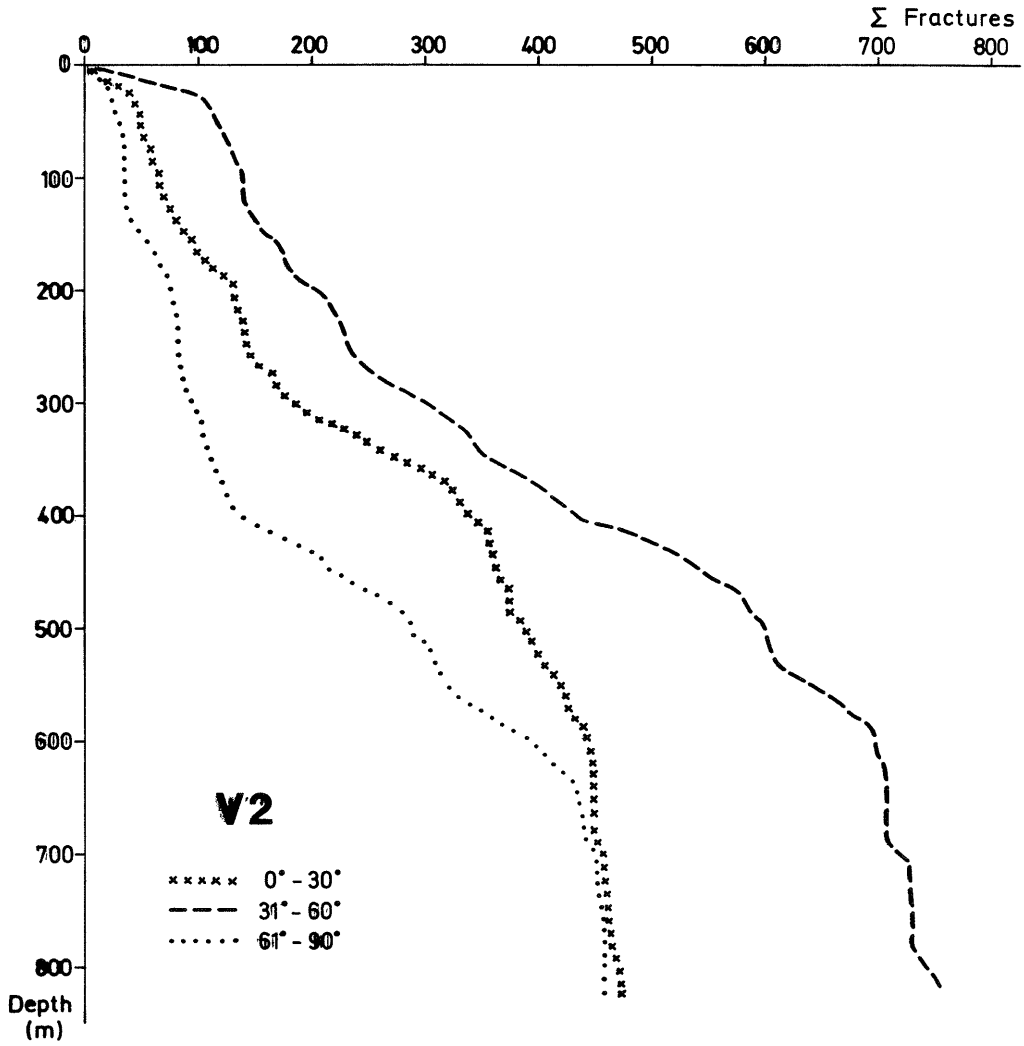

Figure 2-10. Cumulative fracture diagram for V2 with regard to dipping of the recorded fractures.

figure owing to the variation in estimation depending on the dipping. The flat-lying fractures show a low frequency below approximately 400 m depth with 0.3 fr/m which decreases down to 0.1 fr/m in the lowermost 230 m. This condition indicates that medium steep or steep fractures dominate the fracture system at depth and the horizontal fracturing become more sparse.

The fracture pattern which predominates in the rock mass at the SGU-site may be established by the fracture orientation data from the boreholes. The information from the boreholes N1 and E1 gives a rock mass dominated by steeply dipping fractures in N30E. Other fracture sets of importance are N30W and N10E, both steeply dipping. However, both of these boreholes are nearly horizontal, which indicates that flat-lying fractures will not be penetrated by the boreholes and consequently they will be underestimated. The vertical boreholes may serve as a tool to evaluate the existence of flat-lying fractures.

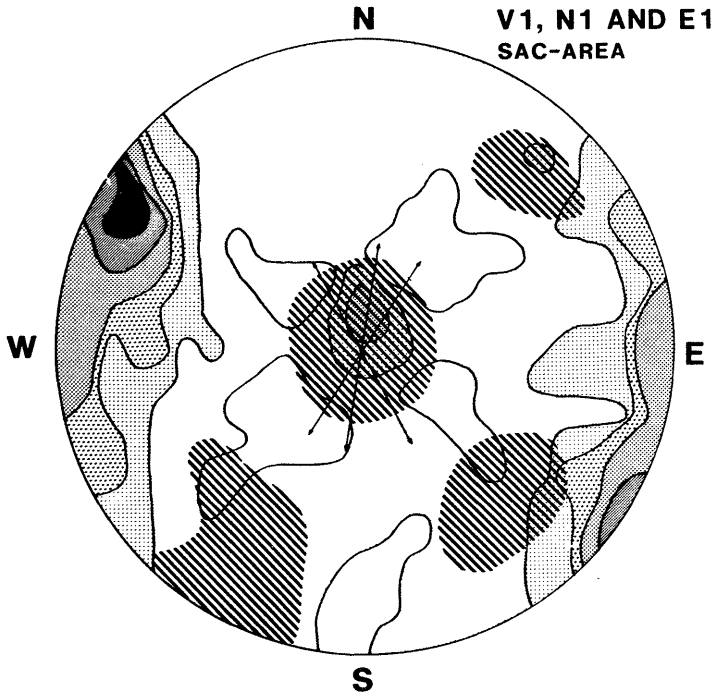

Figure 2-11. Fracture sets obtained at the SGU-site and from the SAC-area (lined parts of the diagram). Semispherical projection, Schmidt net - lower hemisphere.

Steep fractures dominate clearly the fracture pattern and make up as much as 40 percent of all fractures in the rock mass adjacent to the SGU-site. Medium steep fractures makes up 31 percent and the remaining 20 percent are attributed to flat lying fractures. Thus it is possible to distinguish the following sets of fractures at the SGU-site.

1 N10E;80E
2 N30E;85E
3 N30W;90
4 Sub-horizontal;25

These sets are shown in the semispherical projection in Figure 2-11.

The obtained orientations from the SGU-area could be compared with the orientations found in the huge stock of fracture data which exists from the SAC-area (Wollenberg, et al., 1980, Olkiewicz, et al., 1979). In that area the following fracture sets were found:

1 NNW-SSE;60N
2 NW - SE;85NE
3 N65W;50SW
4 Horizontal

These sets are also included in Figure 2-11. As seen in the figure there is a difference between the fracturing at the SGU-site and at the SAC-area, but some resemblance may be found. The difference may be an effect of the sedimentary structures which could have effected the fracturing of the granite. This is also indicated in Figure 2-3. There seems to be a change in orientation of the fracture system which probably is governed by the configuration of the leptite syncline. Closer to the contact between granite and leptite the fracturing is affected by the syncline, while at farther distances it seems to be more independent with increased upright and orthogonal fracturing of the granite.

3 HYDROLOGY

3.1 Hydraulic units

The hydraulic properties of a crystalline rock mass such as the Stripa granite is characterized by fractures, faults and other discontinuities which transect the rock. The granitic rock matrix is, from a practical point of view, almost impervious and the main flow paths are constituted by the fracture system, zones of fractured or crushed rock and other structural discontinuities. As shown in previous sections, there exists a number of discontinuities, some of which are associated with the synclinal structure of the sedimentary sequence and others more independent of it. However, as the dominant tectonization took place before or immediately at the intrusion of the pluton, the granite is intersected only by a few larger fracture zones.

The dominant ruptural deformation is concentrated in the superficial part of the rock, which shows a rather high fracture frequency and a high hydraulic conductivity. This more fractured part of the rock mass extends down to about 250 m depth. Below this level the rock becomes more sparsely fractured, with fractures which are sealed to a great extent. The fracturing continues to decrease and reaches its lowest frequency below the 1 100 m level (c.f. Figure 2-8).

In the deep-seated rock mass the water flow seems to be channelled in a few zones of fractured rock, where the zone found in the lowermost part of V1 is an extreme example of these flow paths. At these deep levels it is probable that the discrete fracture flow is of minor importance.

The mine itself is one of the most important structures governing the water flow in the area. It acts as a drain, with a drainage threshold which was successively lowered as the mining continued. During the SAC-program, efforts were put into the establishment of the draining effect of the mine. As reported by Gale (1982) piezometric recordings taken at different levels in SBH-1, SBH-2, SBH-3 and DbhV1 show that there is a downward gradient above the excavations. Around the test areas, the groundwater gradients are directed towards the excavations.

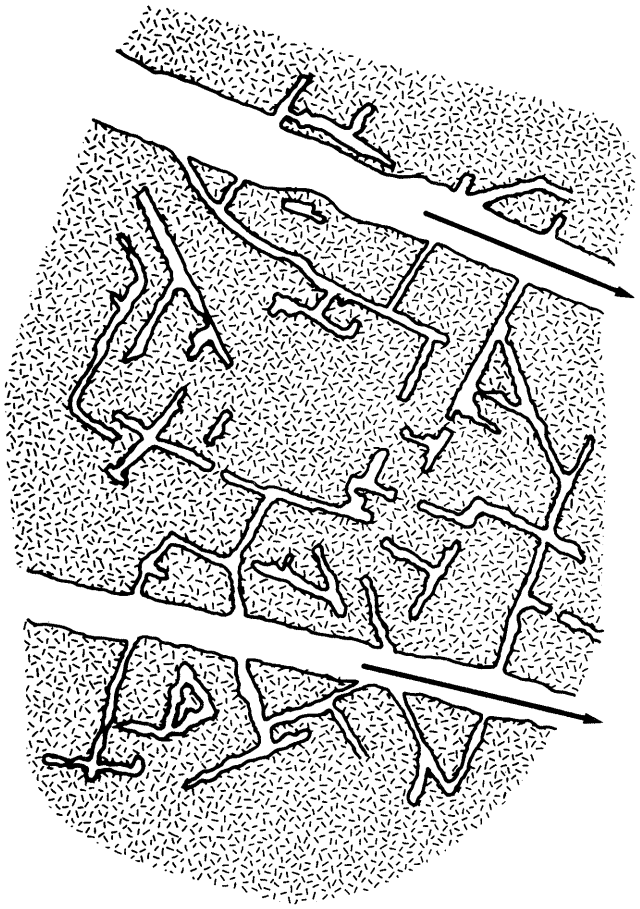

Figure 3-1. Schematic representation of the geometric relationship between the different porosities in a rock mass. The arrows denote an arbitrarily chosen direction of water flow within fractures forming the kinematic porosity. The smaller fractures and pores represent the diffusion and the residual porosity (Norton and Knapp, 1977).

3.2 Porosity of the intact rock material

According to Norton and Knapp (1977) the total porosity in a fractured medium, Θ_T, may be expressed as

$$\Theta_T = \Theta_K + \Theta_D + \Theta_R,$$

where Θ_K = effective flow porosity or kinematic porosity (1),
Θ_D = diffusion porosity (1),
Θ_R = residual porosity (1).

The kinematic porosity represents the fractures through which the dominant fluid flow proceeds, while the diffusion and residual porosities refer to fractures or pores in which no or very limited flow occurs. The fractures making up the residual porosity

are not connected with those included in either the kinematic or the diffusion porosity. Figure 3-1 illustrates the geometric relationship between the different porosities.

In a fractured rock mass the interconnected fractures comprise the kinematic porosity which in a two-dimensional section of unit area can be defined as

$$\Theta_K = e_1 + e_2 + \ldots\ldots + e_n.$$

With equal fracture apertures and spacing, equation (11) becomes

$$\Theta_K = ne,$$

and with three sets of water-bearing joints with equal properties the kinematic porosity will be

$$\Theta_K = 3ne.$$

Calculations of the porosity based on measurements in drill-holes will result in different porosity values depending on the penetration of the drill-hole in different sets. Moreover, the existing joint sets in fact have different fracture properties, a point discussed by Parson (1972) and A. Carlsson (1979).

Snow (1968) reports a study of fracture spacing, fracture apertures and kinematic porosity, and presents a method of determining the kinematic porosity from water-pressure tests. With equal penetration in three equal joint sets, the following relation was obtained

$$\Theta_K = 2.4\ ne.$$

This equation, together with those above, demonstrates a relationship between the kinematic porosity, fracture spacing and fracture apertures.

The rock matrix has a very low hydraulic conductivity where the microfractures constitute the majority of flow paths. The conductivity is estimated to be in the range 10^{-13} - 10^{-16} m/s, depending on the degree of microfracturing. Although the conductivity is low, the storativity is fairly high, the total porosity according to laboratory tests are in average 0.47%. The determinations are summarized in Table 3-1. The porosity measurements are made on 12 samples from N1 and 6 samples from V1. The results are very consistent, with a minimum value of 0.36% and a maximum of 0.61%.

Most of the pores and fractures included in the total porosity are not actively contributing to the flow porosity. The flow porosity is estimated to be in order 10^{-5} - 10^{-4} which is only 2-20 permille of the total porosity.

Table 3-1. Porosity obtained by laboratory tests on drill cores from the boreholes.

Borehole	Number of samples	Mean porosity	Std deviation
E1			
N1	10	$4.6 \cdot 10^{-3}$	$\pm 0.8 \cdot 10^{-3}$
V1	8	$4.7 \cdot 10^{-3}$	$\pm 0.5 \cdot 10^{-3}$
V2			

However, in the heavily fractured part of V1, the flow porosity is higher and estimated from the hydraulic tests to be in the range $1\text{-}5 \cdot 10^{-4}$.

3.3 Hydraulic conductivity of the rock mass

3.3.1 General

A naturally fractured formation is in general represented by a tight matrix broken up by fractures of secondary origin. The fractures vary considerably in size from voids and interconnected channels to fine cracks. Some of the fractures are assumed to be continuously throughout the formation and to represent the paths of principal hydraulic conductivity. The rock matrix consisting of the fine disinterconnected cracks has a lower hydraulic conductivity but generally a higher primary porosity.

The transient behaviour of groundwater pressure versus time depends on the hydraulic conditions around the tested section. In general the flow situation may be described as linear, radial or spherical. A radial flow is usually prevailing when the conditions around the tested section are not hydraulically favoured by a fracture along the section. Instead the flow is radially out from or in to the section in one or more fractures perpendicular or inclined to the borehole. In the radial flow case, no flow is assumed along the direction of the borehole. Thus two imaginary no flow boundaries are assumed at the ends of the test section and perpendicular to the section.

In the radial flow case in natural fractured formations, the matrix has a "delayed" response to pressure changes that occur in the surrounding fractures. Such nonconcurrent responses cause

pressure depletion or inpletion of the fracture relative to the matrix which in turn induces matrix-to-fracture crossflow. The response of the fracture fluid to pressure changes is almost instantaneous, whereas that in the rock matrix is much slower. The period of transient crossflow takes place immediately after the fracture pressure response and before the matrix and the fracture pressures equilibrate, after which the formation acts as a uniform medium with composite properties (Streltsova-Adams 1978; Streltsova and McKinley 1984).

The spherical flow case may occur after a longer time when the influence has reached longer distances from the test section. The shorter the test section, the better are the conditions for spherical flow.

Linear flow is a one dimensional flow which exists whenever there is a fracture of high hydraulic conductivity along the test section. In the case of a fracture parallel to by not intersected by the test section, the linear flow behaviour might occur during certain conditions regarding distance and contrast in hydraulic conductivity between fracture and rock matrix.

3.3.2 Testing techniques

The groundwater system at the Stripa Mine has successively been affected by the mining activities. As the mine was sunk, new flow paths were activated and the drainage threshold was successively lowered. The groundwater system was almost continously in balance with the drainage from the underground drifts, i.e. the groundwater system was in a steady state condition. In 1976 the mining was terminated, but the drainage pumping continued. After the mining, only minor additional impacts affected the system. This gave a hydraulic situation which was well suited for hydrogeological studies underground, any controlled disturbance should take place in an affected but steady groundwater system.

A number of techniques may be applied to the underground hydraulic testing. However, requirements and demands from other activities and research programs make some of the probable techniques less suitable. In order to obtain accurate water sampling and analytical results, the groundwater system should be contaminated as little as possible with external water and other chemical compounds. This condition calls for a testing technique where the groundwater should be extracted rather than injected. Other test programs within the project, as for instance, the Buffer Mass Test, is strongly dependent on a undisturbed supply of groundwater and pressure build-up, which calls for a minor extraction and disturbance on the water head around the mine.

However, as the hydraulic testing takes place deep underground, in the potential sink made up by the mine, it was found conveni-

ent to utilize the existing potential field for the testing, i.e. to use the natural drainage for water extraction as the main tool and to measure the pressure build-up after shut in and the fall-off after release. By this technique, no foreign water is introduced into the groundwater system, and the disturbances on the head should be in a natural sense. This technique was used as the main tool both in single hole tests and in interference tests between different boreholes. However, as a test effort, water injection tests were carried out in order to compare the results from different techniques.

Thus, the following techniques are used for the hydraulic testing included in the program:

Single hole tests

- Build-up tests
- Fall-off tests
- Single packer fall-off tests
- Double packer injection tests

Multiple hole tests

- Build-up tests with selected transmitter and receiver holes
- Fall-off tests with selected transmitter and receiver holes

The procedure for build-up and fall-off tests are normally single hole tests where the pressure change in a sealed off section is monitored. The tests are carried out only for selected sections of the boreholes (Carlsson and Olsson, 1985a).

The packer system is lowered into the borehole to the actual depth. When the system is in the correct position, the packers are inflated with nitrogen gas. The flow from the innermost test section, between the inner packer and the bottom of the hole, is thus packed off and the pressure in the section begins to increase. The main test section, between the packers, continues in free flowing conditions and the flow rate is recorded. After a few hours, the downhole valve is closed and the actual build-up test section continues for about five days after which the valve is reopened. During this stage, the pressure build-up in the main test section as well as in the inner section is monitored.

The test cycle ends with deflation of the packers and thus, a pressure relief in the inner section. By this procedure, a completed test at one level requires one week including installation, free flowing and pressure build-up and fall-off. The technique has been used for 10 test sections in borehole N1, 13 in E1 and 8 in V2.

As a complement to the build-up tests, water injection tests were carried out in boreholes V1, N1 and E1. These tests were made as hydraulic loggings of the entire boreholes in 10-meter sections (Carlsson and Olsson, 1985b).

The tests were initiated with a short build-up period after which the water injection was started and continued for 2 hours. A 2 hour or longer period of fall-off monitoring completed the test cycle. In order to identify the pressure trancience on which the injection was superposed, the information from the initial stage and the fall-off period was analysed with respect to the pressure build-up.

The total testing time for a ten meter section thus become 5-6 hours including installation and testing.

Three different interference tests were also conducted during the program, i.e.:

- Interference test between V1 and V2
- Interference test between V1, V2, N1 and E1
- Interference test between N1 and the BMT-area

In each of these tests, a specific test section in one of the boreholes was used as a source hole where the pressure disturbance was to be introduced. The other boreholes acted as receiver holes where the resulting pressure change was recorded.

3.3.3 Results

A great number of hydraulic tests have produced values on the hydraulic conductivity of the Stripa granite. Tests exist from the surface boreholes as well as from subsurface holes in different test sites, from the large scale ventilation test and from the large scale injection test. This huge stock of values provides a good base for determinations of the water flow in the granitic rock mass around the mine. Table 3-2 summarizes the range in results from the SAC-program.

Thus, it is seen that in the surface boreholes the conductivity is at its maximum, about 5 E-8 m/s, while it is 1 E-9 m/s or lower in the tests made down in the mine. The large scale tests, ventilation and injection tests, which both are measures of the gross conductivity gave low values. 1 E-11 and 4 E-11 respectively. Those latter values are probably representative for the rock mass including minor zones of fractured rock.

The hydraulic tests carried out in the current program, were all made as pressure build-up tests, where the natural water flow into the boreholes was used for the build-up. The tests were analysed according to conventional interpretation techniques. An example of a test is shown in Figure 3-2.

Table 3-2. Hydraulic conductivity values of the Stripa granite obtained during the SAC- and the current program.

Test type	Conductivity range m/s
Injection surface holes	5 E-11 - 5 E-8
Injection ventilation drift	1 E-12 - 1 E-9
Ventilation test	1 E-11
Large scale injection	4 E-11
V1, fracture zone	7 E-8
V1, rock mass	5 E-11
V2, rock mass	1 E-10
E1	5 E-12 - 4 E-8

Two zones have been found with relatively high conductivity, one 40 m wide zone in V1 (40 m along the borehole) with a conductivity of 7 E-8 m/s and one 2 m wide zone in E1 with 4 E-8 m/s. Beside these zones, the obtained conductivity is lower than E-9 m/s.

3.4 Hydraulic head

The hydraulic head in the rock is determined by geological, hydrometeorological and topographical factors. In the current situation it is also, to a very high degree, dependent on the geometrical configuration of the mine.

The hydrometeorological conditions in the Stripa area and on an annual basis can be described by a mean precipitation of 780 mm, an annual evapotranspiration of 480 mm and a run-off of 300 mm (9 1/s sq.km). The climatic conditions are humid and in the run-off term both the recharge and the discharge of groundwater are included.

The geological factor, which determines the hydraulic conductivity and thus the rate of the groundwater flow in the bedrock, points to a rather low conductivity and consequently a low groundwater flow even at high hydraulic gradients. In the upper part of the bedrock the groundwater level in general follows the topography.

The hydraulic head was measured in boreholes both from the mine and from the surface. Measurements of the head are normally made in short sections (2-10 m) in boreholes tightly sealed off by packers. When starting such measurements the head is usually in

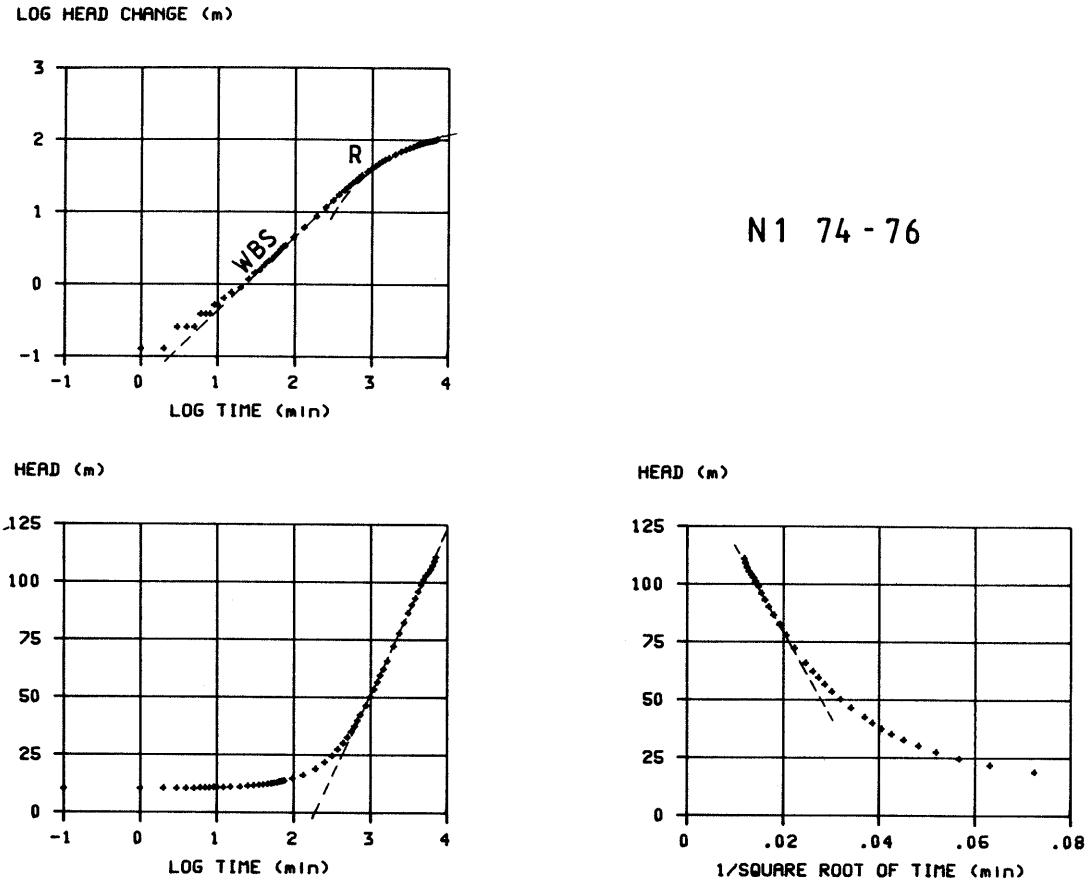

Figure 3-2. Graphs of test section 74-76 m in borehole N1. It is seen that the test is dominated by well bore storage (WBS) in the initial stage. After this period the flow becomes radial as shown by the log-time versus head plot. At the end the flow enters a spherical regime as seen in the third diagram.

a transient state and the monitoring has to be carried out under a longer period. As regards the procedure, it is described in Gale (1982) and in Carlsson and Olsson (1985).

Registrations of hydraulic head in boreholes have been carried out earlier by Olkiewicz, et al, (1979), Witherspoon, et al, (1980) and Gale (1982).

3.5 Model calculations

Preliminary and rough calculations were made of the groundwater conditions and the groundwater inflow to the mine. The calculations were based on available data on hydraulic conductivity and topographical conditions. The calculations were performed for a vertical plane laid out from the center of Lake Rosvalen, through the mine and further on about 4 km towards NNW. In total

the section was 7 km in length and 2.6 km in depth. The mine was illustrated as two horizontal drifts, each 1 000 m in length, at the levels 410 m and 290 m, respectively, in the mine system. The height of the drifts was taken as 70 m.

The calculations were carried out using a finite-element program and assuming two-dimensional flow at steady state. The lower and vertical boundaries of the studied plane were set as no flow boundaries. The groundwater head at the upper boundary was given as the ground-surface. At the mine the head was set as the datum level.

As results of the calculations the head distribution around the mine was given together with the inflow to the mine. The calculations were performed in a vertical plane and the total inflow to the mine was estimated by assuming the same inflow per m of mine along the whole mine.

The hydraulic conductivity of the rock mass was given different values to illustrate different possible conditions in the rock. The conductivity distribution versus depth is given in Figure 3-3. The results of the calculation given as distance of influence on the head and the water inflow are summarized in Table 3-3.

The actual inflow to the mine for the period Jan. 1983 - Sept. 1984 was recorded to be about 470 l/min on the average.

The result from the calculations based on decreasing conductivity values versus depth (Case B) is more reliable as it is based on actual test results from the area. The groundwater head for this distribution is given in Figure 3-4, where the impact of the mine is clearly visualized.

It should be noted that the calculated inflow value doesn't take the flow in fractured zones into account. These zones, as the one in V1, are probably the cause for the major part of the actual inflow to the mine.

The interference tests made in the mine show that the flow in fractured zones may originate from great distances. The results show that there is a clear interconnection between boreholes V1 and V2 and between N1 and the BMT-area. On the other hand, it is also clear that no interconnection was obtained between V2 and N1 or between E1 and N1. A slight influence was noted between the fractured zone in V1 and the innermost part of N1.

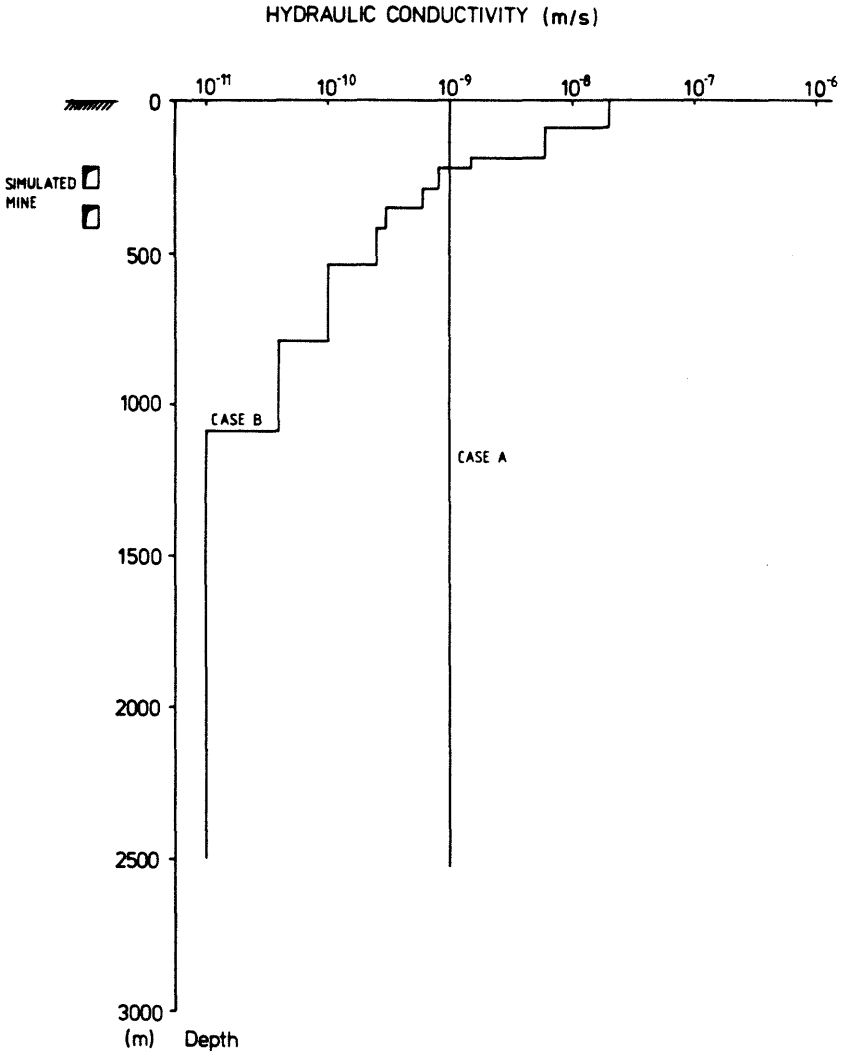

Figure 3-3. Hydraulic conductivity versus depth used in the model calculations.

Table 3-3. Results of numerical calculations of the distance of influence and the groundwater inflow to the Stripa mine.

Assumptions made regarding the K-value of the rock mass	Horizontal distance for 50 m influence at the mine level of 400 m, in km	Groundwater to the mine in l/min
Case A Hom. condition with K=1.E-9 m/s	0.8	73
Case B Hom. condition with decreasing K-value from 2.E-8 down to 3.E-11 m/s	0.45	96

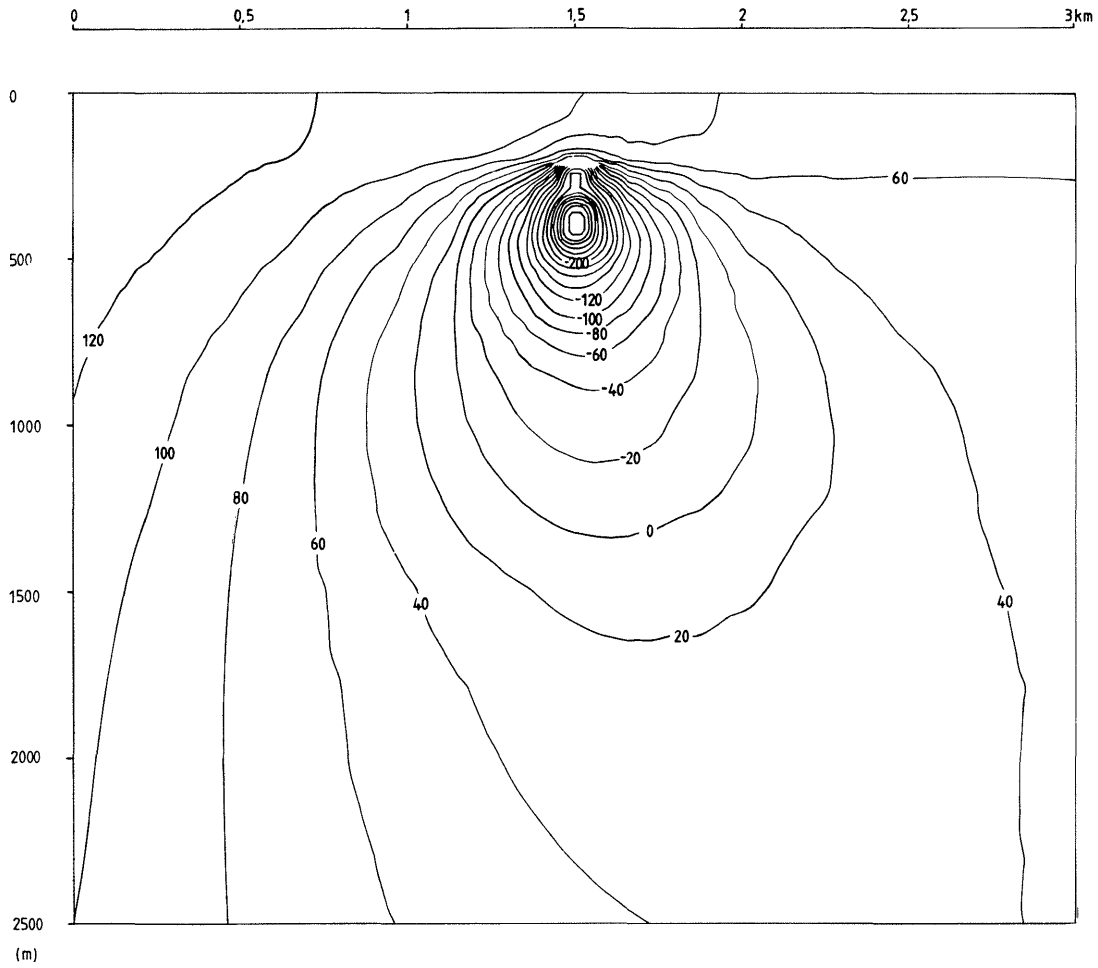

Figure 3-4. Groundwater head around the mine calculated by numerical method, case B.

3.6 Dewatering of the granite

The pressure sink made up by the mine has significantly affected the groundwater conditions in the granite. Over the years a continous water inflow has taken place and as the mine was sunk the drainage threshold was lowered. After the mining activities were terminated in 1976, the drainage pumping continued and the groundwater recharge from the surface and from adjacent areas balanced the groundwater discharge in the mine. After the mining, only minor impacts on the groundwater system was introduced, and then mainly from different boreholes which also acted as drainage structures in the rock mass.

The total effect from the drainage on the groundwater system is a shorter residence time for the groundwater. The recharge from the surface is more quickly flowing down to deeper levels in the rock mass, i.e. those levels which are of interest for water sampling and analysis. Also the groundwater flow from adjacent areas

is faster which leads to a more complex mixing of different groundwaters. These conditions are of great significance for the interpretation of the hydrogeochemical data; a foreign groundwater may be sampled in the granite.

The total discharge from the mine amounted to about 470 l/min as an average value for the period January 1983 to December 1984. This discharge gives a total discharged volume of water from the mine since the start of the SAC program to the end of 1984 of almost 2 million cu. m. Thus, a most significant discharge of groundwater. Also, the boreholes made for the present program gives a most significant discharge, especially for the borehole V2, which was drilled as early as 1978 and presently deepened to its present depth. This borehole has been free-flowing for most of the time, and it is only in connection to various tests that this borehole has been packed off. Borehole V1 contributes greatly to the total discharge due to its high yield. As regards borehole N1 it has been packed off during most of the time as a consequence of its influence on the buffer mass test. In Table 3-4, the total estimated discharge from the main boreholes are summarized. The values given represent the total discharge since the drilling of the boreholes till the end of 1984. The figures are based on the recorded discharge in relation to the borehole history, and are therefore only rough estimates. In total, the errors on the given figures are in the range of 10 per cent.

Table 3-4. Total discharge in the boreholes since the drilling of the holes till the end of 1984.

Borehole	Total discharge cu. m
N1	567
E1	432
V1	11.312
V2	2.756

4 GROUNDWATER CHEMISTRY

4.1 Introduction

Numerous chemical analyses of Stripa groundwaters have been obtained since 1977. Both major and trace constituents have been determined and presented in three separate reports (Fritz, et al., 1979, 1980; Nordstrom, 1983a) along with preliminary interpretations. Additional discussions of the groundwater chemistry have been reported by Nordstrom (1982, 1983b) and Fritz, et al. (1983). The initial findings can be summarized as follows:

1. Some of the deeper groundwaters (>700 m) have unusually elevated salinity, up to 700 mg Cl/L.

2. The more saline water at depth has a markedly different water chemistry than the shallow groundwaters; i.e., it is an Na-Ca-Cl- SO_4 type water.

3. The pH increases to the range of 9-10 with depth.

4. Dissolved inorganic carbon becomes very low with increasing salinity, reaching 9 mg HCO_3/L.

These findings, along with the isotopic data, have led to much discussion and controversy regarding the origin and evolution of the Stripa groundwaters. This chapter presents the chemical data and selected element ratios for comparison with known types of saline fluids such as seawater.

4.2 Methods of sample collection and preservation

Beginning in June, 1981, groundwater samples have been collected from packed-off zones by pumping water from tubing connected to the packer sample tube at the borehole. A peristaltic pump transported the groundwater to a flow cell arrangement closed to the atmosphere where on-site measurements of pH, EMF (electromotive force), temperature, and specific conductance are obtained. Measurements of pH were made with a glass electrode calibrated at sample temperature with pH 7 and 9 buffers. As an accuracy check, a pH 10 buffer was occasionally measured after the sample; and if the deviation was greater than about 0.05 pH units, then the electrode was recalibrated and the sample remeasured. A platinum electrode with a calomel reference was used for EMF measurements and corrections made for the reference potential from

the data of Ives and Janz (1961), to derive the Eh value. ZoBell's solution provides a check on the EMF measurements (Nordstrom, 1977).

All samples were filtered by pumping the water from the same closed line system with the peristaltic pump directly to a precleaned plastic plate filter fitted with an 0.1 micrometer Millipore membrane. The membrane was preleached with at least 1 liter of groundwater before collecting samples for analysis. One sample set (81WA202, N1) was unfiltered due to a broken membrane, and when this problem was noticed a second filtered sample was collected. The unfiltered sample was saved for a comparison of the effect of filtration. Sample preservation techniques varied according to the particular constituents being analyzed. Samples for determination of major cations and trace elements were collected in teflon or polyethylene bottles and acidified with ultrapure nitric acid to a pH <1.5.

Samples collected for Fe (II, III) and As (III, V) were acidified with ultrapure hydrochloric acid to a pH <1.5. Mercury was preserved with the addition of potassium permanganate solution (Avotins and Jenne, 1975), and zinc acetate was added for the preservation of sulfide.

A duplicate set of water samples was collected at each site, during the June field trip, for an interlaboratory comparison of analyses. One set was analyzed by the U.S.G.S. and the other set by S.G.U.. Each set consisted of a 250-ml teflon bottle for cations and trace metals, a 250-ml polyethylene bottle for nitrate, nitrite, phosphate and ammonia, a 250-ml polyethylene bottle for iron (II, III) and arsenic (III, V), a 1-liter glass bottle for mercury, a 50-ml glass bottle for bromide and iodide, a 250-ml polyethylene bottle for anions, a 50-ml glass bottle for dissolved organic carbon (D.O.C.), and a 2-liter or 1-gallon polyethylene bottle for sulfide.

4.3 Methods of analysis

Most metals were analyzed by plasma emission spectrophotometry using both DCP (direct-current plasma) and ICP (inductively-coupled plasma) sources. Selected samples were also analyzed for Na, K, and Li by AAS (atomic absorption spectrophotometry) for a check on accuracy. Rb and Cs were analyzed by flame emission spectroscopy, Hg was analyzed by flameless atomic absorption spectrophotometry, and iron was done by the ferrozine colorimetric method (Gibbs, 1976) in addition to ICP. Anions were done by IC (ion chromatography) except for nitrogen and phosphorus species which were analyzed by colorimetry on an autoanalyzer. Selected samples were additionally analyzed for fluoride by ISE (ion-selective electrode), and H_2S was analyzed by ISE only.

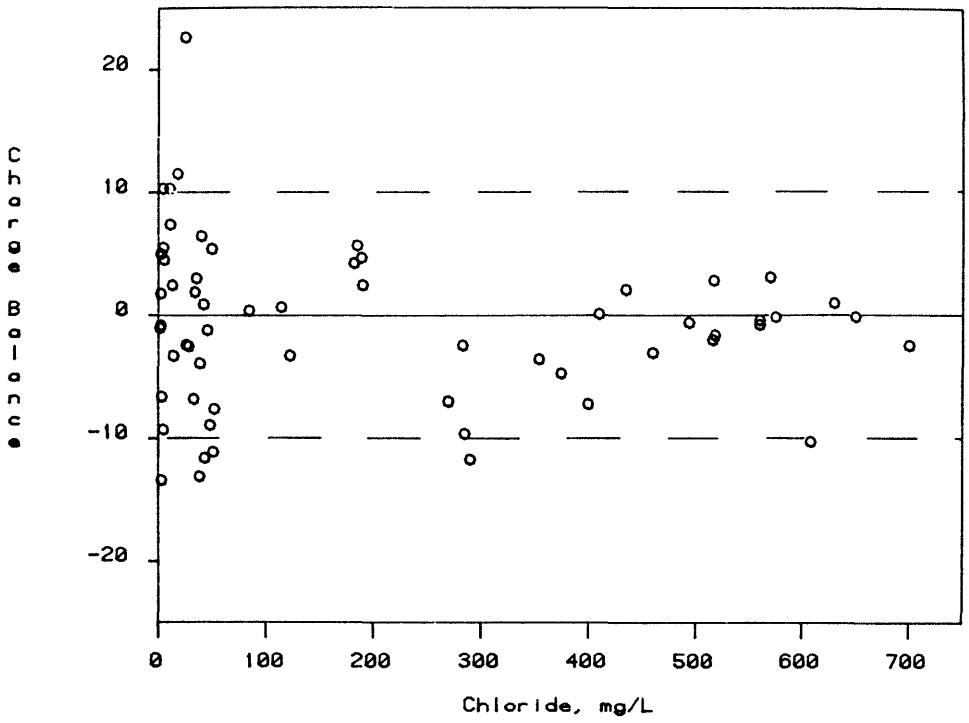

Figure 4-1. Charge balance errors as a function of Cl concentration.

4.4 Accuracy and precision

Precision was occasionally checked by determining the reproducibility on selected samples, and was usually found to be less than 5%. Accuracy was determined by (1) interlaboratory comparison, (2) analysis by an alternate method, and (3) charge balance errors.

The interlaboratory comparison is described in detail in Nordstrom (1983a). The results showed that discrepancies were usually within 5% after cross-checking and revising the initial values. Charge balances were also exceptionally good (<4%) for this one group of samples. Charge balance error was calculated from the following equation:

$$200\ \left(\frac{\text{meq./L, cations} - \text{meq./L, anions}}{\text{meq./L, cations} + \text{meq./L, anions}}\right)$$

For all of the analyses given in Table 4-1, the charge balance was calculated and plotted as a function of chloride concentration as shown in Figure 4-1.

Nearly all the values fall in the range from +10% to -10% with a slight decrease in the dispersion at higher chloride concentrations. These results suggest the determinations for major constituents are accurate. Most analytical determinations, other than those in the interlab comparison, can be considered accurate to

about 10%. Greater errors are occasionally found in the anion data, especially Cl and SO_4. The reasons for these discrepancies are not known.

Table 4-1. Stripa water analyses (in mg/L except where otherwise noted).

Drillhole/Site	Stream	Stream	SW1	T.P.	T.P.	PW1
Sample Code No.	10	11	81WA217	9	----	18-1
Sampling Interval (m)	----	----	----	----	----	----
Date Collected	770912	770912	811008	771209	831003	770927
Temperature (°C)	12.9	9.3	10.1	13.2	10.0	9.5
pH	6.5	6.73	6.96	7.57	7.42	7.85
Cond (uS/cm)	25	31	31.5	152	130	263
Eh(mV)	----	----	468	----	474	----
Total Alkalinity (mg/L, HCO_3)	6.1	8.6	9	48.8	74	206.2
Charge Balance (%)	-13.4	-6.6	1.77	7.39	0.9	-5.06
Species						
Ca	3.5	4.5	3.5	26	20	37
Mg	0.5	1.0	1.2	5.5	4.3	12
Na	1.7	1.8	2.0	6.9	5.3	24
K	0.4	0.6	0.83	1.9	1.8	1.1
SO_4	7.5	9.0	6.1	15	8.1	13
F	----	----	0.51	----	0.79	----
Cl	2.9	3.3	2.3	11	8.3	16
Br	----	----	0.014	----	----	----
I	----	----	0.003	----	<.005	----
PO_4	<0.01	<0.01	0.05	<0.01	<.02	0.20
SiO_2	3.8	4.4	5.35	6.2	5	8.6
B	----	----	<0.005	----	<.005	----
NO_2	----	----	<0.005	----	<.005	----
NO_3	0.41	0.48	1.3	1.66	<.1	----
NH_4	----	----	0.03	----	.04	----
Al	----	----	0.055	----	<.01	----
Fe (total)	0.23	0.39	.183	0.43	.12	<0.01
Fe^{2+}	----	----	0.174	----	----	----
Mn	----	----	0.015	----	.03	----
Cu	----	----	<0.005	----	<.001	----
Zn	----	----	0.018	----	.002	----
Pb	----	----	----	----	<.01	----
Co	----	----	<0.005	----	.011	----
Ni	----	----	----	----	<.001	----
Cr	----	----	----	----	<.005	----
V	----	----	----	----	<.01	----
Mo	----	----	<0.005	----	<.01	----
Li	----	----	<.005	----	.006	----
Sr	----	----	0.011	----	.065	----
Cs	----	----	----	----	----	----
Rb	----	----	0.005	----	.019	----
Be	----	----	----	----	<.003	----
Ba	----	----	0.011	----	.042	----
DOC *	4.9	4.9	----	5.0	----	0.8

* Dissolved Organic Carbon

Table 4-1. Stripa water analyses (in mg/L except where otherwise noted).

Drillhole/Site	PW5	PW5	PW5	PW2	PW3	PW3
Sample Code No.	21-3	21-10	21-11/25	23-10/20	20-3	20-4
Date Collected	771006	771007	771010-12	771024-26	771026	771026
Temperature (°C)	7.7	7.7	7.6	7.0	----	----
pH	7.35	6.6	6.85	7.6	7.2	7.2
Cond (uS/cm)	98	104	94	105	245	245
Eh (mV)	----	----	112	----	----	----
Total Alkalinity (mg/L, HCO_3)	83.6	61.0	78.7	102.5	197	197
Charge Balance	4.5	5.5	10.3	-1.0	2.46	10.3
Species						
Ca	19	18	23.6	21.2	69	66
Mg	4.5	4.5	4.8	5.7	4	3.7
Na	4.5	4.9	4.5	4.3	4.3	4.6
K	1.4	1.4	1.1	1.9	2.4	3.4
SO_4	13	14	10.1	2.8	8.4	9.0
Cl	5.2	4.7	4.4	1.5	13	10.7
PO_4	<0.01	0.03	----	----	<0.01	----
SiO_2	8.8	7.8	9.9	13.6	11.4	12.0
NO_3	2.27	2.47	----	----	0.74	----
Fe (total)	2.45	6.25	----	----	3.4	----
DOC	5.2	5.2	----	----	0.7	----

Table 4-1. Stripa water analyses (in mg/L except where otherwise noted).

Drillhole/Site	WT3	PW5	PW3	PW1	PW2	drillwater
Sample Code No.	70-1	21-29	20-8	81WA215	81WA216	25-1
Sampling Interval (m)	----	----	----	0-80	0-80	----
Date Collected	790501	790515	790516	811008	811008	771107
Temperature (°C)	6.0	5.8	7.5	11.2	10.2	10.0
pH	6.62	6.2	7.58	5.11	6.13	8.1
Cond (uS/cm)	63	50	230	50	82	----
Eh (mV)	----	263	370	463	490	----
Total Alkalinity ($mg/L, HCO_3$)	34.1	17.3	210	12	20	118
Charge Balance	5.0	-0.8	1.22	-9.29	-3.28	11.5
Species						
Ca	8.9	5.7	64.5	4.0	13	46
Mg	1.58	1.5	4.34	1.1	2.5	11
Na	4.69	2.7	5.8	3.7	2.5	8.0
K	1.47	1.1	1.8	1.1	1.7	2.1
SO_4	7.4	13.1	10.4	10	12	28
F	----	----	----	0.30	0.22	----
Cl	2.3	2.3	3.2	4.5	14	18
Br	----	----	----	0.014	0.023	----
I	----	----	----	0.002	0.003	----
PO_4	----	----	----	<0.02	<0.02	<0.01
SiO_2	9.4	10.0	12.2	13.5	10.5	12
B	----	----	----	<0.005	<0.005	----
NO_2	----	----	----	<0.005	<0.005	----
NO_3	----	<0.4	<0.4	0.80	4.3	12.6
NH_4	----	----	----	0.04	<0.02	----
Al	----	----	-----	0.12	0.090	----
Fe (total)	----	1.73	<0.05	.068	.037	0.03
Fe^{2+}	----	----	----	.031	.031	----
Mn	----	----	----	0.027	0.010	----
Cu	----	----	----	0.051	<0.005	----
Zn	----	----	----	0.12	0.027	----
Co	----	----	----	<0.005	<0.005	----
Mo	----	----	----	<0.005	<0.005	----
Li	----	----	----	<0.005	<0.005	----
Sr	----	----	----	0.016	0.033	----
Rb	----	----	----	<0.005	0.008	----
Ba	----	----	----	0.018	0.022	----
DOC	----	----	----	----	----	3.0

Table 4-1. Stripa water analyses (in mg/L except where otherwise noted).

Drillhole/Site	dripwater	dripwater	SBH3	R1	R1	R1
Sample Code No.	26-3	27-4	85-15	53-7	53-20	53-29
Sampling Interval (m)	340-360	360-410	89-104	0-60	0-60	0-60
Date Collected	771117	771117	790527	781117	790502	790517
Temperature (°C)	----	----	8.0	11.9	11.7	10.0
pH	8.35	8.1	7.89	9.0	8.89	8.95
Cond (uS/cm)	----	----	162	202	199	208
Eh (mV)	----	----	----	158	37	131
Total Alkalinity (mg/L, HCO_3)	129	104	142.5	97.7	97.4	101.5
Charge Balance	-2.5	-2.4	1.0	0.9	3.0	-13.1
Species						
Ca	52	81	33.9	14.1	15.4	14.8
Mg	3.5	6	4.5	0.29	0.27	0.31
Na	38	45	12.5	49.0	44.7	43.5
K	0.6	2.9	1.7	0.20	0.17	0.19
SO_4	89	147	8.8	2.3	3.0	3.1
F	----	----	----	----	----	4.3
Cl	28	26	3.7	42.1	35.4	38.3
Br	----	----	----	----	----	<0.1
PO_4	<0.01	<0.01	----	----	----	----
SiO_2	9.6	9.4	12.5	11.7	11.2	11.9
NO_3	1.12	75	----	----	----	----
Fe (total)	0.05	0.04	----	<0.05	----	<0.05
Mn	----	----	----	<0.05	----	----
DOC	1.7	2.0	----	----	----	----

Table 4-1. Stripa water analyses (in mg/L except where otherwise noted).

Drillhole/Site	R1:4	R9	H-2	M3	M3	M3
Sample Code No.	81WA204	79-5	38-2	16-5	16-23A	42-2
Sampling Interval (m)	0-60	----	----	3-10	3-10	3-10
Date Collected	810604	790522	780601	770926	771019	780607
Temperature (°C)	12.0	----	15.0	10.8	----	15
pH	8.96	----	8.2	----	8.7	8.93
Cond (uS/cm)	215	----	----	----	210	----
Eh (mV)	57	----	----	97	92	----
Total Alkalinity (mg/L, HCO_3)	95	68.4	81.1	83.01	78.7	74.4
Charge Balance	1.9	5.4	-8.3	-7.6	8.32	0.52
Species						
Ca	15	18.0	11.8	15	14.1	14.2
Mg	0.18	0.25	0.32	<0.5	0.3	0.31
Na	49	40.6	51.5	43	50.8	54.5
K	0.10	0.13	0.35	0.3	0.2	0.29
SO_4	3.2	1.3	4.0	2.1	1.4	1.0
F	4.7	----	----	----	----	----
Cl	34	49.6	60.2	52	49.3	65.8
Br	0.3	----	----	----	----	----
I	0.014	----	----	----	----	----
PO_4	<0.1	----	----	<0.01	----	----
SiO_2	12	12.1	11.8	11.6	12.0	12.0
B	0.15	----	----	----	----	----
NO_2	<0.005	----	----	----	----	----
NO_3	0.5	----	----	0.24	----	----
NH_4	<0.01	----	----	----	----	----
Al	0.005	----	----	----	----	----
Fe (total)	0.046	<0.05	----	0.07	----	----
Fe^{2+}	.016	----	----	----	----	----
Mn	<0.005	----	----	----	----	----
Cu	<0.003	----	----	----	----	----
Zn	<0.005	----	----	----	----	----
Co	<0.005	----	----	----	----	----
Mo	0.038	----	----	----	----	----
Li	0.020	----	----	----	----	----
Sr	0.12	----	----	----	----	----
Rb	<0.002	----	----	----	----	----
Ba	0.006	----	----	----	----	----
DOC	4.0	----	----	0.7	----	----

Table 4-1. Stripa water analyses (in mg/L except where otherwise noted).

Drillhole/Site	M3	M3	M3	M3	E1	E1
Sample Code No.	42-35	81WA205	----	----	81WA218	----
Sampling Interval (m)	3-10	3-10	3-10	3-10	003-300	003-300
Date Collected	790517	810604	831109	840223	811111	820323
Temperature (°C)	13	12	14	15	10.5	10.4
pH	8.98	8.84	9.14	9.04	----	9.2
Cond (uS/cm)	----	210	235	235	175	180
Eh (mV)	207	----	136	98	-1	----
Total Alkalinity ($mg/L, HCO_3$)	86	86	92	93	84	103
Charge Balance	-8.91	-3.9	-8.2	-6.7	22.6	-4.0
Species						
Ca	14.7	14	14	14	20	22
Mg	0.25	0.23	0.22	0.22	0.32	0.81
Na	47.8	47	40	42	45	30
K	0.24	0.12	0.31	0.30	0.80	2.3
SO_4	3.6	4.9	6.5	5.1	6.8	10
H_2S	----	0.026	----	----	----	----
F	5.0	5.0	5.4	5.1	3.1	2.2
Cl	48.1	38.5	36	36	25	22
Br	<0.1	0.3	0.16	<5	.16	.078
I	----	0.013	0.011	0.021	0.006	----
PO_4	----	<0.1	<0.2	<0.2	<0.02	<0.02
SiO_2	11.4	12	12	11	11.8	13.3
B	----	0.18	0.16	0.23	0.10	.041
NO_2	----	<0.005	<.005	<.005	<0.005	<0.005
NO_3	----	0.6	<.1	<.1	0.10	<0.1
NH_4	----	<0.01	<.02	<.02	<0.02	<0.02
Al	----	.0055	<.01	<.001	<.005	0.06
Fe (total)	<0.05	.008	.01	<.005	.071	.009
Fe^{2+}	----	.005	----	<.01	.0055	----
Mn	----	<0.005	.001	<.001	0.005	.05
Cu	----	<0.003	<.001	<.001	<0.005	<0.005
Zn	----	<0.005	<.001	<.001	0.073	<0.01
Cd	----	----	----	----	----	<0.005
Hg	----	----	----	<.01	----	----
Pb	----	----	<.01	<.01	----	<.01
Co	----	<0.005	<.005	<.005	<.005	<0.005
Ni	----	----	≤.001	≤.001	----	<0.005
Cr	----	----	.004	<.001	----	<.005
V	----	----	.01	<.005	----	<.005
Mo	----	0.056	.07	0.11	0.049	<.005
Li	----	0.020	.032	0.024	0.019	.021
Sr	----	0.14	0.15	0.13	0.13	0.17
Cs	----	0.047	----	----	----	----
Rb	----	<0.002	<.005	<.005	<.005	<.005
Be	----	----	<.003	<.003	----	<.003
Ba	----	<0.003	.004	<.005	0.003	0.027
DOC	----	----	----	----	1.3	----

Table 4-1. Stripa water analyses (in mg/L except where otherwise noted).

Drillhole/Site	E1	E1	N1	N1	N1	N1	
Sample Code No.	----	----	81WA209	81WA214	----	81WA202	
Sampling Interval (m)	003-300	127-129	003-300	003-300	003-300	010-300	
Date Collected	840306	820323	810819	811006	820603	810603	
Temperature (°C)	10.3	----	10.4	11.5	10.0	10.1	
pH	8.9	----	8.91	8.93	8.71	8.85	
Cond (uS/cm)	185	----	190	215	195	190	
Eh (mV)	110	----	-39	-4	-185	13	
Total Alkalinity (mg/L, HCO_3)	87	----	81	72	75	77	
Charge Balance	-2.8	----	6.44	-11.1	-3.9	-1.2	
Species						**Filtered**	**Unfiltered**
Ca	18	----	23	21	21	23	22.5
Mg	0.23	----	0.57	0.21	0.77	0.12	0.22
Na	36	----	37	33	30	35.5	35.5
K	0.17	----	0.61	0.38	2.2	0.12	0.19
SO_4	8.7	13	0.45	0.30	1.0	0.6	----
H_2S	----	----	----	----	----	0.026	----
F	3.4	2.0	3.5	3.3	3.4	.070	----
Cl	22	23	40	51	40	45.5	----
Br	0.11	.078	0.42	0.50	.38	0.5	----
I	0.005	----	0.014	0.016	----	0.015	----
PO_4	<.02	----	<0.02	<.02	<.02	<0.1	----
SiO_2	13	----	11.1	11.8	13.5	12	15
B	0.049	----	0.07	.084	.045	0.094	0.10
NO_2	<.005	----	<0.005	<.005	<.005	<.005	----
NO_3	<.1	----	<0.2	.40	1.0	0.7	----
NH_4	<.02	----	<.02	.02	<.02	<.01	----
Al	.017	----	0.080	.033	.007	.059	0.56
Fe (total)	<.01	----	.15	.07	.033	.017	0.16
Fe^{2+}	<.01	----	.003	.035	----	.009	.018
Mn	0.004	----	<0.01	<.005	<.01	<.005	<.005
Cu	<0.001	----	<.005	<.005	<.005	<.003	0.043
Zn	<.001	----	<.010	<.005	<.01	<.005	0.024
Cd	----	----	----	----	<.005	----	----
Pb	<.01	----	----	----	<.01	----	----
Co	<.005	----	<.005	.010	<.005	<.005	<.005
Ni	0.007	----	----	----	<.005	----	----
Cr	<.001	----	----	----	.005	----	----
V	<.005	----	----	----	<.005	----	----
Mo	0.040	----	.050	.046	<.005	.049	.054
Li	0.017	----	.020	.022	.023	.019	.017
Sr	0.12	----	.15	0.16	0.16	0.16	0.17
Cs	----	----	----	----	----	0.035	0.066
Rb	<.005	----	<.005	<.005	<.005	0.003	0.003
Be	<.003	----	----	----	<.003	----	----
Ba	0.008	----	.005	<.003	----	0.003	0.004
DOC	----	----	1.2	----	----	----	----

Table 4-1. Stripa water analyses (in mg/L except where otherwise noted).

Drillhole/Site	N1:2	N1:1	N1	N1	N1	N1
Sample Code No.						
Sampling Interval (m)	151-251	252-300	123-125	203-205	271-273	274-276
Date Collected	840126	840126	820830	820906	820914	820923
Temperature (°C)	10.3	10.5	10.2	10	10.5	10.4
pH	8.99	8.89	8.73	8.43	8.85	8.79
Cond (uS/cm)	215	200	355	250	205	221
Eh (mV)	45	39	-243	-146	-108	-64
Total Alkalinity (mg/L, HCO_3)	87	81	39	55	75	63
Charge Balance	-6.8	-11.6	-3.25	2.3	-15.8	.028
Species						
Ca	22	23	29	24	22	26
Mg	0.18	0.20	0.45	0.42	0.29	0.09
Na	29	29	60	35	29	30
K	0.25	0.19	0.27	0.26	0.45	0.21
SO_4	0.67	0.46	0.9	0.1	2.7	.50
F	3.35	3.35	3.1	3.3	3.1	3.0
Cl	33	43	122	58	48	50
Br	.32	.38	1.5	----	0.57	.64
I	.015	.017	.038	.021	.012	.017
PO_4	<.02	<.02	.03	<.02	<.02	<.02
SiO_2	12	12	10.3	12.2	10.3	10.3
B	0.12	0.12	.054	.063	.047	.036
NO_2	<.005	<.005	<.005	<.005	<.005	<.005
NO_3	<.1	<.1	<.1	<.1	<.1	<.1
NH_4	<.02	<.02	<.02	.06	<.02	.03
Al	<.001	<.001	0.09	.05	<.01	<.01
Fe (total)	<.01	<.01	.15	.006	.007	.021
Fe^{2+}	<.01	<.01	----	----	----	----
Mn	.004	.003	<0.01	<.01	<.01	<.01
Cu	<.001	<.001	<.005	<.005	<.005	<.005
Zn	<.001	<.001	<.01	<.01	<.01	<.01
Cd	<.001	<.001	<.005	<.005	<.005	<.005
Pb	<.01	<.01	<.01	<.01	<.01	<.01
Co	<.005	<.005	<.005	<.005	<.005	<.005
Ni	.007	.008	<.005	<.005	<.005	<.01
Cr	<.001	<.001	<.005	.007	<.005	<.005
V	.005	.005	<.005	<.005	<.005	<.005
Mo	.040	.047	<.005	<.005	<.005	<.005
Li	.022	.022	.033	.026	.024	.033
Sr	0.13	0.15	0.22	0.19	0.16	0.19
Rb	<.005	<.005	<.005	<.005	<.005	<.005
Be	<.003	<.003	<.003	<.003	0.047	0.010
Ba	<.005	<.005	0.16	.19	.10	.065

Table 4-1. Stripa water analyses (in mg/L except where otherwise noted).

Drillhole/Site	V1	V1	V1	V1	V1	V1
Sample Code No.	----	81WA212	81WA213	----	81WA206	----
Sampling Interval (m)	000-506	004-506	004-506	006-506	000-408	100-505
Date Collected	810409	810921	811006	810326	810604	831003
Temperature (°C)	----	15.5	14.5	----	10.3	13.2
pH	----	9.10	9.11	----	9.73	8.95
Cond (uS/cm)	----	----	1650	----	510	1540
Eh(mV)	----	----	135	----	22	162
Total Alkalinity (mg/L, HCO_3)	12	12	11	10	18	11
Charge Balance	2.1	-0.29	-0.67	-1.0	2.5	-3.0
Species						
Ca	160	146	146	143	27	138
Mg	.64	0.55	0.57	.93	<.005	0.56
Na	280	248	246	257	116	217
K	1.6	2.4	2.4	2.2	0.24	1.9
SO_4	91	90	90	89	11.5	85
F	4.2	4.5	4.1	3.7	4.6	4.5
Cl	620	560	560	580	190	500
Br	----	5.9	5.8	----	2.0	5.5
I	----	0.14	0.14	----	0.061	0.10
PO_4	<.3	<.02	<.02	<.3	<0.1	<.02
SiO_2	----	13	13.5	----	14	13
B	----	0.21	0.20	----	0.24	.023
NO_2	<.005	<.005	<.005	<.005	<.005	<.005
NO_3	6.1	6.4	7.8	6.5	2.5	6.4
NH_4	<.01	<.02	<.02	<.01	<0.01	<.02
Al	----	.02	.009	----	0.032	<.01
Fe (total)	<.005	.0053	.004	<.005	.019	<.01
Fe^{2+}	----	.0046	.002	----	.010	----
Mn	.007	<.01	<.005	<.005	.008	<.01
Cu	<.005	<.005	<.005	<.005	<.003	<.001
Zn	<.005	.051	.020	.027	<.005	<.001
Pb	<.010	----	----	<.010	----	<.01
Co	<.005	<.005	<.005	<.005	<.005	<.005
Ni	<.005	----	----	<.005	----	<.001
Cr	<.005	----	----	.010	----	<.005
V	----	----	----	----	----	<.01
Mo	----	.010	.013	----	.050	<.01
Li	----	0.15	0.15	----	.020	0.20
Sr	2.4	1.7	1.7	1.9	.20	1.3
Cs	----	----	----	----	.078	----
Rb	----	<.005	.005	----	.009	.035
Be	<.003	----	----	<.003	----	<.003
Ba	.038	0.025	0.027	.024	<.003	.025
DOC	----	----	----	----	1.1	----

Table 4-1. Stripa water analyses (in mg/L except where otherwise noted).

Drillhole/Site	V1	V1	V1	V1	V1	V1
Sample Code No.	----	----	----	----	----	81WA203
Sampling Interval (m)	100-505	100-505	100-505	100-505	100-505	410-506
Date Collected	831019	831105	831207	840111	840208	810603
Temperature (°C)	12.1	11.5	12.2	12.6	12.2	10.6
pH	9.15	9.25	9.2	9.24	9.30	9.31
Cond (uS/cm)	1625	1420	1460	1580	1540	1420
Eh(mV)	225	126	127	102	120	-56
Total Alkalinity (mg/L, HCO_3)	12	14	11	11	17	9.25
Charge Balance	7.4	-6.1	2.93	-1.93	-1.53	1.1
Species						
Ca	144	138	149	146	152	172
Mg	0.51	0.46	0.48	0.47	0.43	0.19
Na	195	208	225	212	208	277
K	2.8	2.9	1.5	1.9	2.4	1.2
SO_4	85	88	85	89	86.5	102
H_2S	----	----	----	----	----	.0026
F	4.5	4.5	4.6	4.5	4.6	4.6
Cl	500	500	517	516	518	630
Br	5.6	5.5	5.4	5.6	5.4	6.5
I	0.16	0.13	.080	.14	.22	0.16
PO_4	<.02	<.02	.28	<.02	<.02	<.1
SiO_2	17	13	10	12	13	13.0
B	.021	0.24	.076	.23	.24	0.25
NO_2	<.005	<.005	<.005	<.005	<.005	<.005
NO_3	<.1	<.1	<0.1	<0.1	<0.1	7.0
NH_4	<.02	<.02	<.02	<.02	<.02	<.01
Al	<.01	<.01	<.001	<.001	.001	.024
Fe (total)	.02	2.0	<.01	<.01	.004	.004
Fe^{2+}	----	0.12	----	----	<.01	.0007
Mn	.002	.002	<.001	<.001	.003	<.005
Cu	<.001	<.001	<.001	<.001	<.001	<.003
Zn	.002	.001	.005	<.001	<.001	<.005
Cd	----	----	<.001	<.001	<.001	----
Hg	----	----	----	----	----	<.005
Pb	<.01	<.01	<.01	<.01	<.01	----
Co	<.005	<.005	<.005	<.005	<.005	<.005
Ni	<.001	<.001	.005	<.001	<.001	----
Cr	<.005	.002	<.001	<.001	<.001	----
V	<.01	.01	<.005	<.005	<.005	----
Mo	<.01	<.01	.011	.050	.090	.027
Li	0.21	0.19	0.14	.075	.14	.085
Sr	1.2	1.2	1.3	1.3	1.4	1.7
Cs	----	----	----	----	----	.074
Rb	.017	<.005	<.005	<.005	<.005	.032
Be	<.003	<.003	<.003	<.003	<.003	----
Ba	.026	.025	.022	.024	.025	.035
DOC	----	----	----	----	----	4.2

Table 4-1. Stripa water analyses (in mg/L except where otherwise noted).

Drillhole/Site	V1	V1	V1	V1	V1	V1
Sample Code No.	81WA208	81WA210	81WA211	81WA207	----	----
Sampling Interval (m)	410-506	410-506	410-506	410-505	092-094	092-094
Date Collected	810819	810908	810911	810713	810114	810116
Temperature (°C)	10.6	10.5	15.5	10.5	----	----
pH	9.27	9.28	9.17	9.54	----	----
Cond (uS/cm)	1340	1420	1580	1600	----	----
Eh(mV)	129	79	----	55	----	----
Total Alkalinity ($mg/L, HCO_3$)	13	16	19	11	65	17
Charge Balance	-2.34	-.021	-.039	3.21	-14	2.2
Species						
Ca	170	167	146	152	36	32
Mg	0.32	0.27	0.81	0.60	4.8	.25
Na	304	290	260	270	74	113
K	2.5	2.5	2.2	2.6	3.0	1.1
SO_4	95	105	92	110	9.6	1.1
F	4.5	4.2	4.4	4.5	2.2	3.2
Cl	700	650	575	570	174	220
Br	6.2	6.6	5.9	6.6	----	----
I	0.11	0.16	0.14	0.16	----	----
PO_4	<.02	<.02	<.02	<.03	<.3	<.3
SiO_2	13.7	13.0	13.0	13.7	----	----
B	0.24	0.22	0.21	0.25	----	----
NO_2	<.005	<.005	<.005	<.005	.037	.037
NO_3	7.0	<.2	1.4	<.10	2.3	2.6
NH_4	<.02	<.02	<.02	.03	.20	.10
Al	<.005	.01	.008	<.005	----	----
Fe (total)	.008	.013	.010	<.01	<.01	<.01
Fe^{2+}	.002	.006	.004	<.01	----	----
Mn	<.01	<.005	<.005	<.01	<.01	<.01
Cu	<.005	<.005	<.005	<.005	.029	.033
Zn	<.010	<.010	<.010	<.005	.078	.020
Co	<.005	<.005	<.005	.009	<.005	<.005
Ni	----	----	----	----	<.005	<.010
Cr	----	----	----	----	<.005	<.005
Mo	.010	.020	.020	.010	----	----
Li	0.18	0.15	0.15	0.19	----	----
Sr	1.8	2.0	1.8	2.0	.147	.192
Rb	<.005	.005	.005	.005	----	----
Be	----	----	----	----	<.003	<.003
Ba	.030	.030	.030	.040	----	----
DOC	4.8	1.0	----	1.6	----	----

Table 4-1. Stripa water analyses (in mg/L except where otherwise noted).

Drillhole/Site	V2	V2	V2	V2	V2	V2
Sample Code No.	----	24-2	----	6-5	6-28	6-30
Sampling Interval (m)	006-822	000-471	000-471	152.3-471	152.3-471	152.3-471
Date Collected	820421	771110	810409	770908	770914	770914
Temperature (°C)	9.2	7.6	----	9.3	8.2	8.2
pH	9.37	9.25	----	9.38	9.54	9.54
Cond (uS/cm)	710	308	----	439	464	464
Eh(mV)	-146	29	----	122	72	72
Total Alkalinity (mg/L, HCO_3)	36	45.8	----	38.6	31.5	31.5
Charge Balance	-6.96	0.66	18.6	4.27	1.72	5.7
Species						
Ca	49	23	34	35	36.8	37
Mg	0.72	<.5	.32	0.5	.09	<.5
Na	142	64	71	96	100	100
K	2.6	5.4	1.1	0.2	0.37	0.2
SO_4	24	3.6	12	6.9	8.0	6.2
F	12	----	5.1	----	----	----
Cl	270	114	120	182	192	185
PO_4	<.02	<.01	----	<.01	----	.01
SiO_2	17	11.2	----	12.6	13.1	12.8
B	.097	----	----	----	----	----
NO_2	<.005	----	----	----	----	----
NO_3	3.4	.15	7.6	.15	----	.15
NH_4	<.02	----	----	----	----	----
Al	.17	----	----	----	----	----
Fe (total)	0.02	.05	<.005	.19	----	.03
Mn	<.01	----	.005	----	----	----
Cu	<.005	----	.005	----	----	----
Zn	<.01	----	.010	----	----	----
Cd	<.005	----	----	----	----	----
Pb	<.01	----	<.010	----	----	----
Co	<.005	----	<.005	----	----	----
Ni	<.005	----	<.005	----	----	----
Cr	<.005	----	<.005	----	----	----
V	<.005	----	----	----	----	----
Mo	<.005	----	----	----	----	----
Li	.057	----	----	----	----	----
Sr	0.51	----	.34	----	----	----
Rb	<.005	----	----	----	----	----
Be	<.003	----	<.003	----	----	----
Ba	.014	----	.032	----	----	----
DOC	----	0.7	----	1.1	----	0.4

Table 4-1. Stripa water analyses (in mg/L except where otherwise noted).

Drillhole/Site	V2:1	V2	V2	V2	V2	V2
Sample Code No.	----	15-4	81WA201	81WA219	29-3	29-34
Sampling Interval (m)	562-822	285-471	356-471	356-471	376.5-471	376.5-471
Date Collected	831129	770915	810603	811119	780130	780222
Temperature (°C)	8.2	8.0	8.0	8.0	7.5	7.0
pH	9.94	9.49	9.53	9.17	9.75	9.7
Cond (uS/cm)	1215	463	960	----	600	600
Eh(mV)	44	7	20 to 79	----	169	144
Total Alkalinity (mg/L, HCO_3)	25	29.0	11.5	28	15.4	12.3
Charge Balance	-2.1	4.7	0.18	-7.15	-2.4	-11.7
Species						
Ca	146	37	104	101	59	55
Mg	<.005	<0.5	0.11	0.29	0.5	0.1
Na	195	100	180	170	125	120
K	0.82	0.2	.0.37	1.0	0.4	0.4
SO_4	35	7.2	44.5	45	19	19
H_2S	----	----	.00023	----	----	----
F	4.8	----	3.9	3.4	----	3.7
Cl	540	189	410	400	283	290
Br	5.1	----	4.0	4.2	----	----
I	0.56	----	0.11	0.11	----	----
PO_4	<.02	.01	<0.1	0.02	<.01	<.01
SiO_2	18	12.8	12	11.8	11.2	17
B	0.39	----	0.20	0.21	----	----
NO_2	<.005	----	<.005	<.005	----	<0.001
NO_3	<.1	0.14	4.8	3.7	0.28	0.05
NH_4	<.02	----	<.01	0.04	----	0.01
Al	.034	----	.01	.015	----	----
Fe (total)	<.01	.02	.088	.085	<.02	0.08
Fe^{2+}	----	----	.008	.016	----	----
Mn	<.001	----	.009	<.005	----	----
Cu	<.001	----	<.003	<.005	----	----
Zn	<.001	----	<.005	.069	----	----
Hg	----	----	.023	----	----	----
Pb	<.01	----	----	----	----	----
Co	<.005	----	<.005	<.005	----	----
Ni	<.001	----	----	----	----	----
Cr	<.001	----	----	----	----	----
V	<.005	----	----	----	----	----
Mo	<.005	----	.051	.071	----	----
Li	0.11	----	.038	.073	----	----
Sr	1.0	----	.99	1.0	----	----
Cs	----	----	.046	----	----	----
Rb	<.005	----	.015	.010	----	----
Be	<.003	----	----	----	----	----
Ba	.019	----	.024	.022	----	----
DOC	----	0.4	4.0	----	0.8	----

Table 4-1. Stripa water analyses (in mg/L except where otherwise noted).

Drillhole/Site	V2	V2:3	V2:2	V2	V2:4	V2
Sample Code No.	29-39	----	----	17-32	----	43-3
Sampling Interval (m)	376.5-471	424-499	500-561	6.3-50	382-423	08-40
Date Collected	780223	831128	840228	771003	840228	780606
Temperature (°C)	7.0	9.0	8.6	8.0	8.0	7.5
pH	9.7	10.04	10.06	8.83	9.51	9.04
Cond (uS/cm)	600	1210	1090	262	1140	----
Eh(mV)	144	52	45	-1	28	-87
Total Alkalinity (mg/L, HCO_3)	12.3	20	18	53.8	11	57.1
Charge Balance	-9.6	-3.7	-1.6	0.4	0.4	39.9
Species						
Ca	61	106	94	18	145	9.8
Mg	<0.5	<.005	0.03	<0.5	0.12	0.26
Na	120	231	218	56	198	93.8?
K	0.8	0.46	0.44	0.4	0.38	----
SO_4	18	67	57	3.3	60	----
F	----	4.6	5.3	----	3.3	----
Cl	285	500	460	84	500	78.5
Br	----	5.3	4.5	----	5.0	----
I	----	0.84	0.14	----	0.11	----
PO_4	<.01	<.02	<.02	<.01	<.02	----
SiO_2	12.8	16	18	11.2	12	----
B	----	0.21	0.34	----	0.13	----
NO_2	----	<.005	<.005	----	<.005	----
NO_3	0.19	<.1	<.1	.20	<.1	----
NH_4	12.8	<.02	<.02	----	<.02	----
Al	----	.063	.009	----	.013	.035
Fe (total)	<0.02	<.01	<.005	0.15	.005	----
Fe^{2+}	----	----	<.01	----	<.01	----
Mn	----	<.001	<.002	----	<.001	----
Cu	----	0.04	.007	----	.003	----
Zn	----	<.001	<.001	----	<.001	----
Pb	----	<.01	<.01	----	<.01	----
Co	----	<.005	<.005	----	<.005	----
Ni	----	<.001	<.001	----	<.001	----
Cr	----	<.001	<.001	----	.007	----
V	----	<.005	<.005	----	<.005	----
Mo	----	0.034	.060	----	.051	----
Li	----	.086	.087	----	0.10	----
Sr	----	1.0	0.89	----	1.1	----
Rb	----	<.005	<.005	----	<.005	----
Be	----	<.003	<.003	----	<.003	----
Ba	----	.007	.009	----	.028	----
DOC	0.6	----	----	0.6	----	----

Table 4-1. Stripa water analyses (in mg/L except where otherwise noted).

Drillhole/Site	V2	V2	V2	V2	V2	V2
Sample Code No.	43-7	59-3	69-1	69-14	----	----
Sampling Interval (m)	08-40	401-428	401-428	401-428	406-410	413-417
Date Collected	781116	781120	790406	790517	821124	821214
Temperature (°C)	8.2	8.0	7.0	8.0	10.0	8.3
pH	9.16	9.6	9.4	9.48	9.36	9.20
Cond (uS/cm)	234	925	830	1000	1410	1200
Eh(mV)	-57	105	----	248	219	-120
Total Alkalinity (mg/L, HCO_3)	----	9.4	----	8.7	13	9
Charge Balance	34.4	-4.81	-1.23	2.15	-10.2	-0.52
Species						
Ca	19.6	110	108	109	156	135
Mg	0.29	0.18	0.17	0.17	0.35	0.37
Na	64	177	176.0	189	218	196
K	0.24	0.55	0.54	0.53	1.3	1.6
SO_4	5.4	55.4	42.3	41.2	77.5	57
F	----	----	----	2.4	2.75	2.5
Cl	90.5	449	437.0	435.0	608	490
Br	----	----	----	<0.1	7.0	5.1
I	----	----	----	----	.50	.14
PO_4	----	----	----	----	<.02	<.02
SiO_2	11.3	10.2	10.4	11.4	9.6	18
B	----	----	----	----	.049	0.69
NO_2	----	----	----	----	<0.005	<0.005
NO_3	----	----	----	----	<0.1	<0.1
NH_4	----	----	----	----	<.02	<.02
Al	----	----	----	----	<0.01	<0.01
Fe (total)	<0.05	<0.05	----	<0.05	.005	.025
Mn	<0.05	<0.05	----	----	<0.01	<0.01
Cu	----	----	----	----	<.005	<.005
Zn	----	----	----	----	<.01	<.01
Cd	----	----	----	----	<.005	<.005
Pb	----	----	----	----	<.01	<.01
Co	----	----	----	----	<.005	<.01
Ni	----	----	----	----	<.01	<.01
Cr	----	----	----	----	<.005	<.005
V	----	----	----	----	<.005	<.005
Mo	----	----	----	----	<.005	<.01
Li	----	----	----	----	.11	.16
Sr	----	----	----	----	1.5	1.3
Rb	----	----	----	----	<.005	<.005
Be	----	----	----	----	.003	<.003
Ba	----	----	----	----	.099	.031

Table 4-1. Stripa water analyses (in mg/L except where otherwise noted).

Drillhole/Site	V2	V2	V2
Sampling Interval (m)	490-494	549-553	584-588
Date Collected	830119	830207	830307
Temperature (°C)	9.3	9.4	9.4
pH	9.85	9.84	9.89
Cond (uS/cm)	1220	1040	960
Eh(mV)	-5	-100	-120
Total Alkalinity (mg/L, HCO_3)	18	18	19
Charge Balance	-2.98	-4.67	1.00
Species			
Ca	89	61	72
Mg	0.39	0.34	<.005
Na	224	198	175
K	0.73	0.69	1.7
SO_4	55	51	48
F	4.2	5.6	6.2
Cl	460	375	325
Br	5.1	4.8	4.4
I	0.24	0.17	0.49
PO_4	<.02	<.02	<.02
SiO_2	15	13	16
B	0.74	1.3	0.47
NO_2	<.005	<.005	<.005
NO_3	<.1	<.1	<.1
NH_4	<.02	<.02	0.02
Al	0.10	<.01	0.11
Fe (total)	.004	.27	.015
Mn	<.01	<.01	<.01
Cu	<.005	<.005	.010
Zn	<.01	<.01	<.01
Cd	<.005	<.005	----
Pb	<.01	<.01	----
Co	<.01	<.01	<.01
Ni	<.01	<.01	<.01
Cr	<.005	<.005	<.005
V	<.005	<.005	<.005
Mo	<.01	<.01	----
Li	0.13	0.12	.070
Sr	1.0	0.74	0.74
Rb	<.005	<.005	----
Be	<.003	<.003	<.003
Ba	.024	.006	----

4.5 Chemical analyses

Table 4-1 contains chemical analyses of Stripa groundwaters and nearby wells and streams for the period 1977-84, including both the data from the SAC program (Fritz, et al., 1979, 1980) and the international program. The analyses have been organized sequentially in a hierarchy as follows:

Borehole or site designation

Size of borehole interval

Chronological sequence

The borehole or site sequence follows the order: surface waters, lakes, ponds, private wells, shallow boreholes, R1, M3, E1, N1, V1, V2. The size sequence proceeds from largest to smallest, and the chronological sequence proceeds from oldest sampling to youngest. The determinations of Fe^{2+} have been included for the first time because the sampling and preservation procedures have been found to be reliable.

Also, the following abbreviations are used: SW = surface water, T.P. = tailings pond, PW = private well, WT = water table and SB = shallow borehole.

A few analyses from the SAC program were not included. These were samples that were either duplicates from the same location and had identical chemistries, or they were samples clearly contaminated by cementing material as indicated by a radical change in chemistry (high pH and Ca).

4.6 Saline groundwaters in central Sweden: Regional program

Southern and central Sweden have been invaded by seawater on two separate occasions during the Holocene. Approximately 10,000 - 9,000 B.P. the Yoldia sea covered a large area directly across central Sweden, reaching levels of 150 - 170 m.a.s.l. on the present land surface. Stripa is located just within these limits (Figure 4-2), and thus, it is possible that Yoldia seawater could have infiltrated the Stripa granite as suggested by Fritz, et al. (1983). The second invasion came through Öresund, and only affected coastal areas (mostly southern and western Sweden), reaching levels of 45-55 m.a.s.l. (Engqvist, 1981). This invasion of the Litorina sea could not have affected the Stripa area.

There are many known occurrences of saline groundwaters (over 800 wells: Nordberg, 1981; Lindewald, 1981; Engqvist, 1981) in central Sweden believed to be the result of entrapped Yoldia/Litorina seawater. A dozen locations were found and sampled to bet-

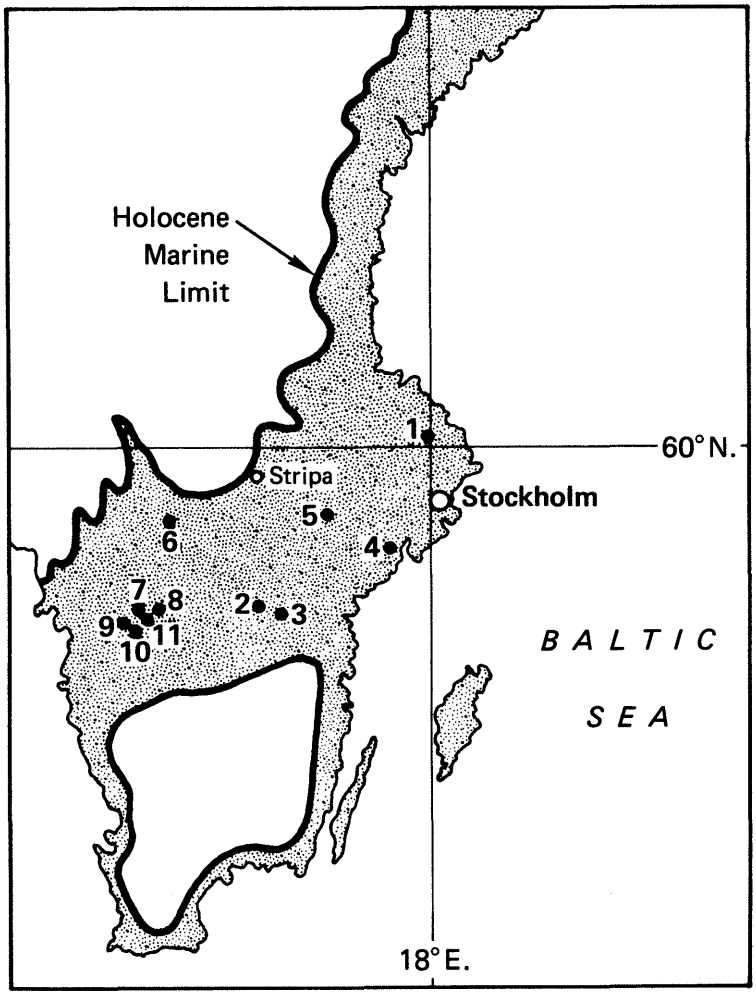

Figure 4-2. Southern and central Sweden showing sampling locations, Stripa and the limits of Yoldia/Litorina sea invasion.

ter identify its chemical characteristics for comparison with the Stripa groundwaters. The sampling locations are given in Figure 4-2, and the analyses are provided in Table 4-2.

4.7 Distribution of salinity with location and time

A more definitive statement can now be made about changes in the water chemistry with respect to location and time. The suggestion has been made that there is a gradual increase in chloride concentrations with depth (Fritz, et al., 1979; Nordstrom, 1983a). Further sampling indicated an abrupt change in chloride below 770 m (Fritz, et al., 1980). With approximately 100 water samples collected and analyzed to date, this question can be addressed more confidently and in more detail.

Table 4-2. Chemical analyses of saline groundwaters in central Sweden (concentrations in mg/L).

Sample	STENE	HÄSSELBY	ÅKER	SMEDTOFTA	ROCKAGÅRDEN	HAMMARÖ
Date Collected	830422	830420	830505	830504	830505	830503
Temp (°C)	5.8	7.8	10.0	6.7	9.5	8.2
Field pH	8.3	8.01	7.64	7.05	7.78	7.5-7.8
Cond (uS/cm)	1280	1750	6200	2850	2600	1710-2000
Eh (mV)	224	223	117	----	180	202
Alkalinity	139	262	931	581	736	254
Charge Balance (%)	-0.8	-5.4	1.0	-1.2	-0.9	-41
Species						
Ca	55	100	57	30	48	27
Mg	6.6	16	76	26	40	22
Na	328	416	1527	803	700	270
K	3.5	5.4	95	47	40	16
SO_4	64.3	84	135	4	91	180
F	1.7	2.0	1.5	1.5	1.6	1.6
Cl	501	700	2100	1100	835	540
Br	2.35	2.43	7.70	3.33	2.02	----
I	0.011	0.016	0.56	0.19	0.16	0.03
PO_4	<0.02	<0.02	0.15	4.0	0.08	0.03
SiO_2	12	11	21	19	26	27
B	0.41	0.41	1.0	0.56	0.48	0.11
NO_2	<0.005	<0.005	<0.005	<0.005	0.015	<0.005
NO_3	<1.0	<1.0	<1.0	<1.0	<1.0	<1.0
NH_4	0.02	0.07	4.5	9.4	1.7	0.54
Al	<0.01	<0.01	<0.01	0.25	0.01	0.01
Fe (total)	0.11	0.10	1.37	5.6	0.50	1.75
Fe^{2+}	0.027	0.033	0.75	5.2	0.24	0.79
Mn	<0.01	0.07	0.12	0.44	0.13	0.56
Cu	<0.005	<0.005	<0.005	<0.005	<0.005	<0.005
Zn	0.01	0.04	0.02	0.01	0.15	<0.01
Cd	<0.005	<0.005	<0.005	<0.005	<0.005	<0.005
Pb	<0.01	<0.01	<0.01	<0.01	<0.01	<0.01
Co	<0.01	<0.01	<0.01	<0.01	<0.01	<0.01
Ni	<0.01	<0.01	<0.01	<0.01	<0.01	0.02
Cr	<0.005	<0.005	<0.005	<0.005	<0.005	<0.005
V	0.010	0.057	0.18	0.071	0.093	0.039
Mo	<0.01	<0.01	<0.01	<0.01	<0.01	<0.01
Be	<0.003	<0.003	<0.003	<0.003	<0.003	<0.003
Li	0.11	0.038	0.13	0.027	0.085	0.042
Sr	1.2	1.5	0.98	0.33	0.88	3.9
Rb	<0.01	<0.01	<0.01	<0.01	<0.01	<0.01
Ba	0.043	0.060	0.045	0.057	0.054	0.11
DOC	4	----	14	21	10	12

Table 4-2. Chemical analyses of saline groundwaters in central Sweden (concentrations in mg/L).

Sample	ST. SUNDBY	SKOFTEBY	ÖSMO-JURSTA	HANGLÖSA	KAGA	WILHELMSLUND
Date Collected	830502	830504	830422	830504	830421	830421
Temp (°C)	8.7	7.4	----	12.5	11.7	10.5
Field pH	8.37	7.93	7.34	8.02	7.38	7.88
Cond (uS/cm)	1920	3750	335	1940	2990	3620
Eh (mV)	283	214	451	266	252	196
Alkalinity	166	879	214	690	164	53
Charge Balance (%)	1.2	-0.85	2.2	1.7	-12	-3.1
Species						
Ca	108	53	75	25	400	386
Mg	6.3	58	8.3	11.5	12	4.0
Na	463	1120	6.3	540	380	587
K	6.4	59	11	22	21	12
SO_4	107	66	15	81	33	1.04
F	1.8	3.0	.18	2.8	.8	1.8
Cl	740	1500	10	450	1400	1630
Br	2.03	5.06	----	1.78	14.3	18.3
I	0.04	0.52	<0.005	0.15	0.080	0.16
PO_4	0.03	3.2	3.5	0.06	<0.02	<0.02
SiO_2	20	18	13	15.5	11	6.6
B	0.29	1.3	0.021	0.80	0.30	0.44
NO_2	<0.005	<0.005	<0.005	0.008	0.055	0.030
NO_3	<1.0	<1.0	45	<1.0	<1.0	<1.0
NH_4	<0.02	3.2	0.04	0.68	0.03	0.72
Al	<0.01	<0.01	<0.01	<0.01	<0.01	<0.01
Fe (total)	0.020	0.076	<0.01	.069	0.22	0.29
Fe^{2+}	0.001	0.031	<0.01	.057	0.021	0.046
Mn	0.02	0.04	<0.01	.07	.20	0.23
Cu	<0.005	<0.005	0.036	.03	<0.005	0.012
Zn	0.02	0.01	0.11	.03	0.27	0.09
Cd	<0.005	<0.005	<0.005	<0.005	<0.005	<0.005
Pb	<0.01	<0.01	<0.01	<0.01	<0.01	<0.01
Co	<0.01	<0.01	<0.01	<.005	<0.005	<0.01
Ni	<0.01	<0.01	<0.01	<.004	<0.004	<0.01
Cr	<0.005	<0.005	<0.005	<0.005	<0.005	0.023
V	0.011	0.13	0.020	<.005	.012	<0.005
Mo	<0.01	<0.01	<0.01	<0.01	<0.01	<0.01
Be	<0.003	<0.003	<0.003	<0.003	<0.003	<0.003
Li	0.069	0.074	<0.003	0.054	0.14	0.37
Sr	1.2	1.6	0.16	.44	8.5	8.1
Rb	<0.01	<0.01	<0.01	<0.01	<0.01	<0.01
Ba	0.028	0.16	0.022	.43	3.5	0.92
DOC	5	18	----	12	3.8	----

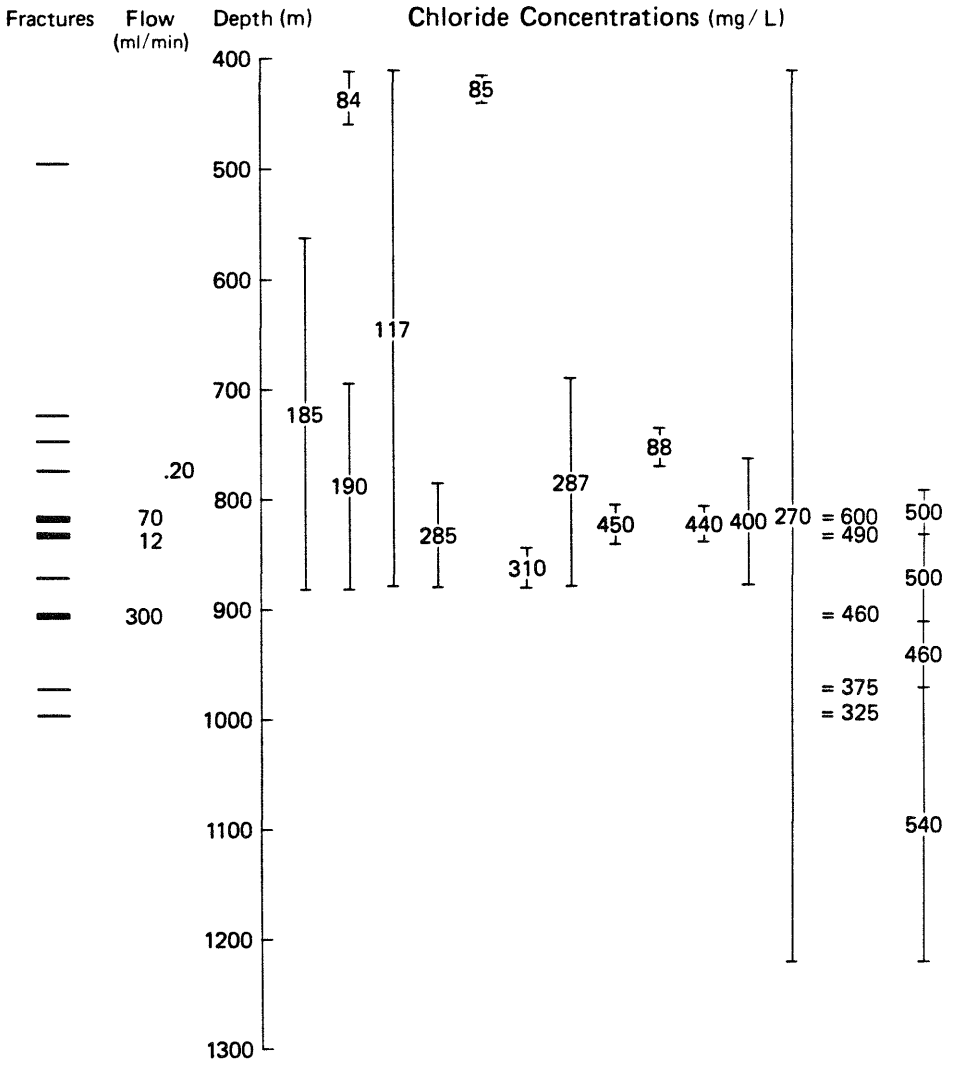

Figure 4-3. Chloride concentrations of sampled intervals in V2 borehole from oldest to youngest (far right).

Several short interval samples have been collected which are indicative of narrow fracture zones, eliminating the possibility of mixing of different zones within the borehole. These narrow intervals can be compared to large intervals to gain an appreciation for chemical variability over different sections of a single borehole. The two best examples are from boreholes V2 and N1. Figure 4-3 shows some of the fracture zones, flows, depth and chloride concentrations that have been measured in the V2 borehole. The chloride concentrations are in chronological sequence from left to right (right-hand side is the most recent in time).

The first, most obvious, observation is that several water samples have been taken over large intervals of the borehole, and the larger the borehole interval the lower the chloride concentration tends to be. In these instances there is a considerable amount of mixing of waters from different fracture zones in the same borehole. Where narrow intervals of the borehole (<50 m) have been sampled, there is considerable variation in chloride

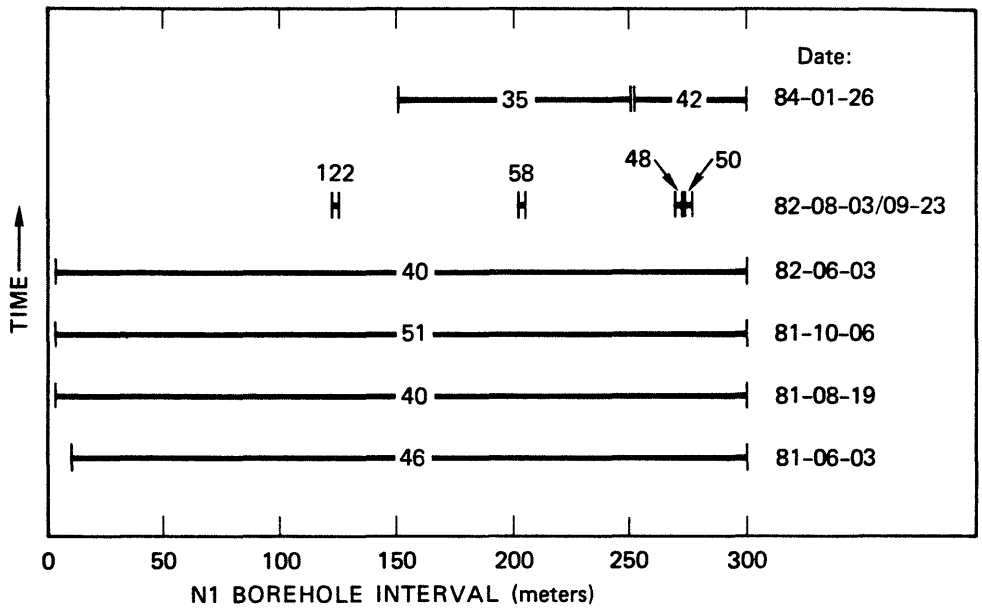

Figure 4-4. Chloride concentrations (in mg/L) of sampled intervals in N1 borehole from oldest to youngest (top).

concentration from 84 mg/L to 600 mg/L. One zone giving 88 mg/L chloride is only 47 m away from another zone having 600 mg/L chloride. There is no clear trend with depth, although the highest salinity tends to be around 800-900 m depth; and samples taken below 800 m are consistently higher in salinity than samples taken from above 800 m. Figure 4-4 shows chloride concentrations at different intervals of the N1 borehole. The sampling dates are shown on the right-hand side. Again it can be seen that when narrow intervals are sampled, zones of distinctly higher salinity can be found. The water chemistry is a very sensitive measure of the location of different types of permeable fracture zones.

The conclusion is that the salinity is quite variable from one fracture zone to the next, the existence of the mine may have had a large influence on diluting the salinity above 800 m, and the geochemical evolution of these groundwaters is closely associated with the fractures of the local rock. This also indicates that there is not enough interconnection between the fractures to allow sufficient mixing to give a more homogeneous water chemistry or a clear pattern of mixing with depth. Mixing in this context simply refers to mixing of groundwater between fracture zones or between water-bearing conduits in the granite. This salinity-depth profile will be called "heterogeneous," in contrast to the type of "homogeneous" profile which has been observed in Sweden and Finland where Baltic seawater (or Yoldia/Litorina seawater) has infiltrated crystalline bedrock. An example of the latter can be seen in Figure 4-5 (Snellman, 1982).

The results from Stripa lead to the conclusion that there is not a continuous increase in salinity with depth, nor is there a

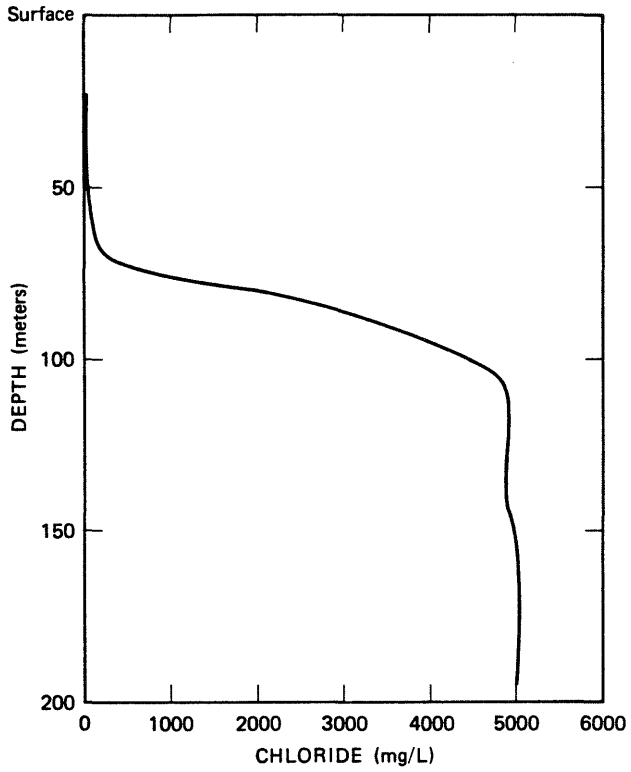

Figure 4-5. Chloride vs. depth profile for Y1 borehole, Loviisa, Finland.

sudden break in salinity below 770 m. Instead, there is an irregular increase in chloride with depth (the heterogeneous profile). In N1, a 2-m interval is discharging water of 120 mg/L chloride at a depth of about 360 m. At 92-94 m in V1 borehole (about 460 m depth), a discharging water contains about 200 mg/L chloride. These and other irregularities indicate that there is no clear break in the salinity with depth, but rather an irregular increase much like the depth profile for hydraulic conductivity.

Detailed mapping of fracture-zone water chemistry shows promise as a tool in finding flow paths in crystalline rock. It might be possible to make permeable connections between boreholes based on similarities in water chemistry.

The heterogeneous profile seen at Stripa suggests an origin other than simple intrusion of saline water from an external source. However, the general chemical characteristics of these waters are very much the same from one fracture zone to another, i.e., independent of salinity (see chapter 5), which implies there is a single type of source or a single type of process accounting for the salty components. This heterogeneous profile may be typical of groundwater in crystalline rocks that have not been intruded by saline waters such as seawater.

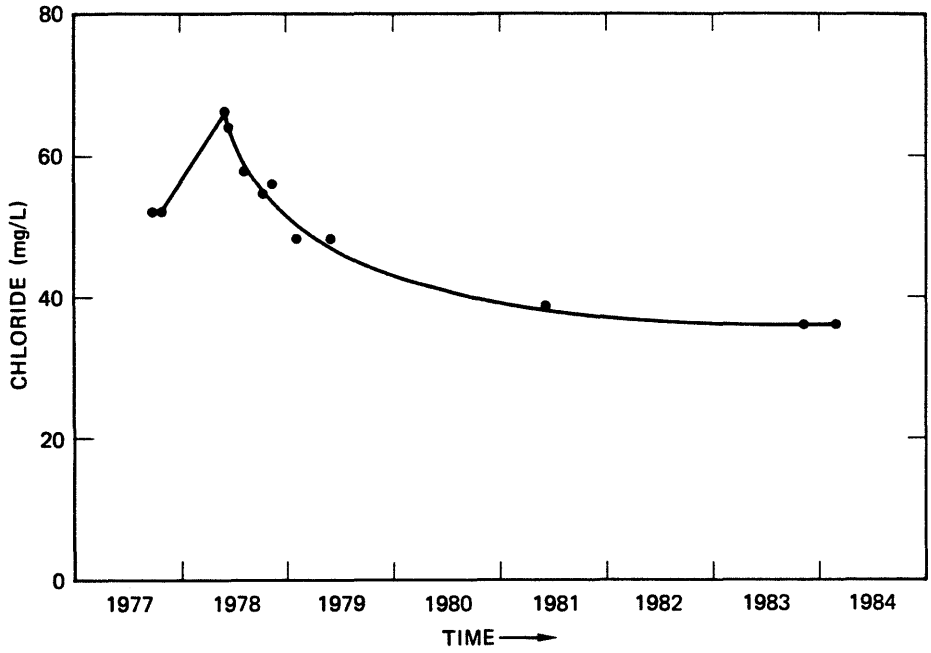

Figure 4-6. Chloride concentrations as a function of time for the M3 borehole.

Chemical variations with time are not exactly clear. The data shown in Figure 4-3 for the V2 borehole suffers from two problems: (1) rarely has the same borehole interval been sampled more than once, and (2) it is known that the discharges from the various fracture zones change with time; and if they don't all change proportionately the same, then the change in chemistry could simply reflect different borehole mixtures obtained by varying hydrologic flow conditions. Comparing the interval 690-880 m in V2, the increase in chloride from 190 to 287 mg/L may be a change in a single fracture system, or it may be due to a slightly different positioning of the packers, or it may be due to different proportions of flows from individual fractures zones.

The M3 borehole has been monitored over a long period of time and shows a recognizable pattern (Figure 4-6). Background chloride concentrations were initially about 52 mg/L. On June 1, 1978, the heater experiments were begun, and one week later chloride values jumped to 66 mg/L. Following that initial increase, the chloride values follow a decay curve leveling off at around 36 mg/L. These data show that a pulse of chloride was released as a result of the start-up of the heater experiments, and with time the chloride decreased to constant values that are significantly lower than the original background. These results could be interpreted in either of two ways. First, if the chloride originates from the rock (such as fluid inclusions), then the thermal gradients could have caused an increase in diffusion of chloride along micro-cracks, causing a pulse of chloride to come out; or it might even have caused some mechanical microfracturing in wa-

ter-bearing zones, which would immediately release a greater amount of chloride from inclusions. Thermal stress experiments on natural quartz grains have shown that water from fluid inclusions is released by microfracturing at less than 100°C up to 550°C (Barker and Robinson, 1984). Second, the thermal stress may have changed the flow direction in fractures so that water at higher chloride concentrations was temporarily rerouted to the M3 borehole. The flow direction may have been altered by the affect of thermal convection on flow, or by changes in porosity and flow channels caused by the heating. Distinguishing these effects would be very difficult without additional information. Further discussion on the effects of the heater experiments on the water chemistry from nearby boreholes can be found in Fritz, et al. (1980).

Other boreholes, such as R1 and V1, do not seem to show any significant chemical variability with time.

4.8 Ion ratios and classification of groundwater

Ion ratios can provide a useful means of distinguishing different water types, sources of water, and their classification (e.g., White, et al., 1963). Although there are limitations to the interpretation based only on ion ratios, these ratios do provide a way of initially characterizing the water chemistry. Chloride is useful for normalizing because it is one of the most conservative common ions in natural waters, and it provides a much clearer picture of depicting the water chemistry than comparing ions with depth or specific conductance. Ratios of ions to chloride can also provide some information on the evolution of saline waters. A good example is provided by Eugster (1980), who describes the origin and evolution of brines at Lake Magadi, Kenya, using chloride as a normalizing factor. The main purpose of this section will be to compare the Stripa groundwater chemistry with other possible sources of salinity, such as seawater, Yoldia seawater, Baltic water, and the sedimentary basin brines in the Cretaceous-Jurassic strata of southernmost Sweden. These four types of saline water are the only ones known to occur in Sweden. Table 4-3 summarizes several ion ratios for these four types of water and for several locations at Stripa.

Permian evaporates transported to Stripa have also been suggested as a source of salinity.

4.8.1 Seawater

Surface seawater has a very constant composition for all major constituents and most minor and trace constituents regardless of location. The occurrence of modern seawater into Swedish ground-

Table 4-3. Ion ratios (by weight) for saline waters and Stripa waters.

	Br/Cl	$(I/Cl)x10^6$	Ca/Mg	Mg/Cl	Ca/Cl	Na/Cl	K/Cl	SO_4/Cl
Seawater	0.00347	3.1	0.32	0.067	0.021	0.55	0.0206	0.14
Baltic water	0.00342		0.32	0.067	0.022	0.55	0.0205	0.14
Yoldia seawater:								
Set I	0.00342	163	4.7	0.052	0.072	0.74	0.0308	0.125
Set II	0.0107	77	65	0.0055	0.29	0.32	0.011	0.012
Skåne brines	0.0055	40-53	22	0.012	0.20	0.50	0.011	0.0023
V1 and V2	0.0107	446	451	0.00107	0.23	0.47	0.0040	0.11
N1	0.0105	359	108	0.0069	0.48	0.68	0.011	0.016
E1	0.0047	192	56	0.016	0.81	1.56	0.048	0.354
Shallow wells	0.0024	330	6.7	0.94	7.1	1.17	0.39	2.3
Surface waters	0.0077	1300	4.8	0.40	1.77	0.65	0.21	2.1

waters is limited to coastal areas, especially near highly populated areas, such as Göteborg and Skåne, where high pumpage rates encourages the intrusion of seawater (Nordberg, 1981). Unaltered modern seawater clearly cannot be entering the Stripa granite.

4.8.2 Baltic seawater

The Baltic sea is a mixture of seawater and fresh waters entering the Baltic region. The dilution factor averages 6.5 for surface Baltic water, but decreases considerably with depth because the denser seawater enters the Öresund (the sound between Denmark and Sweden) along the sea bottom. Since the Baltic is a relatively simple mixture, many of the element ratios should be the same as those of seawater. Extensive investigations by Kremling (1969, 1970, 1972) at 21 stations from the Öresund to the Bothnian Bay and the Gulf of Finland show that even with considerable dilution the ion ratios deviate very little from seawater (Table 4-3). Coastal Baltic seawater intrusion also occurs in some coastal aquifers along the east coast (Sund and Bergman, 1981), but direct intrusion from the modern Baltic cannot be the source of saline components in the Stripa groundwaters because ion ratios are incompatible.

4.8.3 Yoldia seawater

As previously mentioned, the Yoldia sea invaded central Sweden some 9,000 years ago and in some places became entrapped in Quaternary clay deposits of low permeability. These waters have chemical compositions which have undergone modification from the original seawater composition by such processes as clay formation, ion exchange, and mineral precipitation (Jacks, 1973,

1978; Agerstrand, et al. 1981). The analyses for these waters shown in Table 4-2 can be grouped into two sets, based on ion ratios. Set I comprises eight samples which have nearly identical Br/Cl ratios averaging 0.00342 (±0.00071) which is indistinguishable from modern seawater and Ca/Mg ratios averaging 4.74 (±5.8). Set II comprises two samples (Kaga and Wilhelmslund) which average 0.0107 for Br/Cl and 65 for Ca/Mg, considerably higher than all of the other samples. Of the remaining two samples, one was found to be entirely diluted with fresh water, and the other was unavailable for Br analysis. Set I is considered to be typical of Yoldia seawater altered by water-rock and biologically-mediated reactions. The ion ratios for this set fall in the same range as those from coastal groundwaters in Finland, which are assumed to be Yoldia or Litorina seawater (e.g., Hyyppä, 1984). Set II has ion ratios that are more comparable to those found at Stripa, especially the Br/Cl, Ca/Mg and Mg/Cl ratios.

Thus, the Stripa groundwaters are not unique in their chemistry, and they are not comparable to Yoldia/Litorina entrapped seawater. Elimination of Holocene seawater as a possible source of the saline components at Stripa means that these components (and probably the groundwater itself) must be older than 10,000 years B.P.

4.8.4 Jurassic-Cretaceous sedimentary basin brines of Skåne

Deep (1 km) subsurface brines are known to occur at Skåne in Jurassic and Cretaceous sedimentary rocks (Brotzen and Assarson, 1951). Chloride concentrations can be as high as 154,000 mg/L, and the general chemical characteristics are similar to other brines in deep sedimentary basins of the world. Ion ratios for these brines (shown in Table 4-3) appear to be roughly intermediate between the altered Yoldia seawater ratios and those of Stripa. Assuming that the saline components at Stripa had a marine origin, then it is possible to interpret them as the extreme case of modified seawater in which the Yoldia waters and the Skåne brines are intermediate steps. The progression from modern seawater ion ratios to the Stripa ion ratios may represent the effect of time, or the effect of temperature, or both. The temperature effect may be important because the Skåne brines are slightly elevated in temperature (up to at least 80°C), and the rocks in the Stripa region have undergone much higher temperature alterations. Further discussion of a possible temperature signature in the Stripa groundwater chemistry is discussed in Chapter 5.

4.8.5 Permian evaporates

Extensive deposits of Permian evaporite beds are found in large areas throuhout Germany, Russia and Poland and the hypothesis is developed in Chapter 7 that some of these may have been eroded and subsequently transported to central Sweden. This suggestion is based on the stable isotope data on dissolved sulfate which are similar to the values for Permian marine sulfates. However, there are no known Permian deposits in Sweden so that transport of dissolved salts over long distances is required. Such transport would involve dissolution and probably redox processes which would tend to destroy and/or dilute the Permian isotopic signature. Furthermore, erosion of Permian deposits such as the Zechstein evaporates is confined to just a few diapiric intrusions composed dominantly of halite and smaller amounts of gypsym, anhydrite and carnallite. Hence the Br/Cl ratio would be dominantly reflected by the ratio found in halite which is considerably lower than seawater and an order of magnitude or more lower than the ratio in the Stripa groundwaters. Finally, the Fennoscandian shield has been an area of uplift and erosion since the Devonian and has not experienced any depositional environments until the Holocene (Brinkmann, 1969). It is very difficult to imagine a scenario that involves erosion, transport and infiltration at some unidentifiable period of time of evaporates so that the subsequent saline water contains the Permian sulfate stable isotope signature but most of the rest of the chemistry has changed.

4.8.6 Stripa groundwaters

The ion ratios listed in Table 4-3 for Stripa groundwaters show several anomalous trends which must be accounted for in any geochemical interpretation:

1. Br/Cl and I/Cl ratios are markedly higher than seawater and modified seawater.

2. Ca/Mg ratios are 1-2 orders of magnitude higher than seawater and modified seawater.

3. Mg/Cl are markedly lower than seawater and modified seawater.

These anomalies cannot be fully accounted for by modern, Holocene, Paleozoic or Mesozoic seawater. An alternative hypothesis, based on fluid inclusion leakage, is presented in Chapter 5.

Another important aspect of the water chemistry is the comparison of ion ratios between various boreholes. From Table 4-3 it would appear that if V1 and V2 are characteristic of one type of

water, then boreholes N1 and E1 are a mixture of V1/V2 type with typical surface waters or shallow groundwaters. E1 is diluted much more with freshwater than N1 because the Br/Cl ratio of E1 is more like a shallow groundwater, and the total chloride concentration is less than N1. A regular trend in nearly all the ion ratios can also be seen in progressing from V1/V2 to the surface waters that indicates a mixture of two sources of dissolved ions. These trends are examined in more detail in Chapter 5.

4.8.7 Dissolved organics and microbial life

A study completed by J.L. Means (1981) showed that the dissolved organics in a water sample collected from an unspecified locality underground at Stripa contained low molecular weight fulvic acid fraction (<700 MW). Much more research is needed to understand the role of organic compounds at Stripa.

More interesting results came from a study by J.M. West (pers. comm.) on the microbiology of 2 samples of borehole water, M3 and the 100 - 505 m interval in V1. The M3 borehole sample was dominated by aerobic heterotrophs and contained smaller concentrations of anaerobic heterotrophs and denitrifying bacteria. These populations would indicate that some small amount of oxygen is present in M3, consistent with the high tritium values and the implication of recent recharge. The water sample from V1, however, contains almost no aerobic heterotrophs and a high concentration of anaerobic heterotrophs with a moderate concentration of denitrifying bacteria. V1 is clearly a more reduced water that can be considered anoxic.

5 WATER-ROCK INTERACTIONS

5.1 Introduction

Preliminary interpretations of water-mineral reactions have been discussed in a qualitative fashion in the earlier reports of Fritz, et al. (1979, 1980) and Nordstrom (1983a, b). In this chapter a more quantitative picture is described based on a much more extensive set of water analyses that have undergone quality control review. There is no question that reactions of the groundwater with the bedrock have taken place to a considerable extent, altering its chemistry, and making interpretations difficult. Several of these reactions can be identified using chloride correlation plots, chemical equilibrium computations, and fluid-inclusion data. Equilibrium computations were done with the WATEQ3 program (Ball, et al., 1980, 1981). The results of these investigations indicate that it is possible to explain the origin and evolutionary processes of the groundwater chemistry by interactions between infiltrating meteoric freshwaters with the crystalline bedrock, such as the granite and the leptite.

5.2 Chloride correlations and mineral reactions

In most hydrogeochemical processes, chloride acts in a strongly conservative manner. It enters into precipitation-dissolution only at high-salt (brine) concentrations, and it rarely enters into oxidation-reduction reactions or adsorption reactions (Feth, 1981). It is, therefore, frequently used as a conservative tracer in deciphering hydrochemical processes. The groundwater chemistry data at Stripa covers a large range of chloride concentrations, and depth profiles are not meaningful due to their heterogeneity. Hence, chloride can be used as a tracer to define the amount of loss (or gain) of other constituents, as well as a normalizing factor to interpret possible sources of saline constituents.

5.2.1 Alkali metals: Na, K, Li

Sodium is frequently conserved in hydrochemical processes in which it is strongly associated with chloride. For example, sodium is preferred over chloride as a reference element for studying fractionation of elements in atmospheric processes (Duce and Hoffman, 1976), and Eugster (1980) has shown that over a large range of evaporative concentration, saline lakes can be strongly

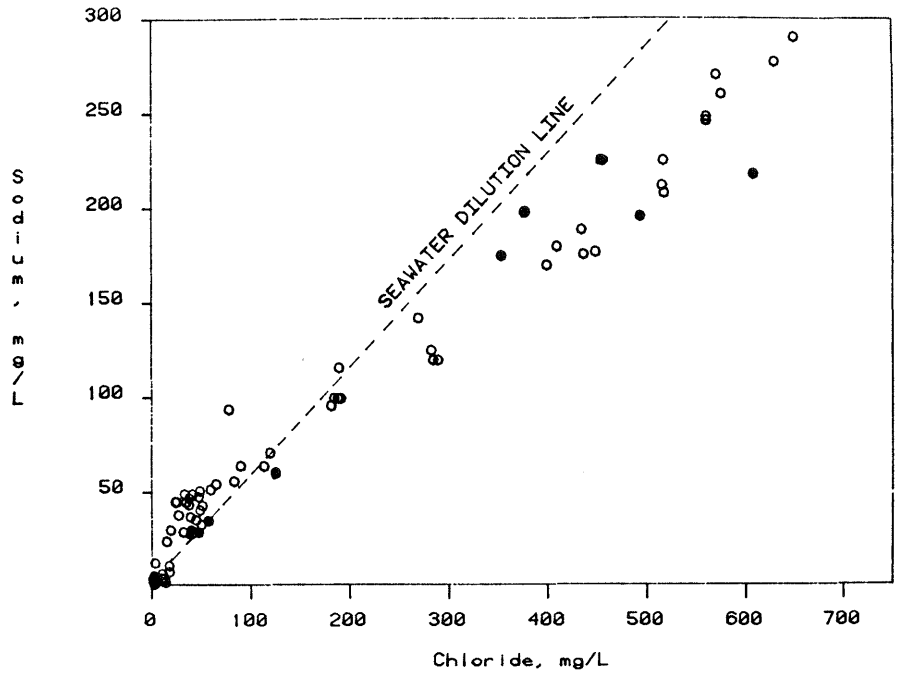

Figure 5-1. Plot of sodium against chloride concentrations. Narrow interval samples representing single water-bearing fracture zones are shown by closed circles in this and following plots.

conservative with respect to both sodium and chloride. There is also evidence for the conservative nature of sodium in natural water during weathering (Graustein, 1981) under certain conditions.

Figure 5-1 plots sodium against chloride for the Stripa waters, and a fairly constant increase is apparent that could be interpreted as a mixing line (showing a small loss of sodium compared to the seawater dilution line). Many of the borehole intervals were so large that mixing did occur between different water-bearing fracture zones in the borehole. To determine whether single fracture zones deviate from this apparent mixing line, the narrow intervals are shown as closed circles. From this comparison (and from several other elements) there is no significant deviation from the mixing line for the individual water-bearing zones within the analytical uncertainty of the data. Hence, there are no major losses of sodium during mixing. Comparison of the Na:Cl correlation with the ratio for seawater shows a trend that suggests a loss of sodium or gain of chloride compared to seawater streamwater mixtures. If this loss is real, it must have occurred before invasion of the saline waters into the Stripa granite, or there would have been a change in slope. The only change in slope that can be demonstrated is shown in the semi-log Na:Cl plot of Figure 5-2. At around 40 mg/L chloride, the sodium values intersect from a steep slope at low concentrations to a lower slope at higher concentrations. This slope change at

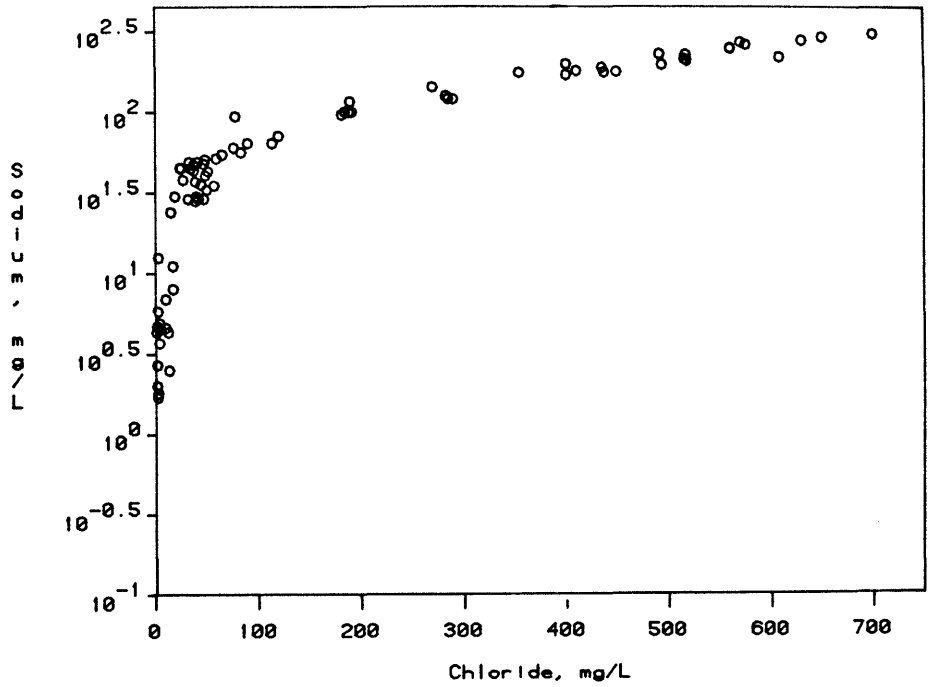

Figure 5-2. Semi-log plot of sodium against chloride concentrations.

40 mg/L chloride is consistent with a few other constituents. For example, the Br/Cl ratio becomes constant above 40 mg/L chloride. This point may mark the change from shallow weathering processes to deep seated processes that are characterized by a different set of reactions. The lower slope that correlates with chloride means that the main source of sodium at higher concentrations is a salty component, and it is not primarily derived from feldspar weathering.

Lithium also shows a similar increase with chloride as sodium, again suggesting a mixing line (Figure 5-3). The lithium concentrations do not cover a very large range, but they are strongly enhanced over the seawater dilution line. Lithium also tends to be conservative in dilute waters, and this is suggested by the Stripa data.

Potassium shows an entirely different trend. There may be a slight increase in potassium at the very highest chloride values (Figure 5-4), but most of the values are fairly low and constant regardless of chloride. This strongly nonconservative trend suggests that the source of the chloride has little or no potassium associated with it, and that either a steady-state weathering rate or a mineral solubility equilibrium is controlling the potassium concentrations. WATEQ computations show that these waters are both undersaturated and supersaturated with respect to illite. However, it is felt that the uncertainties in (a) the solubility product constant for illite, (b) some of the aluminum determinations, and (c) some of the potassium determinations are

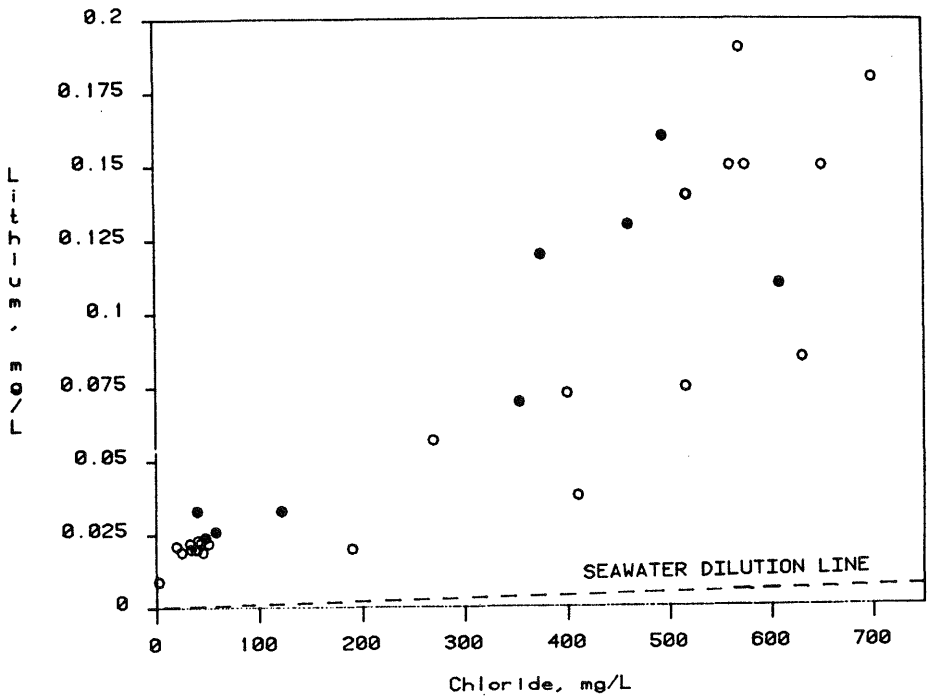

Figure 5-3. Linear plot of lithium against chloride concentrations.

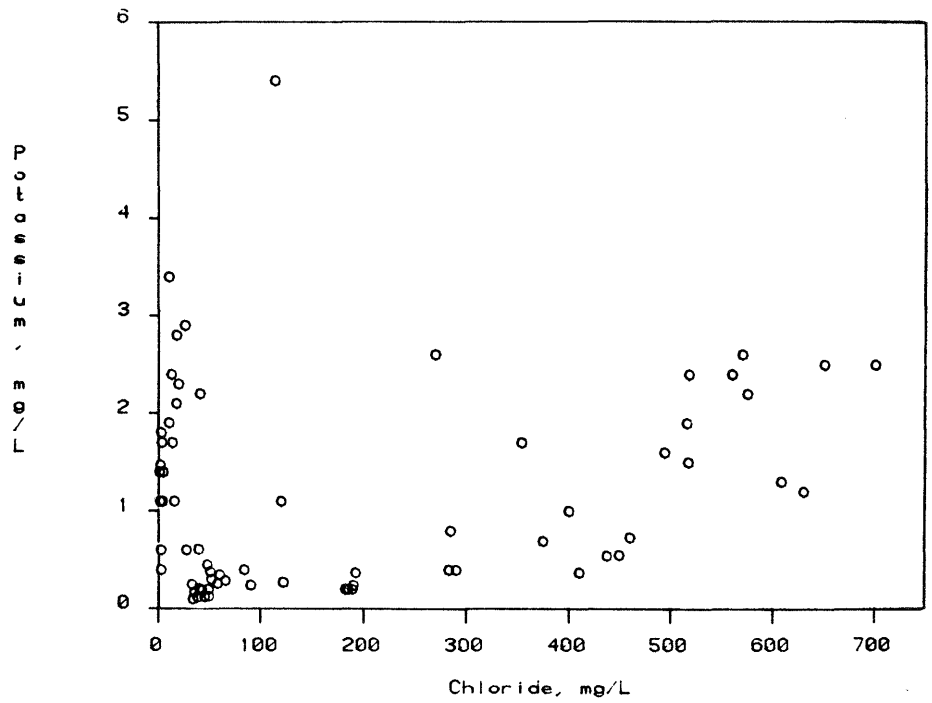

Figure 5-4. Plot of potassium against chloride concentrations.

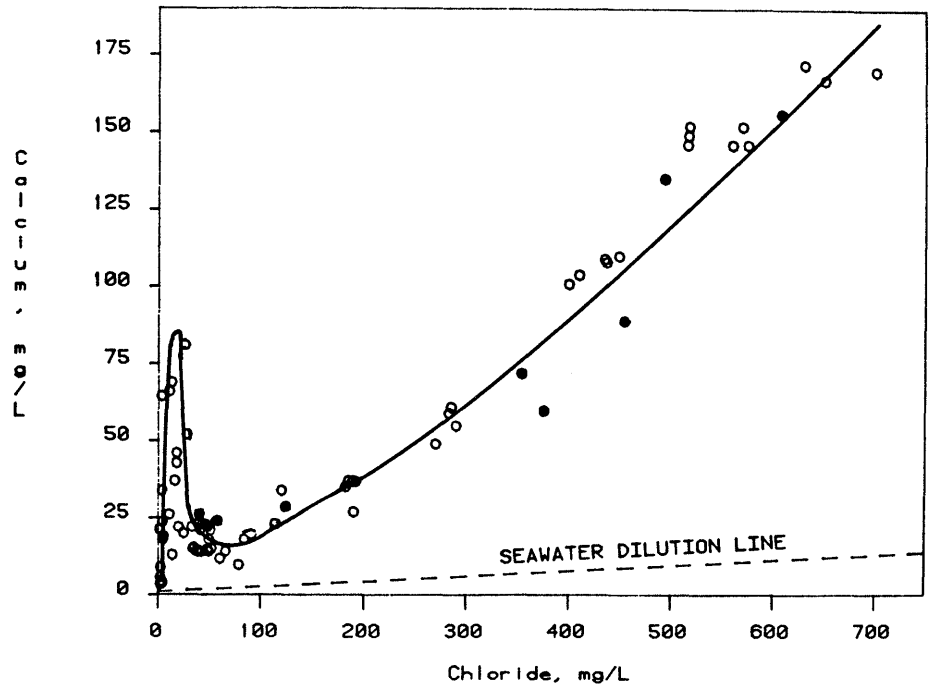

Figure 5-5. Plot of calcium against chloride concentrations.

such that it is difficult to claim equilibrium saturation for this mineral. This solubility control appears likely, but is not proven.

5.2.2 Alkali-earth metals (Ca, Mg, Sr, Ba) and carbonate geochemistry

The correlation plot for calcium against chloride, shown in Figure 5-5, has several significant features. The general trend with depth (see Figure 5-7) shows increasing calcium concentrations to a depth of about 100 m where the concentrations peak, and then they decrease with increasing chloride to about 50 mg/L chloride (strikingly close to the change in slope for the sodium vs. chloride plot). Thereafter a steady, almost linear, increase is observed that corresponds to depths of about 360 m (N 1 borehole) and deeper. The Ca/Cl slope is strongly enhanced above the seawater dilution line. The initial increase in calcium at less than 100 m depth suggests calcite dissolution up to saturation where the peak in the curve occurs. Having reached calcite saturation, the groundwater then precipitates calcite at increasing chloride concentrations. This evolutionary sequence is similar to that outlined by Fritz, et al. (1979) and Jacks (1978).

The pH of groundwaters is often regulated by equilibria in the $CaO-CO_2-H_2O$ system, i.e., by calcite solubility, CO_2 solubility, and the aqueous carbonate equilibria. The general features of this equilibria in groundwater have been described by Langmuir (1971) and summarized by Freeze and Cherry (1979). A schematic evolutionary diagram applicable to Stripa is shown in Figure 5-6.

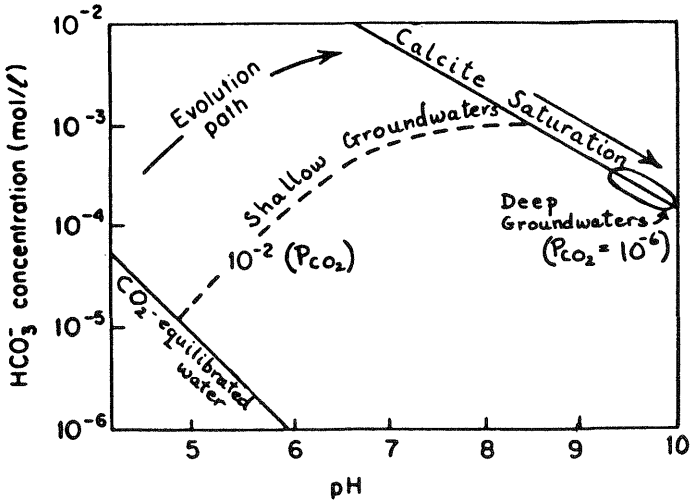

Figure 5-6. Schematic evolutionary diagram of bicarbonate, pH and P_{CO_2} during calcite dissolution.

Shallow dilute groundwaters have pH values near 6, and carbon dioxide partial pressures (P_{CO_2}) about 10^{-2} bars. Under these conditions, calcite is unstable and tends to dissolve under partially closed conditions to reach the high pH values of around 8 at saturation. If calcite then begins precipitating, the pH should be maintained close to 8. The deep groundwaters, however, have pH values of 9-10, and the calcium concentrations have increased considerably. This unusual situation is displayed more clearly in Figure 5-7 where the plots for calcium, bicarbonate, pH and calcite saturation index (S.I.) are shown as a function of chloride concentration. The S.I. is defined as the log of the ion activity product, AP, divided by the solubility product constant, K (Drever, 1982). The bicarbonate alkalinity mimics the first part of the calcium curve, reaching a peak at around 200 mg/L and then steadily decreasing at higher salinities, suggesting calcite precipitation is active over the remaining range of salinity. This interpretation is confirmed by the S.I. for calcite which shows undersaturation for the most dilute groundwaters less than 100 m depth, reaching saturation at a pH of 8 (coincident with the peaks in the bicarbonate and calcium curves). The S.I. continues to increase to one-half an order of magnitude supersaturated where it remains constant in spite of increasing calcium concentrations. This behavior can be explained if the bicarbonate concentrations are decreasing due to calcite precipitation which in turn is being driven by calcium input from some other source. Calcium input may be derived from the weathering of plagioclase feldspar or from the same saline source as the chloride. The strong correlation of calcium with chloride suggests the latter is the dominant process. It is important to note, however, that feldspar weathering must play a role to maintain the high pH values and part of the calcite supersaturation. The rise to pH = 8 can be accounted for by closed-system calcite dissolution, but once saturation is reached, calcite precipitation will not allow the pH to increase any further. The fact

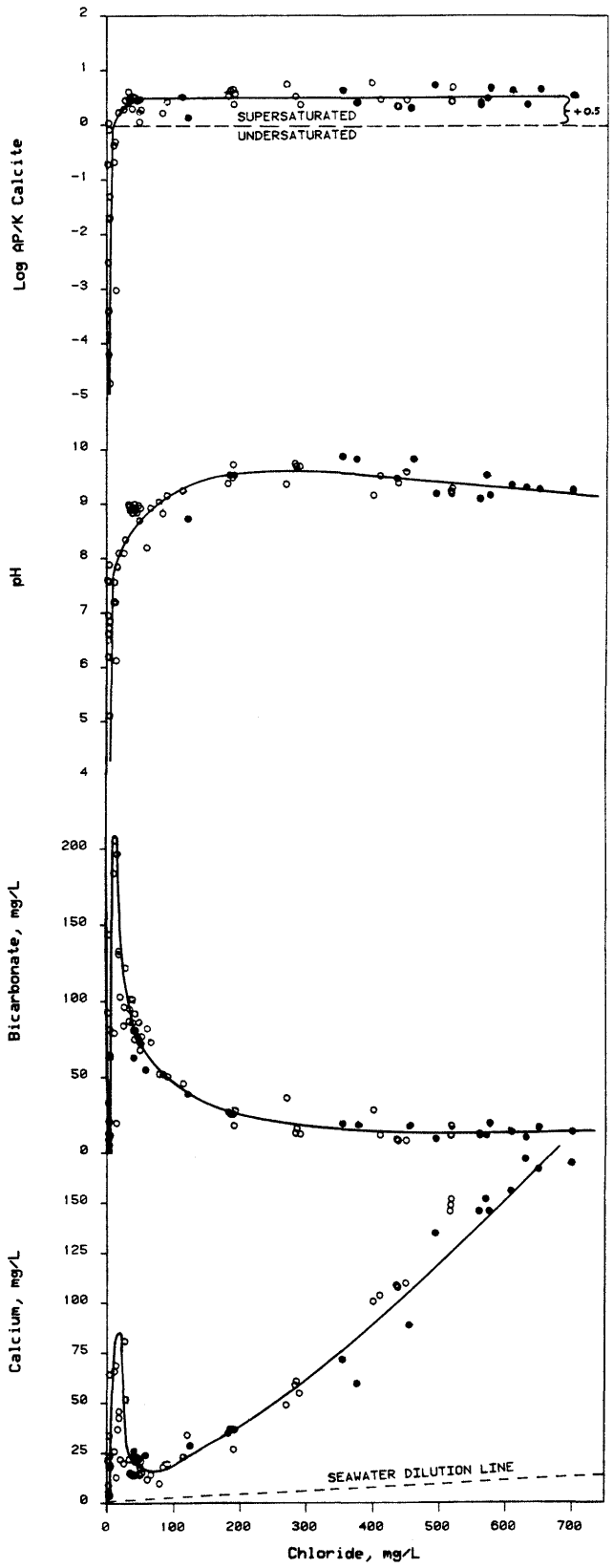

Figure 5-7. Trends in carbonate geochemistry with Cl concentrations.

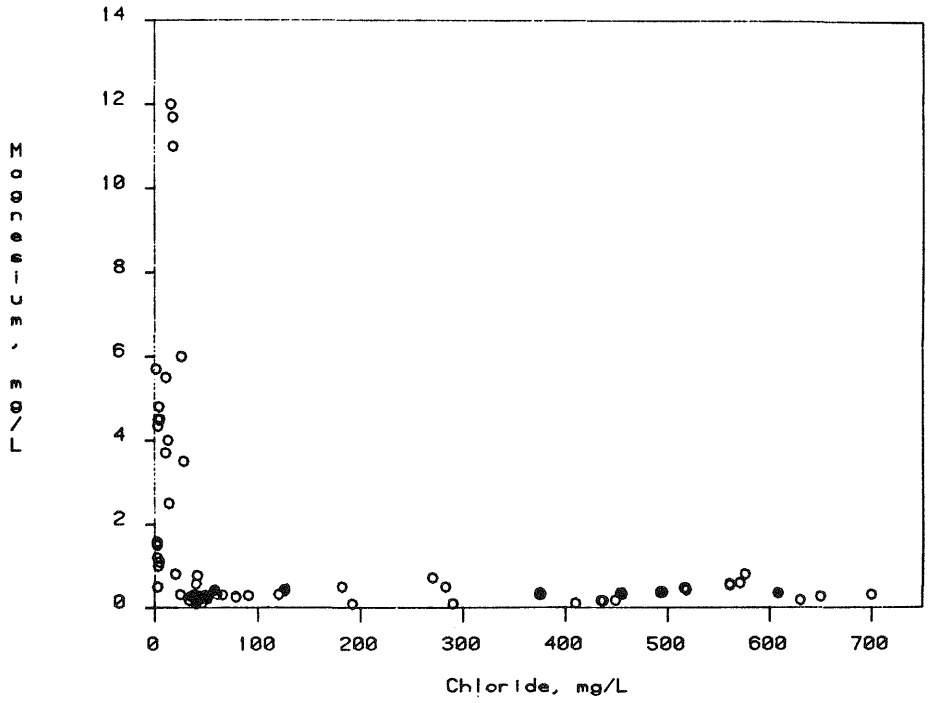

Figure 5-8. Plot of magnesium against chloride concentrations.

that the pH continues to increase to almost 10 suggests that silicate (feldspar) hydrolysis is the primary factor behind calcite precipitation until the calcium concentrations begin to increase again. At that point the saline input may be just as important as feldspar dissolution in maintaining calcite supersaturation.

The degree of calcite supersaturation shown in Figure 5-7 is probably a real supersaturation because errors in the thermodynamic data (Plummer and Busenberg, 1982), and the analytical data (shown by the scatter in the points) are less than this amount. The combined error from these two sources does not exceed about 0.25 log units, which is about half of the degree of supersaturation.

This outline of the carbonate geochemistry of deep groundwaters at Stripa complements and extends the earlier discussions of Jacks (1978), and provides a general picture that should be applicable to most deep groundwaters in crystalline rocks of similar salinity.

Magnesium concentrations range from 2-12 mg/L in the shallow subsurface, and generally reflect chemical weathering of magnesium silicates by carbonic acid (Keller et al., 1963). As the carbonate alkalinity decreases below about 50 mg/L, the magnesium is fixed below 1 mg/L. This change in magnesium concentration corresponds to about 40 mg/L chloride, shown in Figure 5-8, which also corresponds to the change in slope of the sodium: chloride plot. The strong lack of correlation with chloride suggests a

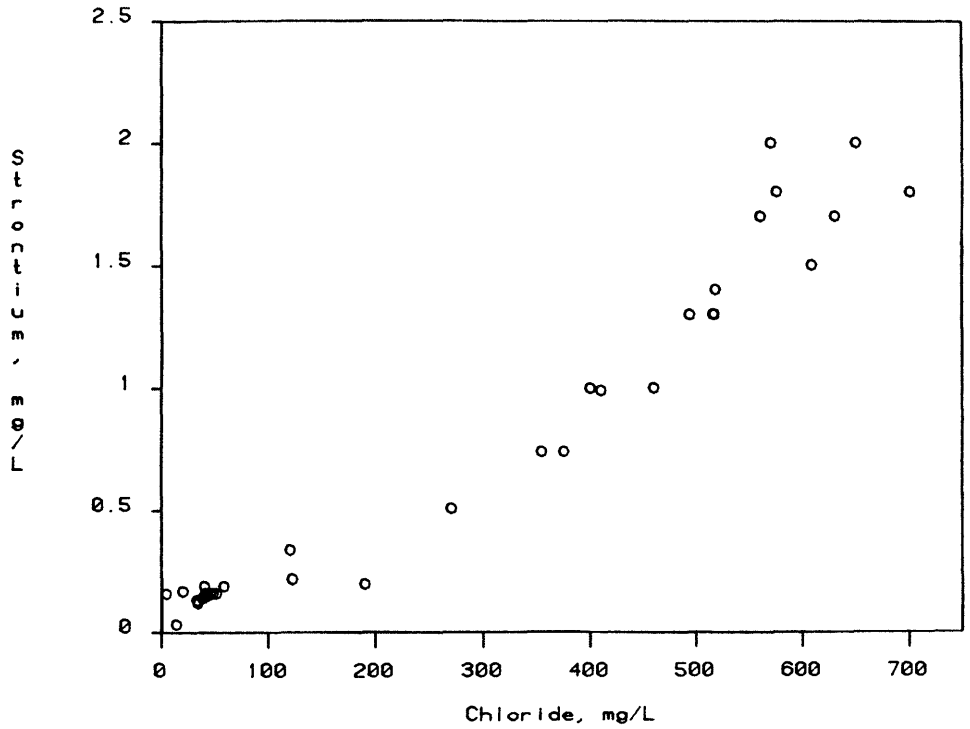

Figure 5-9. Plot of strontium against chloride concentrations.

greatly reduced weathering rate of magnesium silicates at depths greater than about 100 m and a possible solubility control. WATEQ computations for the S.I. values of sepiolite, $Mg_4Si_6O_{15}(OH)_2 \cdot 6H_2O$, and pure Mg-chlorite (magnesium-clinochlore, both 7A and 14A), $Mg_5Al(Si_3Al)O_{10}(OH)_8$, indicate a range of a few orders of magnitude covering both undersaturation and supersaturation. The range of S.I. primarily reflects the complexity of the mineral formula and, secondarily, the uncertainties in the analytical determinations of magnesium and aluminum which are larger than the uncertainties in most other constituents. Even with improved analytical data no firm conclusions could be drawn because the range of Fe-Mg, Al-Fe, and Al-Si substitution in chlorite produces such a range of solubility (as well as increased uncertainties) as to be obviously ambiguous. S.I. computations for magnesite, $MgCO_3$, and dolomite, $CaMg(CO_3)_2$ are all undersaturated for the whole range of chloride concentrations.

The plot in Figure 5-8 does make an important point, however, that at chloride concentrations up to 700 mg/L there is no corresponding increase in the magnesium concentrations. Sodium and calcium both increase in spite of calcite precipitation, but magnesium doesn't increase, not even where the magnesium silicate saturation values are 1-2 orders of magnitude undersaturated. This observation suggests that little or no magnesium is being contributed along with sodium, calcium, and chloride from the saline source. The magnesium content is orders of magnitude lower than the calcium content, and can't be simply explained by ion exchange phenomena. This result contrasts sharply with the inter-

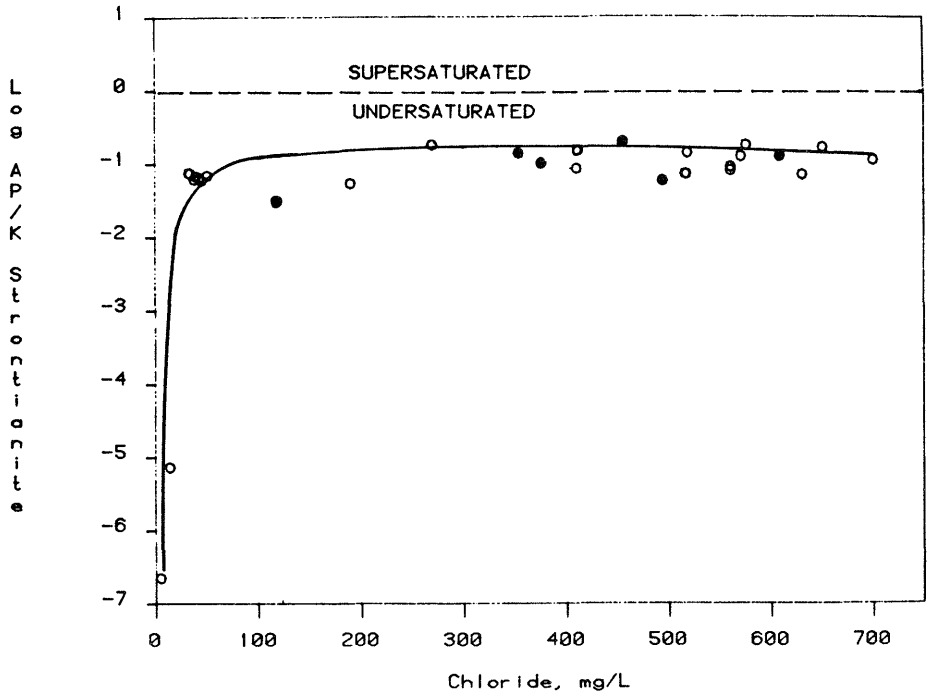

Figure 5-10. Plot of the S.I. for strontianite against chloride concentrations.

pretation of Jacks (1978), and will be discussed further in Section 5.3.

Strontium in natural waters might be regulated by the solubility of celestite, $SrSO_4$, or strontianite, $SrCO_3$. The chloride correlation plot in Figure 5-9 shows an increase in strontium comparable to the plots for sodium and calcium. Strontium is an important component of the saline source. All of the Stripa waters are undersaturated with respect to celestite because of the relatively low salinity of these waters, and because celestite is more soluble than strontianite. The S.I. values for strontianite are plotted in Figure 5-10, and demonstrate a constant undersaturation of about one order of magnitude for all the water samples. Other than a small amount of substitution into calcite there is no solubility control on strontium concentrations. The constant amount of undersaturation most likely reflects the constant S.I. of calcite and the removal of carbonate alkalinity by calcite precipitation. The carbonate content is kept so low that strontianite saturation is simply never reached.

Barium does not correlate with chloride as shown in Figure 5-11. The highest barium concentrations are found in the four short interval samples of the N 1 borehole. N 1 borehole waters also contain some of the highest concentrations of H_2S (up to 0.03 mg/L), and these results may indicate enough sulfate reduction is occurring in N 1 so that barite might dissolve. The S.I. values for barite shown in Figure 5-12 indicate barite undersaturation in all but the deepest (V 1 and V 2) boreholes where satura-

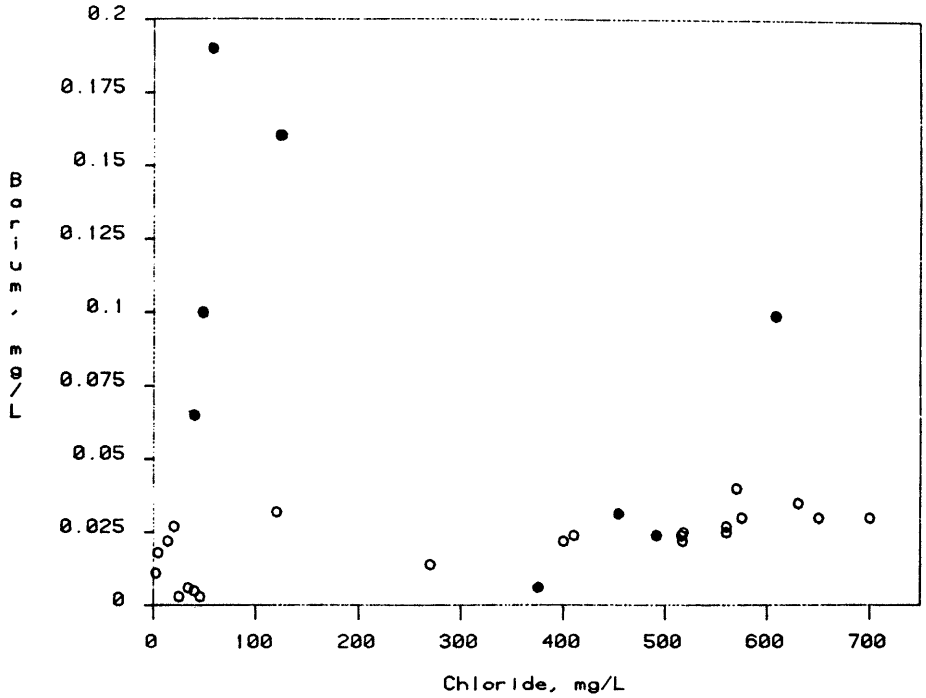

Figure 5-11. Plot of barium against chloride concentrations.

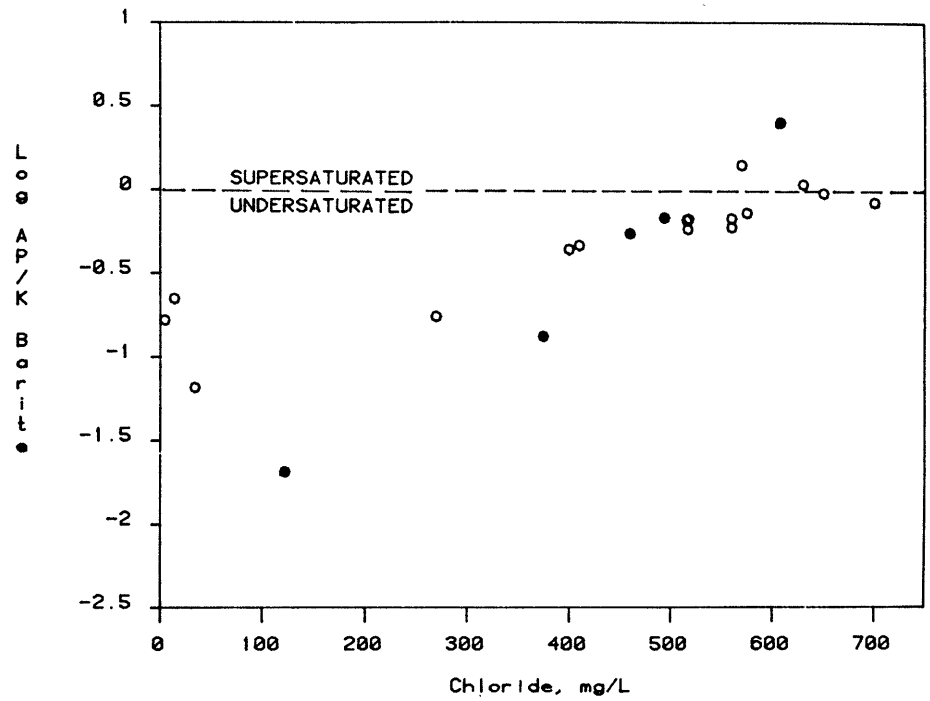

Figure 5-12. Plot of the S.I. for barite against chloride concentrations.

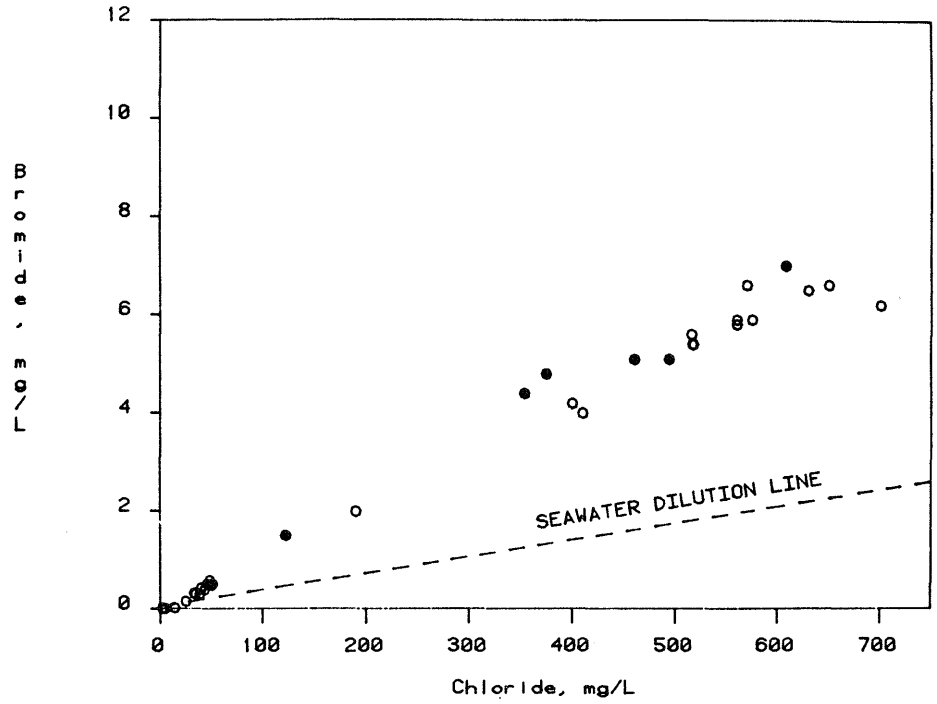

Figure 5-13. Plot of bromide against chloride concentrations.

tion is reached. This saturation equilibrium would explain the low and constant concentration of barium at the higher chloride concentrations.

5.2.3 Halogens (F, Cl, Br, I) and fluorite solubility

Both bromide and iodide correlate very strongly with chloride, and Br/Cl and I/Cl ratios are strongly enhanced relative to seawater (Figures 5-13 and 5-14). The seawater dilution curve for iodide is congruent with the horizontal axis for the scale shown in Figure 5-14. These linear correlations are strong evidence for a simple mixing of a saline source with fresh groundwaters. The saline source might be the intrusion of a saline aquifer from somewhere originally external to the Proterozoic bedrock, or it might be internal to it, i.e., it might be salt from within the granite and leptite being leached. This latter possibility does not mean that two water bodies are mixing, but rather that the bulk groundwater is mixing with a source of salt whose water volume is negligible relative to the bulk groundwater. The former possibility should show distinct trends in D and ^{18}O isotope content with salinity, and the latter possibility wouldn't. In any event, two-component mixing is indicated, and bromide and iodide are associated with the saline source.

Fluoride shows no correlation with chloride and strongly indicates a mineral reaction-controlling process (Figure 5-15). The mineral fluorite is fairly common as a fracture-filling, and would provide an obvious solubility control on fluoride concentra-

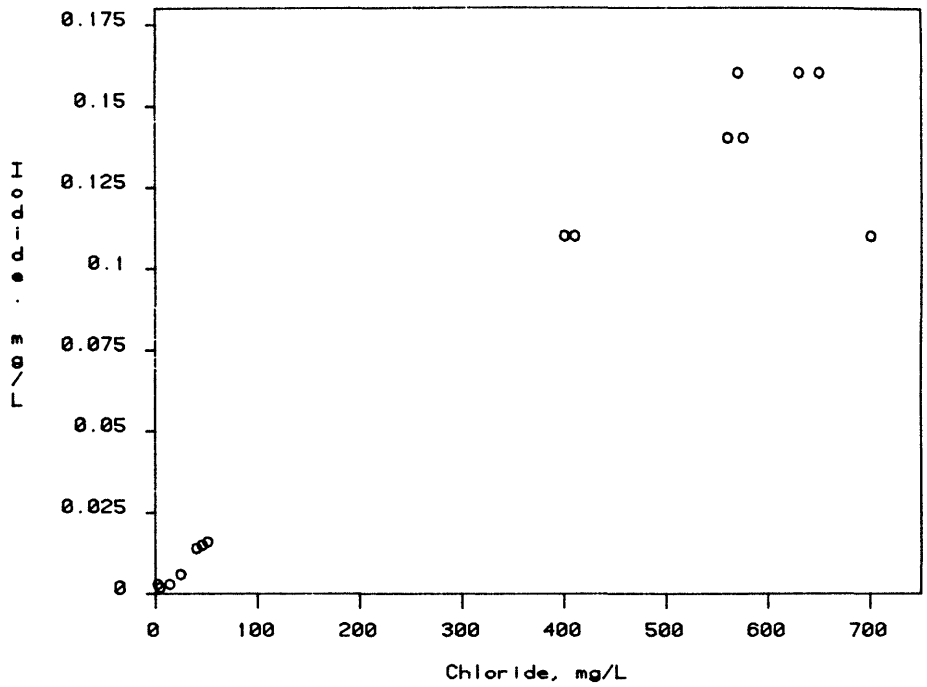

Figure 5-14. Plot of iodide against chloride concentrations.

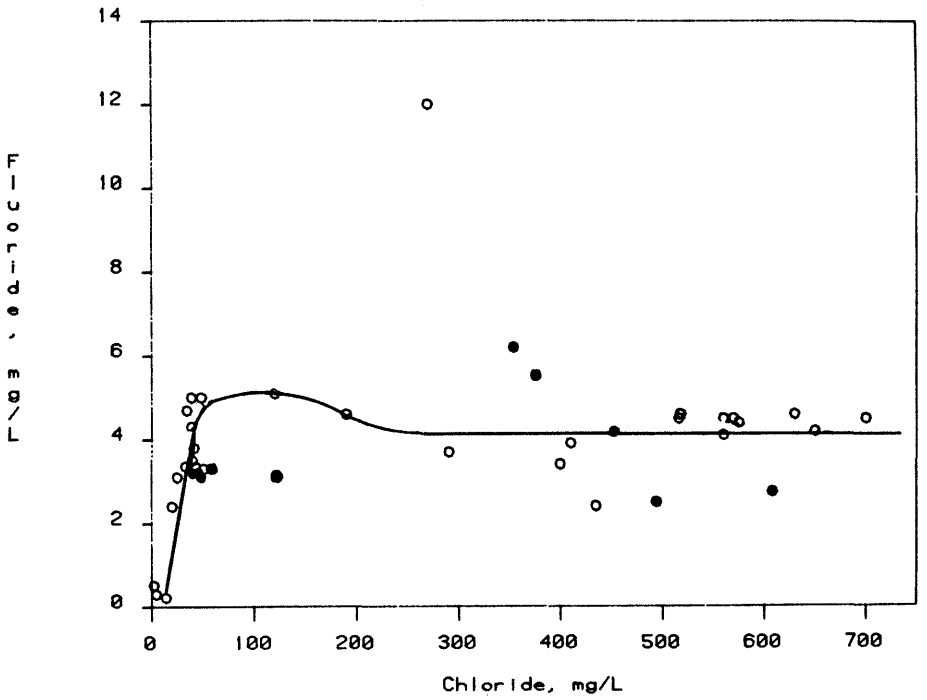

Figure 5-15. Plot of fluoride against chloride concentrations.

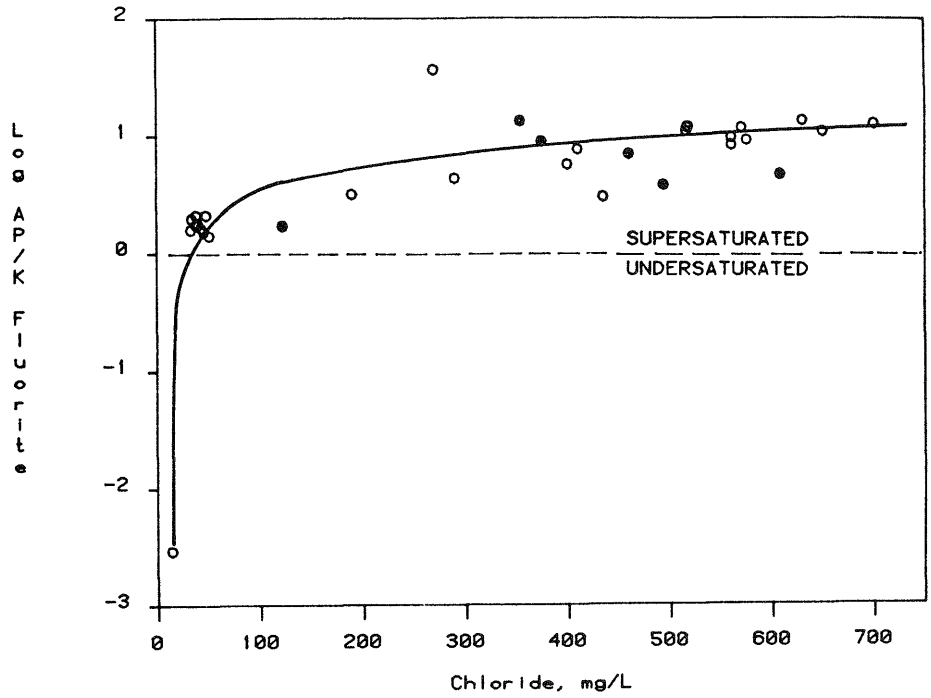

Figure 5-16. Plot of the fluorite S.I. against chloride concentrations.

tions. S.I. values for fluorite are shown in Figure 5-16 where up to an order of magnitude supersaturation exists, although the values are very constant with increasing chloride. The K_{sp} used for fluorite is believed to be about 0.3 log units too insoluble based on more recent data (see citations by Ball, et al., (1979). If this correction is made, the values would only be supersaturated by about one-half an order of magnitude just like the calcite S.I. values. It is difficult to say just how real this amount of supersaturation is, but it can be concluded that fluorite solubility controls the fluoride concentrations in the Stripa groundwaters, and that modern-day precipitation of fluorite in the fractures seems likely.

5.2.4 Aluminosilicate reactions

Although it has been mentioned that there are some large uncertainties in the aluminum determinations, partly due to contamination problems and partly due to analytical errors, it is nevertheless possible to make some constructive statements about aluminosilicate reactions.

Samples collected from V 1, V 2, R 1, and M 3 boreholes between June and November, 1981, have more reliable aluminum values than the rest of the samples analyzed. These particular samples have been analyzed for aluminum by three different analysts and by two, three, or sometimes four independent methods. The values are generally in agreement within about 10%. WATEQ computations

on these sample results show consistent undersaturation with respect to gibbsite, and random under- and oversaturation with respect to kaolinite. It is safe to say that gibbsite solubility does not play a role in regulating aluminum concentrations, and that some more complex aluminosilicate phase probably is. Kaolinite, chlorite, illite, smectite, or a combination of these, may be important as solubility controls, but neither the thermodynamic data nor the precision on the aluminum, potassium, or magnesium concentrations allow such statements to be made with much certainty.

A noteworthy observation that came out of the WATEQ computations is the consistent slight supersaturation with respect to prehnite and laumontite in all of the V 1 and V 2 waters. These two minerals are very common fracture-fill minerals in granitic rocks (e.g., Tullborg and Larson, 1982; Kerrich, 1984), and are commonly found in geothermal mineral assemblages of 100-350°C (Bird, et al., 1984) along with wairakite, epidote, and chlorite. The WATEQ results indicate these minerals are also present in the Stripa granite (and leptite) fractures, although they haven't yet been identified. The presence of laumontite generally indicates low-temperature metamorphism up to about 200°C, and prehnite and epidote indicate temperatures of 200-350°C (Zen and Thompson, 1974; Bird and Helgeson, 1981; Bird, et al., 1984). Both in progressive burial metamorphism and in geothermal alteration, the appearance of large amounts of chlorite usually occurs at temperatures of 150°C and higher (Boles and Franks, 1979; Zen and Thompson, 1974). In fact, prehnite, wairakite, laumontite, and epidote are important "zone markers" or "index minerals" for the intensity of alteration by temperature and pressure gradients (Schiffman, et al., 1984; Zen and Thompson, 1974). Epidote and chlorite are common in the Stripa fractures, and the occurrence of laumontite and prehnite should be expected from the above discussion. Further fracture mineralogical studies should be done to find if they occur.

5.2.5 Iron chemistry and redox potentials

Nineteen of the Stripa groundwater samples have had Fe(II) and Fe(III) determinations made, and fourteen of these also have Eh measurements so that a direct comparison can be made between the redox potential measured with the platinum electrode, Eh(Pt), and the Fe(II/III) redox potential, Eh(Fe). The Fe(II/III) potential is calculated after correcting for the distribution of species and activity coefficients with the WATEQ program in the same manner as Nordstrom, et al. (1979). The comparison in Figure 5-17 shows that there is a rather poor correlation. The iron concentrations (nearly always below 0.060 mg/L) are simply too low to adequately equilibrate at the electrode surface. A few samples compare rather well, and this may be due to waiting a longer pe-

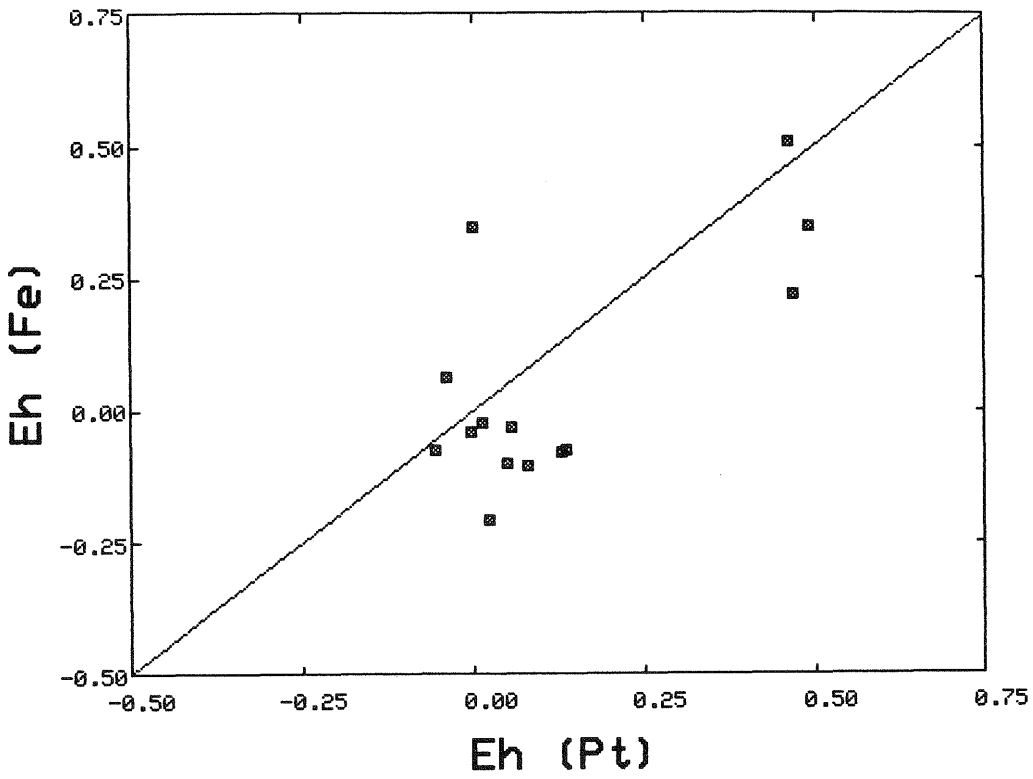

Figure 5-17. Comparison of the platinum electrode potential, Eh(Pt), against the ferrous-ferric redox potential, Eh(Fe) in volts. The straight line represents the 1:1 correlation.

riod of time for the electrode measurement to reach a steady value. It is very common for the electrode to slowly drift toward lower potentials, and the drift rate seems to decrease with time as it approaches the calculated Fe(II/III) couple. More analyses and more careful electrode measurements might improve the correlation, but they won't change the conclusion that these waters are very poorly poised. With respect to radioactive waste containment, this means that leaking radionuclides are likely to dominate the redox reactions, and reaction rates will be more important than equilibrium processes. It also means that there is very little dissolved iron to react with and coprecipitate radionuclides.

Since both $Fe^{2+}_{(aq)}$ and $Fe^{3+}_{(aq)}$ can be measured in these groundwaters, and their activities calculated, it is possible to examine directly the saturation state of both reduced and oxidized iron minerals. It is noteworthy that in many samples the concentration of $Fe^{3+}_{(aq)}$ is as large as, or larger than, the concentration of $Fe^{2+}_{(aq)}$. In Figure 5-18 the saturation indices for ferri-

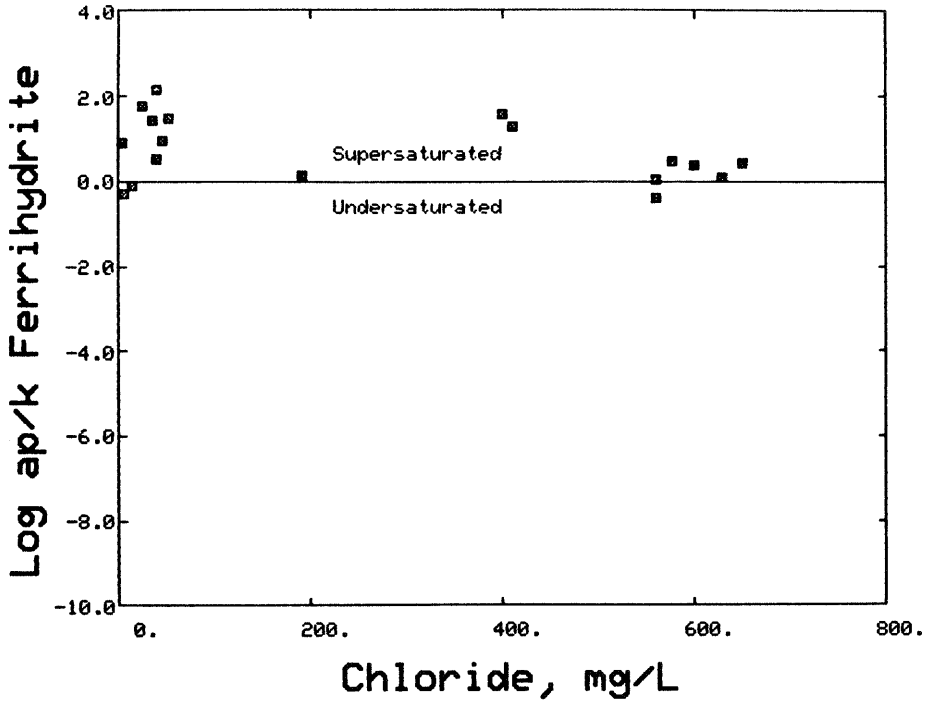

Figure 5-18. Plot of the ferrihydrite S.I. against chloride concentrations.

hydrite are plotted against chloride concentrations. Ferrihydrite is a poorly crystalline form of ferric hydroxide with a pK of 37-39 (Schwertmann and Taylor, 1977). This mineral phase has commonly been confused with amorphous ferric hydroxide, and the research of Schwertmann (1979) indicates that "amorphous" ferric hydroxide usually turns out to be ferrihydrite. The WATEQ S.I. computations use the most soluble pK for ferrihydrite, and according to Figure 5-18, the water samples are either saturated or supersaturated by up to two orders of magnitude. This amount of supersaturation seems unreasonable, and it is concluded that some of the samples must be contaminated with iron, either from drilling or sampling. Three important observations indicate that active precipitation of ferric hydroxides within the boreholes is governing the iron chemistry and the iron redox potentials: (1) ferrihydrite supersaturation is common; (2) the lowest iron redox potentials tend to correlate with the lowest $Fe^{3+}_{(aq)}$ concentrations, as they should; and (3) some of the more recent platinum electrode potentials are as low in Eh as the lowest iron redox potentials shown in Figure 5-17. Hence, the iron chemistry may be dominated by active precipitation of ferrihydrite, and only careful long-term monitoring of a continuously flowing borehole might provide true background values of ferrous and ferric iron.

5.2.6 Sulfate

The data for sulfate shows slightly different trends compared to other ions that may be due to either a different source of sulfa-

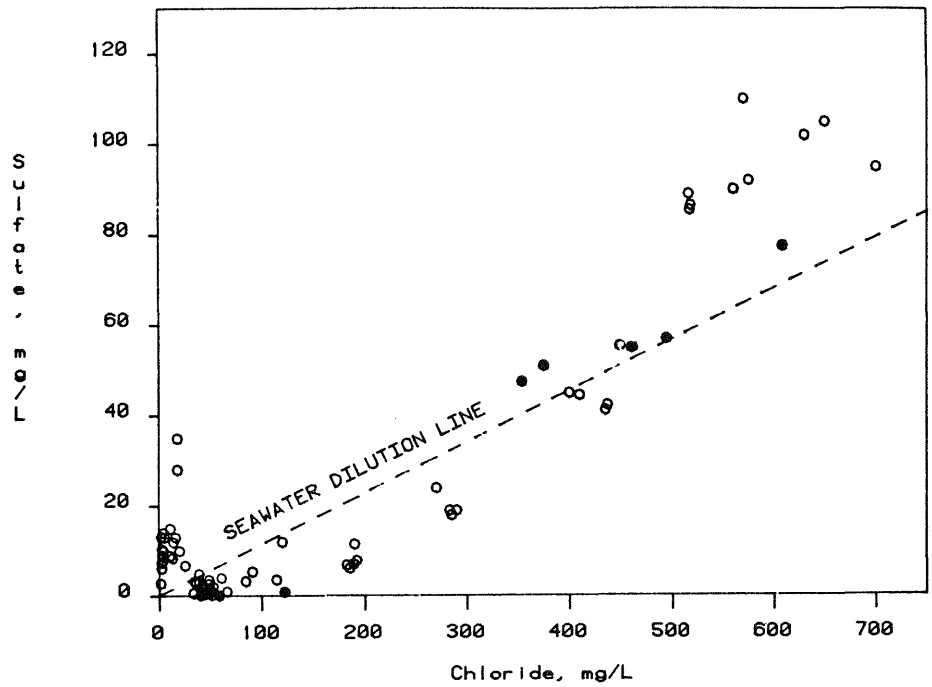

Figure 5-19. Plot of sulfate against chloride concentrations.

te or the effect of redox processes, or a combination of both. The chloride correlation plot for sulfate is given in Figure 5-19.

Clearly sulfate increases with increasing chloride, but it seems to increase in an almost exponential fashion, rather than linearly.

This observation may be more apparent than real, but the higher salinity waters do have a higher SO_4/Cl ratio than the lower salinity waters, and the lowest ratios are encountered in the N 1 borehole. This may indicate that sulfate reduction is more important in the N 1 borehole than for the deeper borehole samples, assuming that a single source of salinity with a distinct SO_4/Cl ratio exists. This suggestion finds some corroboration in the sulfate stable isotope data (Chapter 7).

5.3 Chemical geothermometers

It was mentioned in Chapter 4 that the Br/Cl, Ca/Mg, and Mg/Cl ratios of the deep groundwaters are anomalous compared to typical Swedish groundwaters and marine-derived water. The possibility of a temperature signature in the water chemistry was also mentioned. These anomalies will now be further explored.

5.3.1 Ca/Mg and Mg/Cl ratios

The magnesium concentrations in the Stripa groundwaters are extremely low, resulting in very high Ca/Mg ratios and very low Mg/Cl ratios. These ratios tend to be 1-2 orders of magnitude different than those for any other type of low-temperature groundwater regardless of origin or age. That is to say, given any type of original water chemistry and an unlimited amount of time, groundwaters do not achieve these anomalous ion ratios seen in the Stripa groundwaters, with one exceptional group. From this observation we can infer that ion exchange and clay formation do not alter the Ca/Mg and Mg/Cl ratios to the extreme values found at Stripa. The exceptional group is geothermal waters. As a group, geothermal waters are the only ones which have similar ratios. This can be explained and demonstrated in three ways: (1) by empirical field observation, (2) by experimental observation, and (3) by theoretical calculation.

Geothermal chemists have pointed out for many years that high Ca/Mg ratios are indicators of high temperatures. White (1970) pointed out that high Ca/Mg ratios are characteristic of high-temperature systems because Mg strongly favors solid phases such as chlorite and smectite at high temperatures, whereas the ability of Mg to react at low temperatures decreases greatly. Hence, seawater, oilfield brines of moderate temperatures, and water in contact with ultramafics have much higher Mg content than any high-temperature groundwater. Another process that affects Ca/Mg and Mg/Cl ratios is dolomitization. However, the change in these ratios during dolomitization do not approach the Stripa values, and Hitchon *et al.*, (1971) pointed out that the statistical relationship between Ca and Mg was not simple, suggesting that dolomitization was not the only process occurring in the western Canadian plains.

Graphical demonstration of the effect of temperature on Ca/Mg and Mg/Cl ratios was first shown by Fournier and Potter (1979) for 50 well waters, and can be seen more quantitatively in Figures 5-20 and 5-21. Approximately 255 groundwater analyses of all types that have *in situ* temperature measurements (or silica geothermometer temperatures) are plotted as log(Ca/Mg) (weight ratio) and log(Mg/Cl) against 1000/T where T is the Kelvin temperature. These are in the form of Arrhenius plots for convenience and increased linearity. The groundwater samples are taken from the published literature, and include both low- and high- temperature groundwaters, carbonate and silicate aquifers, freshwater and brine compositions, and very old and very young waters. The sources of data are given in Table 5-1. In spite of the very large range of groundwater age and composition, it is clear that temperature is the overriding factor affecting the Ca/Mg and Mg/Cl ratios. Note the distinct increase in Ca/Mg and decrease in Mg/Cl above about 100°C. These plots support the observation that Mg is a very temperature-sensitive parameter.

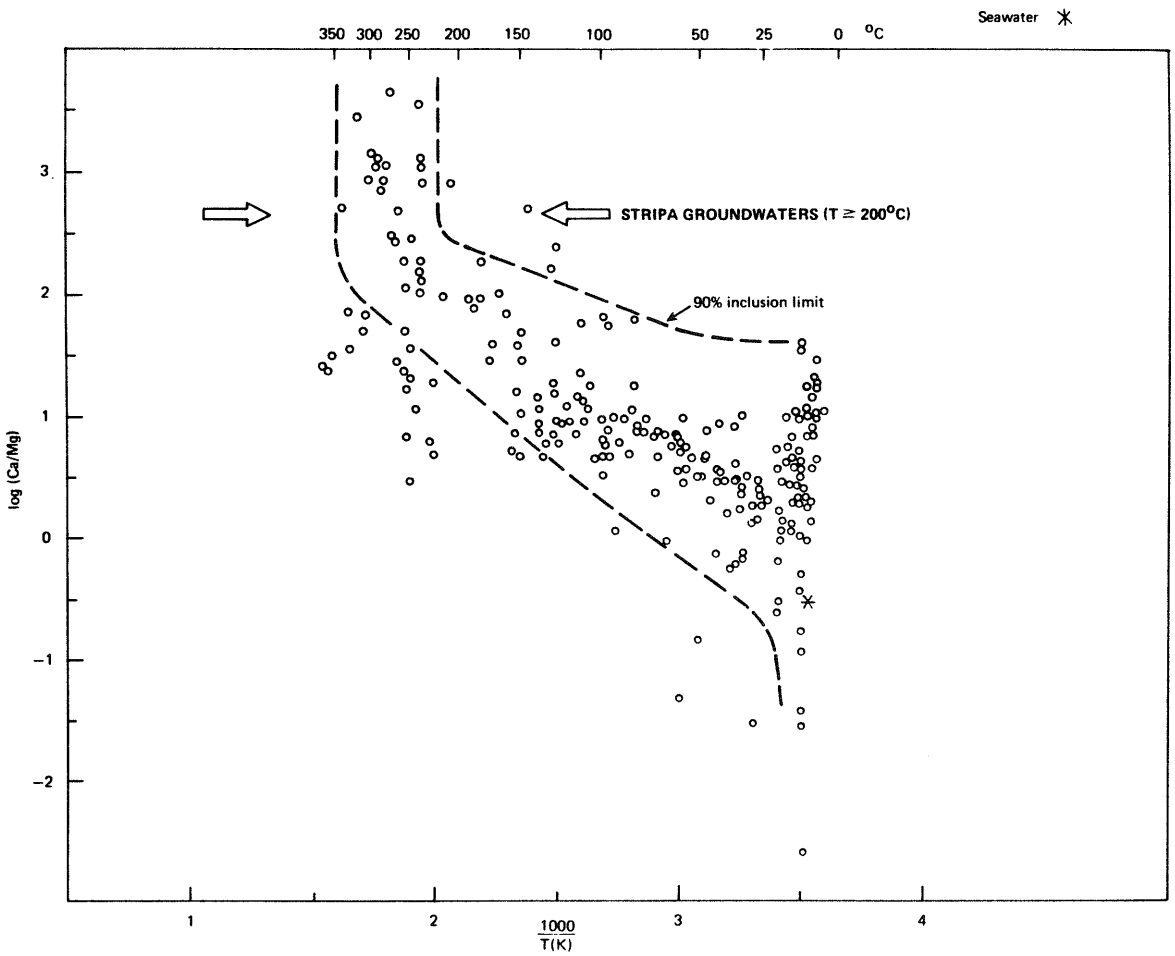

Figure 5-20. Plot of log (Ca/Mg) against 1000/T.

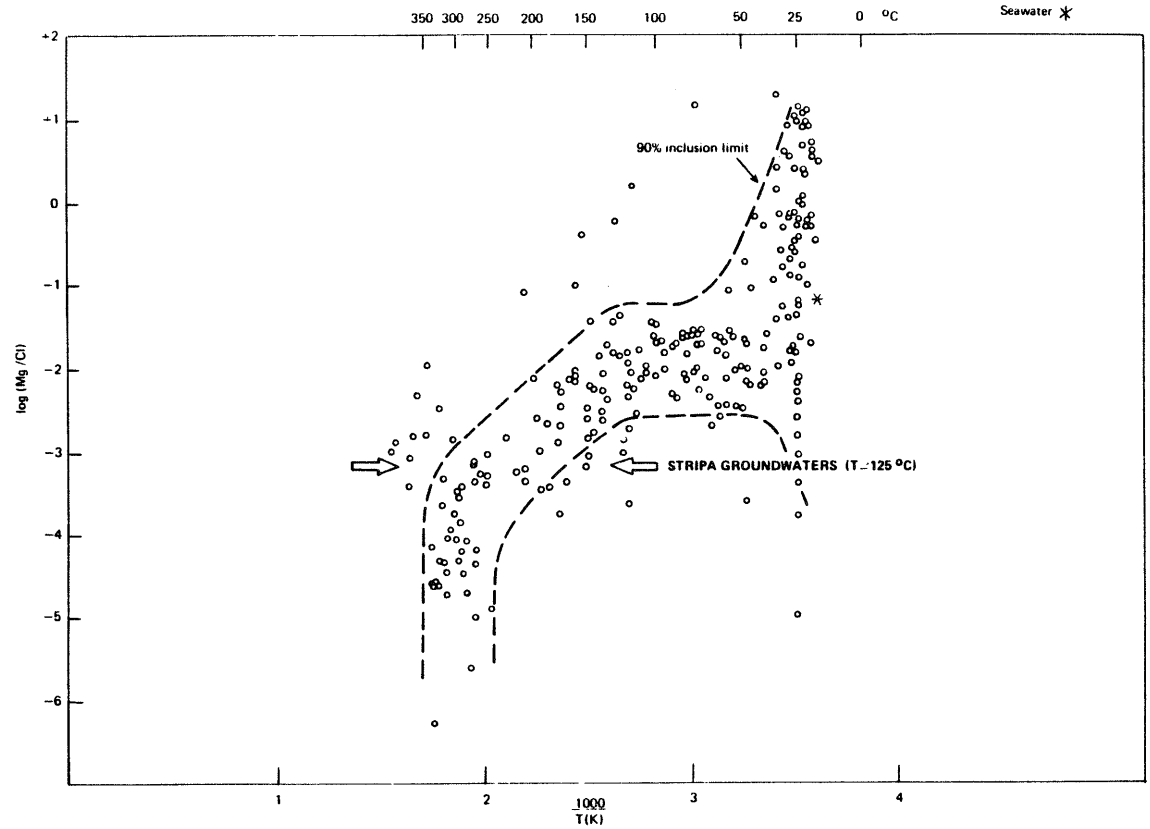

Figure 5-21. Plot of log (Mg/Cl) against 1000/T.

Table 5-1. Literature sources for data plotted in Figure 5-20 and 5-21.

Arnorsson, S., Björnsson, A., Gislason, G. and Gudmundsson, G. (1975), in Proc. Second United Nations Symposium on the Development and Use of Geothermal Resources 2, 853-864.

Arnorsson, S., Gronvold, K. and Sigurdson, S. (1978) Geochim. Cosmochim. Acta 42, 523-536.

Back, W. (1966) U.S. Geol. Survey Prof. Paper 498-A, 42 pp.

Barnes, I., Downes, C. J. and Huston, J. R. (1978) Am. J. Sci. 278, 1412-1427.

Brown, D. W. and Gulbrandsen, R. A. (1973) J. Res. U.S. Geol. Survey 1, 105-111.

Capuano, R. M. and Cole, D. R. (1982) Geochim. Cosmochim. Acta 46, 1353-1364.

Feth, J. H., Roberson, C. E. and Polzer, W. L. (1964) U.S. Geol. Survey Water-Supply Paper 1535-I, 170 pp.

Fusillo, T. V. and Voronin, L. M. (1981) U.S. Geol. Survey Open-File Report 81-814, 38 pp.

Helgeson, H. C. (1968) Am. J. Sci. 266, 129-166.

Hem, J. D. (1970) U.S. Geol. Survey Water-Supply Paper 1473, 363 pp.

Hitchon, B. and Friedman, I. (1969) Geochim. Cosmochim. Acta 33, 1321-1349.

Hitchon, B., Billings, G. K. and Klovan, J. E. (1971) Geochim. Cosmochim. Acta 35, 567-598.

Kharaka, Y. K., Callender, E. and Carothers, W. W. (1977), in Proc. Third Geopressured-Geothermal Energy Conference, 1, 121-165.

Kharaka, Y. K., Carothers, W. W. and Brown, P. M. (1978) Soc. Petroleum Eng. AIME 7505, 5 pp.

Kharaka, Y. K., Lico, M. S., Wright, V. A. and Carothers, W. W. (1979), in Proc. Fourth United States Gulf Coast Geopressured-Geothermal Energy Conference: Research and Development, 168-193.

Langmuir, D. (1971) Geochim. Cosmochim. Acta 35, 1023-1045.

Miller, T. P., Barnes, I. and Patton, W. W., Jr. (1975) J. Res. U.S. Geol. Survey 3, 149-162.

Robertson, E. C., Fournier, R. O. and Strong, C. P. (1975), in Proc. Second United Nations Symposium on the Development and Use of Geothermal Resources, 1, 553-561.

Rye, R. O. and Haffty, J. (1969) Econ. Geol. 64, 629-643.

Truesdell, A. H., Thompson, J. M., Coplen, T. B., Nehring, N. L. and Janik, C. J. (1981) Geothermics 10, 225-238.

White, A. F., Claassen, H. C. and Benson, L. V. (1980) U.S. Geol. Survey Water-Supply Paper 1535-Q, 34 pp.

White, D. E. (1968) Econ. Geol. 63, 301-335.

White, D. E. (1981) Econ. Geol. 75th Ann. Vol., 392-423.

Mineralogical evidence from field studies in both geothermal areas associated with magmatism and/or tectonics and geothermal areas associated with deep basin burial metamorphism indicate that large quantities of chlorite/montmorillonite are produced as the temperature increases above 100-150°C (Boles and Franks, 1979; McDowell and Elders, 1983; Ellis and Mahon, 1977). Chlorite formation at high temperatures removes large quantities of magnesium from the fluid phase.

Several experimental water-rock investigations have shown that large depletions in dissolved magnesium result from chlorite formation (Hawkins and Roy, 1963; Ellis and Mahon, 1967; Bischoff and Dickson, 1975; Dickson, 1977; Mottl and Holland, 1978; Seyfried and Bischoff, 1979; Seyfried and Mottl, 1982) regardless of rock type. In all of these experiments at 150°C or higher, magnesium was strongly depleted due to the growth of a magnesium silicate phase.

Thermodynamic equilibrium computations also support the strong temperature dependence of the Ca/Mg and Mg/Cl ratios. A notable example is the work of Ryzhenko, et al. (1981) in which the affect of pressure, temperature, CO_2 and rock/water ratio were varied in equilibrium computations involving a rock of granitic and another of basaltic composition. One of the results was that magnesium was strongly depleted under nearly all conditions when the temperature increased and when the rock/water ratio increased.

These investigations demonstrate that orders of magnitude variations in Ca/Mg and Mg/Cl ratios, especially when compared to seawater, can only be accounted for by high-temperature formation of magnesium silicates, generally chlorites, and cannot be representative of low-temperature clay formation or ion exchange processes.

5.3.2 Na-K-Ca and silica geothermometers

The classical Na/K, Na-K-Ca, and silica geothermometers are good temperature indicators for geothermal waters (Ellis and Mahon, 1977). Unfortunately, low-temperature re-equilibration prevents the use of the silica geothermometer, and re-equilibration may easily affect the Na/K and Na-K-Ca geothermometers, given sufficient time. It is noteworthy that when the Ca correction to the Na/K geothermometer is applied, the calculated temperature increases by at least several tens of degrees. However, the calculated temperatures fall in the range of 10-28°C, only slightly higher than the actual measured temperatures. This geothermometer, if reliable, reflects a low temperature origin.

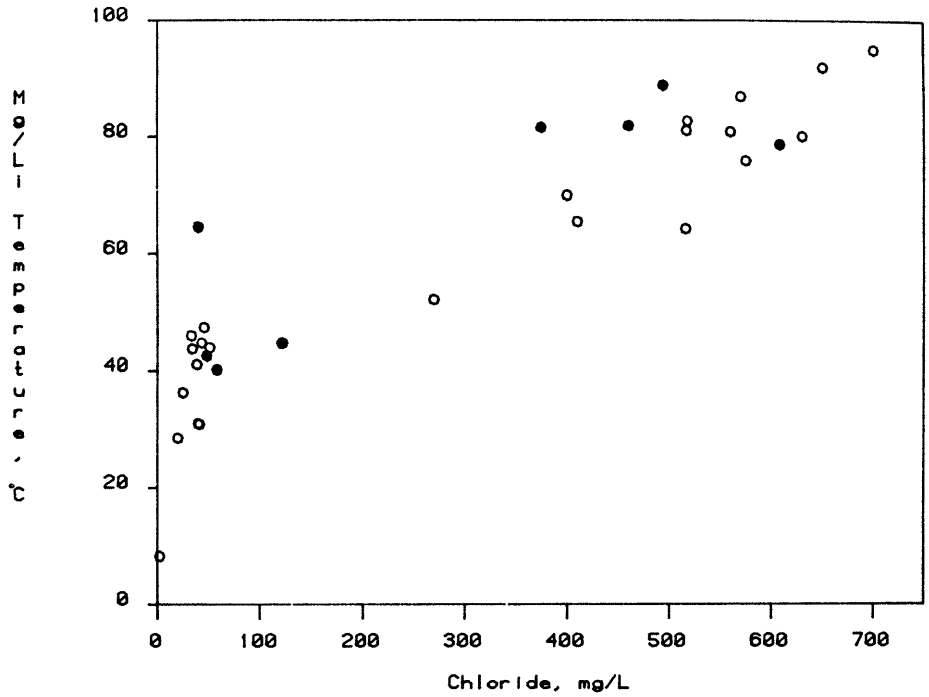

Figure 5-22. Mg/Li geothermometer temperature against chloride concentrations.

5.3.3 The Mg/Li geothermometer

A new geothermometer has been described by Kharaka, et al. (1985) that has been found to be reliable over the range of 40-350°C and often gives the best results for temperatures of 40-70°C. This geothermometer takes advantage of the fact that Li tends to increase with temperature, whereas Mg decreases with temperature, according to the empirical equation:

$$t(^{\circ}C) = \frac{1900}{4.67 + \log(\sqrt{Mg/Li})} - 273$$

where the magnesium and lithium concentrations are in mg/L. A plot of the Mg/Li temperatures against chloride concentrations is shown in Figure 5-22 for the Stripa groundwaters. A consistent trend is apparent, indicating temperatures of 80-95°C at the highest chloride concentrations. These temperatures overlap significantly with some of the fluid-inclusion homogenization temperatures in the Stripa granite. Although the correlation in Figure 5-22 reflects a mixing line, the saline end-member appears to carry a high-temperature signature.

5.3.4 Conclusions from geothermometry

Several ion ratios are anomalous in the Stripa groundwater chemistry. These ratios, such as Ca/Mg, and Mg/Cl, are difficult to explain by low-temperature processes such as clay-mineral formation. They are consistent, however, with processes that occur at high temperatures. Since high temperatures have not occurred at Stripa for several millions of years, these anomalies might be explained by the leakage of fluid inclusions from the Stripa granite (and/or the leptite). Fluid inclusions incorporated in the granite would carry a high-temperature signature and, if they leaked into the groundwater regime, would explain a high-temperature signature in a low-temperature environment. One of the most direct approaches to test such a hypothesis is to leach fluid inclusions from the granite and compare the Br/Cl ratios of the leachate with those in the groundwater.

5.4 The fluid-inclusion hypothesis and rock-leaching studies

5.4.1 Introduction

Fluid inclusions are common in igneous and metamorphic rocks, but they are rarely larger than 1 mm and frequently go unnoticed. They can account for more than 50% of the chloride content of granitic rocks (Fuge, 1979), and they have the potential for playing a role in water-rock interactions when the rock/water ratio becomes very high (i.e., very low porosity). In two comprehensive reviews Roedder (1972, 1984) has discussed nearly all aspects of fluid inclusions, and these references should be consulted for further details.

If fluid inclusions might enter into a groundwater system, then several general questions must be addressed, such as: Can they leak? How? How fast? Are there enough fluid inclusions? Do they contain sufficient salt content?

Although no one has specifically addressed the question of whether fluid inclusions can leak significantly into groundwater systems, Roedder and Skinner (1968) did address the general question as to whether they leak during sample preparation or experimentation. They concluded that if adequate care was used in sample preparation, leakage was rare, but leakage due to surficial fractures formed during inadequate sample preparation was responsible for earlier reports of widespread leakage. Sawing, grinding, and polishing rock samples can produce surficial microfractures which penetrate the sample by more than 1 mm.

Fracturing the granite can easily lead to exposure of large quantities of fluid inclusions, both directly and by slow leakage,

from microfractures. Leakage may occur either by diffusion or by mass transport. Diffusion through solid mineral grains is too slow of a process to be important. Diffusion along microcracks would be driven by the concentration gradient if the inclusions were more saline than the groundwater. Microfractures, likely to be abundant near major fractured zones, might be large enough for mass movement of the fluid. If a small volume of groundwater flows by a large surface area of rock (a typical situation in deep crystalline rocks) containing abundant inclusions, then the accumulation of some salinity from this source seems quite probable.

Another important observation is the common occurrence of fluid inclusions as planar structures in crystalline rock. These fluid-inclusion planes are usually secondary features which reflect the microfracturing and rehealing of the rock. Such fluid-inclusion planes cut across mineral grain boundaries, and are parallel to and coincident with microjoints[1]. Wise (1964) found evidence for younger, smaller planes of fluid inclusions reopening older fluid-inclusion planes. These older planes represent Precambrian joint systems, and they controlled the orientation of subsequent fracturing during Laramide orogeny (late Cretaceous to early Tertiary). Dale (1923) found numerous examples of fluid-inclusion planes that were parallel and coincident to microfractures in granites and gneisses from New England. He provides some striking examples of fluid-inclusion planes becoming microfractures of the same strike and dip. Large numbers of very small inclusions have been found on mineral grain boundaries of fractured mineral surfaces by electron microscopy (Sella and Deicha, 1962a,b, 1963).

Microcracks and micropores are common in igneous rocks, and have been investigated for their effect on the physical properties of the rock, especially electrical resistivity, compressibility, and permeability (Brace, et al., 1972). Relatively few microcracks are induced by drilling (Nur and Simmons, 1970), and the effects of surface grinding and polishing can be removed by ion thinning (Brace, et al., 1972; Sprunt and Brace, 1974). These microcavities have been found both along grain boundaries and within mineral grains (Sprunt and Brace, 1974), they have been found to connect, to form larger microcracks when placed under subcritical stress (Tapponier and Brace, 1976), they are more common in rocks with a higher water content than those that are "drier" (Montgomery and Brace, 1975), and they are more abundant in sodic feldspar than in quartz or potassium feldspar (Sprunt and Brace, 1974; Montgomery and Brace, 1975). This last observation is particularly important because many of these microcavities are identical in description to fluid inclusions, and are

---

[1]Microjoints are not necessarily microscopic in character, but rather a distinct size class of jointing on a small scale.

thought to be fluid inclusions by Sprunt and Brace (1974) and Montgomery and Brace (1975); and yet little is known about fluid inclusions in feldspars. Most fluid-inclusion studies are done on relatively transparent minerals, such as quartz, fluorite, and calcite. Feldspars are notoriously difficult to study for fluid inclusions because of their opacity, and nothing is really known about the distribution of inclusions between quartz and feldspars in a granite. If the results of Montgomery and Brace (1975) are valid for most granites, then the density of fluid inclusions in sodic feldspar must be considered greater than in coexisting quartz grains, and the volume contained by fluid inclusions could take up to 2% of the feldspar. Fluid inclusions may be, in fact, the reason for the turbid, opaque appearance of feldspars (Folk, 1955) and the milky white appearance of quartz (Roedder, 1972, 1984).

Thus, fluid-inclusion planes can be zones of weakness where fracturing has a higher probability of occurring, and fractured groundwater zones would have direct access to the highest density of fluid inclusions. This close relationship between fluid-inclusion planes and microfractures/microjoints could make the accessibility of fluid inclusions to the groundwater nearly instantaneous in response to tectonically- or anthropogenically-derived changes in rock stress. It may not be necessary for fluid inclusions to be transported any significant distances in order for them to mix with the groundwaters; only microfracturing needs to occur. The microfracturing would depend on tectonic events and man-made disturbances. The amount of inclusion fluid in the groundwater may depend upon the rate of microfracturing relative to the groundwater flow rate, in addition to the length of the flow path and the rock/water ratio.

Investigations of fluid inclusions in the Stripa granite have followed along three complementary lines: (1) direct measurements of fluid inclusions by standard techniques, (2) chemical analysis of inclusions by leaching studies, and (3) microcavity porosity and salinity measurements.

5.4.2 Fluid-inclusion measurements and volumetric considerations

The fluid-inclusion study by Lindblom (1984) that is summarized in Chapter 2, has demonstrated that there should be more than sufficient fluid-inclusion salt in the Stripa granite to account for the salinity of the groundwater, assuming near-static hydrologic conditions. There is, on the average, 17 liters of inclusion fluid per cubic meter of granite, assuming that there is a comparable amount of inclusions in feldspars as in quartz. This fluid averages around 3 wt. % NaCl or about 0.0105 wt. % Cl for the granite. In other words, there is about 278 grams of chloride per cubic meter of granite. The porosity of the granite is about 1%, i.e. about 100 times more rock than water. Hence, there are

278 grams of chloride per 10,000 cubic centimeters of groundwater. Assuming static groundwater conditions, that would produce a concentration of 28 g/L chloride if all the fluid inclusions were opened. The maximum observed concentration is 700 mg/L, which only requires about 2.5% of the total fluid-inclusion chloride. Therefore, on volumetric grounds it is certainly feasible for fluid inclusions to be the primary source of chloride in the Stripa groundwaters. A simple test of this hypothesis is to compare the Br/Cl and I/Cl ratios from fluid-inclusion leachates with those in the groundwater.

5.4.3 Preliminary fluid-inclusion leaching study

Nine samples of V 1 and V 2 drillcore were leached according to the procedures of Roedder, et al. (1963) and Hall and Friedman (1963). Rock fragments about 1 cm across were cleaned in a sonic bath (some samples were electrolytically cleaned until it was found that no further contaminants were removed by this additional step) and then vacuum dried, crushed in an iron pipe under vacuum, the water extracted, and the remaining fragments subject to a one-minute leach with doubly-distilled water. The leachate was filtered after one minute, and then another one-minute leach was obtained. Five or six successive leaches were made until the chloride concentrations were no longer detectable. Determinations of F, Cl, Br, and SO_4 were performed by ion chromatography, and I was determined by the standard colorimetric method based on iodide-catalyzed cerium reduction (Whittemore, pers. comm.).

The results and the average values for Br/Cl and I/Cl are shown in Table 5-2. The ratios for Br/Cl and I/Cl are consistently high and identical to the groundwater ratios. This comparison provides the strongest evidence yet for the association between fluid inclusions and the groundwater salinity.

5.4.4 Microfractures: porosity and salinity measurements

A cooperative investigation is underway (involving D.K. Nordstrom, I. Neretnieks and K. Skagius) to determine the porosity of microfractures and the salinity of the microfracture fluid in the Stripa granite. Cores taken from V 1 and V 2 are cored again along the length about every 3-4 cm. These smaller cores (60-90 cm^3) are leached in 7-10 ml of distilled water for two weeks, and then the solution is analyzed for Cl, Br, I, F, and SO_4. The core is then blotted dry, weighed, put under vacuum, then heated at 90°C for three days, and reweighed. The weight loss gives an estimate of the water content, and when combined with the chloride concentrations, they give an estimate of the chloride concentrations in the microfractures. Next, the core is ground up in a mortar and pestle to approximately 50-400 mesh

Table 5-2. Anion analyses on fluid-inclusion leachates of Stripa granite in preliminary study (in mg/L).

	Cl	Br	I	F	SO_4	Br/Cl	I/Cl x 10^4
V1-445A							
leach #1.	9.95	0.085	--	0.35	51	.0085	--
2.	3.60	0.037	--	0.49	29	.0103	--
3.	1.42	<.01	--	0.33	11	--	--
4.	0.31	<.01	--	0.17	3.6	--	--
5.	<0.12	<.01	--	0.16	2.1	--	--
6.	<0.12	<.01	--	0.18	1.2	--	--
V1-445B							
leach #1.	7.27	0.058	0.00165	0.31	0.17	0.0080	2.2
2.	2.86	0.027	--	0.34	0.10	0.0094	--
3.	0.57	<0.01	--	0.33	<0.1	--	--
4.	<0.1	<0.01	--	0.43	<0.1	--	--
5.	<0.1	<0.01	--	0.27	<0.1	--	--
V1-445C							
leach #1.	4.47	0.050	0.0021	0.21	1.6	0.0112	4.7
2.	2.11	<0.01	--	0.15	1.1	--	--
3.	0.36	<0.01	--	0.11	0.23	--	--
4.	<0.3	<0.01	--	0.09	0.15	--	--
5.	<0.3	<0.01	--	0.11	<0.1	--	--
6.	<0.3	<0.01	--	0.04	<0.1	--	--
V1-505							
leach #1.	6.18	0.082	0.0050	0.40	0.53	0.0133	8.1
2.	2.45	0.031	--	0.13	1.2	0.0127	--
3.	0.77	<0.01	--	0.08	0.27	--	--
4.	0.38	<0.01	--	<0.1	0.40	--	--
5.	0.28	<0.01	--	<0.1	0.26	--	--
V1-408							
leach #1.	2.79	0.027	0.001	0.18	0.70	0.0097	3.6
2.	3.11	<0.01	--	<0.1	0.15		
3.	0.50	<0.01	--	<0.1	0.11		
4.	0.50	<0.01	--	<0.1	0.071		
5.	0.31	<0.01	--	<0.1	<0.05		
V2-363							
leach #1.	8.78	0.090	0.0032	0.58	1.85	0.0103	3.6
2.	3.42	0.031	--	0.37	0.98	0.0091	--
3.	0.70	--	--	0.31	0.37	--	--
4.	0.34	--	--	0.29	0.29	--	--
5.	0.10	--	--	0.24	0.18	--	--
V2-404							
leach #1.	5.00	0.045	0.0019	0.45	0.53	0.0090	3.8
2.	1.87	0.017	--	0.22	0.24	0.0091	--
3.	0.58	<0.01	--	0.13	<0.05	--	--
4.	0.22	<0.01	--	0.11	<0.05	--	--
5.	0.24	<0.01	--	0.12	<0.05	--	--
V2-445							
leach #1.	4.70	0.049	0.0013	0.40	0.44	0.0104	2.8
2.	1.44	0.016	--	0.085	<0.05	0.0111	
3.	0.28	<0.01	--	0.40	<0.05	--	
4.	<0.1	<0.01	--	0.10	<0.05	--	
5.	<0.1	<0.01	--	0.28	<0.05	--	
V2-471							
leach #1.	3.69	0.035	0.0020	0.69	2.54	0.0095	5.4
2.	1.51	<0.01	--	0.45	0.76	--	
3.	0.56	<0.01	--	0.20	0.27	--	
4.	0.26	<0.01	--	0.20	0.29	--	
5.	0.20	<0.01	--	0.20	0.09	--	

Leachates:
Average Br/Cl = 0.0101($\pm$0.0015) n = 15
Average I/Cl = 4.28×10^{-4}($\pm 1.8 \times 10^{-4}$) n = 8

Groundwaters:
Average Br/Cl = 0.0107 ($\pm$0.001) n = 25
Average I/Cl = 4.46×10^{-4}($\pm 4.1 \times 10^{-4}$) n = 24

Table 5-3. Preliminary data on Stripa granite leachates for crushed and uncrushed samples.

	Cl(ug/g of rock) Uncrushed	Cl(ug/g of rock) Crushed	Microfracture salinity Cl(mg/l)
V11/1	2.6	11.2	3680
V11/3	1.3	20.6	862
V12/1	1.5	15.0	356
V12/3	0.61	10.4	492
V13/1	0.73	11.6	518
V13/3	6.8	9.2	5390
V21/1	1.7	18.9	1410
V21/3	3.8	17.5	3030
V22/1	2.6	19.9	2030
V22/3	3.2	17.6	2050
V23/1	3.3	13.7	4730
V23/3	2.3	14.8	3060

(0.3-0.03 mm diameter) and leached again in distilled water for 15 minutes, filtered, leached again in distilled water for 15 minutes, and filtered again. These measurements have been done on the same samples that were used for fluid-inclusion analysis by Sten Lindblom. Preliminary results, shown in Tables 5-3 and 5-4 demonstrate that the microfracture chloride concentrations are sometimes equal to, but usually greater than, the groundwater chloride concentrations, and less than the fluid-inclusion concentrations. These concentrations may not be the same as those that exist in situ, but this experiment does show that fluid inclusions can leak out of the rock matrix, and that fresh groundwater can enter microfractures and mix with the fluid inclusions. This premise is further verified by the halogen ratios summarized in Table 5-5. The Br/Cl and I/Cl ratios are nearly identical in the crushed and uncrushed samples, and nearly the same as the groundwater ratios. Thus, we have demonstrated an association between the salt in the inclusion fluid, in the microfracture fluid, and in the groundwater. It is very noteworthy that the I/Cl ratios that we have determined are higher than any recorded from the published literature on natural waters.

5.4.5 Literature survey of halogens in granites

Relatively little information is available on the halogen content and halogen ratios in granitic rocks. The lack of data is partly due to the very low concentrations of Br and I and the inherent difficulties in analyzing for them. Another reason may be lack of interest. A literature survey, however, has revealed some fascinating trends in halogen content and ratios.

Typical average halogen concentrations and ranges of measured values for granites are shown in Table 5-6. The water-soluble portion of the halogens is, of course, more important from a ground-

Table 5-4. Analyses of F, Cl, Br and SO_4 (in mg/L) for Stripa Granite Leachates. (a) is first leach, (b) is second leach. Number in parentheses refer to one standard deviation.

SAMPLE	F	Cl	Br	I	SO_4
V1,11	0.03	2.60	-	.0112	0.318
V1,11a	0.08	11.2	0.126	.0226	1.49
V1,11b	0.17	5.98	0.048	.0255	1.41
V1,13	2.10	1.26	0.016	.0094	0.701
V1,13a	0.74	20.6	0.240	.0393	1.84
V1,13b	1.31	5.73	0.126	.094	2.002
V1,21	2.22	1.55	0.014	.0044	0.391
V1,21a	1.11	15.0	0.190	.067	1.10
V1,21b	1.45	6.92	0.076	.250	1.54
V1,23	2.18	0.61	0.013	.0042	0.593
V1,23a	1.42	10.4	0.186	.192	1.37
V1,23b	1.59	2.65	0.055	.0117	1.33
V1,31	3.00	0.73	0.024	.0054	0.483
V1,31a	1.32	11.6	0.218	.0206	1.23
V1,31b	1.99	2.95	0.067	.107	1.54
V1,33	2.27	6.80	0.022	.0056	0.378
V1,33a	1.21	9.19	0.159	.0225	1.37
V1,33b	1.62	3.81	0.094	.0164	1.41
V2,11	1.35	1.73	0.022	.0057	1.02
V2,11a	0.60	18.9	0.234	.0246	2.40
V2,11b	0.61	8.82	0.078	.213	1.95
V2,13	1.59	3.84	0.033	.0053	0.860
V2,13a	0.78	17.5	0.126	.304	1.95
V2,13b	1.04	10.1	0.220	.071	2.20
V2,21	1.59	2.58	0.033	.0053	0.530
V2,21a	0.88	19.9	0.269	.0364	1.05
V2,21b	1.19	4.44	0.049	.0182	1.54
V2,23	1.54	3.24	0.033	.0077	0.546
V2,23a	0.56	17.6	0.140	.0284	1.82
V2,23b	1.12	13.7	0.220	.286	2.20
V2,31	0.061	3.26	0.011	.0059	0.362
V2,31a	0.14	13.7	0.213	.0497	2.17
V2,31b	0.31	35.6	0.153	-	2.79
V2,33	0.09	2.29	0.007	.0046	0.353
V2,33a	0.65	14.8	0.164	-	0.427
V2,33b	0.21	8.44	0.184	.0310	2.33
Mean, uncrushed	1.50(.975)	2.54(1.68)	.0210(.009)	.00623(.00214)	.545(.219)
Mean, crushed(a)	.791(.427)	15.0(3.88)	.189(.049)	.0734(.0910)	1.52(.547)
Mean, crushed(b)	1.05(.600)	9.10(8.94)	.114(.065)	.102(.101)	1.85(.461)

Table 5-5. Weight Ratios for Stripa Granite Leachates.

SAMPLE	SO_4/Cl	Br/Cl	$(I/Cl)x10^3$	I/Br
V1,11	.122	-	4.31	-
V1.11a	.133	.0112	2.01	.179
V1,11b	.236	.0080	4.26	.531
V1.13	.556	.0127	7.46	.588
V1.13a	.089	.0116	1.90	.164
V1,13b	.349	.0220	16.4	.746
V1,21	.252	.0090	2.84	.314
V1,21a	.073	.0126	4.45	.353
V1,21b	.222	.0110	36.1	3.29
V1,23	.974	.0213	6.90	.323
V1,23a	.131	.0178	18.4	1.03
V1,23b	.502	.0208	4.42	.213
V1,31	.661	.0328	7.39	.225
V1.31a	.106	.0188	1.77	.0945
V1,31b	.522	.0227	36.3	.491
V1,33	.056	.0032	.824	.254
V1,33a	.149	.0173	2.45	.142
V1,33b	.370	.0247	4.30	.174
V2,11	.590	.0127	3.29	.259
V2,11a	.127	.0124	1.30	.105
V2,11b	.221	.0088	24.1	2.73
V2,13	.224	.0086	1.38	.161
V2,13a	.111	.0072	17.4	2.41
V2,13b	.218	.0218	7.03	.323
V2,21	.205	.0128	2.05	.161
V2,21a	.053	.0135	1.83	.135
V2,21b	.347	.0110	4.10	.371
V2,23	.168	.0102	2.38	.233
V2,23a	.105	.0079	1.61	.203
V2,23b	.161	.0161	20.9	1.30
V2,31	.111	.0034	1.81	.536
V2,31a	.158	.0155	3.63	.233
V2,31b	.078	.0043	-	-
V2,33	.154	.0031	2.01	.657
V2,33a	.029	.0111	-	-
V2,33b	.276	.0218	3.67	.168
Mean, uncrushed leachate	.339(.29)	.0118(.0088)	3.55(2.4)	.337(.174)
Mean, crushed leachate(a)	.105(.039)	.0131(.0037)	5.16(6.4)	.494(.739)
Mean, crushed leachate(b)	.271(.15)	.0160(.0071)	14.7(12.9)	.940(1.08)

Table 5-6. Average halogen concentrations and range of values for granites.

	Average(ppm)	Range(ppm)	Reference
Cl	200	10-1,180	Fuge(1974)
Br	0.5	0.13-5.01	Fuge(1974)
I	0.2	0.04-0.72	Fuge(1974,1978)

Table 5-7. Water-soluble halogens in granites.

	% of Total Halogen	Reference
Cl	20-100	Faber(1941), Behne(1953), Fuge(1979)
Br	(20-100)	Behne(1953)
I	60-100	Fuge(1978)

water viewpoint, and from Table 5-7 it's clear that a large fraction, usually most, of the halogen content is readily leached by water. This amount represents the fluid-inclusion salt of the rock. If we assume that 50% of the chloride in a granite is water soluble, then 0.010% Cl is the average amount of fluid-inclusion chloride in a granite. From this we can calculate that there are 260 grams of leachable chloride in 1 m^3 of granite. This value is very similar to the value obtained for the Stripa granite.

Additional verification of the soluble nature of chloride in igneous rocks has been demonstrated in at least three experimental studies. Ellis and Mahon (1967) showed that anywhere from 3 to 1000 ppm Cl could be leached from igneous rocks subject to temperatures of 250-600°C. The maximum amount extracted was 50-100% of the total chloride in the rock (for a water/rock ratio of 1:1). Moore, et al. (1983) forced distilled water through cylinders of two different granites at temperatures of ambient to 300°C, and collected and analyzed water samples at regular intervals. At room temperatures the Cl concentrations ranged from 20 to 132 mg/L, and the last samples collected after 30-60 ml of water flow still had 20-50 mg/L Cl coming through with no sign of a decrease (Moore, pers. comm.). In one run a total of 2.3 mg Cl had been extracted with 42 ml of distilled water. Since the granite cylinders were about 1025 g each (assuming a density of 2.6), with an estimated leachable Cl content of .01%, then the total leachable chloride would be about 103 mg. If about 50 times more water had been passed through, then all of the leachable chloride should have been extracted. This amount would be equivalent to a total water/rock ratio of 5:1. Alternatively, the data is amenable to a rough estimation of the time necessary to wash out all the soluble chloride. 2.3 mg Cl was extracted in about 7 days at a pore pressure of about 100 bars. Assuming a

constant extraction rate, it would take nearly a year to wash out all the chloride from this volume of rock.

The third study is in progress on the Carnmenellis granite (Edmunds, et al., 1983, 1984). Groundwaters in this granite have high salinities (up to 19300 mg/L), and it has been demonstrated that significant quantities of chloride can be leached from the granite. However, the investigators have stated that the salinity is not derived from fluid inclusions, but rather leached from primary minerals (Kay, 1984) having the same Br/Cl ratio as seawater (Edmunds, et al., 1984).

There are precious few determinations of the Br and I content of granites, and even fewer published data where the ratios Br/Cl and I/Cl are available. The best data seems to be that of Fuge (1974, 1978), who suggests that the average Br concentration for granites is 1 ppm, and the average I concentration is 0.2 ppm. Combining these values with an average Cl content of 0.02% for granites, the ratios become Br/Cl = 0.005 and I/Cl = 0.001 which are noticeably higher than seawater values. Fuge (1978, 1979) also noted that close to 100% of the total iodine content was water-soluble, whereas lower proportions of chlorine were water-soluble (30-70%). Assuming that 50% of the Cl in the average granite is water-soluble, and 100% of the Br and I is water-soluble, then the water-soluble leachates would have Br/Cl = 0.010 and I/Cl = 0.002. These values are nearly identical to those at Stripa, and are considerably higher than values found in most other types of rock, mineral, or natural water. They are, however, very consistent with the studies by Behne (1953), who found a Br/Cl ratio of 0.0125 for 14 granites; Vinogradov (1944), who found a Br/Cl ratio of 0.010 for crystalline rocks; and Kozlowski and Karwowski (1974), who found a Br/Cl ratio of 0.015 ($\pm$0.013) for 34 fluid-inclusion extracts from hydrothermal quartz in several massifs from lower Silesia. This consistency suggests that a high-temperature process may be responsible for enriching the Br/Cl ratio relative to seawater. The only known explanation is the partitioning of halogens into the hydroxyl site of micas and amphiboles. At high temperatures a larger amount of chloride can substitute for this site, but little or no bromide or iodide can substitute because their ionic size is too great. Hence, there should be an enrichment of Br/Cl and I/Cl in the residual fluid and any fluid inclusions remaining from that process. The degree of enrichment probably depends very heavily on temperature and residence time of the fluid at that temperature. At temperatures of 200-300°C in active geothermal areas that contain modern-day seawater, there is no change in the Br/Cl ratio (Truesdell, et al. 1981). Thus, longer residence times and higher temperatures are probably required.

6 OXYGEN-18 AND DEUTERIUM CONTENTS

6.1 Introduction

Oxygen-18 and deuterium measurements have been performed on the Stripa groundwaters since the beginning of the LBL-KBS project. Basic principles and a first discussion of results can be found in Fritz, et al., 1979, 1980. All data obtained within the framework of the entire Stripa project by several laboratories (Gesellschaft für Strahlen- und Umweltforschung mbH München (GSF), International Atomic Energy Agency (IAEA), Université de Paris-Sud (UPS), University of Waterloo (UW)) are presented in Table 6-1.

All samples for ^{18}O and ^{2}H determinations in water were collected in tightly sealing bottles and prepared according to standard procedures which include CO_2-equilibration at constant temperature. Results are then expressed as per mille ($^{o}/oo$) deviations (δ-values) from the SMOW reference (Standard Mean Ocean Water). A $\delta^{18}O = +10$ $^{o}/oo$ then signifies that the samples has 10 $^{o}/oo$ more ^{18}O than the standard.

Analytical reproducibility in each laboratory is better than ± 0.2 $^{o}/oo$ for ^{18}O and ± 1.0 $^{o}/oo$ for deuterium. However, between laboratories minor differences do exist. This is shown in an intercomparison of ^{18}O and ^{2}H data between different laboratories (Table 6-2) as well as the data listed in Table 6-1. These differences do not affect the interpretation of the results.

6.2 General considerations

Stable isotope analyses are used to distinguish waters from different origins or they may be used to study reactions between rocks and minerals. The first case assumes that ^{2}H and ^{18}O concentrations are conservative whereas modifications of isotopic compositions may occur in the second case.

6.2.1 Conservative stable isotope contents

Conservative stable isotope contents are characteristic for many "normal" groundwater systems in which ^{2}H and ^{18}O contents are defined by recharge processes and remain unchanged during groundwater flow. This natural labelling has recently been reviewed in IAEA publications 1981, 1983a, 1983b. For practical purposes, two observations are of particular importance

Table 6-1a Summary of ^{18}O and ^{2}H Data on Surface Waters and Shallow Groundwaters at the Stripa Test Site. All analyses were done at University of Waterloo (UW) unless otherwise indicated.

NAME	STRIPA NO. KBS-LBL	DATE	$\delta^{18}O$ °/oo SMOW	$\delta^{2}H$ °/oo SMOW	ANAL.
PONDS AND LAKES					
Tailing pond 3	1	77-09-07	- 9.2	-76.3	
" " 3		78-06-16	-10.8	-78.0	
" " 3		78-11-23	- 9.3	-76.0	
" " 3	9	77-09-12	--	--	
STREAMS					
Herr gard Sauna	4	77-09-07	- 9.1	-73.4	
Danshuttegard Bridge	5	77-09-07	- 9.1	-73.4	
" "		78-11-23	- 9.6	-77.0	
" "		82-06-10	-10.7	-80.8	UPS
" "		83-03-23	-11.2	-81.8	UPS
Into tailings pond	72	79-05-06	-12.7	-93.0	
WATERTABLE WELLS AND SEEPS					
WT - 2	71	79-05-5-18	-14.2		
WT - 3	70	79-05-01	-12.5		
WT - 7	54	78-08-24	-11.8	-81.3	
seep at SBH 3	73	79-05-06	-12.1	-89.0	
PRIVATE WATER SUPPLY WELLS					
Private well 1	18	77-09-27	-10.8	-81.3	
" " 1	83	79-05-18	- 9.6	-82.0	
" " 1		82-06-10	-11.56	-82.5	UPS
Private well 2	19	77-09-28	-11.0		
" " 2	23	77-10-24	-11.0	-81.0	
" " 2		77-10-25	-10.8		
" " 2		77-10-27	-11.0	-79.1	
Private well 3	20	77-09-28	-10.6		
" " 2		77-10-26	-10.9	-76.3	
" " 2		79-05-16	-13.4		
Private well 4	80	79-05-17	-11.4		
" " 4		82-06-09	-12.91	-93.4	UPS
Private well 5	21	72-10-06	-10.9		
" " 5		77-10-07	-11.1	-83.7	
" " 5		77-10-11	-11.1		
" " 5		77-10-12	-11.0	-81.7	
" " 5		79-05-15	-13.1		
SBH-3					
89-104 m	85	79-05-23/24	-11.7	-83.0	
" "		79-05-25	-11.5	-83.0	
" "		79-05-26	-11.7	-80.0	
" "		79-05-27	-11.3	-82.0	
DRIP WATER AT OLD MINE LEVELS AND FLOWING WATER IN OLD MINE					
mine discharge	2	72-09-07	- 9.1	-74.6	
135 m level, drip	75	79-05-14	-11.4*, -11.5		
157 " " , "	76/77	79-05-11	-11.5*, -11.5	-84, -82	
310 " " , "	78	79-05-11	-11.0	-79	
360-360 m level, drip	26	77-11-17	-10.8	-79.4	
" " " , "		77-11-18	-10.9		
360-410 m level, drip	8	77-09-08	-10.8		
" " " , "		77-11-17	-10.7	-79.4	
" " " , "	8	79-05-15	-11.0*	-79	
Flooded drift at 380 m	64	78-11-24	-11.4	-82	

* Average of more than one analyses done on different samples collected during the stated sampling period.

Table 6-1b. Summary of ^{18}O and ^{2}H Data from borehole M 3.

NAME	STRIPA NO. KBS-LBC	DATE	$\delta^{18}O$ °/oo SMOW	$\delta^{2}H$ °/oo SMOW	ANAL.
M 3	16	77-09-21	-11.8	-86.9	UW
		77-10-19	-11.8	-87.7	UW
		77-11-29	-11.9		UW
		78-01-24	-11.9		UW
		78-02-24	-11.9		UW
	35	78-05-30	-12.2	-87.2	UW
	42	78-08-15	-12.4		UW
		78-09-19	-12.3		UW
		78-11-17	-12.3	-88	UW
		78-11-27	-12.4		UW
		79-02-12	-12.2		UW
		79-05-02	-12.2		UW
		79-05-17	-12.6	-90	UW
	87	79-11-21	-12.3	-90	UW
		81-06-04	-12.3	-87	UW
		81-07-09	-12.60	-90.6	UPS
		82-06-10	-12.32	-87.7	UPS
		83-03-23	-12.20	-85.9	UPS
		83-11-09	-12.02	-88.9	IAEA
		84-02-14	-12.1	-90	UW
		84-02-23	-11.95	-86.3	IAEA

Table 6-1c. Summary of ^{18}O and ^{2}H Data from Boreholes at the 330 m Level Excavation.

NAME	STRIPA NO. KBS-LBL	DATE	$\delta^{18}O$ °/oo	$\delta^{2}H$ °/oo	ANAL.
R 1	53	78-08-29	-12.1	-86.0	UW
R 1	53	78-09-19	-12.0	-87.0	UW
	53	78-11-17	-12.2	-86.0	UW
		78-12-08	-12.3	-86.0	UW
		79-05-17	-12.3	-87.0	UW
		81-06-04	-11.9	-82.0	UW
R 3	46	78-06-16	-12.3	-90.6	UW
R 9	79	79-05-22	-12.5	-92.0	UW
HG-3	47	78-06-16	-12.3	-88.8	UW
HG-4	48	78-06-16	-12.2	-87.7	UW
SGU-hori. 338 m	28	77-12-07	-12.1	-88.0	UW
Vent. drift combined	65	78-11-24	-12.2	-90.0	UW
S 1	50	78-09-15	-12.1	-87.0	UW
S 4	51	78-09-14	-12.3		UW
		78-11-27	-12.1		UW
S 5	52	78-09-14	-12.5	-89.0	UW
		78-11-27	-12.4		UW

Table 6-1d + e

Table 6-1d. Summary of ^{18}O and ^{2}H Data from Stripa Borehole E 1.

NAME	INTERVAL	DATE	$\delta^{18}O$ °/oo SMOW	$\delta^{2}H$ °/oo SMOW	ANAL.
E 1		81-11-11	-12.7	-94.0	UW
	3-300 m	81-11-17	-12.80	-95.4	UPS
	127.5-129.5 m	82-03-23	-12.00	-86.4	GSF
	0-267 m	82-06-10	-12.66	-90.5	UPS
	0-267 m	82-06-10	-12.53	-91.3	GSF
	open	84-02-14	-12.30	-92.0	UW
	3-300 m	84-03-06	-12.34	-90.4	IAEA

Table 6-1e. Summary of ^{18}O and ^{2}H Data from Borehole N 1.

NAME	INTERVAL	DATE	$\delta^{18}O$ °/oo SMOW	$\delta^{2}H$ °/oo SMOW	ANAL.
N 1	3-300 m	81-08-19	-12.6	-89.5	IAEA
		82-06-10	-12.97	-93.6	UPS
		82-06-03	-12.8	-88.9	IAEA
			-12.6	-89.8	
		82-06-03	-12.82	-93.7	GSF
	123-125 m	82-08-30	-13.3	-93.4	IAEA
		82-08-30	-13.59	-98.6	GSF
	203-205 m	82-09-06	-13.1	-92.6	IAEA
		82-09-06	-13.50	-97.7	GSF
	271.10-273.10 m	82-09-14	-13.0	-92.4	IAEA
		82-09-14	-13.11	-94.8	GSF
	276-276 m	82-09-23	-13.2	-91.4	IAEA
		82-09-23	-13.37	-97.4	GSF
	3-300 m	83-03-23	-12.75	-90.0	UPS
	10-119 m	84-02-14	-13.5	-96	UW
	120-150 m	84-02-14	-13.5	-97	UW
	151-251 m	84-02-14	-12.5	-93	UW
	252-300 m	84-02-14	-12.9	-94	UW
	151-251 m	84-01-26	-12.43	-90.5	IAEA
	252-300 m	84-01-26	-12.47	-90.3	IAEA

Table 6-1f Summary of ^{18}O and ^{2}H Data from Borehole V 1.

NAME	INTERVAL	DATE	$\delta^{18}O$ °/oo SMOW	$\delta^{2}H$ °/oo SMOW	ANAL.
V 1	409-506 m	81-06-03	-12.8	-93	UW
		81-07-13	-13.0	-94	UW
		81-08-19	-13.0	-94	UW
		81-09-08	-12.9	-94	UW
		81-09-11	-13.0	-94	UW
		81-09-21	-13.0	-94	UW
		81-07-09	-13.25	-91.5	UPS
		81-08-19	-12.5	-89.6	IAEA
		81-08-28	-12.92	-91.7	GSF
		81-08-28	-12.91	-92.2	GSF
		81-09-08	-12.80	-91.6	GSF
	5-506 m	81-11-17	-13.08	-91.9	UPS
		82-06-10	-13.10	-93.0	UPS
	10-505 m	83-03-22	-12.93	-91.2	UPS
		83-03-05	-12.9	-95	UW
	100-505	83-10-03	-12.40	-91.0	IAEA
		83-10-19	-12.73	-94.0	IAEA
		83-11-05	-12.86	-91.3	IAEA
		83-12-07	-12.45	-94.0	IAEA
		84-01-11	-12.54	-90.3	IAEA
		84-02-08	-12.69	-91.3	IAEA
		84-02-14	-12.9	-93	UW

- infiltrating waters were not subject to evaporation before or during recharge and climatic conditions determine the stable isotope contents in the recharge area. They decrease with the number of condensation stages of the initial vapour, i.e. mainly with temperature. Altitude effects, seasonal effects and paleoclimatic effects are the result. On a delta^{2}H - delta^{18}O diagram, sample points usually follow a straight line with a slope of about 8.

- Water can evaporate before or during the recharge event: stable isotope contents increase with the amount of evaporation, following a variable slope which is lower than 8 on a delta^{2}H - delta^{18}O diagram.

A crucial parameter for the discussion of the origin of a given water is the deuterium excess (Dansgaard, 1964), which is defined as

$$d \text{ (per mil)} = \text{delta}^{2}H - 8\ \text{delta}^{18}O$$

Values of d are generally close to 10 °/oo in present day oceanic precipitation (Craig, 1961; Yurtsever and Gat, 1981) and, depending on the slope, are obviously much lower for evaporated waters. The d-value is a reflection of the origin and history of a vapour mass. Since in any given area meteorological regimes are not subject to major ultra-annual fluctuations, this value re-

Table 6-1g Summary of ^{18}O and ^{2}H Data on Samples from Borehole V 2 (410 m hole).

NAME	INTERVAL	STRIPA NO. KBS-LBL	DATE	$\delta^{18}O$ °/oo SMOW	$\delta^{2}H$ °/oo SMOW	ANAL.
V 2	8-39 m	(43)	78-06-06	-12.6	-90.7	UW
			78-11-20	-12.4	-90.0	UW
		(86)	79-09-06	-12.6	-92.0	UW
			79-09-14	-12.6		UW
	6.3-50 m	(17)	77-09-22/10-20	-12.2	-88.8	UW
	6.3-50 m	(17)	77-09-22/10-20	-12.0	-89.0	UW
	332-359 m	(68)	79-03-16	-12.2		UW
	401-428 m	(59)	78-11-20	-13.2	-95.0	UW
	401-428 m	(69)	79-04-06	-13.6	-98.0	UW
			79-04-24	-13.6, -13.7		UW
			79-05-04	-13.7		UW
			79-05-17	-13.3	-96, -98	UW
	356-470 m		81-06-03	-13.6	-97.0	UW
	0-356 m		81-11-	-13.19	-96.2	UPS
	356-471 m		81-11-30	-12.9	-93.1	IAEA
	6-822 m		82-04-21	-12.8	-90.2	IAEA
	6-822 m		82-04-	-12.84	-91.9	GSF
	406-410 m		82-11-24	-13.0	-91.4	IAEA
	406-410 m		82-11-24		-92.4	UPS
	406-410 m		82-11-24	-13.22	-95.1	GSF
	413-416.74 m		82-12-14	-12.8	-92.5	IAEA
			82-12-14	-13.30	-95.9	GSF
	490-493.74 m		83-01-19	-12.77	-89.3	IAEA
	549-552.74 m		83-02-07	-12.35	-91.1	IAEA
			83-02-07		-88.2	IAEA
	0-822 m		83-03-		-90.0	UPS
	490-493.74 m		83-01-	-13.13	-94.2	GSF
	549-552.74 m		83-02-07	-13.03	-93.2	GSF
	382-423 m		84-02-14	-13.10	-94.0	UW
	424-490 m		84-02-14	-13.10	-94.0	UW
	500-561 m		84-02-14	-13.0	-94.0	UW
	562-822 m		84-02-14	-12.8	-92.0	UW
			83-11-29	-12.62	-92.4	IAEA
	424-499 m		83-11-28	-12.74	-95.9	IAEA
	382-423 m		84-02-28	-12.70	-94.8	IAEA
	500-561 m		84-02-28	-12.70	-93.5	IAEA

mains rather constant in the average annual precipitations at a given location. However, major modifications would be introduced if:

- vapour originating in closed, evaporating basins and from evapotranspiration were added to the condensing atmospheric vapour.

- a global change in climatic conditions of oceanic vapour formation and meteorological circulation patterns were to occur (paleoclimatic effect).

The former case is recognized in the Mediterranean basin (Gat and Carmi, 1970) where d values reach +22 °/oo, whereas the latter case is strongly suspected for some ancient groundwaters, e.g. in deep confined aquifers of the Sahara (Gonfiantini et al., 1974; Fontes, 1981) and in Saudi Arabia (Hötzl et al. 1980) where values as low as 5 °/oo are found. Direct evidence for d values lower than present and close to +5 °/oo were recently obtained on Antarctic ice core profiles from the last glaciation (Jouzel pers. comn.). The lower d values are probably due to an average relative humidity over the oceans higher than at present, reflecting cooler conditions over tropical and equatorial oceanic masses (Merlivat and Jouzel, 1979). A modern example for the dependence of d-values on the origin of the vapour is seen in precipitations over Canada where Pacific/Arctic dominated weather regimes in Western Canada produce rain with $d < 5$ °/oo and the warmer Gulf of Mexico and Atlantic regimes provide precipitations with d-values close to +10 °/oo (Fritz et al., in prep.)

Deuterium excess values can thus be an important tool for groundwater identification because studies limited to one isotope can not characterize the origin of the initial vapour. Thus variations in delta-values might only be due to local conditions of recharges in general climatic conditions. However, by definition, deuterium excess values accumulate both ^{2}H and ^{18}O analytical errors which typically are between 2 and 3 °/oo of the d-value. Therefore, accurate and repeated measurements are required in order to obtain reliable values for this parameter.

The requirement of reliable analyses for the determination of d values is clearly emphasized by the data given in Table 6-2 and which compares isotope data obtained by participating laboratories on two samples. Although all laboratories clearly establish the isotopic difference which exists between the two samples, the d-values calculated from these data vary by about 4 °/oo. This is outside the possible difference which might exist between different Stripa waters and, therefore, make the consideration of this calculated parameter somewhat problematic.

6.2.2 Non-conservative stable isotope contents

Non-conservative stable isotope contents are found under special hydrogeochemical conditions such as:

- geothermal environments where exchange between ^{18}O rich minerals and water causes an increase of the ^{18}O contents in the waters (see e.g. Truesdell and Hulston, 1980);

- environments with fluids rich in CO_2 and H_2S. If their oxygen or hydrogen contents are significant with respect to the atomic contents of oxygen and hydrogen in the water, isotopic ex-

Table 6-2. Results of Intercomparison of Samples MIX and VTW.

MARCH 1984

	MIX		VTW	
Laboratory	δD	$\delta^{18}O$	δD	$\delta^{18}O$
Neuherberg	-45.0	-5.50	-82.6	-11.5
Waterloo	-49.0	-5.48	-81.0	-11.4
Uppsala	--	-5.89	--	-11.72
Paris		-5.68		-11.52
Krakow	-47.6	-5.50	-84.2	-11.66
IAEA	-47.6	-5.56	-83.5	-11.27
Mean	-47.3	-5.60	-82.8	-11.51
σ	1.7 (excl. Paris)	0.16	1.4 (excl. Paris)	0.16

change between gas and water will be significant. Exchange with gaseous carbon dioxide will deplete the water in ^{18}O and H_2S exchange produces an increase in the ^{2}H content of the water. These are not common phenomena.

- crystallization of clay minerals during weathering of feldspars and micas causes under closed system conditions, an enrichment in oxygen 18 and a depletion in deuterium (see Savin, 1980); i.e. the residual fractions of oxygen and hydrogen in the water may be significantly depleted in ^{18}O and enriched in ^{2}H respectively (Fritz and Frape, 1982). A similar effect can also be observed if exchange takes place between clays or micas and limited amounts of water as may be the case in low-permeability rocks.

6.3 Discussion

Histogrammes depicting the distribution of ^{18}O in groundwater at different depths and environments from the Stripa area are shown in Figure 6-1 whereas Figure 6-2 presents a summary of ^{18}O and ^{2}H data. Both show that consistent and substantial differences do exist.

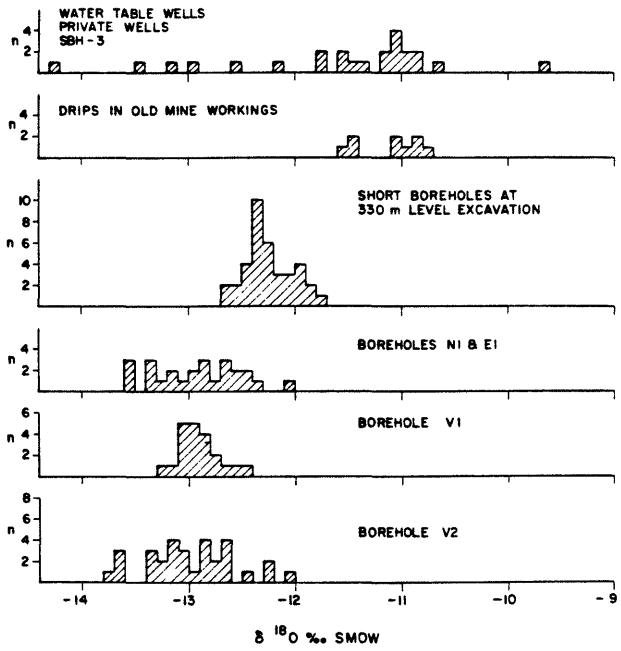

Figure 6-1. The oxygen-18 contents in different types of groundwaters at Stripa. Note, that shallow groundwaters and old mine drips are the only waters which contain substantial amounts of tritium. All data listed in Table 6-1 are shown.

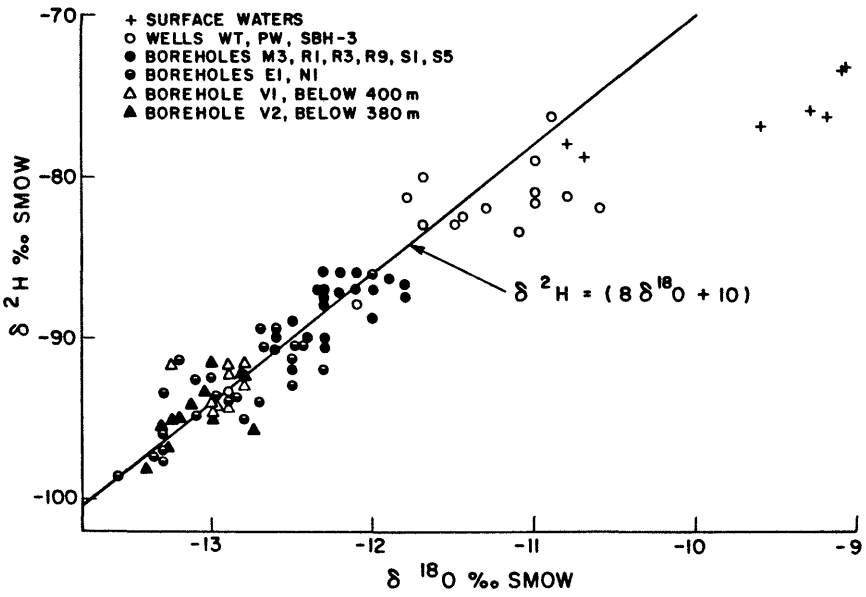

Figure 6-2. $\delta^{18}O$ versus $\delta^{2}H$ in Stripa groundwaters. Only samples collected from short boreholes or between limited packer intervals are shown. For clarity not all data points listed in Table 6-1 are shown.

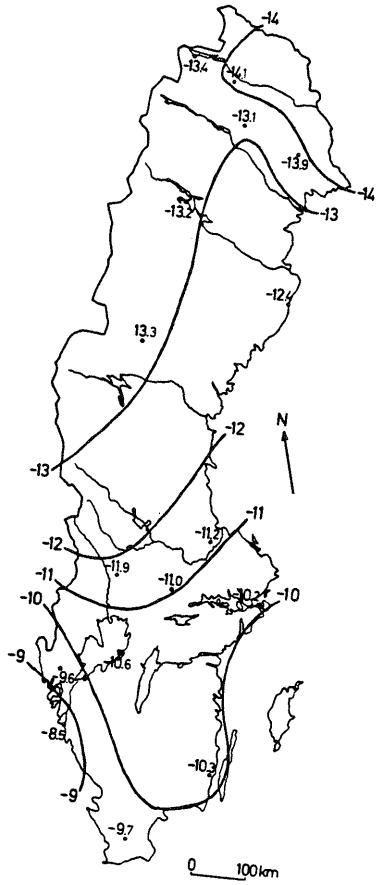

Figure 6-3. Average annual ^{18}O content in precipitation over Sweden (From Burgman, et al., 1981).

Surface waters in the Stripa area lie on or to the right of the global meteoric waterline. This shift indicates surface evaportion. Such evaporated water can also be found in some shallow wells (e.g. PW 1) although this is an exception because the majority of all shallow groundwaters are close to or on the meteoric waterline. The best "definition" of the isotope contents of shallow groundwaters is probably provided by "drips" in the old mine workings. These waters are rich in tritium (77 to 160 T.U.) and represent a rather well mixed reservoir whose average composition is close to -11 °/oo (see Figure 6-1 and Table 6-1). Most shallow groundwaters in private and watertable wells closely agree with this value, which is also the average annual ^{18}O content in local precipitations (Figure 6-3, Burgman et al., 1981).

Deep groundwaters are depleted in heavy isotopes as compared to shallow groundwaters and waters discharging from boreholes at the 300 m levels. The ^{18}O and deuterium contents place them on the meteoric waterline (Figure 6-2). Deviations most probably re-

flect the analytical differences discussed above. They are thus normal groundwaters which have preserved their composition since infiltration.

However, heavy isotope contents of deep groundwaters are rather variable between different boreholes and within a given well, depending on the packer intervals that were sampled. Nevertheless, the data for boreholes such as M 3 or specific levels in V 2 indicate consistent isotopic differences over a 7-year period, although, minor time-variations do occur. As in most confined aquifers, these are small.

D and ^{18}O contents of deep groundwater (Boreholes V 1 and V 2) are similar and in the case of borehole V 2 indicate a small decrease with depth (a decrease of about 6 °/oo in deuterium and 0,7 °/oo in ^{18}O was observed in 1978-79 and about 3 °/oo in deuterium and 0,4 °/oo in ^{18}O in 1981-83). This trend has not changed much over the seven years period although some variations are observed and are attributed to the fact that samples were measured in different laboratories and at different time. It should be noted that the differences in question are of the order of 2-3 times the analytical error.

Isotopic differences between samples from the different levels within the same borehole are an indication that different fracture systems deliver different types of water. Mixing may occur between, at least, two different types of waters, in order to explain observed compositions at the different levels. However, the rather regular change in chemical and isotopic compositions with depth in borehole V2 is probably a result of mixing in the borehole rather than a reflection of mixing between fracture systems.

Considering only the most saline waters in the deep portions of boreholes V 1, V 2 and possibly N 1, a depletion in ^{18}O by up to 2.5 °/oo with respect to the shallow groundwaters is observed. Comparing this figure with common altitude gradients for isotope contents in precipitations, this isotopic difference could imply an altitude difference of several hundred meters between areas of recharge of shallow and deep groundwaters (possibly exceeding 500 m). However, this signifies that regional flow systems would have to be invoked. Under those conditions the chemistry of the deep Stripa waters would reflect an evolution in a multitude of different rock types and could not be discussed in terms of a geochemical evolution within the Stripa granitic rock mass.

Exceptional precipitation events can sometimes be called upon to explain differences in heavy isotope contents of groundwaters since it is known that heavy precipitations can be depleted if compared to average values at any given location (Yurtsever and Gat, 1981). However, it is unlikely that such events can account for the differences seen in the Stripa groundwaters.

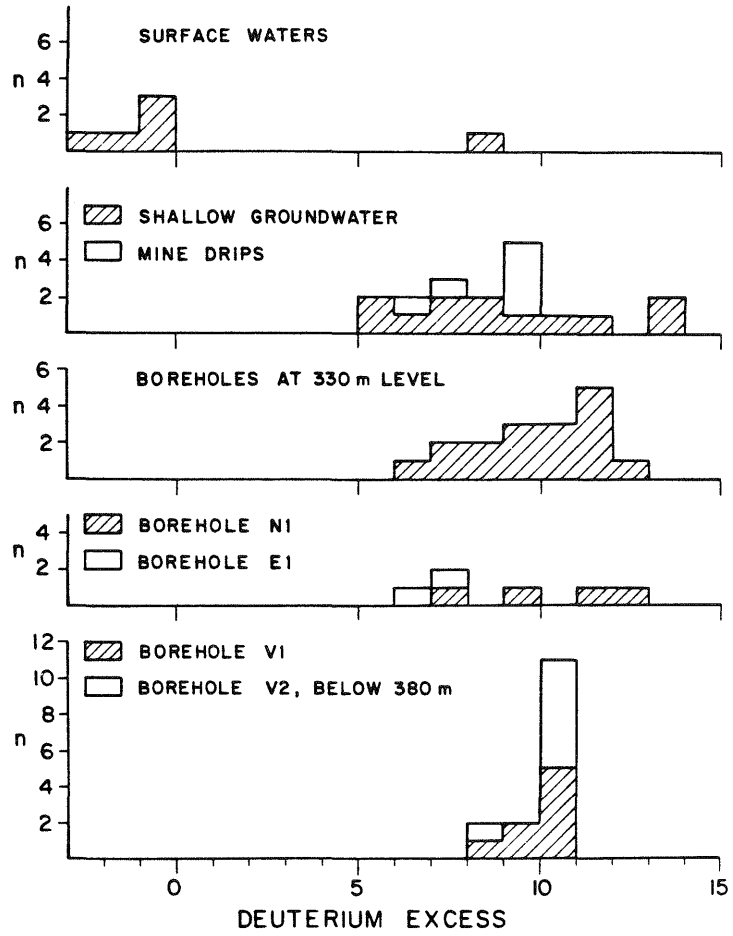

Figure 6-4. Deuterium excess (in $^{o}/oo$) in Stripa groundwater samples. Only samles analyzed by UW are shown.

An evolution outside the granitic type rocks at Stripa may also have occurred if the waters had a local origin. However, their lower heavy isotope contents must then reflect paleoclimatic conditions. The observed ^{18}O difference between water recharge and the deep waters agrees well with differences observed at localities in Germany (Eichinger, et al., 1984), the UK (Bath, et al., 1979) and Austria (Andrews, et al., 1984) where groundwaters which formed during interstadials (> 25 ka) and during postglacial cold periods (> 12 ka) have similarly lower heavy isotope contents. The deep Stripa groundwaters would then be at least 10 ka old. Tritium and ^{14}C data do not contradict this statement.

As mentioned above, a possibly important parameter for interpreting the origin of a given water is the deuterium excess (Dansgaard, 1964). The deuterium excess of the Stripa groundwaters is shown in the histogrammes of Figure 6-4. The data show that the deeper waters have essentially the same d-values as the shallow waters. Minor differences can be due to analytical variability and, furthermore, some of the shallow groundwaters are influenced by evaporated surface waters with d-values as law as -2.7.

This similarity of d-values between deep, old groundwaters and shallow, young groundwaters is also observed in waters with estimated ages between 20 and 30 ka which are found in a Triassic aquifer in the UK. (Bath, et al. 1979). The ^{18}O contents of the old waters are also about 2 °/oo below modern recharge values. Both observations compare well with our findings at Stripa. On the other hand, younger, postglacial (about 12 ka) groundwaters found in the Tertiary basin of S. Germany have d-values which are about 6 °/oo below modern but are paralleled by a 2 °/oo decrease in ^{18}O (Eichinger, et al., 1984); similar, lower d-values are recognized in Pleistocene groundwaters throughout North Africa (Moser, et al., 1983).

Can the similarity of d-values in shallow and deep groundwaters at Stripa be used to argue that the deep waters must be pre- or inter-glacial (> 25 ka) in nature? One may not be able to answer this question conclusively but there is little doubt that the lower ^{18}O contents in the deep, saline groundwater at Stripa reflect cooler recharge conditions. Burgman, et al., (1981) established a temperature coefficient of 0.547 to a network of Swedish meteorological stations which would signify that the isotopic difference between shallow and deep groundwaters reflects a change in average annual temperature of 3-4 °C. This assumes that groundwaters always reflect the compositions of average annual precipitations. However, it must be noted that some shallow groundwater reflect the seasonal variations of precipitation and can reach the low values of the deep groundwaters. If, in the past, selective recharge had occurred, then the lower heavy isotope contents of the deep water would not necessary reflect climatic change. Fortunately isotope data on deeper but young groundwaters (as represented by mine drips) show a smoothing of such variations and suggest that the observed isotopic differences reflect climatic differences rather than selective recharge.

It is very unlikely that glacial meltwaters participated in the formation of the deep groundwaters. These waters are considerably more depleted in ^{18}O than the lowest values we observed and thus only a minor percentage of the deep water could have such an origin. Such a mixture would require mixing before the waters enter the fracture systems at Stripa, an interpretation which would greatly complicate the hydrogeological regimes in this area.

The origin of the waters which discharge from different boreholes at the 300-360 m levels is not easily defined, despite the fact that they display a remarkable constancy in time of their isotopic compositions. This is especially true for the waters in M 3 which since 1977 discharged several times 10^5 liters of water. In terms of their ^{18}O and ^{2}H contents most waters at these levels fall between the compositions of the shallow and deep waters. Thus, they could be considered as mixed waters although chemical and tritium data do not substantiate this interpretation.

Table 6-3. Cl^- and ^{18}O Contents in Samples Collected 1984-02-13.

Borehole	Interval	Cl^- mg l^{-1}	^{18}O ‰
M 3		34.5	-12.4
N 1	10 - 119	185	-13.5
	120 - 150	148	-13.5
	151 - 251	29.0	-12.5
	252 - 300	37.1	-12.9
V 1	0 - 550	553	-12.9
V 2	382 - 423	467	-13.1
	424 - 490	487	-13.1
	500 - 561	430	-13.0
	562 - 822	526	-12.8

The problem is further compounded by analyses done on samples collected from specific intervals in borehoe N 1 (Table 6-3). The $\delta^{18}O$ values range from -12.5 to -13.5 which corresponds to values seen in M 3, for example, and the deep waters. These data would indicate that some of the fractures encountered in N 1 discharge waters which are similar to the deep saline waters. Tritium data appear to exclude that hydraulic connection exists, although the chlorinities are highest in the isotopically light samples and could lend some support to this view.

Hydraulic testing, however, exclude a direct link because the fractures carrying low ^{18}O water in N1 do not connect hydraulically with V 1 or V 2. The testing does indicate that the deeper portion of N1 connects with the BMT area and the R 1 borehole.

6.4 Regional saline groundwater survey

A regional survey of saline groundwaters was undertaken in order to determine whether Stripa groundwater was geochemically and isotopically unique or whether it was necessary to propose more regionally valid interpretations. The results of ^{18}O and ^{2}H analyses are listed in Table 6-4, their location is seen in Figure 6-5.

Comparison with the isotopic composition of average annual rainfall at the different localities establishes that all but three samples could have a local origin. However, samples 2, 3 and 4 have ^{18}O and ^{2}H contents which are lower than would be expected for modern recharge. Their formation occured in a cooler clima-

Figure 6-5

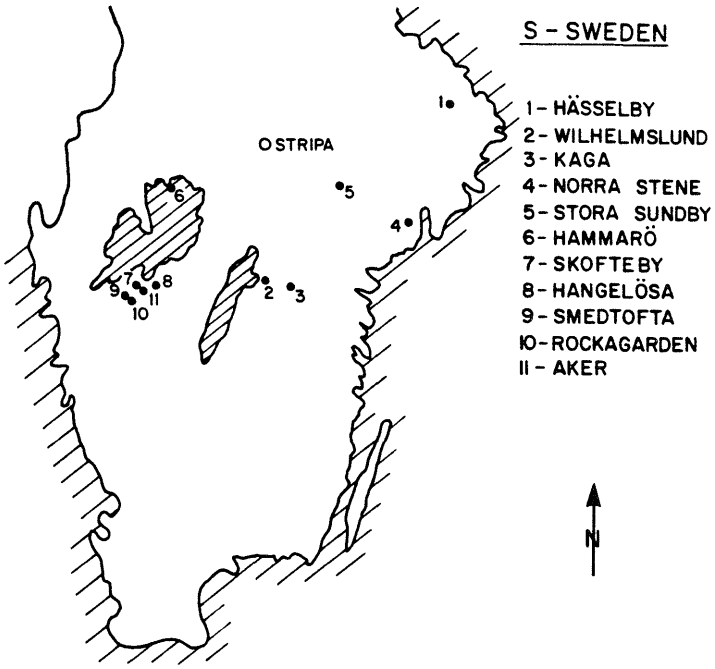

Table 6-4 ^{18}O and ^{2}H in groundwater in South Central Sweden. Collected 84-04-22.

Locality	Aquifer rock	$\delta^{18}O$ °/oo	$\delta^{2}H$ °/oo	Lab
HÄSSLEBY	Crystalline rock	-11.22	-77	IAEA
		-11.27	-81.1	GSF
WILHELMSLUND	Cambrian Sandstone	-12.33	-83.5	IAEA
		-12.57	-87.3	GSF
KAGA	Crystalline rock	-13.98	-98.0	IAEA
		-15.12	-109.7	GSF
NORRA STENE	Crystalline rock	-14.32	-102.2	IAEA
		-14.53	-106.5	GSF
STORA SUNDBY	Crystalline rock	-11.92	-83.7	IAEA
		-12.03	-88.1	GSF
HAMMARÖ	Crystalline rock	-11.78	-86.3	IAEA
		-12.44	-90.2	GSF
SKOFTEBY	Quatern. sediments	-8.25	-60.1	IAEA
		-9.08	-63.5	GSF
HANGELÖSA	Crystalline rock	-9.80	-64.8	IAEA
		-9.94	-70.0	GSF
SMEDTOFTA	Quatern. sediments	-9.31	-64.0	IAEA
		-9.83	-68.8	GSF
ROCKAGÅRDEN	Quatern. sediments	-9.03	-60.6	IAEA
		-8.99	-63.0	GSF
AKER	Quatern. sediments	-8.80	-58.0	IAEA
		-8.44	-60.6	GSF

te, whereas the Kaga (No. 3) and Norra Stene (No. 4) samples are depleted in heavy isotopes even with respect to Stripa waters. It is interesting to note that the Kaga sample is one of two samples that has a Br/Cl ratio significantly higher than seawater and an anomalously high Ca/Mg ratio. The other sample is Wilhelmslund. In this respect these resemble the deep Stripa waters. For further discussions, see sections 4.6 and 4.8.3.

6.5 Conclusions

Stable isotope analyses are well suited to characterize different groundwaters in the project area. Results show that the Stripa groundwaters are normal meteoric waters which have not been subject to surface evaporation or secondary isotope exchange processes with rocks and minerals. Their compositions reflect recharge conditions.

The lower ^{18}O and ^{2}H contents of the deep waters indicate an infiltration during a cooler climate than exists today in this area. In this respect, these waters are similar to low ^{18}O, low ^{2}H waters encountered in the regional survey and is suggested that these waters are relatively old. "Age" estimates will be attempted on the basis of other data presented here.

However, it is important to notice that at Stripa in general low heavy isotope contents are paralleled by increasing salinities, although the parallelism is far from perfect. Therefore, one can suggest that the observed compositions are not only due to the mixing of two different water types but also to geochemical reactions which modify chemistry and total dissolved solids. That mixing occurred is relevant for the discussion of water "ages" (Fritz, et al., 1983).

Remarkable are the differences which exist for both chemistry and isotopic compositions in adjacent fracture systems. This may reflect different flow paths. The appearance of isotopically light water in fractures in different boreholes may reflect hydraulic connection even where hydraulic testing was not sufficient to substantiate this.

7 STABLE ISOTOPE GEOCHEMISTRY OF SULPHUR COMPOUNDS

7.1 Introduction

Sulphur geochemistry in the Stripa groundwater system is of special interest because (1) large variations in sulphate content occur in groundwaters from different boreholes, (2) there is a rather systematic increase of sulphate concentrations with chloride at depth, from less than 1 mg l^{-1} to well over 100 mg l^{-1}, (3) both reduced and oxidized forms of aqueous sulphur occur and (4) the presence of solid sulphides (such as pyrite and chalcopyrite) are found in the rock matrix and on fracture surfaces.

The discussion of available data is preceded by a basic review of natural isotopic variations in sulphur compounds.

7.2 Variations of stable isotope contents of sulphur compounds

Biological and chemical reactions involving oxidized and reduced sulphur compounds generally cause very significant isotope fractionations for both sulphur and oxygen isotopes. The sulphur-34 and/or oxygen-18 differences between two compounds 1 and 2 in a geochemical cycle of sulphur are expressed as α or ε, standard notations for all environmental isotopes (Friedman and O'Neil, 1977):

$$\alpha \text{ (alpha)} = R_1/R_2 \text{ and } \varepsilon \text{ (epsilon)} = \alpha - 1 \simeq \ln \alpha \simeq \delta_1 - \delta_2$$

where

$$\delta = \left(\frac{R_s}{R_{ST_D}} - 1\right) \times 1000$$

and

$$R = {}^{34}S/{}^{32}S \text{ or } {}^{18}O/{}^{16}O$$

Epsilon is also called the "enrichment factor" which directly describes isotopic differences between two compounds. For convenience epsilon is generally expressed in per mil (i.e. multiplied by 10^3). Standards are

the troilite phase from the Canyon Diablo meteorite (CD) for ^{34}S

and

Standard Mean Ocean Water (SMOW) for ^{18}O.

Equilibrium isotope effects are generally very high for sulphur compounds especially at low temperatures (Friedman and O'Neil, 1977).

However, elements such as sulphur enter into metabolic cycles and isotope effects may occur under the influence of biocatalysts which increase rates of chemical and isotopic reactions. Under these conditions isotope effects are no longer controlled by equilibrium but by kinetic fractionations. Kinetic isotope fractionation effects are not only temperature dependent but depend also upon environmental conditions and are defined within ranges rather than as precise values. Biochemical catalysts "prefer" light isotopes which results in heavy isotope concentrations in the unmetabolized fraction.

Due to the occurrence of kinetic and reservoir effects during the formation of reduced species, a large range of ^{34}S contents is observed in natural sulphides. For instance, sedimentary pyrites may show $\delta^{34}S$ values from -50 to 70 °/oo (Krouse, 1980) but are generally depleted in ^{34}S with respect to coexisting sulphates. When formed at high temperatures from deep (crustal or mantle) sulphur, volcanic H_2S remains generally close to the standard troilite and shows $\delta^{34}S$ values near zero or slightly negative.

Fortunately, in most aquifer systems, reducing conditions are not frequent and because the solubility of reduced sulphur species is low, the most frequent form of dissolved sulphur is sulphate.

Oceanic masses provide the main reservoir of sulphate.

The isotopic composition oceanic sulphate is very constant because of a steady state process between input (river) and output (precipitation and reduction):

$\delta^{18}O\ (SO_4^{2-}) = +9.5$ SMOW

$\delta^{34}S\ (SO_4^{2-}) = +20.0$ CD

Meteoric sulphates from oceanic rains and aerosols (unpolluted by industrial dusts and smokes) show marine values (Mizutani and Rafter, 1969; Rightmire et al., 1974).

During sulphate precipitation in the form of gypsum as anhydrite an isotopic fractionation occurs. Experimental and field values of epsilon for gypsum and anhydrite fall in the range of:

$4.0 >$ epsilon(^{18}O) > 3.0 °/oo (Lloyd, 1968; Pierre, 1982)

and

$3.4 >$ epsilon(^{34}S) > 1.4 °/oo (Thode and Monster, 1965; Pierre, 1982).

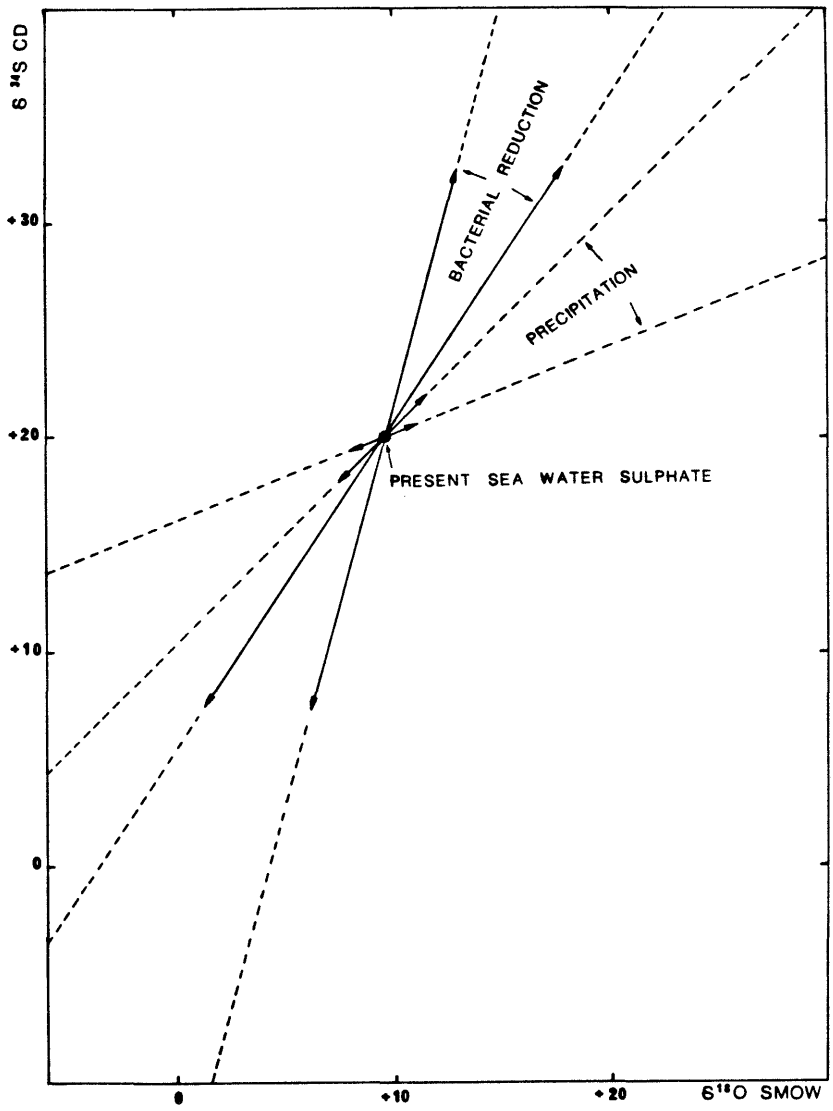

Figure 7-1. Sulphur 34 and oxygen 18 evolution of present day aqueous oceanic sulphate during crystallization of sulphate and sulphate reduction. Solid arrows: one stage process.

As a consequence, after precipitation, the remaining aqueous sulphate is depleted in heavy isotopes and further precipitation stages lead to solid sulphate depleted in ^{34}S and ^{18}O with respect to the initial aqueous SO_4^{2-} (Figure 7-1). Thus, marine Mg-K sulphates show ^{34}S contents below average ocean values (Nielsen and Ricke, 1964).

7.2.1 Redox systems

Reduction hardly occurs at low temperatures except if sulphate reducing bacteria are present in the environment, e.g. Desulfovibrio desulfuricans. Kinetic enrichments and steady state conditions become predominant. Whereby, products from this biosynthesis are depleted in heavy isotopes by 40 $\pm$10 °/oo (Claypool et al., 1980). Therefore, the remaining portion of SO_4^{2-} is enriched in heavy isotopes. Under quilibrium conditions, the isotopic difference (epsilon$_r$) would be about 80 °/oo at 30°C (Friedman and O'Neil, 1977).

The behaviour of oxygen isotopes during sulphate reduction can only be investigated indirectly since CO_2 - the most common resulting oxygen bearing compound in the reaction - is mixed with environmental CO_2 and reequilibrates with water. However, the remaining aqueous SO_4^{2-} becomes less enriched in ^{18}O than in ^{34}S by approximately 1/4, (Rafter and Mizutani, 1967; Mizutani and Rafter, 1969). One assumes that typical values of epsilon$_r$(kin) for ^{18}O are close to +10 °/oo (Claypool et al., 1980). However, rates of kinetic reactions are generally specific for a given environment and, therefore, values of epsilon$_r$(kin) may exhibit a large range of variations. Mizutani and Rafter (1969, b) report values of the ratio epsilon^{34}S(kin)/ epsilon^{18}O(kin) between -7.8 and +23.5 °/oo. In reducing evaporitic ponds, Zak et al. (1980) and Pierre (1982) found values close to +1.5 for this ratio.

7.2.2 Sulphide and H_2S oxidation

Reduced sulphur is quickly transformed into S^0, SO_3^{2-} and finally SO_4^{2-} when groundwater circulation reaches an oxidizing zone and/or mixes with superficial waters saturated with oxygen. However, besides inorganic processes, oxidation may occur through biological (bacterial) activity (Thiobacillus thiooxidans).

Further experimental data are still needed about sulphur isotope fractionation occurring during oxidation. It is generally found (see Krouse, 1980; Pearson and Rightmire, 1980) that the pure chemical process is not fractionating whereas slight depletion in ^{34}S may occur through bacterial formation of SO_4^{2-} (Kaplan and Rittenberg, 1964).

The atoms of oxygen participating in the formation of the sulphate ion from H_2S(for HS^- and S^{2-}) may have several origins. It has been shown by Lloyd (1967, 1968) and by Mizutani and Rafter (1969 a, b) that the oxygen involved in the process comes from environmental water as well as from dissolved (molecular) oxygen.

According to Lloyd (1968), the isotopic balance requires that a proportion of 1/4 of the oxygen atoms be supplied by the water and 3/4 by dissolved oxygen. The incorporation of water oxygen

into the sulphur bond would occur without fractionation. The admixture of dissolved oxygen occurs with an isotope fractionation effect, where:

$\delta^{18}O$ (aqueous SO_4^{2-}) = $\delta^{18}O$ (dissolved oxygen) - epsilon ox.

The isotope enrichment factor epsilon ox. is 8.7 °/oo (Lloyd, 1968). If dissolved oxygen is of atmospheric origin and not modified by organic processes one finds $\delta^{18}O(ox)$ = 23.5 °/oo (Kroopnick and Craig, 1972). However, isotopic exchange processes are ocurring between water sulphite ions so that the respective participation of H_2O and O_2 in the oxidation are given by:

$\delta^{18}O$ (SO_4^{2-}) = 0.66 $\delta^{18}O$ (environmental H_2O) + 4.9

This leads to sulphate ion with a $\delta^{18}O$ close to +5 °/oo of oxidation takes place in sea water ($\delta^{18}O$ = 0) and to -3.7 °/oo in water with an ^{18}O content of -13 °/oo (Stripa deep water).

According to Cortecci (1973), however, the proportions of atmospheric and water oxygen participating in the formation of sulphate ion approach stoichiometric proportions, where:

$\delta^{18}O(SO_4^{2-})$ oxidation =

$\{2[\delta(O_2) - 8.7 + \delta(H_2O)]2 + \delta(O_2) + \delta(H_2O)\}/4$

i.e. +9.6 and +3.1 in waters with $\delta^{18}O$ = 0 and -13 °/oo respectively.

However, this picture may also be modified if dissolved oxygen is partially used for metabolic respiration. In that case an oxygen enrichment occurs in the remaining fraction of the initial dissolved oxygen of atmospheric origin (Fontes and Michelot, 1983).

This brief discussion shows that more data are needed before isotope effects caused sulphate production through oxidation of reduced sulphur can be fully evaluated. Nevertheless, for practical uses one can assume that oxidation processes in groundwater preserve ^{34}S contents of the initial reduced sulphur and produce ^{18}O contents much lower than those known for marine evaporites.

7.2.3 Oxygen isotope equilibrium between sulphate and water

Lloyd (1967) as well as Longinelli and Craig (1967) established that ionic SO_4^{2-} in the oceanic reservoir is far from isotopic equilibrium with sea water.

This disequilibrium is probably due to the extremely slow rate of reaction of the S-O bond with water at neutral pH. Values for this reaction rate have been experimentally determined by Lloyd

(1968) for different pH values in the temperature range 298 to 721 K. From these values Pearson and Rightmire (1980) derived the following relationship between halftime of reaction $t_{1/2}$, temperature T in K, and pH:

$$\log t_{1/2}(\text{hours}) = 2.15 \times 10^3 \times T^{-1} + 0.44\ pH - 3.09$$

which theoretically could provide a geochronometer since the distance to equilibrium is time dependent.

However, care should be taken in any attempt to use this formula for time estimates in groundwater systems, because:

(a) to obtain the experimental data base, experiments were performed over limited ranges of time (some months). Low temperature runs were thus conducted at very low pH; therefore extrapolations to conditions f normal environments and to long periods (e.g. milenia) would be risky since no error estimate is available;

(b) kinetic isotopic reactions may interfere in the $SO_4^{2-} - H_2O$ system as well as catalytic or inhibiting effects, specifically during biochemical reduction or oxidation:

(c) equilibrium values for isotope fractionation effects between SO_4^{2-}, HSO_3^- ions and water at low temperature are still under discussion.

Furthermore, it must be remembered that the residence time of any aqueous compound is not necessarily that of the groundwater in which is dissolved.

7.3 Sampling and analyses

Because of the highly variable SO_4^{2-} content (from less than 1 to about 100 ppm) in the Stripa waters the amount of water collected during this phase of the program varied from 2 to 60 litres.

Where necessary (well N 1) the water sample was treated with reagent grade HCl in order to remove H_2S and HS^- whose further oxidation may modify the stable isotope content of aqueous SO_4^{2-}. In the case of surface water, precipitation of sulphate on a 25 litre sample was unsuccessful.

Samples were treated with a solution of barium chloride in order to precipitate SO_4^{2-} as barium sulphate. Barium carbonate is then removed by H^+ addition and a further precipitation step is made. The final barium sulphate rinsed and dried, is allowed to react with pure graphite at about 1000°C under vacuum. CO_2 and carbon monoxide are produced. The latter is converted into CO_2. An aliquote of BaS produced through the reduction is dissolved and con-

verted into Ag_2S and oxidized in pure and dry oxygen at torch temperature. Oxygen and sulphur isotope contents are then determined through CO_2 and SO_2 analyses on a VG Micromass 602 D mass spectrometer. Uncertainties are about ± 0.25 on both measurements.

A number of samples were collected on an experimental basis with ion exchange resins. The result are encouraging and further studies will be undertaken using this method.

A sample of 250 ml of water is also collected for SO_4^{2-} determination and ^{18}O measurement in the water.

7.4 Results and discussion

All data are summarized in Table 7-1, and graphically shown in Figure 7-2.

7.4.1 Aqueous sulphate in subsurface waters

Representative points of shallow groundwaters (three measurements) fall within a heavy isotope range which was previously considered as intermediate between marine sulphate (sea spray) and sulphates resulting from oxidation of reduced species of sulphur (Fritz et al., 1983, Fontes and Michelot, 1983). Such values were also observed in New Zealand (Mizutani and Rafter, 1969c), in Italy (Cortecci and Longinelli, 1970) and attributed to a mixture of sea spray and sulphates produced through oxidation of fuel-sulphur.

A detailed study of ^{34}S and ^{18}O contents of meteoric sulphate in Poland (Trembaczowski and Halas, 1984) show a rather constant $\delta^{34}S \simeq +3.7$ °/oo and a $\delta^{18}O$ strongly correlated to that of precipitation water: $\delta^{18}O(SO_4^{2-}) = 16.0 \pm 0.9 + (0.38 \pm 0.07)\ \delta^{18}O(H_2O)$. For Stripa this relationship yields a $\delta^{18}O$ value of about +12 °/oo, using the average ^{18}O content of -11 °/oo for the local precipitation (Burgman et al., 1981). Thus the intercept value (+16 °/oo) or slope do not apply for the Stripa groundwaters. Another possibility is that these sulphates contain a component very depleted in heavy oxygen such as oxidized sulphides. Sample PWI is probably affected by a secondary enrichment in heavy isotopes due to a partial reduction of the SO_4^{2-} bulk facilitated through water stagnation (the same well shows a low deuterium excess which indicates an evaporation effect from the well).

Shallow aqueous sulphates do not seem to have any connection with sulphates of V 1 and V 2.

Table 7-1 ^{18}O and ^{34}S contents of aqueous sulphates from Stripa.

Borehole	Interval	Date	$\delta^{18}O$ SMOW	$\delta^{34}S$ CD	Lab
PW 1		79/05/18		+7.6*	UW
		82/06/10	+4.28	+5.13	UPS
PW 3		79/05/16		+8.3	UW
PW 4		79/05/17	-1.7	+2.8	UW
		82/06/09	+1.02	+3.60	UPS
WT 2		79/05/05		+5.2*	UW
SBH 3	89-104	79/05/28		+7.2	UW
M 3		78/11		+16.5	UW
		78/11		+17.6	UW
		79/05		+13.2	UW
		79/05		+12.6	UW
		79/05		(+14.2)	UW
		79/11/21		+12.6*	UW
		79/11/22		+13.0*	UW
		82/06/10	+0.78	+11.28	UPS
		84/02/14	+0.9**, +3.3	+13.0**, +13.4	UW
R 1		78/08/09	+8.8	+20.7	UW
E 1		84/02/14	+5.7**	+5.8	UW
N 1	3-300	82/06/10	+5.27	+27.92	UPS
	151-251	84/02/14	+11.1**	+39.3**	UW
	252-300	84/02/14	+11.7**	+27.3**	UW
V 1	409-506	81/06/03	+7.80	+12.84	UPS
	409-506	81/07/09	+7.30	+12.85	UPS
	5-506	81/11/17	+8.10	+13.96	UPS
	5-506	82/06/10	+7.81	+13.79	UPS
	100-505	83/10/03	+7.58	+13.84	UPS
	100-505	83/10/19	+7.58	+14.08	UPS
	100-505	83/12/07	+8.26	+14.54	UPS
	100-505	84/01/11	+7.83	+13.91	UPS
	100-505	84/02/08	+7.55	+14.38, +14.3**	UPS
		84/02/14	+7.4**, +7.6	+13.9	UW
V 2	401-428	78/11/20	+8.5	+17.4	UW
	401-428	79/05/04		+20.1	UW
	356-470	81/06/03	+7.95	+15.04	UPS
	406-410	82/11/24	+7.54	+15.35	UPS
	424-499	83/11/28	+9.15	+18.94	UPS
	562-822	83/11/29	+9.72	+25.50*	UPS
	382-423	84/02/14	+7.7**, +8.1	+16.6**, +17.3	UW
	424-490	84/02/14	+8.7**, +8.6	+21.6**, +22.0	UW
	500-561	84/02/14	+9.4**, +9.3	+27.2**, +27.0*	UW
	562-822	84/02/14	+9.6**, +9.8	+29.1**, +27.8	UW
	382-423	84/04/26	+8.70	+14.90	UPS
	424-499	84/04/26	+9.58	+21.60	UPS
	500-561	84/04/26	+10.59	+24.30	UPS
	562-822	84/05/03	+10.06	+24.80	UPS
Hässelby		83/04/20	+14.0	+24.9	UPS
		83/04/20	+9.9	+26.9	UW
Kaga		83/04/21	-0.3	+5.1	UPS
Nora Stene		83/04/22	+8.0	+18.3	UPS
		83/04/22	+7.7	+23.2	UW
Storå Sundby		83/05/02	+8.5	+18.0	UPS
		83/05/02	+7.7	+20.1*	UW
Hammarö		83/05/03	+10.8	+14.9	UPS
		83/05/03	+8.7	+17.0*	UW
Skofteby		83/05/04	+18.4	+69.7	UPS
		83/05/04	+12.4	+74.6	UW
Hangelösa		83/05/04	+17.9	+42.1	UPS
		83/05/04	+15.1	+46.1	UW
Rockagarden		83/05/05	+17.8	+44.3	UPS
		83/05/05	+11.8	+47.7	UW
Aker		83/05/05	+19.3	+74.7	UPS
		83/05/05	+15.1	+79.6	UW

* Average value.
** Sample collected using ion exchange resines.

UPS: Université Paris-Sud, France.
UW: University of Waterloo, Canada.

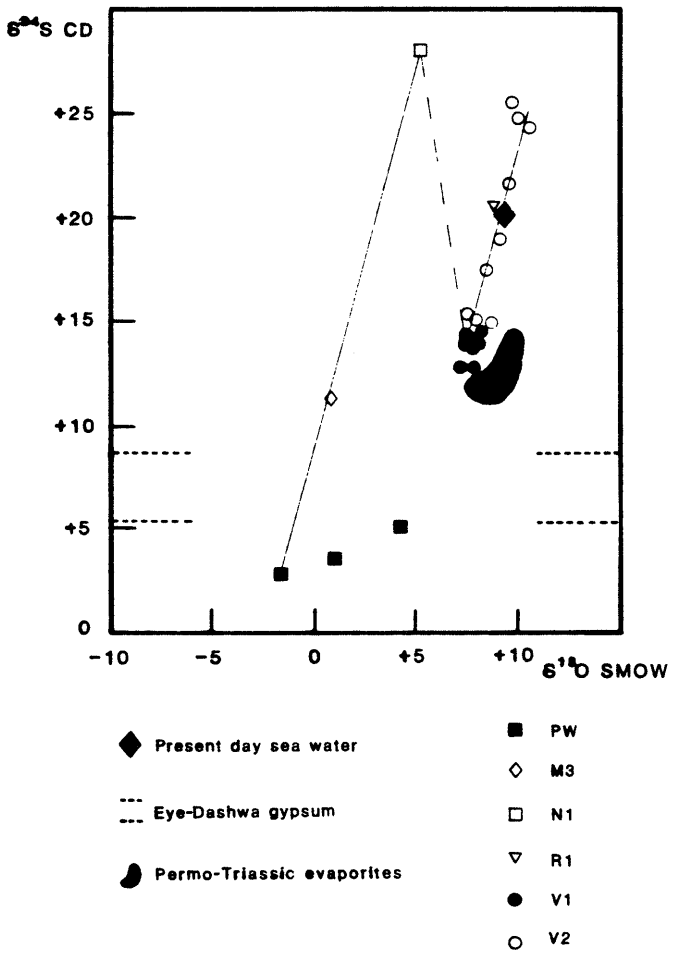

Figure 7-2. Oxygen 18 vs sulphur 34 contents in aqueous sulphates from Stripa.

7.4.2 Aqueous sulphate in deep waters

The sulphates of Stripa groundwaters may have several origins corresponding to various ages:

a) recent sea water intrusions, i.e. lateral intrusion;

b) Holocene Baltic sea intrusion, i.e. vertical and/or lateral intrusion;

c) leaching of fluid inclusions or some form of rock sulphate;

d) leaching of evaporites or contribution of associated brines.

In addition, geochemical reactions especially redox processes involving biological activities may have modified the original sulphate concentrations and compositions. This, however, is

least likely for V I, whose waters show rather constant isotopic compositions and highest sulphate concentrations.

In the $\delta^{34}S$ - $\delta^{18}O$ diagram (Figure 7-2) most of the points from V 1 fall close to the range of sea water derived sulphates as documented by the average values, where SO_4 has $\delta^{18}O = 7.76 \pm 0.29$ and $\delta^{34}S = +13.80 \pm 0.59$.

This could reflect different sources, e.g.:

1) a succession of biogeochemical processes which could have given such a heavy isotope content starting from any sulphur species;

2) a true sedimentary origin with preservation of the original heavy isotope content.

Hypothesis (1) would, for instance, imply the following geochemical pathways:

a) a dissolution of a fossil evaporite with a ^{34}S content close to +14,

b) a complete reduction of this sulphate which maintains a sulphur 34 content of +14 °/oo,

c) an oxidation of the reduced sulphur by dissolved oxygen considerably enriched in heavy isotopes through an intense respiration process.

Condition (a) requires an evaporite source.

Condition (b) requires that reduction products remain homogeneized after completion of the reaction, i.e. a stagnant flow regime.

Condition (c) implies a transfer from the reducing to an oxidizing reservoir.

This scheme appears somewhat complicated (despite the fact that it represents one of the most simple pathways to reach the observed heavy isotope contents) and therefore preservation of original sedimentary compositions appears probable.

7.4.3 Discussion of the various possible origins of the aqueous sulphate

- Hypothesis (a): No hydraulic data are available on a possible penetration of present day marine waters or Baltic seawater to the Stripa region. However, V 1 aqueous sulphate has an average ^{34}S content much lower than modern open marine sulphate. A

contribution of sulphate produced through oxidation of reduced sulphur species could account for this low ^{34}S content. However such a process would have led to a significant decrease of the ^{18}O content of the sulphate which cannot be recognized. Furthermore, in the case of a supply of sulphate derived from reduced sulphur into a bulk of sulphate of marine origin the following balance should match simultaneously where m, c and s stand for marine continental and Stripa waters respectively:

$W_m + W_c = W_s = 1$: water balance

$W_m \delta^{18}{}_m(H_2O) + W_c \delta^{18}{}_c(H_2O) = W_s \delta^{18}{}_s(H_2O)$: ^{18}O balance in water

$W_m \times C_m(SO_4) + W_c \times C_c(SO_4) = W_s \times C_s(SO_4)$: SO_4^{2-} balance

$W_m \times C_m(SO_4) \times \delta^{18}{}_m(SO_4) + W_c C_c(SO_4) \delta^{18}{}_c(SO_4) = W_s \times C_s(SO_4) \delta^{18}{}_s(SO_4)$: ^{18}O balance in SO_4^{2-}

$W_m \times C_m \times \delta^{34} + W_c \times C_c \times \delta^{34}{}_c = W_s \times C_s \times \delta^{34}{}_s$: ^{34}S balance

$W_m \times C_m(Cl) + W_c \times C_c(Cl) = W_s \times C_s(Cl)$: chloride balance

$W_m \times C_m(Br) + W_c \times C_c(Br) = W_s \times C_s(Br)$: bromide balance

With the following additional constraints for the marine component:

$C_m(Cl) = 7.1\ C_m(SO_4)$ $\quad$ $\delta^{18}{}_m(H_2O) = 0$ $\quad$ $C_m(Cl) = 17000$

$\delta^{34}{}_m(SO_4^{2-}) = +20$ $\quad$ $\delta^{18}{}_m(SO_4^{2-}) = +9.5$ $\quad$ $C_m(Br) = 65$

This system can not obey the necessary constraints W_m, W_c, C_m, $C_c \geq 0$, except for $W_m \leq 0.03$:

W_m	W_c	$\delta_c{}^{18}(H_2O)$	$C_c(SO_4)$	$\delta_c{}^{18}(SO_4)$	$\delta_c{}^{34}(SO_4)$	$C_c(Cl)$	$C_c(Br)$
0.01	0.99	-12.9	76.8	+7.2	+11.8	434	5.9
0.02	0.98	-13.1	53.2	+6.2	+8.1	265	5.3
0.03	0.97	-13.2	29.0	+3.3	-2.0	928	4.7

The discussion of such a small contribution appears meaningless. However, the continental component would be very rich in salts (SO_4^{2-}, Cl^- and Br^-) the origin of which would be difficult to explain.

Table 7-2 Stable isotope contents of waters and aqueous sulphates from Baltic Sea.

Sampling Depth	Cl^- mg l^{-1}	SO_4^{2-} mg l^{-1}	^{18}O (H_2O) °/oo SMOW	^{2}H (H_2O) °/oo SMOW	^{18}O (SO_4^{2-}) °/oo SMOW	^{34}S (SO_4^{2-}) °/oo CD
- 50 m	4200	560	-6.97	-57.7	+6.93	+19.22
-200 m	7800	870	-5.64		+8.83	+19.40

It is concluded that a supply of marine sea water can not be invoked.

Therefore hypothesis (a) which, furhermore, is not in agreement with other geological and chemical data (Nordstrom, 1983) will be discarded.

- o Hypothesis (b): Another possible source of sulphate in the Stripa system are the Quaternary precursors of the Baltic Sea, e.g. Yoldia or Littorina seas (Fritz et al., 1983). We have no data for these waters but measurements of ^{34}S and ^{18}O contents of Baltic Sea sulphates show that the marine isotopic signature is rather well-preserved even when the water is highly diluted (Table 7-2). Since the heavy isotope content of open ocean SO_4^{2-} has remained constant through the entire Quaternary (Claypool et al., 1980) a simple intrusion of Holocene Baltic Sea (hypothesis b) cannot provide an explanation for the origin of deep groundwater SO_4^{2-} in the Stripa system. In that case a "minor admixture of isotopically light sulphate" (Fritz et al., 1983) could hardly account for the observed differences for the same reasons as above.

- o Hypothesis (c): Fluid inclusions of granite contain sulphate (Nordstrom, 1983, and this report). However, the concentration is low (less than 20 ppm in the rock according to our measurements). Because of this scarcity, it was not yet possible to determine the stable isotope content of this sulphate and to discuss its origin. Measurements of ^{36}Cl indicates the chloride is not in secular equilibrium with the granite, although it might be leaching out of the leptite. Thus the sulphate is probably not coming directly from the granite. However, dissolution of secondary sulphate could be possible even if no solid sulphate was recorded from fracture filling minerals.

  Fracture sulphate (gypsum) was observed in Eye-Dashwa lakes pluton (Ontario). The sulphur 34 content of this gypsum ranges from +5.3 to +8.5 (Kaminemi, 1983). This range, much below ^{34}S contents of Stripa aqueous SO_4^{2-} (Figure 7-2), is attributed to a preservation of sedimentary Precambrian sulphate. Furthermore, the ^{18}O content is not available. Since a complete discussion of the origin of the sulphate is hardly possible without the knowledge of ^{18}O values (Michelot et al., 1984), one can-

not draw any further conclusion on the comparison with the Stripa system.

- o Hypothesis (d): Leaching of evaporites would probably have to involve Permian deposits since Zechstein evaporites have heavy isotope contents which are very close to those observed in sulphates from borehole V 1 (Claypool et al., 1980). Since borehole V 1 shows the highest sulphate content of the system, its heavy isotope content should have been the most preserved from significant modification due to partial reduction or further mixing. No Permian deposits are presently known in these regions of Sweden. However, recent paleogeographical reconstructions (Ziegler, 1982) map a Permian gulf in the Oslo region. Permian salts may thus have been deposited in the Fennoscandian peninsula and successively dissolved giving rise to dense solution which could have infiltrated the Fennoscandian shield.

  An alternative hypothesis takes into account the occurrence of gypsum, anhydrite and complex sulphate salts of Permian age throughout Northern Germany and Poland. Rivers from the catchment area of the Southern shore of the Baltic may have discharged diluted solutions of these sulphates into a "pre-Baltic" basin isolated from open ocean. Infiltrations would have brought this sulphate into the Stripa groundwater system. A very similar explanation may involve small supplies of Permian brines to the deep groundwater system (Michelot et al., 1984). Sulphates from evolved (post halite) brines would be slightly depleted in ^{18}O (and subsidiary in ^{34}S) by previous gypsum, anhydrite (and polyhalite) crystallization. It should be noted that heavy brines (denser than Baltic seawater) have been found in southern most Sweden (Smellie, 1984, pers. comm.) with a Br/Cl ratio close to 0.0114 and from southern Finland (Kankainen and Hyyppä, 1984).

  Regardless of the "origin" of this Baltic sulphate the question arises as to when this infiltration could have occurred and whether it took place before or after the last glacial period (assuming that no infiltration occurred during glacial times which still requires confirmation).

7.4.4 In-situ reactions involving sulphur compounds: V 2, N 1, M 3, and R 1

All these boreholes show variable but much lower SO_4^{2-} contents than V 1. Most of them contain reduced species of sulphur.

The ^{18}O isotope contents of V 2 appears sometimes much higher than those of V 1. Furthermore, values lie along a line with a slope close to 4. This is indicative of a partial reduction of a small amount of the initial sulphate bulk by bacteria. A partial

bioreduction of SO_4^{2-} could also explain the much smaller ratio SO_4^{2-}/Cl^- in V 2 ($\simeq$ 0.11) than in V 1 ($\simeq$ 0.16). The reduction line passes through V 1 values confirming that V 1 contains the initial, not reduced, bulk of sulphate.

For samples very depleted in sulphate (N 1, M 3 and R 1) the heavy isotope content may also have been modified by a partial reduction of sulphate (e.g. in R 1) or oxidation of reduced sulphur (e.g. in M 3). A very pronounced partial reduction could also account for the very high ^{34}S of N_1. For both N 1 and M 3, the reduction process might have occurred from an initial sulphate completely different from V 1 and which could be the shallow sulphate (see Figure 7-2). This hypothesis, which would imply an hydraulic connection between surface and the upper part of the deep groundwater system, still requires further measurements and investigations.

7.4.5 Regional survey of saline groundwaters

Heavy isotope contents of aqueous sulphates show extreme variations (about 70 °/oo in ^{34}S and 20 °/oo in ^{18}O). Values are not scattered: oxygen 18 contents follow an asymptotic trend to about +20 °/oo (Figure 7-3). Similar large variations have been reported from areas in which successive cycles of reduction and oxidation may occur (Gilkelson et al., 1981; Basharmal in Fritz, 1983). As suggested by Fritz (1983) the evolution may be due to the combination of (i) a Rayleigh process (incomplete reduction with removal of the reduced species through precipitation or degassing), (ii) a reaction between SO_4^{2-} and H_2O which tends toward isotopic equilibrium. Calculations of the various fractions of remaining sulphate after one single stage after reduction process in closed system give reasonable values for the initial content in aqueous SO_4^{2-}, assuming (i) a kinetic enrichment factor of 40 °/oo during reduction (Claypool et al., 1980), and (ii) on unique initial bulk of aqueous sulphate defined by the heavy isotope content of sample from V 1 (see Table 7-3). This enhances the possibility of V 1 to be representative of the regional bulk of aqueous sulphate: it would also strongly suggest that high contents in aqueous SO_4^{2-} in the region are:

- mainly derived from a common source;
- independent from their geological location.

Sample nr 3 in granite has a relatively low SO_4^{2-} content (35 ppm). It could represent either the oxidation of a reduced sulphur species previously derived from the same SO_4^{2-} bulk, or a SO_4^{2-} supply of meteoric origin as in the Stripa shallow water (see PW4).

At 10°C (average temperature for these groundwaters), the enrichment factor epsilon$^{18}(SO_4 - H_2O)$ is approximately +35 °/oo. At equilibrium the aqueous SO_4^{2-} of sample nr 11, which is the most enriched, should reach a ^{18}O content close to +25 °/oo. None of the

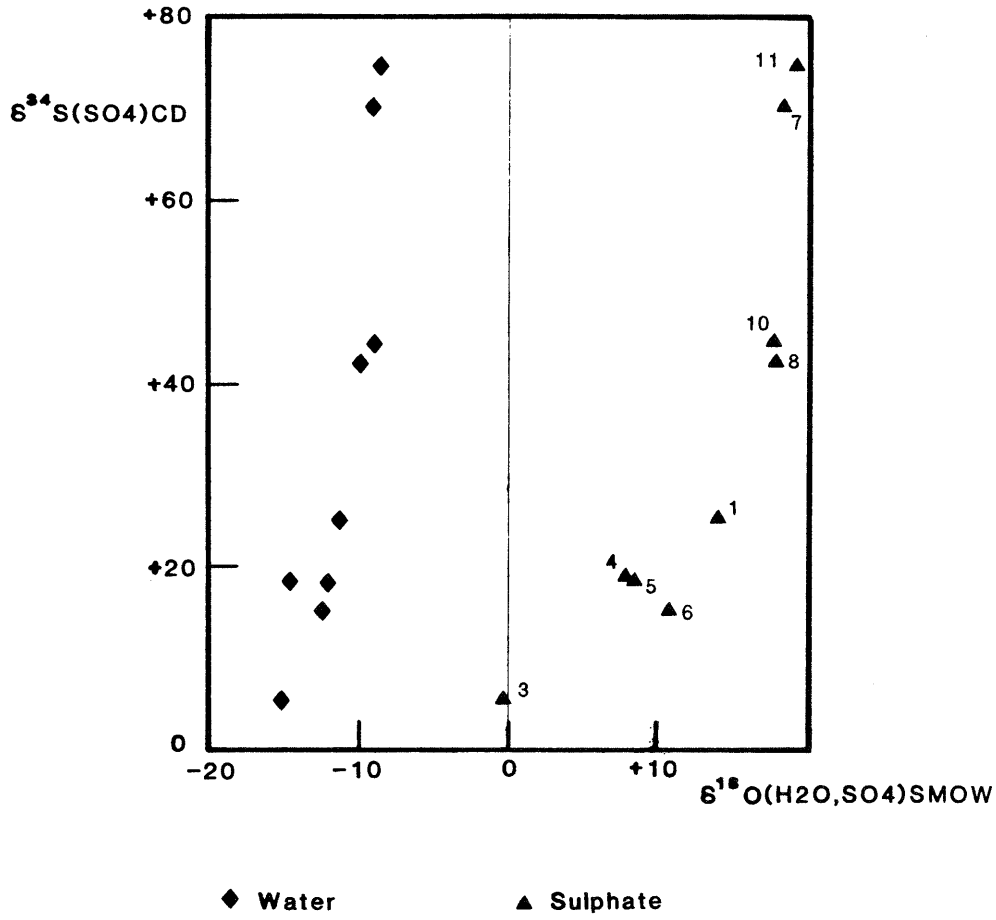

Figure 7-3. Oxygen 18 vs sulphur 34 contents in aqueous sulphates from central Sweden wells.

aqueous sulphate appears to be in equilibrium with the groundwater.

Theoretically one could then evaluate the residence time of SO_4^{2-} ions within a groundwater system through the knowledge of environmental temperature and pH which control the reaction. Satisfactory agreements are reported between ^{14}C and $^{18}O(SO_4^{2-})$ age estimations from a carbonate aquifer in Manitoba (Mkumba, in Fritz, 1983).

In the case of sample nr 11, a half-reaction time of 8360a is calculated at T = 283 K and pH = 7.64: according to Pearson and Rightmire (1980) equation, the corresponding time t of contact between water and aqueous sulphate is thus given by:

$$A = epsilon_{eq} \ (1 - e^{-(\ln 2/T_{1/2})t})$$

with:

$$A = \delta^{18}O(SO_4^{2-}) - \delta^{18}O(H_2O).$$

Table 7-3. Regional program sulphates.

Nr	^{34}S °/oo CD	f	$(SO_4^{2-})_i$ ppm
11	+74.7	0.22	545
7	+69.7	0.25	264
10	+44.3	0.47	200
8	+27.8	0.70	116
1	+24.9	0.76	113
4	+18.3	0.89	85
5	+18.0	0.90	122
6	+14.9	0.97	186

Calculation of the remaining fraction of SO_4^{2-} (f) and of the SO_4^{2-} initial content ($(SO_4^{2-})i$):

(Single Rayleigh reduction process, assuming:

- epsilon ^{34}S = 40 °/oo ≃ delta $^{34}S(SO_4^{2-})$ - delta $^{34}S(S^{2-})$

- delta $_0$ = delta $_{V1}$ = +13.8 °/oo)

The time contact is approximately 19,000a. This surprising age (since the Fennoscandian peninsula was covered by ice at that time) is, however, probably irrelevant.

As a working hypothesis, it is proposed that, more than time, the microenvironmental pH is the main controlling factor in that system. Through processes of oxidation-reduction the microenvironment of the reaction has become highly acid during oxidation steps:

$$H_2S + 3/2\ O_2 = SO_3^{2-} + 2\ H^+$$

or

$$H_2S + 3/2\ O_2 = HSO_3^- + H^+$$

Before the drop in pH is buffered through release of cations from the matrix, the rate of the isotopic reaction between SO_3^{2-} or HSO_3^- and water is greatly increased. Furthermore, recent data obtained on very old ^{14}C groundwaters from Saharian "Continental Intercalaire" (the world's largest confined aquifer) suggest that isotopic equilibrium between SO_4^{2-} and H_2O within neutral range of pH, is probably longer to reach than indicated from the extrapolation of Lloyd's experimental data (Fontes and Guendouz,

1984). As discussed before the SO_4^{2-} - H_2O "chronometer" should be carefully reassessed before any attempt of age estimation.

In conclusion, it appears that:

- redox processes may play a major role in the control of heavy isotope contents of the regional aqueous SO_4^{2-} and any age estimation from the ^{18}O content of the sulphate is probably risky.

- Stripa deep groundwaters from V 1 could be representative of the initial isotope and SO_4^{2-} contents of a regional supply of sulphate of sedimentary origin.

The conclusions of the stable isotopes of sulphate are not in agreement with those of the hydrochemistry. The necessary reconciliation of all of the data requires further research including efforts to find the possible source materials for sulphate either locally (from rocks along the groundwater flow path) or regionally. This research is being performed in the ongoing Phase II investigations.

8 THE CARBON AND OXYGEN ISOTOPIC COMPOSITIONS OF AQUEOUS CARBONATE AND CALCITES

8.1 Introduction

Within the Stripa project a large number of ^{13}C, ^{14}C and ^{18}O analyses were carried out on aqueous and solid carbonates. The analytical work was initially done within the LBL-KBS programme by the University of Waterloo (UW) and the International Atomic Energy Agency (IAEA). Dr. J.F. Barker, Dr. J. Gale and Mr. D. Reimer participated in this phase (Fritz, et al., 1979). Subsequent analyses were done by UW, the University of Paris-Sud (UPS) and the University of Bern (UB).

The following discussion is based on all data available and explores first the ^{13}C contents of aqueous carbon (TIC). Thereafter, the ^{14}C abundances in different water are discussed with the aim to evaluate this tool for the determination of residence times. The last section deals with the isotopic composition of fracture calcites and their role as indicators of hydrologic/geochemical processes.

8.2 Sampling and analyses

8.2.1 Aqueous carbonate

Samples for ^{13}C and ^{14}C measurements were collected either by precipitation of all aqueous carbonate (TIC) with $BaCl_2 \times 2\ H_2O$ or were shipped in aqueous form to the laboratory and extracted by acidification with phosphoric acid. Sampling methods are indicated in Table 8-1.

Precipitation with $BaCl_2 \cdot 2\ H_2O$ is a standard procedure which produces very reproducible results for both ^{13}C and ^{14}C determination. However, the low alkalinities of the deep Stripa waters proved to be a challenge and a number of different arrangements were used. For example, a number of 60 l bottles were filled in series to minimize air contamination, and precipitation had to be done with fresh, decarbonated reagents. After a precipitation, samples were shipped as alkaline slurry to the laboratories or washed with boiled, distilled water before filtration. The lowest ^{14}C contents were measured by the latter method, which, therefore appears to be most reliable. For samples collected in

a flow-through shipping system developed by UW for the LBL/KBS project phase as well as most other samples which relied on large volumes some air contamination may have occurred.

To overcome this, three samples were collected by UPS accelerator measurements through the UB. The results are encouraging, although it appears that again air contamination cannot be excluded. This is especially true for samples which were shipped as water to UPS and extracted there.

Samples for ^{13}C-TIC analyses (usually 500 ml H_2O) based on acid extraction were poisoned with $HgCl_2$ before shipment. Results are expressed as permille differences (δ °/oo values) from the PDB standard. Analytical precision is better than ± 0.15 °/oo and overall reproducibility is better than about ± 0.5 °/oo.

8.2.2 Fracture calcite

Fracture calcites were collected from borehole fractures and fracture surfaces exposed in the excavation. Since most samples were very small, no chemical or mineralogical analyses were attempted. Isotope analyses were done via a reaction of the calcite with 100% H_3PO_4 at 25°C and results are expressed as permille differences from the PDB standard for ^{18}O and ^{13}C. However, for the determination of isotope fractionation factors etc. it is necessary to use $\delta^{18}O$-SMOW (Standard Mean Ocean Water) values which are obtained using the following conversion formula

$$\delta^{18}O_{SMOW} = 1.03086\ \delta^{18}O_{PDB} + 30.86$$

8.3 Aqueous carbon

The carbon isotopic composition of the aqueous carbon is a direct reflection of the geochemical history of a groundwater. This evolution begins in the recharge environment and continues in the subsurface where mineral-water interaction will dominate. The possible expected changes in ^{13}C contents are summarized in Figure 8-1. It shows that in most recharge environments the uptake of isotopically depleted soil-CO_2 produces $\delta^{13}C$ values in the aqueous carbon which are close to -20 °/oo, more positive values are found in high pH environments, lower values where low pH values dominate. The subsequent dissolution of carbonate minerals will usually cause an enrichment in ^{13}C and values as high as 0 °/oo can be reached if the incongruent dissolution of dolomites occurs. Biological processes can further modify the isotopic composition of the aqueous carbon and generate $\delta^{13}C$ values as high as +20 °/oo if methane production occurs or very negative values where organic compounds are oxidized.

The results of ^{13}C and ^{14}C analyses on aqueous carbonate in the Stripa groundwaters are summarized in Table 8-1. They show relative uniformity which a first indication that the carbon geochemistry of these different waters has a similar history. Furthermore, all $\delta^{13}C$-TIC values are below -10 °/oo, which is a strong suggestion (see Figure 8-1) that biogenic processes are important.

8.3.1 Shallow groundwaters

Geochemically least evolved are watertable wells in which the carbon geochemistry is largely determined by the PCO_2 of the soil-zone and the pH of the water. The lowest ^{13}C contents are found in watertable well WT2 which has a $\delta^{13}C$ = -23.2 °/oo PDB and a pH = 5.1. Assuming open system equilibration the soil-CO_2 would be close to -23.0. Chemical data agree with this since the field measured alkalinity corresponds to 2.9 ppm HCO_3 and the water is saturated with atmospheric oxygen. The water in this well represents most closely the recharge condition for present day (and past?) Stripa groundwaters.

Calcite dissolution probably occurs in the shallow groundwaters at Stripa yet only deeper waters are saturated with respect to calcite. This is graphically shown in Figure 8-2; saturation indices for calcite were calculate with the WATEQF speciation programme by Plummer, et al. (1976). This figure is from Fritz et al, (1979), and a more complete picture is seen in Figure 5-7.

The uptake of calcium carbonate carbon in the shallow groundwaters is in agreement with the observed isotope data if, as suggested above, the open system uptake of soil-CO_2 does occur and if subsequently a closed system dissolution of calcite occurs with calcite - $\delta^{13}C$ below about -5 °/oo.

The required, non-marine calcite values are encountered in the fracture calcites of the Stripa rocks. Watertable well WT3 already has 33.1 ppm HCO_3, a pH = 6.6 and a $\delta^{13}C$ = -21.8, all of which suggest that carbonate dissolution has already taken place.

Further evolved are the waters in the private wells, whereby especially the deeper ones reach calcite saturation. This is achieved through the dissolution of carbonate minerals. However, the $\delta^{13}C$ values of PW 2, 3 and 4 are amongst the highest of all samples measured and model calculations (Fritz, et al., 1979) show that they must have dissolved a calcite with higher $\delta^{13}C$ values than found on the fractures of the crystalline rocks. This could be represented by a local marble which has a $\delta^{13}C$ = -1.4 °/oo PDB. PW 1 and 5 are sunk into granitic rocks and their water did not see carbonate with such high $\delta^{13}C$ values.

Table 8-1 The carbon isotopic composition of aqueous inorganic carbon in Stripa groundwaters.

Location	Interval (m)	Date	$\delta^{13}C$ TIC	$\delta^{13}C$-$BaCO_3$	^{14}C pmC
Tailing pond		77-09-12	-23.2		
Watertable wells					
WT-2		79-05-05/18	-23.2		
WT-3		79-05-01	-21.8		
Private wells					
PW 1		77-09-27	-15.2		
		79-05-18	-14.0		
PW 2		77-10-24/27		-15.0	53.8[b]
		77-10-24/27	-15.2	-14.9	54.1[c]
PW 3		79-05-16	-13.4		
PW 4		79-05-17/24	-13.7	-14.1	52.1[c]
PW 5		77-10- 6/13	-19.1	-18.1	89.3[b]
		79-05-15	-22.3		
SBH-3	89-104	79-05-22/28	-15.6	-15.2	62.8[c]
M3	~ 10	77-09-09/21	-13.2	-15.8	2.5[b]
		77-11-15/23	-16.8		3.5[c]
		79-05-02/10	-16.2	-16.3	6.4[c]
		79-11-11/12	-15.9	-16.9	2.8[c]
		79-11-20/22	-16.0	-15.8	3.3[c]
		84-03	-15.9(-16.7)[d]		
R1	~ 30	78-08-09/26		-16.2	4.5[c]
		78-11-17/24	-17.1	-19.0	6.6[c]
		79-05-02/08	-16.4	-17.7	7.0[c]
		79-05-09	-16.1		
R9	~ 30	79-05-22	-15.5		
N-1 horiz.	252-300	84-02-14	(-17.3)[d]		
	151-251		-15.9(-17.1)		
	120-150		(-13.0)		
	10-119		(-14.0)		
		83-		-23.1±2.4	3.95±3.83[e]
		84-		-18.7±3.2	16.06±0.33[f]
E-1	openhole	84-02-14	(-17.6)		
V-1	10-550	84-02-14	(-23.4)		
V-2	6-50	77-09-09/20	-16.1	-15.5	6.0[b]
	8-40	78-06-08	-16.6	-15.7	2.1[c]
		78-11-16/20	-16.5		2.0[c]
		79-09-11/13	-15.9	-16.9	2.8[c]
	below 50	77-09- 8/14	-18.3	-16.9	
	below 280	77-09-14/20	-18.6	-17.8	
	below 380	78-06-12/24	-18.7	-17.5	13.6[c]
	332-359	79-01-31 to 03-16		-18.2	
	400-428	78-11-20	-16.9		
		78-11-22 to 12-20		-13.3	19.4[c]
	400-428	79-04- 6/27		-13.3	7.8[c]
		79-05- 7/11	-14.0	-13.6	5.5[c]
		79-05-18/21	-14.4		
	0-428	77-10-24/26	-16.1	-15.9	5.1[c]
				-18.5	4.7[c]
V-2-3	424-499	83-11-28		-35.6±7.8	14.67±0.75[f]
V-2-4	562-822	84-02-15	(-19.6)		
	500-561	84-02-15	(-30.8)		
	424-490	84-02-15	(-28.3)		
	382-423	84-02-15	(-16.9)		

a The $\delta^{13}C$, TIC (Total Inorganic Carbon) values refer to samples collected and acid extracted specifically for ^{13}C analyses, whereas the $\delta^{13}C$ - $BaCO_3$ values were obtained on barium carbonate precipitated from large volumes for ^{14}C analyses. The $\delta^{13}C$ - TIC, values are considered to be more reliable.

b ^{13}C-$BaCO_3$ and ^{14}C analyses done at Intern. Atom. Energy Agency, Vienna, Austria.

c ^{13}C-$BaCO_3$ and ^{14}C analyses done at Univ. of Waterloo, Waterloo, Canada.

d Samples were shipped to UW in plastic bottles. All other TIC samples were collected in glass bottles.

e Analyses done by accelerator measurements by the University of Bern on barium-carbonate.

f Analyses done by accelerator measurement by the University of Bern on acid-extracted CO_2.

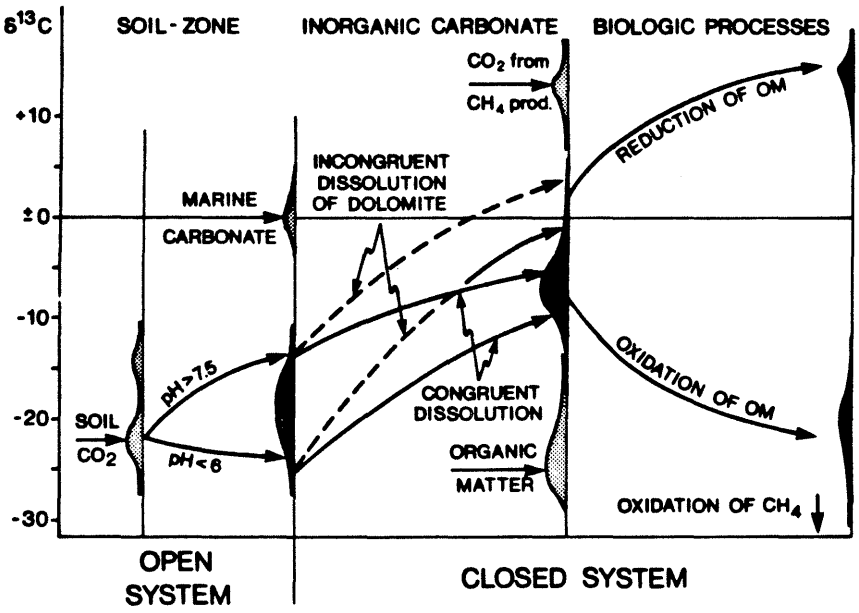

Figure 8-1. Possible range of $\delta^{13}C$ values in the aqueous carbonate of groundwaters. Dark areas indicate expected $\delta^{13}C$-TIC values whereas shaded areas represent source terms.

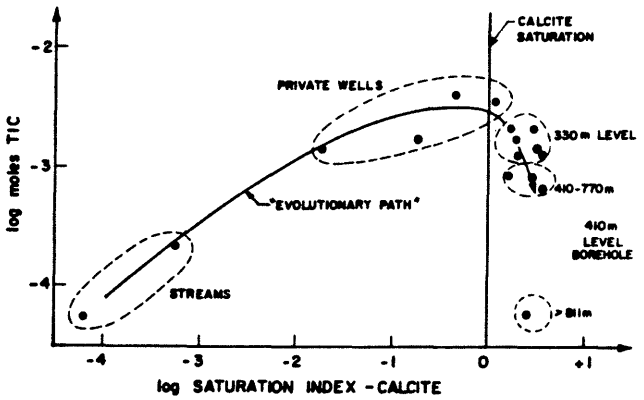

Figure 8-2. Total inorganic carbonate and calcite saturation in Stripa groundwaters. From Fritz, et al. (1979).

8.3.2 Deep groundwaters

All deep groundwaters collected at various mine levels and different boreholes are slightly supersaturated with respect to calcite. As indicated in Figure 8-2, this supersaturation appears to be paralleled by a loss of inorganic, aqueous carbon (TIC) which suggests that calcite precipitation is occurring. The precipitation of calcite will preferentially remove some ^{13}C but the isotope effects are small and significant shifts towards lower $\delta^{13}C$ values can only be expected if more than 70% of the TIC is removed as calcite (Figure 8-3). No actual calculations can be per-

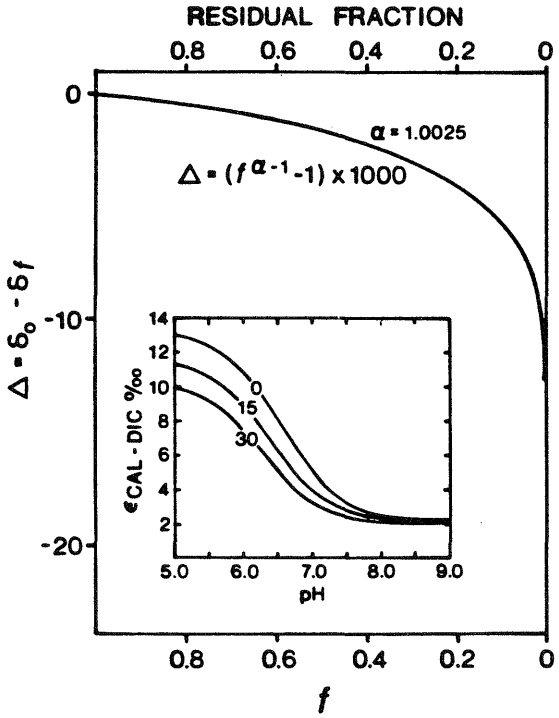

Figure 8-3. Isotope effects caused by precipitation of calcium carbonate from solution. Since the enrichment factors (α) cause preferential removal of ^{13}C in the solid phase the residual fraction of the aqueous carbon (f) becomes depleted in this isotope.

formed because nothing is known about initial TIC contents in the deep waters. However, the more saline waters have considerably less TIC than the shallow, fresh groundwaters and if this difference is applicable to the evolution of the deep groundwaters then $\delta^{13}C$ values may have been affected by calcite precipitation.

The similarity of $\delta^{13}C$-values in deep and shallow waters is remarkable and suggests a) that either no carbon is added to the waters following an initial evolution similar to what was seen in the shallow wells in crystalline rocks or b) that carbon added has an isotopic composition similar to the TIC of these waters.

A case could be made for both situations and, indeed one may have to assume that in some samples only a loss had occurred whereas others have seen the addition (followed by loss?) of carbon. The latter is recognized in groundwaters which discharge today from V-2 at depth between 424 and 560 m. They display very low $\delta^{13}C$ values of -35.6, -30.8 and -28.3 °/oo (Table 8-1). These values are probably not due to the loss of carbon by carbonate precipitation but may reflect the presence of CO_2 which was generated by oxidation of organic matter or methane. A characteristic feature of many Stripa calcites are low $\delta^{13}C$-values and such CO_2 may well play an important role, both for ^{13}C and ^{14}C concentrations as will be shown below.

Based on the information available to date, it appears safe to conclude that the carbon in the aqueous carbonate of the Stripa groundwaters has largely a biogenic origin. The agreement between deep and shallow waters could suggest similar evolutionary path at least as far as the carbon geochemistry of these waters is concerned. The addition of marble or marine carbonate is not found to be an important factor.

8.4 Carbon-14 measurements

The basic concept underlying the carbon-14 dating requires that waters infiltrating through vegetated soils become charged with soil-CO_2 before they become part of a groundwater reservoir. Because this soil-CO_2 has a partial pressure up to two orders of magnitude higher than the atmospheric CO_2, it dominates the carbon isotope content of infiltrating water. Its ^{14}C activity is very close to the ^{14}C activity of the atmosphere. If no other carbon were added, and only decay altered the ^{14}C contents of the dissolved carbonate, this residual activity would be a function of time only, where

$$A_{measured} = A_{initial} \cdot e^{-\lambda t}$$

with A = ^{14}C activity in pmC and λ = decay constant.

Unfortunately, most groundwaters get their aqueous carbonate not only from the soil reservoir, but also from the aquifer carbonates and other sources. These are normally free of ^{14}C and their carbon will therefore "dilute" the ^{14}C contents of the initial soil carbon. The measured ages then become too old.

Many attempts have been made to quantify this geochemical dilution and to establish correction factors which would permit recalculation of the water ages. Three approaches have been taken:

- a statistical approach;
- chemical analyses to assess the amount of rock carbonate dissolution and precipitation;
- ^{13}C is used as an indicator for dead carbon contributions from isotopically distinct sources.

The statistical approach does not attempt to understand the geochemical processes which control the carbon geochemistry of a groundwater. For crystalline terrains, Geyh (1972) proposed "correction factors" which reduce the initial activity by 0 to 20 percent. The numerical value of such "q" factors thus varies between 1 and 0.8 and appears in the decay equation as

$$A_m = qA_0 e^{-\lambda t}.$$

This approach is not very satisfactory primarily because the q-factors were developed only on data from water samples which contained tritium and, therefore, any further geochemical dilution occurring in waters older than 25 to 30 years could not be taken into account.

The ^{14}C contents of the aqueous carbon of a groundwater is strongly dependent on the carbon geochemistry of the system. The simplest "chemical" correction factor is derived from a comparison of initial versus final carbonate content. Such comparison implies (1) no carbon loss through mineral precipitation and (2) that isotope exchange/loss with the rock matrix was not important. Both processes do, however, take place, and more sophisticated models based on a total assessment of the geochemistry of a groundwater and its evolution have been developed. These models combine geochemical considerations with observed ^{13}C variations (Reardon and Fritz 1978; Wigley et al., 1978; Fontes and Garnier, 1979).

If the $\delta^{13}C$-TIC is used as an indication for the uptake of inorganic carbon, then a carbon isotope mass balance in a two component system will lead to the following relationship to obtain an approximate correction factor q:

$$q = \frac{\delta^{13}C\text{-TIC} - \delta^{13}C\ CARB}{\delta^{13}C\text{-soil} - \varepsilon - \delta^{13}C\ CARB}$$

$\delta^{13}C$-TIC is the measured $\delta^{13}C$ value of the sample, $\delta^{13}C$-CARB is the value for the dissolving rock-carbonate, $\delta^{13}C$-soil is the isotopic composition of the soil-CO_2 and ε is the pH dependent isotopic difference between soil-CO_2 and inorganic carbon TIC under open system equilibrium conditions. This value will be close to 0 $^{o}/oo$ for recharge environments with pH close to 5 - such as found at Stripa but becomes important as the pH in the recharge area rises and the system remain open to equilibration with soil-CO_2. Where recharge conditions cannot be estimated, ε is usually neglected.

The final choice of how to transform ^{14}C ages obtained on aqueous carbonate into water ages depends on the amount of information available. For the Stripa project, samples were collected from private wells in the area as well as from all flowing wells and boreholes in the underground working area, in an attempt to understand as completely as possible the geochemistry and isotopic evolution of the Stripa groundwaters.

Finally, it is again necessary to address the concept of water "age" since it might appear that here it is used to describe the "age" of a single water mass. This is not so, since at best one could talk about "mean residence times" of a groundwater. How-

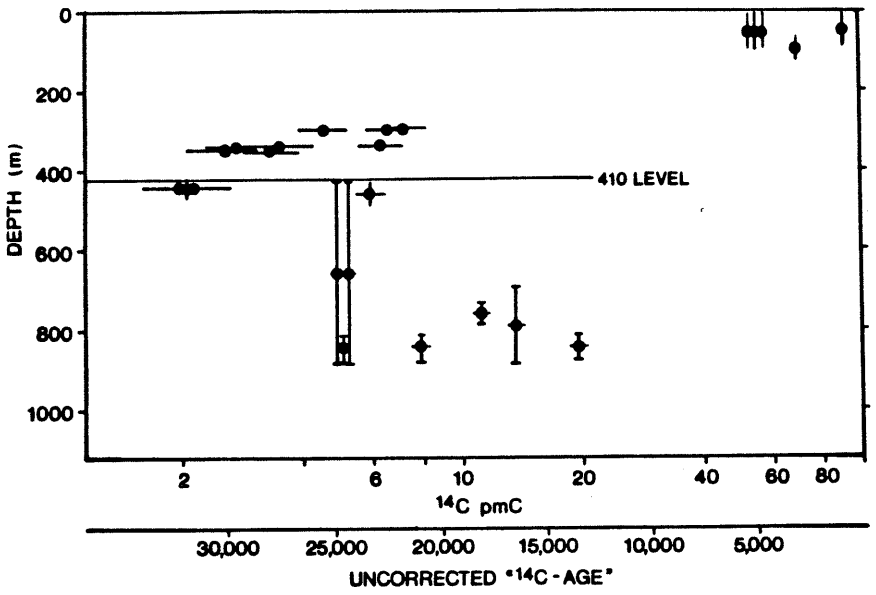

Figure 8-4. Radiocarbon measurements on Stripa groundwaters. The data do not include the accelerator measurement given in Table 8-1.

ever, even this term may be misleading because as has been mentioned in Section 6 of this report, it is quite likely that many of the waters collected in this study represent mixtures of two or more components. For example, a saline old component may have been added to less saline, younger groundwaters and the radiocarbon measurement would reflect the average of the two carbon sources. Thus, it is suggested that absolute age determinations are not possible for the Stripa groundwaters and, instead, such analyses were used to assess the relative "age" of the different aqueous geochemical systems in the Stripa granite.

All ^{13}C and ^{14}C results obtained on aqueous carbonates are listed in Table 8-1. Four of these samples come from shallow private wells from farms in the vicinity of the mine, and the remainder from flowing boreholes at the test site and from the flowing well V-2 at the 410-m level. The ^{14}C-ages for all or much of their water should be modern, i.e., have a ^{14}C activity corresponding to at least 100 pmC. It is unlikely that in the shallow wells an old, low ^{14}C water mixed with modern water and one can assume that the lower activity levels document a significant dilution of initial activity as a result of geochemical reactions.

8.4.1 Shallow groundwaters

The dilution of initial activities has been evaluated on the basis of chemical and isotope analyses, using model calculations where the measured carbon isotopic composition can be compared with a theoretical composition calculated for assumed initial

conditions and different evolutionary paths (Reardon and Fritz, 1978).

The principal conclusions of these calculations are summarized as follows (Fritz, et al., 1979).

- soil CO_2 with a $\delta^{13}C = -23$ °/oo has equilibrated with the infiltrating water at pH = 5,
- the ^{14}C activity of the soil CO_2 was between 100 and 130 pmC, and
- ^{14}C-free rock carbonate with an average $\delta^{13}C$ value below about -5 °/oo dissolved under closed system conditions. As will be shown below, most fracture calcites analyzed in this study fit this requirement and the only exception is a sample of marble from the Stripa area (SBH-3) which had a $\delta^{13}C = -1.4$ °/oo.

These assumptions are not unreasonable: The low pH implies a pCO_2 of 10^{-2} atm which is normal for soils in these environments where, under moss covers, pCO_2 values can be even higher. The ^{14}C activities will be above 100 pmC for very young waters and at about 100 pmC for the somewhat older shallow systems. The surface environments are usually free of carbonate and most dissolution must occur in closed systems within the fractures. This explains why a ^{14}C dilution exists: if this dissolution took place in contact with the soil atmosphere then the ^{14}C activities of the aqueous carbonate would remain close to modern even if the carbonate were free of ^{14}C. The calculation suggests that the $\delta^{13}C$ values of this carbonate should be more negative than the -1.4 °/oo measured on the marble and that fracture calcites deposited much earlier are now partially redissolved by infiltrating groundwaters. Such dissolution must have taken place wherever the shallow waters are in contact with carbonate, since most of the samples of shallow waters are undersaturated with respect to calcite.

The dilution factors (q) derived for the shallower samples vary from about 0.7 to 0.5. The ultimate correction factor for deeper waters could be larger, since these shallow waters have not reached calcite saturation, and will continue to dissolve calcium carbonate. Exchange with carbonate minerals and diffusive loss into the rock matrix will be of no importance in these shallow systems.

8.4.2 Deep groundwaters

The total carbonate contents of the groundwaters decrease with depth and one could assume that the "evolution" from shallow to deep groundwater involves calcite precipitation. This is possible because the pH and Ca concentrations of the waters increases,

and thus maintain calcite saturation. Hydrolysis and dissolution of silicate minerals are probably responsible for this pH increase. If calcite dissolution were paralleled by precipitation, then the observed chemistries could also be explained by closed system dissolution.

The removal of calcium carbonate from solution has little effect on the ^{14}C activities, because the ^{14}C isotope effects are only twice those known for ^{13}C. Thus a 2 °/oo decrease in ^{13}C corresponds to a 4 °/oo or 0.4 percent decrease in ^{14}C activity. This change is within analytical error. One exception could the incongruent dissolution of dolomite. However, since this mineral has not been found this possibility can be disregarded. Thus, in correcting measured ^{14}C ages, only dilution occurring during carbonate uptake until calcite saturation is reached has to be taken into account. Applying this correction to the results presented in Table 8-3, the waters discharging at the 330-m level would have an mean residence time between 23,000 and 25,000 years. Samples from the shallow part of the deeper V-2 hole tend to be slightly younger ..... apparently!

In these deep and possibly old waters the possibility of ^{14}C exchange between the fracture calcites and the aqueous carbon will also have to be considered, because other studies have shown that it could be important - at least in systems where fine grained carbonate is exposed to migrating groundwater (Mozeto et al., 1984). There, however, the aqueous carbon approaches isotopic equilibrium with the carbonate minerals. We have no indication that this is the case at Stripa.

Neretnieks (1980) showed that diffusive loss of radiocarbon into the rock matrix can become very significant, depending on fracture spacing and width. For example, for a 2 m fracture spacing and a fracture opening of 0.1 mm the ratio of actual to measured water ages can become as high as 100. However, the most important fracture systems at Stripa appear to have larger openings and smaller spacing and, therefore it is felt that at least the deep, saline waters, are little affected by this process.

The question also arose as to whether the subsurface production of ^{14}C might be possible in an environment locally enriched in uranium bearing minerals. An evaluation by researchers at the University of Arizona (Zito, et al., 1980) concluded that this may well be possible, although the amounts involved would probably not exceed the equivalent of a few pmC. Further work in uranium bearing fracture systems is, however, warranted because the theoretical data must be supported by field evidence before they become acceptable.

The most important problem in this study was the collection of uncontaminated samples. Because of the low carbon contents up to several thousand litres of water had to be processed which cau-

sed considerable sampling problems. The high variability of the ^{14}C activities listed in Table 8-1 for the V-2 borehole attest to this. However, a continuous stripping device was constructed and directly connected to the flowing borehole. CO_2 was evolved by continuous acidification and flushing with purified N_2. The gas was absorbed in a 5N NaOH solution. Two samples from the deepest portion of V-2 were collected and measured 7.8 and 5.5 pmC. Assuming that both still show minor contamination with atmospheric CO_2, then the mean residence time of these waters would be greater than about 25,000 years. This assumes that geochemical corrections based on carbonate dissolution-precipitation, as described earlier, can be applied.

The new accelerator techniques should be able to overcome such problems. Table 8-1 list three results which show, however, that problems may persist even if much smaller samples are collected: N-1 was sampled twice and one results is comparable to the lower ^{14}C contents measured by conventional techniques whereas the second yielded much higher radiocarbon concentrations. It is not certain whether some contamination occurred or some young water components are present induced by a changing flow pattern. The well should be resampled. However, the measurement for V-2 is also much higher than conventional determinations and provides a strong indication that contamination had occurred.

8.5 Fracture calcites

Fracture mineral studies using environmental isotope analyses were, to date, limited to studies of fracture calcites, but will be expanded in the future. Calcites were collected from cores of a number of boreholes but no attempts were yet made to classify the calcites and associated minerals. All results are listed in Table 8-2. The oxygen and carbon isotopic composition of calcite which form in isotopic equilibrium is determined by the ^{18}O in the water, the ^{13}C of the aqueous carbon and the temperature. Figure 8-5 compares measured ^{18}O and ^{13}C data whereas Figure 8-6 and 8-7 show equilibrium fractionation effects for δ^{18} and ^{13}C respectively.

Calcium carbonate occurs on many fractures in the Stripa granite, usually in association with quartz, epidote, chlorite and mica, (Carlsson and Olsson, 1983). These assemblages are thus different from those investigated by Tullborg and Larson (1982) in the crystalline rocks at the Finnsjön test sites or the Gideå test site which was studied by Tullborg and Larson (1983). There, calcite is often found in association with prehnite and laumontite. For comparison, Tables 8-3 and 8-4 show electronmicroprobe analyses of the dominant fracture mineral at Stripa and Finnsjön respectively, which document that, indeed, the mineralogical composition of the fractures fills analyzed are different

Table 8-2 Carbon and oxygen isotopic compositions of fracture calcites from Stripa boreholes.

		Fracture calcite	
Borehole	Depth (m)	$\delta^{13}C$ PDB (°/oo)	$\delta^{18}O$ PDB (°/oo)
SBH-1	106.43	-10.7	-11.1
	107.85	- 7.0	
	124.03	- 4.5	
	132.31	- 9.0	
	152.90	-10.1	
		-12.4	-11.5
	174.67	- 6.8	
	178.35	-13.2	- 9.5
	189.95	-11.3	
	206.63	-11.6	
	247.11	- 8.3	-10.3
	278.40	- 4.1	-23.7
		- 3.9	
	305.7	-15.2	
	306.20	- 3.8	-21.7
SBH-2	9.4	- 1.4 (marble)	
	79.43	-13.5	
	92.43	- 6.5	
	99.43	-11.1	-12.7
	103.82	+15.3	
	104.27	+13.0	
OV2 BHH1	9.54	- 9.6	- 9.8
BHH3	6.64	- 9.7	- 9.8
BHH6	1.64	- 6.4	-15.8
Back wall of time-scale room ^{14}C: below detection limit			
		- 4.2	
V1	493	- 8.4	-20.9
	495	-16.2	-17.4
	495	-35.7	-13.4
	496	-16.8	-19.3
	497	-14.3	-17.4
V2	316.69	-18.9	-18.2
	317.75	-17.1	-17.9
	318.61	-14.3	-16.8
SBH-3	18.36	- 4.8	-22.5
	24.09	- 4.2	-20.5
	24.2	- 4.7	-21.5
	65.8	- 4.4	-23.3

unless the Ca-mica analysed by Reimer (1980) are in reality prehnite. Unfortunately, however, no efforts have yet been undertaken to study the Stripa fractures with the same techniques as applied at Finnsjön. This is a shortcoming which will be corrected in future studies.

If present groundwaters in the Stripa granite were to deposit calcite then the temperature of deposition would be between 5 and 15°C. Using this range and the fractionation effects shown in Figure 8-6 and 8-7, it is possible to calculate the isotopic composition of calcites which could be deposited. This range is indicated in Figure 8-5. It is noteworthy that this range does not comprise any samples below 300 m which could suggest that the deep waters at present do not precipitate any significant amount of calcite.

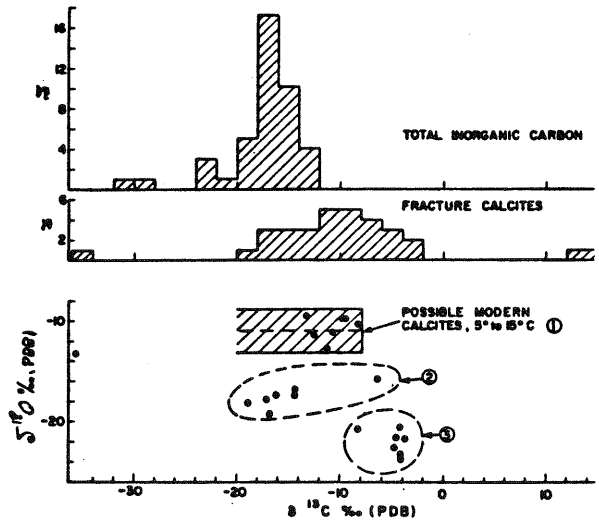

Figure 8-5. The oxygen and carbon isotopic composition of calcites from the Stripa granite.

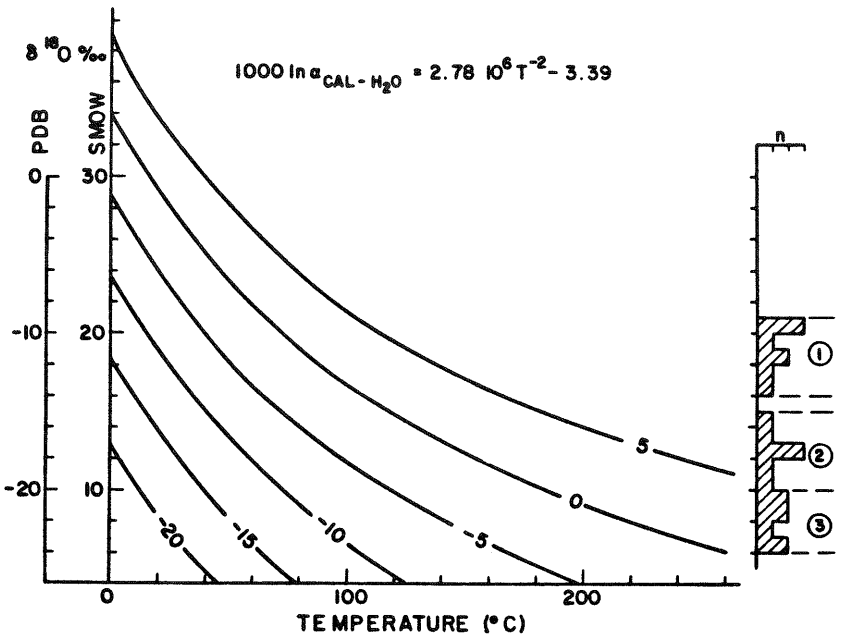

Figure 8-6. Equilibrium isotope effects for ^{18}O in the calcite water system. The histogram show $\delta^{18}O$ values for Stripa calcites. The conversion $\delta^{18}O$ PDB to $\delta^{18}O$ SMOW is by the following equation:

$$\delta^{18}O \text{ SMOW} = 1.03086 \ \delta^{18}O \text{ PDB} + 30.86.$$

In total 3 groups of calcite appear to exist:

Group I would be modern calcites in possible isotopic equilibrium with the water.

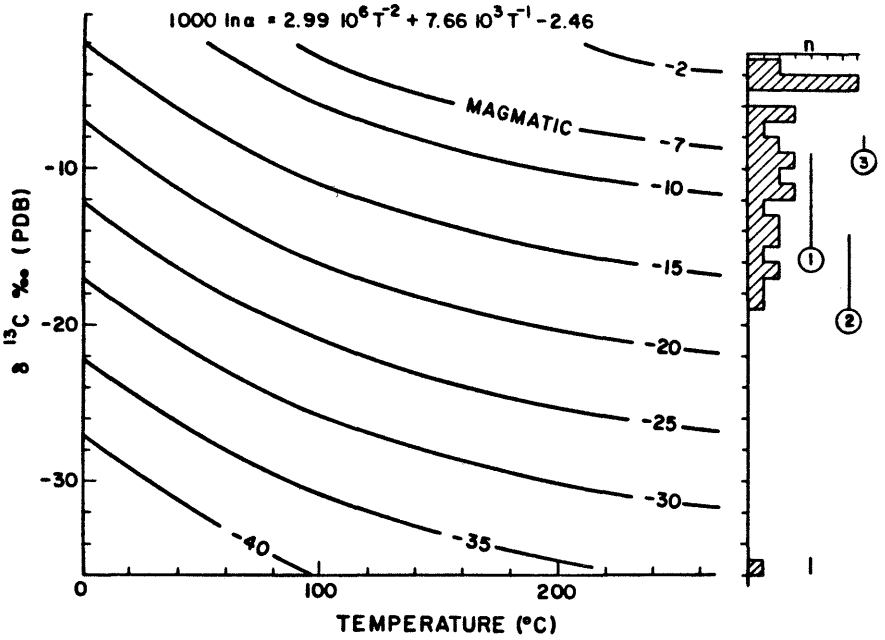

Figure 8-7. Equilibrium carbon isotope effects in the CO_2 - $CaCO_3$ system. The histogram shows $\delta^{13}C$ values of Stripa calcites with indications to which group they might belong.

Group II has the same range of $\delta^{13}C$ values as seen in Group I but distinctly lower ^{18}O values and

Group III comprises samples with relatively high $\delta^{13}C$ but very low $\delta^{18}O$ values.

The "modern" calcites (group I, Figure 8-5) are isotopically comparable to many of the "open fissure" calcites noted by Tullborg and Larson (1982). This is especially true if only ^{18}O where considered which has a much narrower range than ^{13}C. Figure 8-8 is a comparison of Stripa, Finnsjön and Gideå data which documents the similarities and differences. This figure shows that the latter prevail.

Tullborg and Larson (1982) recognized for Finnsjön at least three calcite generations on the basis of fluid inclusion data, mineralogical assemblages and oxygen isotopic compositions. Their group I has $\delta^{18}O$ values above -10 °/oo (PDB) and shows also the highest $\delta^{13}C$ values. Both open and sealed fissures occur and their genesis can possibly be linked to the participation of seawater. This group is only recognized at Finnsjön and does not appear at Stripa or Gideå. Finnsjön Group II appear to be a mixture of "modern" and hydrothermal calcites whereas group III at Finnsjön represents hydrothermal calcites collected below 300 m depth. These latter calcites are associated with prehnite and laumontite.

Table 8-3 Microprobe analyses on Stripa fracture minerals.

CHLORITES

SAMPLE		DEPTH (m)	COMPOSITION AS WT. % OXIDE SiO_2	Al_2O_3	FeO	MgO	CaO	Na_2O	K_2O	TOTAL
Slant 1	A	19.7	24.4	19.9	35.8	7.1	nd	nd	nd	87.2
	B		28.4	18.8	28.9	5.2	tr	nd	1.2	82.5
Slant 1	A	16.9	21.4	17.8	35.2	4.7	nd	nd	tr	79.1
	B		24.7	20.7	37.1	6.2	nd	nd	nd	88.7
	C		23.9	20.2	36.2	5.0	nd	nd	tr	85.3
	D		23.9	20.6	36.8	6.1	nd	nd	nd	87.4
Slant 1	A	27.8	24.6	19.5	37.9	5.8	nd	nd	tr	87.8
	B		25.6	19.7	35.7	6.5	nd	nd	tr	87.5
	C		37.5	19.2	26.9	4.4	nd	3.3	tr	91.3
V-2	A	19.1	23.0	19.6	37.2	4.4	nd	nd	nd	84.2
	B		22.6	17.8	34.9	6.9	nd	nd	nd	82.2
	C		25.7	21.9	34.2	5.6	nd	nd	tr	87.4
	D		26.7	21.6	32.9	3.6	nd	nd	1.5	86.3
	E		31.7	19.9	25.1	8.1	tr	nd	2.1	86.9
V-2	A	14.65	31.4	20.5	21.6	5.4	5.1	nd	1.8	85.8
V-2	A	409.9	26.8	19.3	20.1	17.8	nd	nd	tr	84.0
	B		27.9	17.4	17.7	21.3	nd	nd	nd	84.3
	C		28.3	18.0	17.7	21.5	nd	tr	nd	85.5
	D		29.1	18.7	18.1	20.2	nd	tr	tr	86.1
	E		28.9	18.2	16.9	21.6	nd	tr	nd	85.6
	F		30.0	20.1	17.1	15.7	nd	tr	1.7	84.6

STRIPA

MICAS - II

SAMPLE		DEPTH (m)	COMPOSITION AS WT. % OXIDE SiO_2	Al_2O_3	FeO	MgO	CaO	Na_2O	K_2O	TOTAL
SERICITE										
Slant 1	A	31.7	46.4	26.4	4.9	2.8	1.5	nd	8.7	90.7
Slant 1	A	19.7	44.1	26.6	3.3	1.1	nd	nd	8.8	83.9
	B		42.8	24.8	11.0	3.1	tr	nd	7.0	88.7
V-2	A	355.7	46.6	26.1	6.0	2.2	3.2	nd	7.8	91.9
V-2	A	14.65	37.0	24.8	18.6	3.7	nd	nd	5.9	90.0
	B		43.2	25.8	8.2	2.8	5.9	nd	6.1	92.0
Ca-MICA										
V-2	A	355.7	38.7	23.0	11.6	5.1	10.8	nd	1.7	90.9
	B		43.0	20.5	9.2	tr	20.1	nd	tr	92.8
	C		36.2	22.1	10.9	1.8	17.3	nd	1.0	89.3
	D		37.4	22.9	10.5	1.3	20.0	nd	tr	92.1
V-2	A	404.2	35.2	24.2	10.2	7.6	11.9	tr	tr	89.1
V-2	A	14.65	40.4	19.7	16.0	2.9	10.2	nd	tr	89.2
V-2	A	9.55	43.8	18.6	11.6	6.3	4.7	nd	1.5	86.5
	B		43.4	22.2	7.5	tr	17.5	1.1	tr	91.7

From: Reimer, 1980 in Fritz et al., 1980.

Table 8-4 Microprobe analyses of minerals. (Contents are given in weight-%).

Laumontite		K_2O	Na_2O	CaO	MgO	Al_2O_3	SiO_2
Fi5:264.4 m		0.53	0.23	11.1	0.1	21.8	52.1
"		0.51	0.34	11.3	0.1	22.2	50.4

Prehnite	TiO_2	CaO	MgO	MnO	Al_2O_3	FeO	SiO_2
Fi5:264.4 m	-	27.3	0.2	-	23.3	1.9	43.6
"	-	27.3	0.1	-	22.6	2.7	43.8
Fi7:335.1 m	-	26.5	0.2	0.1	23.1	1.7	44.8
"	0.1	26.4	0.2	-	22.9	1.8	44.4
Fi7:379.5 m	0.1	27.7	0.1	-	21.2	3.7	41.8
"	-	27.8	0.2	-	21.9	3.1	41.4

Calcite		BaO	CaO	CO_2	MnO	SrO	MgO	FeO
Fi7:41.1 m		-	54.5	43.2	0.2	0.1	0.8	0.4
"		-	54.7	44.2	0.5	-	1.0	0.4
"	(Prismatic)	0.1	55.5	42.9	0.3	-	0.6	-
"	"	-	56.0	42.8	0.1	-	0.7	-
"	"		55.8	44.5	0.1	0.1	0.6	-
Fi7:335.1		0.2	55.8	43.8	0.2	0.1	0.6	-
"		-	55.6	44.2	0.3	-	0.7	-
Fi7:494.2		-	55.9	43.3	-	-	0.4	-
"		0.2	55.8	43.3	0.1	0.1	0.4	-
Fi7:519.1		-	56.1	44.4	0.1	0.1	0.6	-
"		-	56.4	43.0	-	-	0.6	-
"	(Prismatic)	-	56.2	43.0	0.1	-	0.4	-
"	"	-	56.2	42.7	-	0.1	0.4	-

From: Tullborg and Larson (1982).

Group II calcites at Finnsjön are characterized by $\delta^{18}O$ values between about -10 and -16 °/oo PDB. The Stripa 1 calcites are also in this range, although they tend to have distinctly lower ^{13}C values than the Finnsjön calcites. A better agreement exists for both ^{18}O and ^{13}C between Stripa 1 and Gideå II. Open fracture calcites occur in these groups and it is safe to assume that most "modern" calcites are represented here. However, some samples at Finnsjön and Gideå come from closed fractures indicating that some hydrothermal calcites are also in these groups.

Stripa 2 calcites are not found at Finnsjön but Gideå Group III samples are similar. At the latter locality only calcites from sealed fractures are found and it is suggested (Tullborg and Larson, 1983) that some of these carbonates are Precambrian. We have not sufficient specific fracture mineral data to discuss this in detail but the Stripa results indicate that hydrothermal calcites are found in these groups. Considering only ^{18}O and assuming for the fluid $\delta^{18}O$ = 0 to +5 °/oo SMOW (typical for magmatic/geothermal waters) the temperature of deposition would be close to 200°C (see Figure 8-6).

At Finnsjön, Group III has the same ^{18}O contents as the Stripa 2 samples yet much higher $\delta^{13}C$ values. The values observed in Finnsjön calcites agree with a hydrothermal origin where ^{13}C- values reflect magmatic/metamorphic carbon dioxide. For the same tempe-

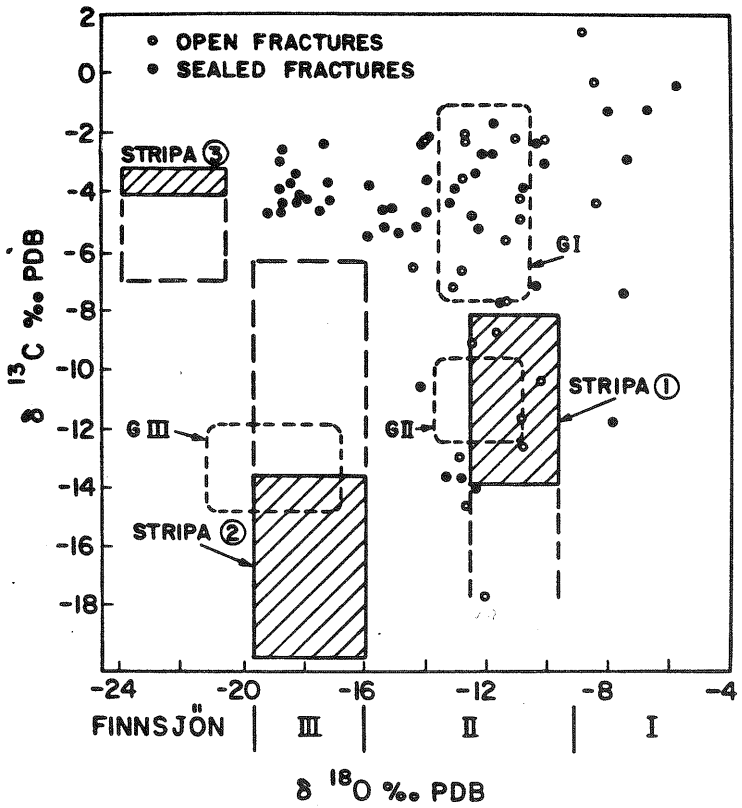

Figure 8-8. Comparison of $\delta^{18}O$ and $\delta^{13}C$ values of fracture calcites from Stripa (shaded area with extensives), Gideå (G_I, G_{II} and G_{III}) and Finnsjön (open and filled circles). The Finnsjön grouping is based on ^{18}O data only and is indicated on the X-axis.

rature regime, the Stripa 2 and Gideå III samples, however, are with two exceptions for Stripa (Table 8-2) in equilibrium with a CO_2 which has a $\delta^{13}C$ close to -15 °/oo (Figure 8-7). This would require the presence of "biogenic" CO_2 during their formation which was possibly generated by the oxidation of organic matter.

The Stripa 3 samples, are found near the surface in SBH-3 and at close to 300 m depth in borehole SBH-1. Similar samples are not found at Finnsjön or Gideå and their genesis presents a special problem. If a hydrothermal genesis is assumed for these samples, then the temperature of deposition would have been between about 250 and 350°C - assuming that the participating fluids were slightly enriched in ^{18}O with respect to SMOW. This in turn would demand, that a carbon dioxide in equilibrium with the calcites have a $\delta^{13}C$ = -2 °/oo. It is thought, however, that such high values could only be generated if marine limestones were available to provide the carbon for the hydrothermal solutions. We would suggest that methane equilibria could also play a role. Note, that these carbon isotope values are very similar to the $\delta^{13}C$ values of the Group III calcites in Finnsjön.

We suggested earlier (Fritz et al. 1979) that it might also be possible to consider these calcites to be glacial meltwater precipitates. Very little is known about the composition of the aqueous carbon in subglacial meltwaters, although the few $\delta^{13}C$ contents of subglacial carbonate precipitates from different environments known to us tend to indicate that either isotopic equilibria with atmospheric CO_2 are approached or that rock carbonate has been taken up and reprecipitated (redeposited) from the glacial melt waters. In both cases the $\delta^{13}C$ values are close to 0 °/oo, and thus quite different from those observed in the present day groundwaters at Stripa. However, the $\delta^{13}C$ values of the Group 3 samples are close to this postulated value. Furthermore, the calculated $\delta^{18}O$ values for water participating in their formation are below -20 °/oo SMOW. Such low values are known from other environments where glacial meltwater infiltration has occurred and would thus support a low temperature origin of these calcites.

Our present data do not suffice to discuss this problem, yet it would be important to document with fluid inclusion data which of the two interpretations is correct. If one could show that indeed glacial meltwaters are responsible for the formation of these calcites, then this observation would contain important information about the depth of actively circulating flow-systems in these environments.

An intriguing element in the Stripa calcites are the "abnormal" values which are found. A calcite from V-I (495 m) yielded a $\delta^{13}C$ = -35.7 °/oo which is close to the values measured in the aqueous carbon from the V-2 borehole. Its $\delta^{18}O$ = -13.4 °/oo (PDB) could reflect deposition at about 16°C from a water with $\delta^{18}O$ = -13.5 °/oo SMOW. These values are close to the actual temperature and present day water composition, this calcite could be a recent precipitate.

The question on the origin of these low ^{13}C values was already addressed above and it was indicated that the oxidation of methane or organic matter might be responsible. Traces of methane were recognized in the deep waters and calcite compositions attest to the past presence of methane producing bacteria in these fracture systems. Two samples from SBH-2 gave $\delta^{13}C$ values of +13.0 and +15.3 °/oo. These values are typical for carbonates whose carbon originated in a CO_2 generated by methane producing bacteria. Such bacteria co-produce isotopically light methane and very heavy carbon dioxide, with typical $\delta^{13}C$ values below -60 °/oo and above +10 °/oo respectively. Reoxidation of such methane could easily produce the low $\delta^{13}C$ values observed elsewhere in these systems. A first carbon-13 analysis on methane from Stripa yielded a $\delta^{13}C$ = -30 °/oo. This value is non-specific although it could indicate that partial re-oxidation had occurred. (Swedish Deep Gas Project, Progress report, 1984.)

8.6 Conclusions

The aqueous carbon in the Stripa groundwaters is dominated by biogenic components. The first organic carbon contribution occurs in the recharge environments where young groundwaters equilibrate with a soil-CO_2 with $\delta^{13}C = \sim -13$ ‰ PDB. This CO_2-uptake is followed by dissolution of carbonate minerals. This appears to be largely a closed system process although locally marbles and other carbonates may outcrop in surface and near-surface environments. Rising pH-values in deeper groundwaters lead quickly to calcite saturation and no further calcite dissolution takes place, but calcite deposition may occur.

This geochemical evolution is also recognized in the radiocarbon contents of the shallow groundwaters where ^{14}C "dilution" does occur. The "dilution" factor" q is estimated to lie between 0.5 and 0.7. Once calcite saturation is reached, decay would dominate ^{14}C abundances unless exchange with exiting carbonate minerals, diffusive loss into the rock matrix or dilution with biogenic carbon dioxide generated by the oxidation of methane and other organic compounds does occur.

Analytical difficulties in these low-carbonate waters are such that it is not possible to come to clear conclusions. However, assuming that the lowest measured values are correct and that decay dominates over other ^{14}C-removing or diluting processes than the deep, saline waters would have mean residence times in excess of 20,000 years.

The ^{18}O and ^{13}C data of the fracture calcites at Stripa reflect the complex geochemical history of the fluids in these rocks. At least four generation of calcites are found, of which two have a low temperature origin. These are the present day precipitates and the "methane" calcites. The former occur all at depths of less than about 300 m. The origin of the low ^{18}O Stripa 3 calcites is unclear and could either represent a high temperature hydrothermal generation or subglacial, low temperature precipitates. If the latter was the case, which would have to be proven through fluid inclusion analyses, the statements about groundwater circulation under ice cover would be possible. All other calcites appear to have originated in thermal environments and/or are related to the genesis and metamorphic history of the granite.

9 THE IN-SITU PRODUCTION OF RADIOISOTOPES AND THE ^{3}H and ^{36}Cl CONTENTS OF THE GROUNDWATERS

9.1 The in-situ neutron flux in the Stripa granite

The estimation of the in-situ neutron flux in geological fractures is very important for assessing underground production of nuclides such as ^{3}H, ^{14}C, ^{36}Cl and ^{39}Ar, some of which have potential for the determination of groundwater residence time.

9.1.1 Neutron production due to ^{238}U spontaneous fission and (α, n) reactions

The in-situ neutron flux in rock formations which are shielded from cosmic ray secondary neutrons is due to the spontaneous fission of ^{238}U and (α, n) reactions with light nuclei, particularly Si, O, Al, Mg. The latter reactions are more significant than the spontaneous fission neutrons and the neutron production rate due to them has been estimated by Feige et al., (1968). The total neutron production rate may be calculated from the equation

$$P = \rho(0.4764\ [U] + 1.57[U] + 0.7[Th])\ \text{neutrons}\ cm^{-3}a^{-1} \qquad (9.1.1)$$

where [U] and [Th] are the U- and Th-contents (ppm) of the rock respectively and ρ is its density (g/cm^3). The first term in this equation is the ^{238}U spontaneous fission neutron production rate whilst the last two terms are the production rates due to (α, n) reactions by α-particles from natural U- and Th-series elements respectively.

Free neutrons decay to protons by β-emission with a half-life of 12 minutes which corresponds to a mean lifetime of 17.3 minutes. Thermal neutrons have a velocity of 2200 m/s at 25°C and in free space such neutrons travel very large distances ($>10^6$ m) in their mean lifetimes. In rock media thermal neutrons undergo scattering and absorption reactions within much shorter distances so that their ultimate fate is absorption. The weighted-mean absorption cross section, σ_m, for a rock matrix may be calculated from the element abundances (N_l, mole fraction) in the rock and their neutron absorption cross sections (σ_i) using the equation:

$$\sigma_m = \sum_{l\,i\,i}^{i} \sigma N \ \text{moles barns/g} \qquad (9.1.2)$$

$$= 0.602 \times \rho \sum_{l\,i\,i}^{i} \sigma N \ \text{atoms/cm}$$

Exact evaluation of this summation requires a complete elemental analysis of the rock. However, a good estimate may be made from data for just 17 elements (Andrews and Kay, 1982) although these include some trace elements which are not often determined. The absorption mean free path, λ_a, for neutrons is then given by:

$$\lambda_a = 1/\sigma_m \text{ cm} \qquad (9.1.3)$$

and the corresponding mean lifetime, t_m, and time constant, λ, for the absorption of thermal neutrons are given by the equations:

$$t_m = \lambda_a/220{,}000 \text{ s}$$
$$\lambda = 1/t_m \text{ s}^{-1} \qquad (9.1.4)$$

This rate constant controls the removal of neutrons from the rock matrix by absorption reactions and the equilibrium between neutron production and absorption is established according to the equation:

$$n_t = \frac{P}{\lambda}(1 - e^{-\lambda t})$$
$$= \frac{P}{\lambda} \text{ when } t > 10^{-3} \text{ s} \qquad (9.1.5)$$

where n_t is the number of neutrons present after time t in 1 cm^3 of rock. Equilibrium is established almost immediately since λ is about 2500 s^{-1}. The thermal neutron flux, ϕ, is then equal to nv $cm^{-2}s^{-1}$ where v is the neutron velocity in cm/s. Estimated neutron production rates, fluxes and absorption data for the Stripa granite and leptite are in Table 9-1.

Table 9-1 Radioelement contents and neutron production rates for the granite and leptite at Stripa.

	U-content ppm	Th-content ppm	ΣσN moles barns	n-production $cm^{-3}a^{-1}$	neutron flux $cm^{-2}s^{-1}$
Granite	44.1	53.4	0.01068[1]	310.0[3]	5.88×10^{-4}
Leptite	5.4[5]	17.9[5]	0.00841[2]	57.2[4]	1.38×10^{-4}

[1] for 8 ppm Li and 4 ppm B

[2] for average basalt; 5 ppm Li, 15 ppm B

[3] for 70% SiO_2

[4] for 60% SiO_2

[5] from Wollenberg et al., 1980 (SAC 36)

9.1.2 Neutron flux measurements with a BF_3 neutron counter

For the experimental determination of the in-situ neutron flux, a high sensitivity boron trifluoride (BF_3) counter was used. Neutrons are detected by their interaction with the ^{10}B nucleus, which produces the ionising nuclei, $^4He^{2+}$ and $^7Li^+$, in the counter. Natural boron consists of two isotopes, 18.8% of ^{10}B and 81.2% of ^{11}B. Neutron capture by ^{10}B produces the compound nucleus, $^{11}B^*$, which dissociates as shown in the decay scheme below. The quoted dissociation energies are partitioned between the α-particles and the lithium recoil nuclei as indicated.

Decay scheme and energy partition for the reaction $^{10}B(n,\alpha)$ Li

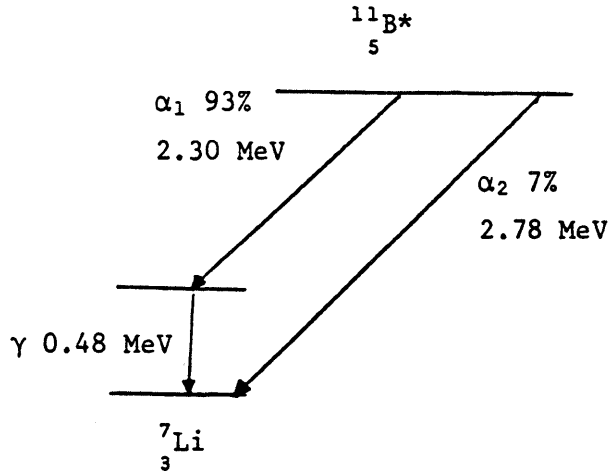

Particles	Kinetic energy, MeV
α_1 + Li recoil nucleus	2.30
α_1	1.47
Li_1 recoil nucleus	0.83
α_2 + Li_2 recoil nucleus	2.78
α_2	1.77
Li_2 recoil nucleus	1.01

Boron may be incorporated in a proportional counter as boron trifluoride gas and this is usually enriched in ^{10}B. The α-particles and lithium recoil nuclei are detected by the proportional counter, and give rise to pulses whose amplitudes are proportional to the particle energies if these are completely stopped in the counter gas. Any γ-radiation background which is present causes very much smaller pulses than the heavily ionising α-particles and lithium recoil nuclei, so it is possible to discriminate against the γ-radiation.

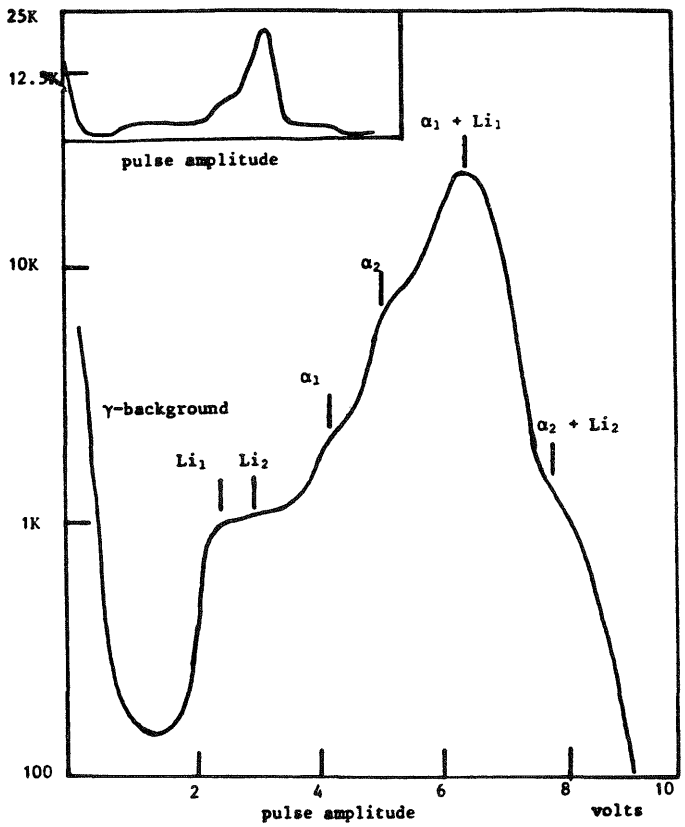

Figure 9-1. Pulse spectrum for BF_3 counter 150EB Ser.No. 8408-290 (inset with linear count scale)

The maximum primary ionisation occurs within the counter when an α-particle and its associated recoil nucleus dissipate all their energy in the filling gas. This primary ionisation is reduced when one of the particles strikes the counter wall before giving up all of its kinetic energy. Figure 9-1 shows a pulse amplitude spectrum for a Centronics 150EB BF_3, neutron counter (1.5 m x 50 mm diameter). This counter was used to measure the neutron flux in various locations in the Stripa mine. The counter has a sensitivity of 242 counts/s for a neutron flux of 1 $cm^{-2}s^{-1}$ and had a negligible background. A count rate of 1 count/minute above background, corresponds to a neutron flux of 7 x 10^{-5} $cm^{-2}s^{-1}$ which could therefore be determined to $\pm$5% (2σ) with a 24-hour count.

Sensitivity of the BF_3 counter for different neutron energies

The cross section of ^{10}B for the reaction $^{10}B(n,\alpha)Li$ is proportional to 1/v where v is the neutron velocity, in the range of neutron energies from 0.001 eV to 10 keV. The (n,α) reaction rate is proportional to the product:

$$\sigma_v n_v v N = \sigma_v \phi_v N \qquad (9.1.6)$$

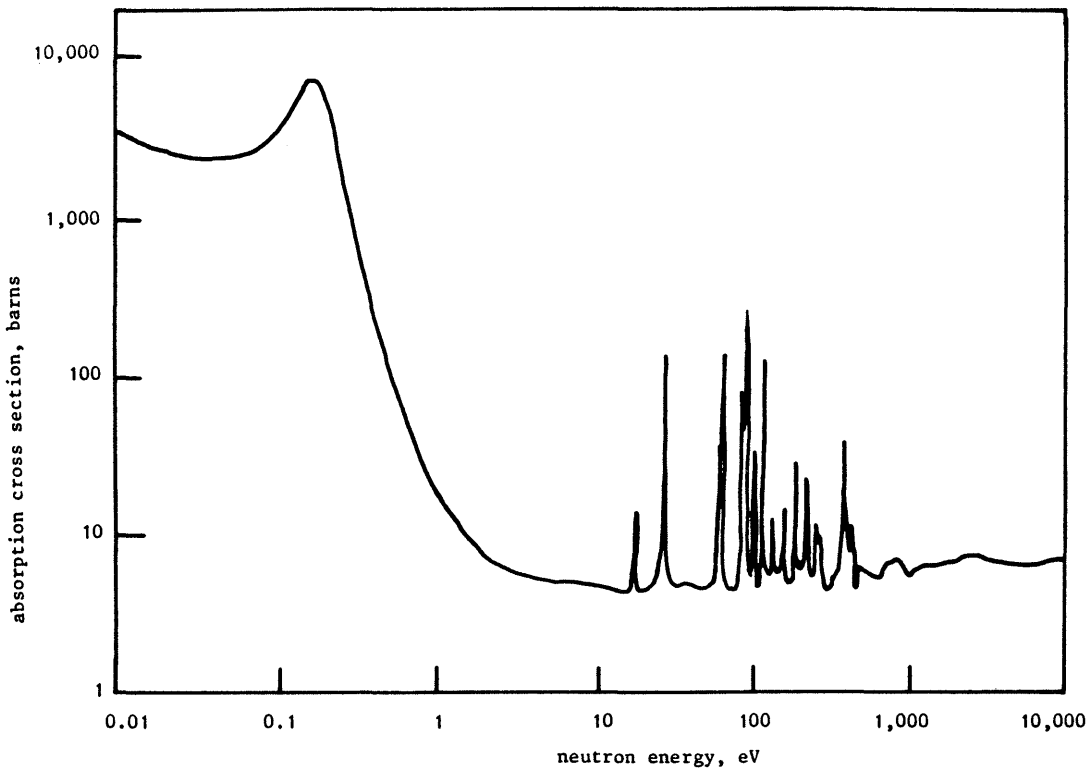

Figure 9-2. Neutron absorption cross section of cadmium as a function of neutron energy

where σ_v and n_v are the cross section (cm^2) and neutron population (cm^{-3}) for neutrons of velocity v, ϕ is the corresponding neutron flux and N is the number of ^{10}B nuclei present. If the 1/v law applies to the neutron cross section, then:

$$\sigma_v = \frac{\sigma_t v_t}{v} \tag{9.1.7}$$

where σ_t and v_t are a reference neutron velocity and corresponding cross section. These may conveniently be taken as the thermal neutron velocity at 25°C (2200 m s^{-1}) and the corresponding cross section. The (n, α) reaction rate is then proportional to:

$$\sigma_t v_t N \int n_v dv = \phi N \tag{9.1.8}$$

where ϕ is the integrated neutron flux in the 1/v proportionality range.

The counter sensitivity of 242 counts s^{-1}/unit flux (1 $cm^{-2}s^{-1}$) can therefore be applied for neutron energies up to 10 keV. Above 10 keV the $^{10}B(n,\alpha)^7Li$ cross section deviates from the 1/v law and becomes significantly less than the ^{11}B neutron-capture cross section. The counter has an enrichment to 90% ^{10}B and above 10 keV the cross sections for the neutron reactions with the two isotopes in the counter become comparable.

Table 9-2 Neutron flux measurements.

	Site	Formation	Count rate, min^{-1}		Neutron flux, $cm^{-2}s^{-1}$		Notes
			Unshielded	Shielded	Thermal x 10^{-4}	Epithermal x 10^{-4}	
1a	Bath	Jurassic Limestone	15.03 ± 0.10	1.11 ± 0.02	9.59	0.76	Surface measurement, elevation 180 m.
1b	Bath	Jurassic Limestone	29.95 ± 0.15	1.92 ± 0.04	19.30	1.32	Surface measurement, 30 m above ground, elevation 210 m
2	Stripa	Leptite	31.68 ± 0.42	2.19E	20.30	1.51	Surface measurement on leptite outcrop, elevation 85 m
3	Stripa	Haematite ore	0.59 ± 0.04	-	<0.41	-	200 m depth in ore body
4	Stripa	Leptite	1.30 ± 0.04	1.00 ± 0.06	0.21	0.69	360 m depth near access shaft
5a	Stripa	Granite	4.18 ± 0.52	0.71E	2.39	0.49	Granitic cavern at 356 m depth by Z shaft in granite outcrop
5b	Stripa	Granite	6.78 ± 0.11	1.15E	3.88	0.79	Borehole H4 in granite wall of cavern
6a	Stripa	Granite	4.91 ± 0.11	0.83E	2.81	0.57	Granitic cavern at 360 m depth, by borehole V1 in SGU site
6b	Stripa	Granite	6.89 ± 0.10	1.17 ± 0.04	3.94	0.81	Borehole 3DP, from access drift to SGU site

E estimated from ratio shielded/unshielded counts for other sites.

The neutron-absorption cross section of Cd is shown in Figure 9-2. The intensity, I_x, of neutrons transmitted through a Cd absorber of thickness x cm, is related to the incident intensity, I_o, by the equation:

$$I_x = I_o \, e^{-\sigma N x} \qquad (9.1.9)$$

where σ is the neutron absorption cross section and N is the number of absorbing nuclei per unit volume. For "thermal neutrons" of energy 0.0253 eV, only 10^{-5} of incident neutrons can pass through a 1 mm thick sheet. For neutron energies above 0.3 eV (1% transmission) cadmium is much less effective as a neutron absorber and above 1.0 eV it is effectively transparent to neutrons. The BF_3, counter response when shielded with 1 mm of Cd metal is hence due largely to neutrons in the energy range 1.0 eV to 10 keV. The difference between the count rates when unshielded and when shielded with cadmium is attributed to neutrons of energy less than 0.3 eV and most are likely to have energies close to 0.025 eV.

9.1.3 Results from neutron flux measurements

The neutron fluxes in the thermal and epithermal (1.0 eV to 10 keV) ranges which were measured in various locations are reported in Table 9-2.

The total measured neutron flux (thermal + epithermal) in 76 mm diameter boreholes in the Stripa granite is 4.7×10^{-4} $cm^{-2}s^{-1}$ and this is in good agreement with the calculated value of 5.88×10^{-4} $cm^{-2}s^{-1}$ (Table 9-1). The epithermal flux is 0.8×10^{-4} $cm^{-2}s^{-1}$ and the epithermal/thermal ratio is 0.2. The total flux in the leptite is 0.9×10^{-4} $cm^{-2}s^{-1}$, and this compares well with the calculated flux of 1.38×10^{-4} $cm^{-2}s^{-1}$. The epithermal/thermal neutron ratio (3.3) is much higher in the leptite than in the granite.

The cosmic-ray secondary thermal neutron flux is dependent upon both altitude and latitude. At Stripa, surface measurements show that it is about 32×10^{-4} $cm^{-2}s^{-1}$ and the corresponding 'epithermal' neutron flux is about 7% of the thermal flux.

9.2 In-situ production of ^{3}H and ^{36}Cl in the Stripa granite

9.2.1 ^{3}H production

The rate of subsurface production may be directly calculated from the experimentally determined neutron flux and the Li-content of the granite. The isotope production equation is:

$$N = \frac{\sigma N_{tg} \phi}{\lambda} (1 - e^{-\lambda t}) \text{ atoms} \qquad (9.2.1)$$

where N is the number of radioactive nuclei with a decay constant λ, which are formed in 1 cm^3 of rock by time t after the start of the reaction. N_{tg} is the number of target nuclei, σ is the cross section for the production reaction and ϕ is the neutron flux. As the ^{3}H-production reaction attains equilibrium after ≅50 years and since 1 T.U. corresponds to one atom of ^{3}H in every 10^{18} atoms of H, the ^{3}H-content of a water-filled fracture, on the assumption that all the ^{3}H formed is trapped by the water, is given by:

$$\text{water } ^{3}H\text{-content} = \frac{N}{6.69 \times 10^{4} f} \text{ T.U.} \qquad (9.2.2)$$

where N is equilibrium number of ^{3}H atoms per cm^3 of rock matrix and f is the fracture porosity. The ^{3}H-content of fracture fluids was calculated for the measured flux of 4.7×10^{-4} $cm^{-2}s^{-1}$ in the

Stripa granite and for the range of observed Li-contents. The results are given in Table 9-3b. The maximum possible ^3H-content of the fracture fluids for total trapping of the ^3H within them is about 1.4 T.U. However, the rock matrix must also contain some H-atoms which will trap a proportion of the ^3H. A typical biotite, for example, contains about 0.5% w/w of H as OH groups. For a 10% biotite content in the granite, the maximum ^3H labelling would correspond to about 2.8 T.U. for the biotite hydrogen. Exchange with flowing fracture fluids could result in their becoming tritiated to the same extent if the progression of fluids along the fracture leads to sufficient contact with biotite. However, if the modal H-content of the rock matrix is greater than 0.05%, as might be the case if alteration minerals are present, the ^3H-labelling effect would be reduced.

In conclusion, it seems probable that some ^3H-labelling of fracture fluids may result from in-situ ^3H production. The extent of this labelling is not likely to exceed 1 - 2 T.U. and is probably less than 0.5 T.U.

Table 9-3a. Lithium content of Stripa Granite (data from K Nordstrom, USGS)

Borehole	Depth m	Average Li ppm	Number of determinations
V1	107	8.4	2
	408	4.6	4
	445	5.5	2
V2	456	1.8	2
	471	2.8	2
	760	28.0	2

Table 9-3b. In-situ production of ^3H in the Stripa granite.

^3H-content (T.U.) of fracture fluid for Li-content of:

Porosity	1.8 ppm	8.0 ppm**	11.00 ppm*	28 ppm
0.01	0.01	0.04	0.055	0.14
0.001	0.09	0.41	0.56	1.43

* The average Li-content derived from the $^3He/^4He$ ratio of radiogenic helium.

** Average of rock analyses.

9.2.2 ^{36}Cl production

Some muon-induced spallation of Ca, K and Ar nuclei may produce ^{36}Cl in the near surface of the granite but these reactions are negligible in comparison with the neutron capture reaction with natural chloride, $^{35}Cl(n,\gamma)^{36}Cl$. The number, ^{36}N, of ^{36}Cl atoms produced in ^{35}N atoms of target nuclei, ^{36}Cl, after irradiation in a neutron flux of ϕ $cm^{-2}s^{-1}$ for time t is given by:

$$^{36}N = \frac{\sigma^{35}N\phi}{\lambda_r}(1 - e^{-\lambda_r t}) \qquad (9.2.3)$$

where σ is the cross section for the n-capture reaction and λ_r is the decay constant of ^{36}Cl ($7.1 \times 10^{-14}s^{-1}$). Equilibrium between ^{36}Cl formation and decay is established after about 1.5 Ma (about 5 half-lives of ^{36}Cl) and the ratio of ^{36}Cl atoms to natural chlorine atoms is then given by:

$$^{36}N/(^{35}N + ^{37}N) = \frac{\sigma\phi}{\lambda_r} \cdot \left(\frac{^{35}N}{^{35}N + ^{37}N}\right) \qquad (9.2.4)$$

$$= \frac{0.7553\ \sigma\phi}{\lambda_r}$$

Since the granite is much older than 1.5 Ma, all the natural chloride which it contains must be labelled with ^{36}Cl. Substitution of the cross section (44×10^{-24} cm^2) and neutron flux (3.9×10^{-4} $cm^{-2}s^{-1}$) into equation 9.2.4 yields a value of 180 atoms of ^{36}Cl per 10^{15} atoms of natural chloride for the atomic ratio of ^{36}Cl in the granitic matrix. The ratio for ^{36}Cl production in the leptite (flux = 0.9×10^{-4} $cm^{-2}s^{-1}$) is 45 atoms $^{36}Cl/10^{15}$ atoms of natural chloride.

9.3 Tritium contents in groundwaters at Stripa

9.3.1 Introduction

Tritium (^3H), the radioactive isotope of hydrogen with a half-life of 12.4 years, is a common tool in hydrology to distinguish between recent water (recharge after 1952) and older water (recharge before 1952) or in special cases to date groundwater up to about 80 years old.

^3H is produced naturally mainly in the atmosphere (in minor amounts also in the lithosphere and hydrosphere) and anthropogenically by the thermonuclear tests (mainly in the period 1952 - 1962) and nuclear facilities. In the atmosphere, ^3H is produced by spallation and by interaction of nucleons with nitrogen (e.g. ^{14}N (n, ^3H) ^{12}C), oxygen and argon. After oxidation to water it reaches the earth and the groundwater by precipitation and takes part in the water cycle.

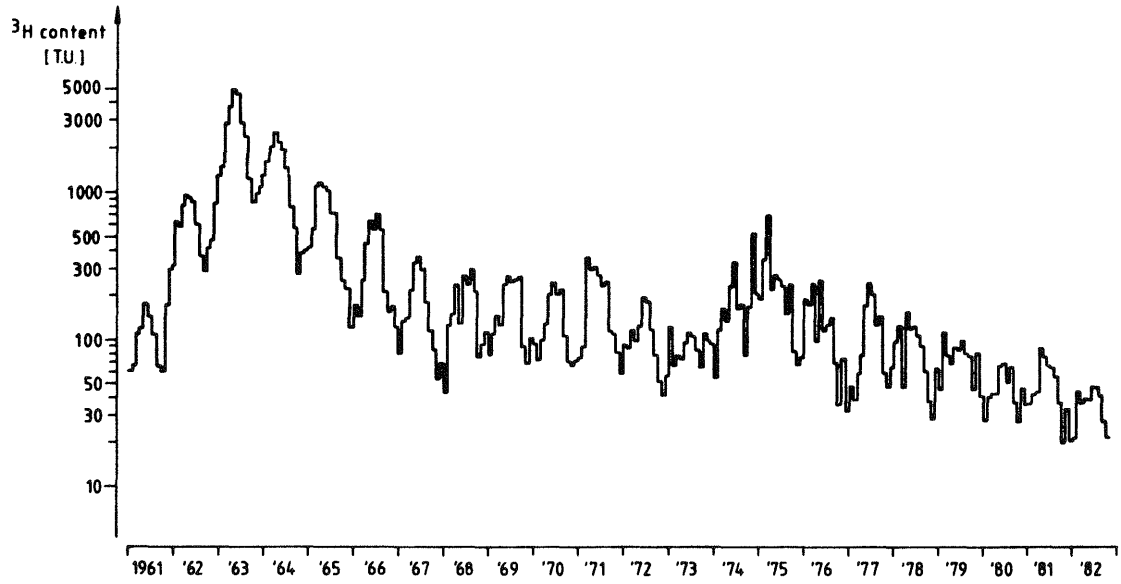

Figure 9-3. Monthly means of ^{3}H contents of precipitation in the catchment area of river Rhine (after WEISS & ROETHER 1975) completed by data since 1974 from upper Bavaria (after MOSER & RAUERT 1983).

The main source of subsurface ^{3}H production is the neutron induced reaction $^6Li(n,^3H)^4He$, where the neutrons originate from α decay of U and Th in the rock material and following processes of (α, n) reactions on light nuclei (comp. FEIGE et al., 1968). The ^{3}H production in groundwater can be neglected because the Li^+ concentration in water is much lower than the Li content of rock.

The ^{3}H concentration of naturally produced tritium in the atmosphere (as water) is in the range of several TU*.

ROETHER (1967) reconstructed the natural tritium level in Central Europe by ^{3}H measurements of old wines and found a mean annual value of 5.5 $\pm$ 0.7 TU for the ^{3}H content of precipitation. This value increased strongly after 1952 by the thermonuclear tests and reached several thousands TU in 1963. After the test-stop the ^{3}H contents in the atmosphere decreased with seasonal periodicity to several tens TU in 1983 (compare Figure 9-3).

---

* The concentration of environmental tritium is expressed in TU. 1 TU (tritium unit) $\triangleq$ $^3H/H = 10^{-18} \triangleq$ 3.2 pCi $^3H/l$ $H_2O \triangleq$ 0.12 Bq $^3H/l$ H_2O.

9.3.2 Measuring techniques

The measurements of the weak β-emitter tritium (maximum β energy 18 keV) can be done after careful sample preparation by β counting in liquid scintillation counters or in gas counters (e.g. EICHINGER et al. 1981) or by the mass-spectrometric determination of ^3He, which is formed by radioactive decay of ^3H (CLARKE et al. 1976). For very low ^3H concentrations an enrichment of ^3H (e.g. by partial electrolysis) before the measurement by β counting is required. Characteristic data of the applied ^3H measuring techniques are summarized in Table 9-4.

Table 9-4 Characteristic data of applied ^3H measuring techniques (measuring room shielded by 75 cm thick walls of Ilmenite concrete; the gas counter is additionally shielded by 40 cm lead (above) and 20 cm iron (all sides)).

	Liquid scint. counting without/with electrolytic enrichment	Gas counting without/with electrolytic enrichment
Volume of water sample (cm^3)	10/400	10/400
Scintillator/Counting gas	13 cm^3 Insta-Gel ® (Packard Co.)	2 bar Propan
Sample container	24 cm^3 polyethylene vial	2.6 l copper counter
Background (cpm)	2.42	0.48
Counting efficiency (%)	24.5	76
Calibration factor (TU/cpm)	57	23
Detection limit (confidence level = 97.5% measuring time = 1000 min)	12/0.6	1.5/0.1

9.3.2.1 Liquid scintillation counting

Samples which are expected to contain higher tritium contents are directly measured in commercial liquid scintillation counters. 10 cm^3 of the water sample are mixed with 13 cm^3 Insta-Gel scintillator (Packard Co.) in polyethylene bottles and counted for a measuring time of about 1000 minutes. With this simple method tritium contents above 12 TU can be detected (detection limit with a confidence level of 97.5%).

9.3.2.2 Gas counting

For the detection of lower ^3H contents, gas counting is preferred in contrast to liquid scintillation counting because of its

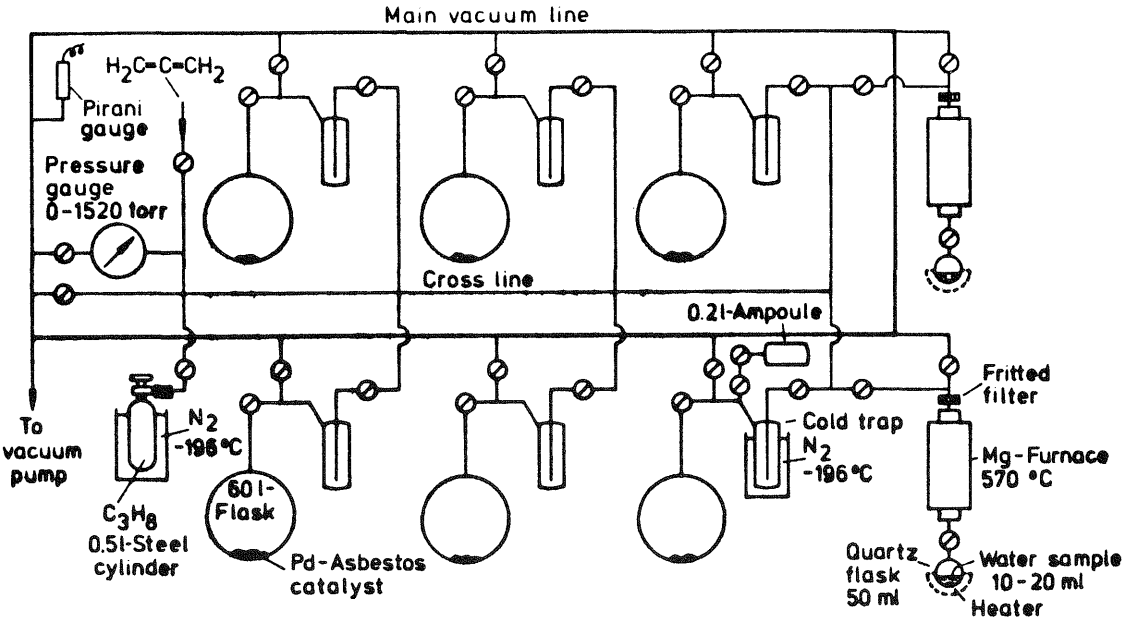

Figure 9-4. Schematic drawing of high vacuum apparatus for synthesis of propane from water samples for ^3H analysis (after WOLF et al. 1981).

higher sensitivity. For ^3H measurement by gas counting the water sample is converted to propane (WOLF et al. 1981) via the reactions (9.3.1) and (9.3.2) in a vacuum apparatus (Figure 9-4).

$$H_2O + Mg \xrightarrow{570^\circ C} H_2 + MgO \qquad (9.3.1)$$

$$2\,H_2 + CH_2 = C = CH_2 \longrightarrow C_3H_8 \qquad (9.3.2)$$

The water sample (10 cm^3) is evaporated from a quartz flask into a furnace filled with magnesium turnings. There the water vapour is completely reduced to hydrogen at 570°C. The produced hydrogen then reacts overnight with propadiene (97-98% of the stoichiometric amount in relation to hydrogen) in a 60 l flask containing palladium catalyst (10% Pd on asbestos). On the following day the synthesized propane is transferred to a 0.5 l steel cylinder for storage before measurement. The propane yield relative to propadiene is 99 $\pm$ 1%.

The ^3H concentration in the propane is counted in a 2.6 l proportional counter at a pressure of 2 bars. The counter is shielded by 40 cm lead (above), 20 cm iron (all sides) and a plastic scintillator anticoincidence shield. The counting system is set up in the basement in a room with 75 cm thick walls made of heavy concrete. For a measuring time of 1000 minutes a detection limit of 1.5 TU (confidence level 97.5%) is achieved.

9.3.2.3 Electrolytic enrichment

At very low ^3H concentrations the ^3H content of the water sample is enriched by partial electrolysis. The applied system consists of 24 batch cells (IAEA type) with stainless steel anodes and mild steel cathodes. With an initial volume of 400 cm^3 and a tritium recovery of 85% the enrichment factor is about 20. With this value the detection limits for liquid scintillation counting and gas counting are reduced to 0.6 and 0.1 TU, respectively.

9.3.3 Results

The results of ^3H analysis of different water samples, obtained at the GSF-Institut für Radiohydrometrie, together with data of FRITZ 1983, FLORKOWSKI 1984 and CARLSSON & OLSSON 1982, are summarized in Tables 9-5 and 9-6. The sampling points for the groundwater samples from southern Sweden are shown in Figure 9-5.

The ^3H concentrations c (TU) are calculated from the measured count rate n_1 (cpm) by means of equation 9.3.3

$$c = \frac{x\,(n_1 - n_o)}{A\,(n_{1,st} - n_o)} = \frac{F}{A}\,(n_1 - n_o) \qquad (9.3.3)$$

where x = ^3H concentration in ^3H standard (TU)

A = enrichment factor

$n_{1,st}$ = ^3H standard count rate (cpm)

n_o = background count rate (cpm)

F = calibration factor (TU/cpm)

For the ^3H results from GSF, the given analytical error $\sigma'(c)$ is related to a 95% confidence level P in the case of a two-sided problem or to P = 97.5% in the case of a one-sided problem and is calculated by means of equation 9.3.4.

$$\sigma'(c) = c\sqrt{\left(\frac{\sigma'(n_1)}{n_1 - n_o}\right)^2 + \left(\frac{\sigma'(A)}{A}\right)^2 + \left(\frac{\sigma'(x)}{x}\right)^2 + \left(\frac{\sigma'(n_{1,st})}{n_{1,st} - n_o}\right)^2 + \left(\frac{(n_{1,st} - n_1)\,\sigma'(n_o)}{(n_1 - n_o)\,(n_{1,st} - n_o)}\right)^2} \qquad (9.3.4)$$

σ' is related to P = 95% or 97.5%, respectively, based on experimentally obtained errors. The relative error of the tritium content in the ^3H standard solution ($\sigma'(x)/x$) was assumed to be 0.02. For the relative error of the enrichment factor ($\sigma'(A)/A$), the experimentally obtained value 0.06 was taken. For enriched samples with very low ^3H concentrations (about 1 TU and lower) the ground contamination during enrichment (0.04 $\pm$ 0.04 TU) was additionally taken into consideration.

Table 9-5 ^{3}H contents of Stripa surface waters, shallow groundwaters at the Stripa test site and groundwaters from southern Sweden.

Sample description	Date	Interval (m)	^{3}H content (TU)	Lab.*
Stream				
Into tailings pond	790506		54 ± 8	UW
Watertable well and seep				
WT-2	790505/18		57 ± 8	UW
Seep at SBH 3	790506		65 ± 8	UW
Private water supply wells				
Private well 1	770927		0 ± 9	UW
Private well 1	790518		13 ± 8	UW
Private well 2	771027		38 ± 10	UW
Private well 3	771026		103 ± 11	UW
Private well 4	790517		4 ± 8	UW
Private well 5	771006		86.2 ± 7.0	IAEA
Private well 5	771007		122 ± 10	UW
Private well 5	771011		98.3 ± 2.3	IAEA
Private well 5	790515		53 ± 8	UW
SBH-3	790523/24	89-104	48 ± 8	UW
SBH-3	790525	89-104	34 ± 8	UW
SBH-3	790526	89-104	55 ± 8	UW
SBH-3	790527	89-104	48 ± 8	UW
Drip water at old mine levels and flowing water in old mine				
135 m level, drip	790514		86 ± 10	UW
157 m level, drip	790511		77 ± 10**	UW
310 m level, drip	790511		159 ± 10	UW
360 m level, drip	790518		86 ± 9	UW
360 - 410 m level, drip	790515		59 ± 8**	UW
Groundwaters from southern Sweden				
Hässelby	830420		4.1 ± 0.6	GSF
Wilhelmslund	830421		2.1 ± 0.6	GSF
Kaga	830421		5.1 ± 0.8	GSF
N Stene	830422		8.3 ± 0.8	GSF
St Sundby	830502		23.7 ± 1.7	GSF
Hammarö	830503		6.5 ± 0.7	GSF
Skofteby	830504		0.0 ± 0.6	GSF
Hangelösa	830504		2.3 ± 0.6	GSF
Smedtofta	830504		12.3 ± 1.1	GSF
Rockagården	830505		0.3 ± 0.6	GSF
Åker	830505		0.5 ± 0.6	GSF

* UW = University of Waterloo, Waterloo, Canada (the analytical error given corresponds to 1σ).

IAEA = International Atomic Energy Agency, Vienna, Austria (the analytical error given corresponds to 1σ).

GSF = GSF-Institut für Radiohydrometrie, Munich-Neuherberg, Fed. Rep. of Germany (the analytical error given is related to a 95% (two sided problem) or 97,5% confidence level (one sided problem) and corresponds to 1.96 σ).

** Average of more than one analysis done on different samples, collected during the stated sampling period.

Table 9-6 ^{3}H contents of Stripa mine waters from different boreholes.

Borehole	Date	Interval (m)	^{3}H content (TU)	Lab.*
M3	770926		0.7 ± 0.3	IAEA
M3	771019		0.5 ± 0.3	IAEA
M3	831109		8.3 ± 0.3	IAEA
M3	831109		9.1 ± 0.6	GSF
M3	840223		10.2 ± 0.3	IAEA
M3	840223		9.2 ± 0.9	GSF
R1	781117		8 ± 8	UW
R1	781208		-6 ± 8	UW
R1	790517		6 ± 8	UW
V1	810828	409-506	0.7 ± 0.1	GSF
V1 (N_2)	810828	409-506	0.7 ± 0.1	GSF
V1	810908	409-506	0.92 ± 0.18	GSF
V1	831003	100-505	1.3 ± 0.2	GSF
V1	831019	100-505	1.3 ± 0.3	GSF
V1	831105	100-505	1.6 ± 0.2	IAEA
V1 (fast filling)	831105	100-505	1.3 ± 0.2	GSF
V1 (slow filling)	831105	100-505	1.2 ± 0.2	GSF
V1 (tritium watch)	831105	100-505	1.3 ± 0.2	GSF
V1	831207	100-505	2.8 ± 0.2**	IAEA
V1	831207	100-505	1.3 ± 0.2	GSF
V1	840111	100-505	1.3 ± 0.3	IAEA
V1	840111	100-505	1.1 ± 0.2	GSF
V1	840208	100-505	1.8 ± 0.2**	IAEA
V1	840208	100-505	1.1 ± 0.2	GSF
V2	820421	6-822	0.95 ± 0.14	GSF
V2	821124	406-410	0.0 ± 0.6	GSF
V2	821214	413-416.74	0.88 ± 0.27	GSF
V2	830119	490-493.74	0.12 ± 0.09	GSF
V2	830207	549-552.74	0.26 ± 0.11	GSF
V2 (3)	831128	424-499	1.3 ± 0.2**	IAEA
V2 (3)	831128	424-499	0.06 ± 0.10	GSF
V2 (1)	831129	562-822	1.8 ± 0.2**	IAEA
V2 (1)	831129	562-822	0.20 ± 0.10	GSF
V2 (2)	840228	500-561	0.2 ± 0.2	IAEA
V2 (2)	840228	500-561	0.08 ± 0.09	GSF
V2 (4)	840228	382-423	0.0 ± 0.2	IAEA
V2 (4)	840228	382-423	0.20 ± 0.11	GSF
E1	811111	3-300	17 ± 2	GSF
E1	820323	127.5-129.5	42.6 ± 3.1	GSF
E1	820610	0-267	20.6 ± 1.8	GSF
E1	840306	3-300	18.6 ± 0.5	IAEA
E1	840306	3-300	19.4 ± 1.4	GSF
N1	820603	3-300	0.19 ± 0.11	GSF
N1	820830	123-125	0.25 ± 0.14	GSF
N1	820906	203-205	0.16 ± 0.10	GSF
N1	820914	271.1-273.1	0.15 ± 0.08	GSF
N1	820923	274-276	0.23 ± 0.09	GSF
N1 (2)	840126	151-251	0.4 ± 0.2	IAEA
N1 (2)	840126	151-251	0.19 ± 0.10	GSF
N1 (1)	840126	252-300	0.4 ± 0.3	IAEA
N1 (1)	840126	252-300	0.12 ± 0.10	GSF
F2	831105		13.8 ± 2.9	GSF

* UW = University of Waterloo, Waterloo, Canada (the analytical error given corresponds to 1σ).

IAEA = International Atomic Energy Agency, Vienna, Austria (the analytical error given corresponds to 1σ; if its value is lower than 0.2 TU it is claimed 0.2 TU).

GSF = GSF-Institut für Radiohydrometrie, Munich-Neuherberg, Fed. Rep. of Germany (the analytical error given is related to a 95% (two sided problem) or 97,5% confidence level (one sided problem) and corresponds to 1.96 σ).

** contamination cannot be excluded.

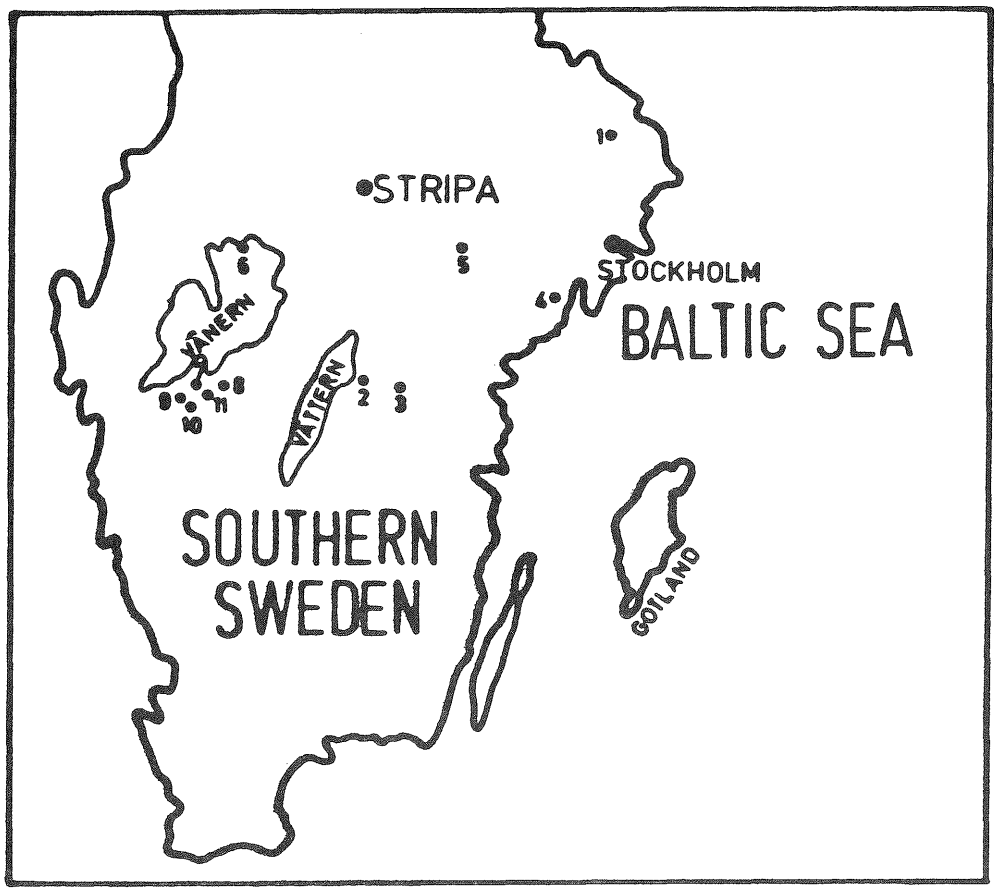

Figure 9-5. Location map for Stripa mine and ^{3}H sampling points in southern Sweden.

1: Hässelby
2: Wilhelmslund
3: Kaga
4: N Stene
5: St Sundby
6: Hammarö
7: Skofteby
8: Hangelösa
9: Smedtofta
10: Rockagården
11: Åker

9.3.4 Discussion

9.3.4.1 Surface waters, shallow waters and groundwaters from southern Sweden

Most of the samples from Stripa surface waters, shallow groundwaters at the Stripa test site and groundwaters from southern Sweden (Table 9-5) show clear influence of bomb-produced ^{3}H (see also FRITZ, et al. 1979) and contain as a whole or at least partially recent water. The ^{3}H contents from the well SBH-3 indicate active circulation of recent waters down to a depth of at least 89-104 m. From Private well 1 (date 770927) and Private well 4, it is not clear, to what extent the samples contain or do not contain bomb-produced ^{3}H, because the measuring technique used is not exact enough to measure in the range below 12 TU.

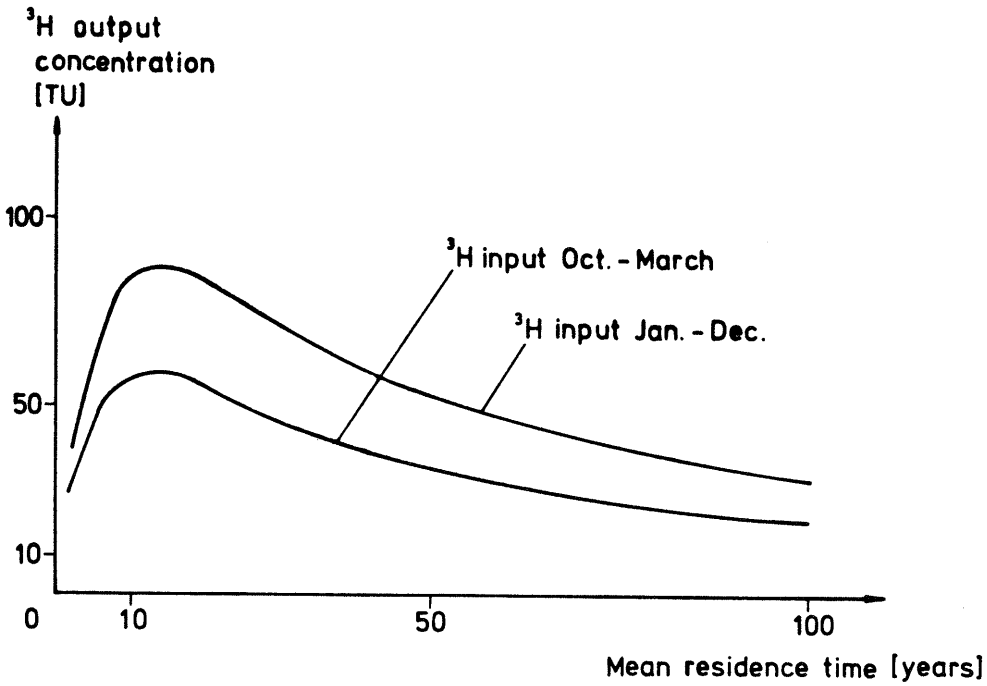

Figure 9-6. ^{3}H contents in groundwaters from Brunswick (sampling year 1982) with different mean residence times calculated by means of the exponential flow model.

Groundwaters from Skofteby, Rockagården and Åker show no detectable influence of bomb-produced ^{3}H and are recharged before the year 1952.

9.3.4.2 Stripa mine waters from different boreholes

The ^{3}H concentrations in waters from different boreholes in the Stripa mine show large differences (Table 9-6). The influence of bomb-produced ^{3}H is shown in the boreholes E1, F2 and M3. The ^{3}H content in M3 increased from 0.6 TU to 9 TU during the last 6 years. The highest ^{3}H content from borehole E1 is measured in the borehole interval 127.5 - 129.5 m. Model calculations by means of the exponential flow model (comp. Figure 9-6) give mean residence times of about 3 or 70 years (^{3}H input Jan. - Dec.) or about 5 or 35 years (^{3}H input Oct. - March) for this sample under the assumption that the ^{3}H input values from southern Sweden are comparable with the ^{3}H input values from Brunswick (Fed. Rep. of Germany). The possibility can not be excluded that this zone is in direct contact with surface water or shallow groundwater. On the basis of these results the statement in FRITZ et al. 1979 has to be revised, that the groundwater at the 330 m-level is essentially free of tritium. It is not possible to decide whether or not the samples from borehole R1 contain bomb-produ-

ced ^3H because of the low sensitivity of direct liquid scintillation counting.

No or at most minor influences of bomb-produced ^3H were found in the samples from boreholes V1, V2 and N1. The variation of the ^3H concentrations with borehole depths (V1, V2) and horizontal borehole distances (N1) are shown in Figure 9-7. The ^3H contents in borehole V1 (interval 100 - 505 m) show no time variation between Oct. 83 and Febr. 84. Results of two contamination tests, carried out on samples from borehole V1 (date 810828 and 831105), show no detectable ^3H contamination. The ^3H content in V2 varies remarkably with the borehole depth. A sample from the whole borehole range shows a ^3H content comparable to that obtained on the sample from the borehole interval 413 - 416.74 m. This suggests that the main flow of the borehole is fed with water from this zone. The ^3H concentration from V1 (interval 409 - 506 m) is comparable to the value of V2 (interval 413 - 416.74 m) and perhaps these waters have the same origin. Figure 9-8 shows that the depths below ground surface of these zones with higher ^3H concentrations are comparable in boreholes V1 and V2. At this time it is not possible to decide whether the ^3H concentrations in these boreholes result from mixing with small amounts of recent water, or from subsurface production of ^3H.

Remarkably low ^3H concentrations, constant over the whole borehole length, have been found in borehole N1. From this water a minimum ^3H model age of 60 years (piston flow model) can be calculated using the following assumptions:

a) the ^3H input value before 1952 is 5.5 TU (after WEISS *et al.* 1979, the ^3H input values from southern Sweden are comparable with the ^3H input values in Central Europe),

b) diffusive loss of ^3H in fractures (NERETNIEKS, 1981) is negligible,

c) no mixing occurs between waters with different ^3H contents and the ^3H concentration decreases only due to radioactive decay.

Because small contamination of the samples during sampling, transport and storage (compare WEISS *et al.* 1976) can not be excluded, this low mean ^3H concentration may indicate a maximum value for the subsurface production of ^3H in groundwater from boreborehole N1.

9.3.5 Conclusions

Surface and shallow groundwaters from the Stripa area show, as expected, high ^3H concentrations and are mainly recharged recently (after 1952). Active circulation of recent water is detected down to a depth of about 100 m.

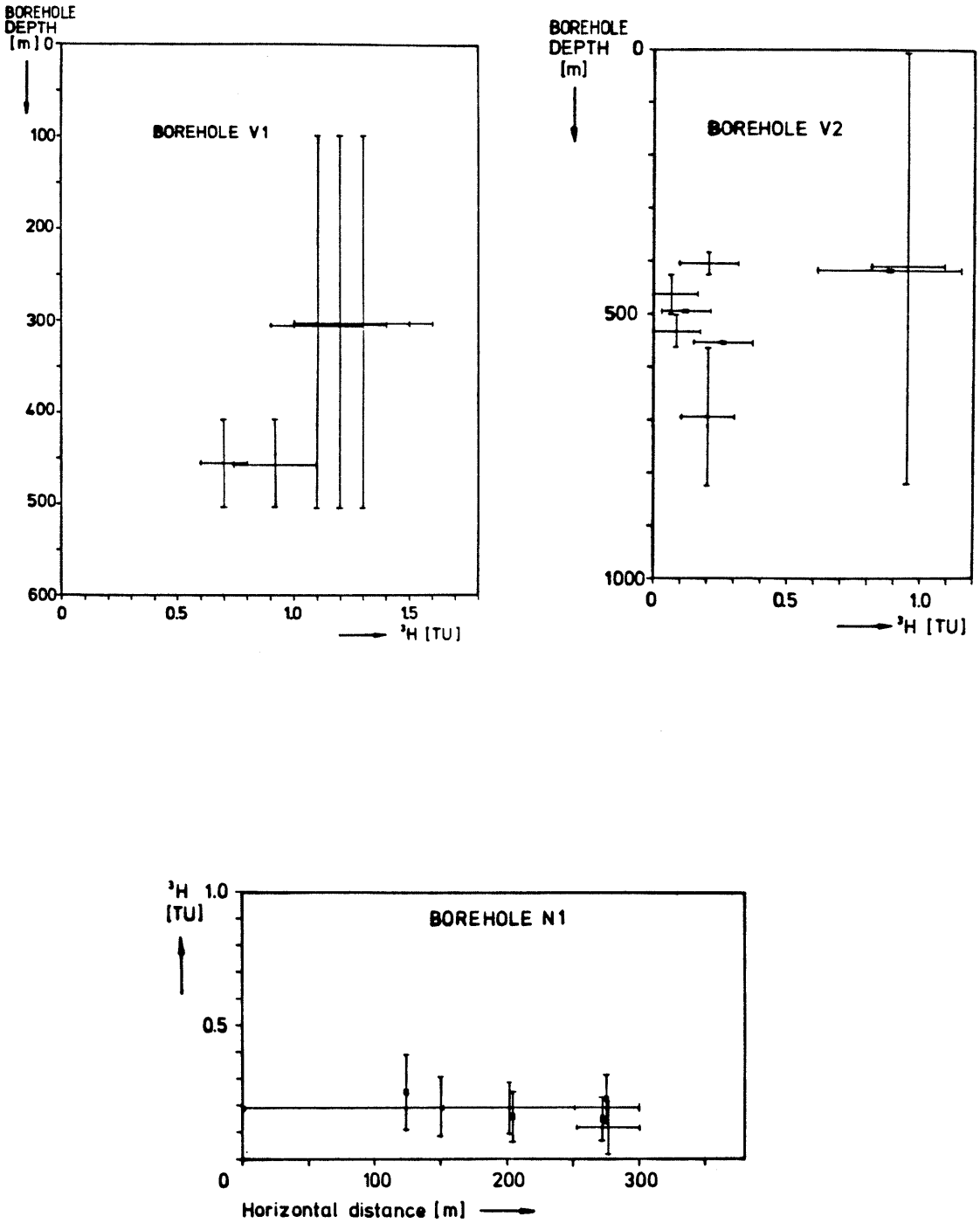

Figure 9-7. Variation of the ^{3}H contents in boreholes V1 and V2 with borehole depths and in N1 with horizontal distance.

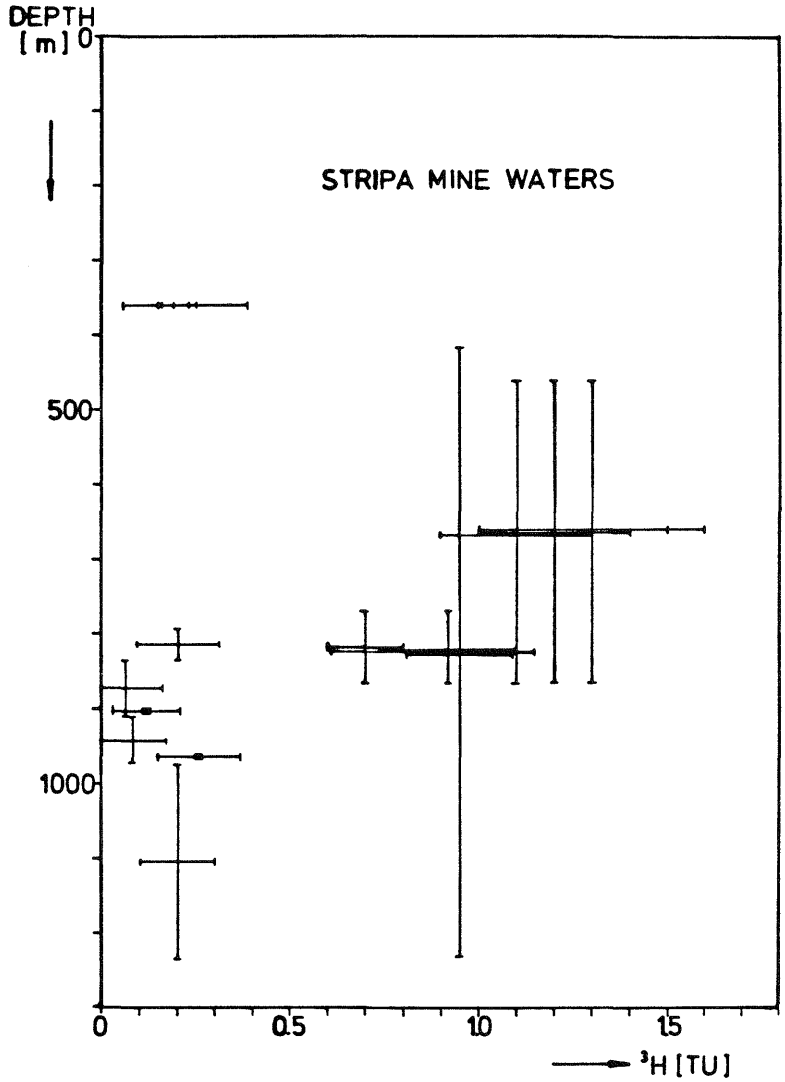

Figure 9-8. Variation of the ^{3}H contents in boreholes N1, V1 and V2 with depth below ground surface.

^{3}H analyses from Stripa mine waters show clearly, that ^{3}H is present partly in remarkable contents. Groundwaters from some boreholes show bomb-produced ^{3}H with indicates residence times of lower than about 30 years (recent recharge). Groundwaters from other boreholes show low but detectable ^{3}H contents. At this time it cannot be decided whether these low ^{3}H contents result from subsurface ^{3}H production and/or by admixture of small amounts of recent water.

Additional measurements and experiments are proposed because an estimation of subsurface production and diffusion of ^{3}H from the rock into the groundwater implies several uncertainties.

A rough estimation of the subsurface ^{3}H production can be done (See Section 9.2.1 and ANDREWS and RAY, 1982) on the basis of U,

Th and Li concentrations in the granite and on fracture minerals using assumptions concerning the effective spectrum of neutron energy and their range.

When calculating that amount of ^{3}H in groundwater, which originates from subsurface production, further problems are imposed by the diffusion of ^{3}H out of the rock into the interstitial water where dilution of the ^{3}H content begins to prevail.

The general problem can be compared with problems of subsurface ^{39}Ar- and ^{37}Ar production. To investigate these processes first experiments were started with irradiation of core material with monochromatic neutrons and detecting the ^{39}Ar- and ^{37}Ar content in the outgassing fraction of Ar (LOOSLI & FORSTER, 1982). These experiments are done as a function of outgassing-temperature and -time and are similar to the experiments of BRERETON (1970). It is proposed to extend the irradiation experiments to the production and detection of ^{3}H. This could be performed in parallel to the ^{39}Ar- and ^{37}Ar experiments and the experiments should be supported by geochemical, mineralogical and gas analyses of Stripa granite and fracture minerals.

9.4 Chlorine-36 in the Stripa groundwaters

9.4.1 Atmospheric sources of ^{36}Cl

Chlorine-36 has properties which make it suitable for the study of confined groundwaters. Its long half-life (3.01×10^{5}a) and the fact that chloride is not removed from solution by mineral interaction or secondary mineral formation would, in principle, permit the detection of very long groundwater residence times. The very high solubility of most natural chloride species ensures that ^{36}Cl remains in solution.

Cosmic-ray production of ^{36}Cl occurs both in the stratosphere and in the troposphere. In the stratosphere, the principle production reaction is proton-induced spallation of ^{40}Ar, whilst in the troposphere the neutron induced reaction, $^{36}Ar(n,p)^{36}Cl$, is more significant. Although stratospheric production is latitude dependent because of the effect of the earth's magnetism on cosmic-ray intensities, mixing is rapid and the stratospheric concentration of ^{36}Cl is uniform. The tropospheric production varies little with latitude. The ^{36}Cl atoms become attached to atmospheric aerosols in the sub-micron size range and these are subsequently removed by precipitation in the lower troposphere. The entry of ^{36}Cl from the stratosphere into the troposphere is seasonally dependent and occurs via the tropopause. The ^{36}Cl fallout rate is consequently higher in middle latitudes than at the

equator or poles (Lal and Peters, 1967). The average fallout rate in Arizona (32°N) is 16 ± 3 atoms $m^{-2}s^{-1}$ (Bentley et al., 1982) and at Stripa (57°N) the rate should be about 14 ± 3 atoms $m^{-2}s^{-1}$, from the latitude dependence which was derived by Lal and Peters (1967).

Nuclear weapon testing at low altitudes resulted in production of ^{36}Cl by neutron irradiation of ocean water, $^{35}Cl(n,\gamma)^{36}Cl$. This caused a large increase in fallout rates (up to 70,000 atoms $m^{-2}s^{-1}$) during the period 1953 to 1964 (Bentley et al., 1982). As the Cl-residence time in the atmosphere is >3 years (Elmore et al., 1982), this 'bomb pulse' of ^{36}Cl was transient and ^{36}Cl fallout rates have returned to the natural level following the cessation of weapon testing in the marine environment. The 'bomb pulse' has been used to study groundwater migration through the unsaturated zone in arid regions.

9.4.2 ^{36}Cl in groundwaters due to cosmogenic ^{36}Cl fallout

The ^{36}Cl content of groundwater may be calculated if it is assumed that the average fallout is incorporated in the total annual precipitation and allowance is made for concentration by evapotranspiration. The groundwater ^{36}Cl content, $[^{36}Cl]$, is:

$$[^{36}Cl] = \frac{F \cdot 3.156 \times 10^7}{R} \left(\frac{100}{100 - E}\right) \text{ atoms/litre} \qquad (9.4.1)$$

where F = fallout rate, atoms $m^{-2}s^{-1}$

R = mean annual rainfall, mm a^{-1}

E = evapotranspiration, %

At Stripa, the cosmic-ray produced ^{36}Cl content of shallow groundwater would be about 1.4×10^6 atoms/litre (R = 780 mm a^{-1}, E = 60%). This is at least 150 times less than the observed ^{36}Cl contents of the Stripa groundwaters (Table 9-7).

As it is not possible that the 'bomb pulse' of ^{36}Cl could be present at all depths in the granite and since the ^{3}H contents of the groundwaters show that there can be little modern water present, it is evident that in-situ production of ^{36}Cl must be occurring in the rock matrix.

9.4.3 Possible use of ^{36}Cl for groundwater studies

The successful use of ^{36}Cl for the determination of groundwater residence times, requires that (i) the ^{36}Cl input of cosmogenic ^{36}Cl at recharge can be determined, (ii) that changes in the ^{36}Cl

total or specific activity can be attributed either to decay of the initial ^{36}Cl or to ingrowth of ^{36}Cl due to in-situ neutron irradiation of chloride in the migrating groundwater, (iii) that the groundwater forms a closed system with respect to chloride which must neither be lost nor gained from the rock matrix. In this discussion, we will assume that the groundwater is sufficiently old and unmixed for there to be no complications due to the bomb pulse of ^{36}Cl. The closed system criterion for chloride in groundwaters is usually the most difficult to justify as groundwaters generally increase in salinity during their evolution. This condition may be relaxed somewhat if in-situ production of ^{36}Cl in the rock matrix is small, as may be the case for some sandstones and limestones.

The number of ^{36}Cl atoms, $^{36}N_t$, present in a groundwater at time t after recharge is given by the equation

$$^{36}N_t = {}^{36}N_o\, e^{-\lambda t} + {}^{36}N_{eq}\,(1 - e^{-\lambda t}) \qquad (9.4.2)$$

decay of cosmic input	ingrowth of ^{36}Cl due to in-situ neutron irradiation of Cl^- in solution (closed system)

If the in-situ neutron flux for the aquifer is small, this equation reduces to the decay term only. Such a simple model has been applied in the case of the confined aquifer in the Great Artesian Basin of Central Australia where the ^{36}Cl activity decreases downdip over a distance of 700 km from the recharge zone (Airey et al., 1984). If the in-situ neutron flux is high and the groundwater is closed to chloride, the ingrowth term controls the ^{36}Cl-activity change with time.

In cases where the groundwater chloride content increases due to interaction with the rock matrix, the specific activity of ^{36}Cl in solution must attain the equilibrium specific activity of ^{36}Cl in the rock matrix, as solution proceeds. No information concerning groundwater residence time can then be deduced, but the admixture of rock chloride with input chloride may be estimated if the residence time is known.

9.4.4 ^{36}Cl contents of the Stripa groundwaters

The total concentration of ^{36}Cl and its specific activity for chloride in the Stripa groundwaters are tabulated in Table 9-7. As shown in Section 9.4.2, the ^{36}Cl contents are much higher than can be attributed to concentration of cosmic fallout by evapotranspiration and must be due to in-situ production. The atomic ratio $^{36}N/(^{35}N + {}^{37}N)$ for the Nl sample is the same, within error, as that estimated for the equilibrium ratio of chloride in the granite matrix. This strongly suggests that the origin of the groundwater chlorinity at this depth is due to water-rock in-

Table 9-7 ^{36}Cl in the Stripa deep groundwaters.

Borehole	Isolated interval m	Depth below surface m	Cl^- ppm	^{36}Cl atoms/ℓ x 10^8	$^{36}Cl/Cl$ ratio x 10^{-15}
N1	203-205	386.7-387	67	2.3 ± 0.4	203 ± 29
V2(A)	0-822	408-1230	300	4.1 ± 0.3	80 ± 7
V1	409-506	766-863	580	6.2 ± 0.7	63 ± 7
V2(B)	406-410	814-818	620	7.0 ± 1.0	66 ± 10

teractions, either by leakage of saline fluid inclusions or by mineral alteration. The enhanced $^{40}Ar/^{36}Ar$ ratios for dissolved Ar in the deep groundwaters suggest that some mineral alteration does occur. For the samples from greater depths in the granite, the ^{36}Cl ratio is much lower than the granite equilibrium ratio and suggests that all of the chloride in solution at these depths may not have been entirely derived from the granite. The deep fracture system may have acquired chloride from some alternative source which has a lower ^{36}Cl atomic ratio than the granite. Two possibilities have been examined, firstly, that some of the groundwater salinity has been derived from interaction with the surrounding leptite during its early recharge history and, secondly, that the deep fracture system was at one time inundated by a solution of an evaporite deposit. The neutron flux in the leptite shows that the ^{36}Cl atomic ratio of its chloride would be only 45 x 10^{-15} compared with 180 x 10^{-15} for the granite. An evaporite deposit would have a very low U-content and negligible Th-content so that the in-situ neutron flux would be extremely low. Evaporated sea water, for example, would contain only 0.1 ppm U in the residual solids. The ^{36}Cl atomic ratio at equilibrium for an evaporite would consequently be negligibly small and a zero value has been assumed for the mixing model discussed below.

The concentration of ^{36}Cl atoms in a groundwater which has derived its total chlorinity, W mg/ℓ, from two sources is given by:

$$^{36}N = W_1S_1 + (W - W_1)S_2 \text{ atoms/ℓ} \qquad (9.4.3)$$

where W_1 is the chlorinity derived from source one and S_1, S_2 are the specific concentrations (atoms/mg) of ^{36}Cl in the two sources. The ^{36}Cl atomic ratio, R, for the mixture is given by the equation:

$$R = \frac{W_1R_1 + (W - W_1)R_2}{W} \qquad (9.4.4)$$

where R_1 and R_2 are the ^{36}Cl atomic ratios for the two chloride sources. The amounts of chloride which must have been derived from granite/leptite and granite/evaporite sources to yield the

Table 9-8 Mixing models and chlorinity sources in the Stripa groundwaters.

Borehole	Cl^- ppm	Cl^- sources (ppm) for mixing with: leptite granite	leptite leptite	evaporite granite	evaporite evaporite	$^{36}Cl/Cl$ (calculated) x 10^{-15}
N1	67	67	0	67	0	180
V2(A)	300	79	221	134	166	80
V1	580	77	503	203	377	63
V2(B)	620	99	521	229	391	66

Values of specific ^{36}Cl content, atoms/mg: granite 3.06×10^6, leptite 7.64×10^5, evaporite 0.

Values of ^{36}Cl atomic ratio: granite 180×10^{-15}: leptite 45×10^{-15}.

observed ^{36}Cl contents of the Stripa groundwaters have been calculated and are listed in Table 9-8. It may be noted that for mixing with a leptite source, the amount of interaction required with the granite at depth is small and most of the chloride is derived from leptite. A more significant interaction with the granite is required by the evaporite mixing model.

It should be noted that both models imply the deep production of ^{36}Cl if the incoming Cl is weak in the granite; this means that the residence time in the granite is not significant.

Figure 9-9 shows the relationship between the ^{36}Cl content and chlorinity for the deep groundwaters. Also shown, are lines for the total derivation of the chlorinity from the granite and from the leptite. Figure 9-10 shows the ^{36}Cl atomic ratio for both mixing models compared to the field data.

The leptite and evaporite mixing models explain the observed ^{36}Cl data equally well but the hydrological implications of the models are different. If the chloride is derived from the granite/leptite model, the deepest groundwaters must undergo considerable evolution in the leptite and <20% of the Cl^- is derived from the granite. There is only a small variation in the extent of interaction with the granite for the different groundwaters. Hydrologically, this implies short flow paths through the granite and progressively longer flow paths through the leptite for the deeper groundwaters. As the Stripa granite is a relatively small intrusion, this is not implausible. The granite/evaporite mixing model implies that the fracture fluids in the system were completely replaced by an evaporite solution at some time in the past and that shallow groundwaters from near the granite outcrop are gradually replacing them. This is also a plausible scenario in the hydraulic sink which has been created by the mine. It is supported by the heavy isotope composition of the dissolved sulphate which suggests that brines of Permian origin provided the sulphate content of the groundwaters (Fontes and Michelot, 1983;

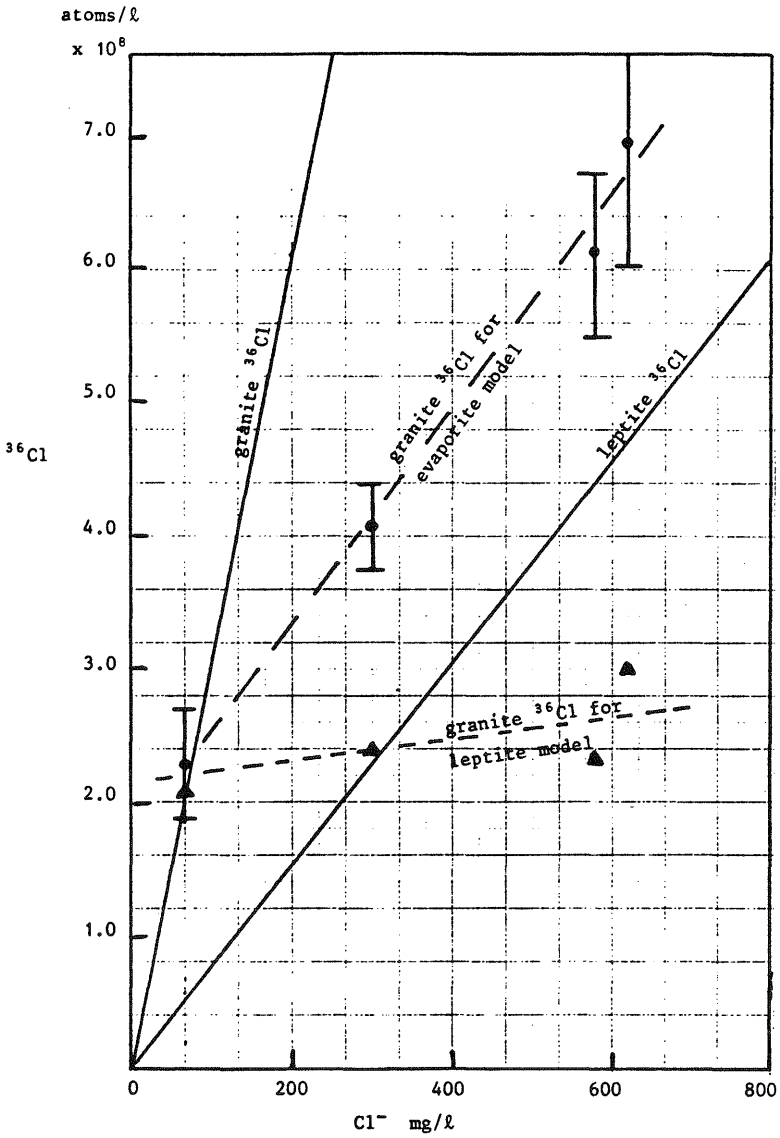

Figure 9-9. The ^{36}Cl content of Stripa groundwaters plotted against their chlorinity. The triangular symbols indicate the granitic component for mixed Cl^- sources from the granite and leptite. Mixed Cl^- sources for the granite evaporite model are coincident with the observed data.

Michelot et al., 1984). The occurrence of evaporites in the region of the Oslo Gulf has been reported in recent restorations of Zechstein times (Ziegler, 1982).

9.4.5 Implications for groundwater residence time

The mixing models which have been discussed above assumed that once the low ^{36}Cl-content evaporite solution or groundwater from the leptite had entered the granite, there was no further increase in the ^{36}Cl-content due to irradiation of the fracture fluids by the neutron flux generated within the granite. Since the mixing models may explain the ^{36}Cl data without such correction,

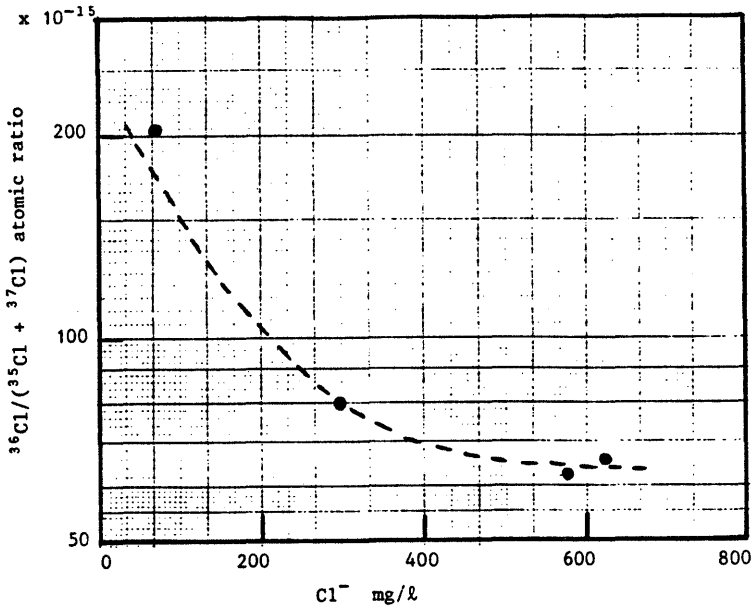

Figure 9-10. The $^{36}Cl/(^{35}Cl + ^{37}Cl)$ atomic ratio of dissolved chloride in the Stripa groundwaters plotted against chlorinity. The broken line is the dilution line for admixture of low ^{36}Cl saline water (Table 8.4.2).

the further ingrowth of ^{36}Cl in the fracture fluids could be smaller than the experimental error on ^{36}Cl-content measurements, which ranges from 7 to 14% for the low ^{36}Cl content deep groundwaters. Application of the ingrowth law (equation 9.4.2) shows that a 14% ingrowth of ^{36}Cl could occur in 70 ka. For the evaporite model, this suggests that the saline incursion into the granite must have occurred less than 70 ka ago and that most of the ^{36}Cl activity has been derived by subsequent interaction of the fluid with the granite. A maximum residence time for the fluids may be calculated on the assumption that no ^{36}Cl has been derived from the granite and that it is entirely due to ingrowth within the fracture fluids. Although this is certainly not so, as it would allow no chemical interaction with the granite, it does establish that, whether or not the mixing model is entirely correct, the deep fluids cannot be older than 170 ka.

These studies are still preliminary because there are only four data points and there are no measurements of ^{36}Cl in the rock matrix to substantiate the calculated value. Further research is under way to resolve these questions.

10 RADIOELEMENTS IN THE STRIPA GRANITE AND GROUNDWATERS

10.1 Radioelement content of the Stripa granite

The uranium, thorium and potassium contents of core samples from boreholes E1, N1, V1 and V2 have been determined by γ-ray spectrometry and are reported in Table 10-1. The U-content of samples from V1 averaged 44.6 ± 10.4 μg/g and from V2 averaged 43.6 ± 3.7. These values may be compared with measurements by Nelson et al., (1979) for the M3 borehole, which has an average U-content

Table 10-1. γ-Spectrometric determination of the U, Th and K contents of the Stripa granite.

Analysis No.	Borehole	Depth m	U-content μg g^{-1}	±	Th-content μg g^{-1}	±	Th/U	K-content %	±
601	N1	22.53- 22.60	42.16	0.25	49.97	0.89	1.19	4.05	0.04
602	N1	282.03-282.11	20.24	0.20	29.00	0.83	1.43	2.98	0.03
603	E1	22.37- 22.43	26.72	0.22	48.88	0.88	1.83	4.34	0.03
604	E1	286.41-286.47	43.35	0.25	50.30	0.89	1.16	4.18	0.04
605	V1	25.51- 25.59	40.83	0.25	59.14	0.91	1.45	3.91	0.04
606	V1	75.45- 75.52	75.17	0.30	55.22	0.90	0.73	4.22	0.04
607	V1	128.44-128.54	39.09	0.24	45.24	0.88	1.16	3.84	0.03
608	V1	186.34-186.41	38.78	0.24	47.17	0.88	1.22	4.05	0.04
609	V1	228.75-228.82	42.89	0.25	47.42	0.88	1.11	3.99	0.04
610	V1	282.47-282.53	48.75	0.26	53.37	0.90	1.09	4.06	0.04
611	V1	330.41-330.49	47.97	0.26	54.38	0.90	1.13	4.16	0.04
612	V1	385.46-385.54	35.40	0.24	52.02	0.89	1.47	4.16	0.03
613	V1	432.29-432.38	42.79	0.25	49.25	0.89	1.15	3.86	0.04
614	V1	498.16-498.25	39.67	0.24	46.22	0.88	1.17	4.27	0.04
615	V1Exc	-	39.18	0.24	44.86	0.87	1.14	4.05	0.04
		Average (605-615)	44.59	10.38	50.39	4.49	1.21	4.05	0.14
625	V2	00.97- 01.06	42.54	0.24	54.80	0.90	1.29	4.27	0.04
626	V2	55.22- 55.31	43.98	0.24	55.78	0.90	1.27	4.27	0.04
627	V2	106.03-106.13	36.13	0.22	41.59	0.86	1.15	3.67	0.04
628	V2	147.08-147.19	38.79	0.23	45.93	0.87	1.18	3.91	0.04
629	V2	196.04-196.15	40.23	0.23	55.51	0.90	1.38	4.25	0.04
630	V2	249.68-249.78	42.34	0.24	56.98	0.90	1.35	4.36	0.04
631	V2	303.10-303.20	42.34	0.24	57.31	0.90	1.35	4.33	0.04
632	V2	348.52-348.61	42.59	0.24	59.32	0.91	1.39	4.32	0.04
633	V2	400.54-400.64	42.95	0.24	59.86	0.91	1.39	4.23	0.04
634	V2	448.79-448.90	43.13	0.24	56.57	0.90	1.31	4.63	0.04
635	V2	503.84-503.95	45.07	0.24	57.26	0.90	1.27	4.34	0.04
636	V2	548.78-548.86	41.90	0.23	52.95	0.89	1.26	4.21	0.04
637	V2	599.21-599.30	42.53	0.23	52.27	0.89	1.23	4.13	0.04
638	V2	645.11-645.19	44.84	0.24	57.01	0.90	1.27	3.86	0.04
639	V2	701.54-701.66	46.47	0.24	58.06	0.90	1.25	4.30	0.04
640	V2	750.93-751.03	47.89	0.25	60.84	0.91	1.27	4.31	0.04
641	V2	800.14-800.25	47.51	0.25	64.46	0.92	1.36	4.36	0.04
642	V2	817.44-817.53	53.74	0.26	70.30	0.93	1.31	4.09	0,04
		Average (625-642)	43.61	3.72	56.49	6.08	1.29±0.07	4.21	0.21

Note: The errors quoted for individual determinations are 2σ errors based on counting statistics. The errors for the set averages are the standard deviation for the set.

of 44.0 ± 24.6 µg/g, som measurements by delayed neutron activation analysis for the 330 m and 410 m levels ranged from 37.3 - 39.9 µg/g (Andrews et al., 1982). Uranium in the granite is concentrated as uraninite within open microfractures in feldspars (Nelson et al., 1979) and it is therefore readily accessible to aqueous leaching and can be almost totally removed from crushed samples by leaching with dilute mineral acids.

The U-content of the granite is uniform throughout the unweathered part of the intrusion and is about 15 times the world average for granites. The Th-content averages 50.4 ± 4.5 µg/g (V1) and 56.5 ± 6.1 µg/g (V2) and the Th/U ratio is 1.2 - 1.29. The Th-content is also greater than the world average for granites but the Th/U ratio is less than the world average (2.8). The remarkably high radioelement contents of the granite are reflected in the high U and Ra found in its groundwaters; by a very high ^{4}He production rate in the granite and by a high neutron production rate due to (α,n) reactions (see section 9.1).

10.1.1 Uranium series equilibria in the Stripa granite

The isotopes ^{238}U, ^{234}U and ^{230}Th are genetically related, being members of the 4n + 2 decay series. (Table 10-3) Radioactive equilibrium throughout this series would be established within 1.25 million years as required by the half-lives in the decay sequence. The equilibria $^{234}U/^{238}U$, $^{230}Th/^{238}U$ and $^{230}Th/^{234}U$ may therefore be used to determine whether or not closed system conditions for U and Th have persisted within the rock over this time scale.

Samples of the Stripa granite from four locations were crushed to sub-micron size and then dissolved in HF in a Teflon pressurised digestion vessel. U and Th were subsequently separated by anion exchange, electrodeposited on stainless steel and determined by alpha-spectrometry. The natural U and Th contents and the various activity ratios are reported in Table 10-2.

The granite from the extensometer drift is in isotopic equilibrium ($^{234}U/^{238}U = ^{230}Th/^{238}U = ^{230}Th/^{234}U = 1$) and has therefore been undisturbed over the last 1.25 Ma. That from the V1 excavation, however, is apparently depleted in ^{230}Th. Since Th is not mobile in natural waters, this can only be explained as a consequence of uranium deposition.

The grey granite (the most typical of the granites at Stripa) from outcrop has a depleted $^{234}U/^{238}U$ ratio. This behaviour is expected when uranium is mobilised by groundwaters and when ^{234}U is preferentially mobilised relative to ^{238}U. The pink granite is in U/Th equilibrium and shows no evidence of uranium loss. Its radioelement contents (both U and Th) are much less than those for the granites at depth. The grey granite has a Th-con-

Table 10-2. Radioelement determinations on Stripa granite.

Sample	U-content µg/g	Th-content µg/g	$^{234}U/^{238}U$	$^{230}Th/^{238}U$ activity ratios	$^{230}Th/^{234}U$
A	19.1 ± 0.8	24.4 ± 0.9	0.74 ± 0.05	1.15 ± 0.04	1.55
	18.5 ± 0.6	27.2 ± 1.9	0.75 ± 0.04	1.27 ± 0.07	1.69
B	24.2 ± 0.7	12.0 ± 0.6	0.98 ± 0.04	0.78 ± 0.03	0.80
	26.1 ± 0.8	15.0 ± 0.7	1.00 ± 0.04	0.94 ± 0.04	0.94
C	38.6 ± 0.9	25.8 ± 1.1	1.00 ± 0.03	1.00 ± 0.03	1.00
	38.2 ± 0.9	24.8 ± 1.2	1.02 ± 0.03	0.91 ± 0.03	0.89
D	36.5 ± 0.8	19.2 ± 1.3	0.99 ± 0.03	0.72 ± 0.03	0.73
	36.0 ± 0.6	16.1 ± 0.9	0.96 ± 0.03	0.61 ± 0.02	0.63

A. Grey granite from outcrop.
B. Pink granite from outcrop.
C. Granite from extensometer drift, 350 m depth.
D. Granite from V1 excavation, 350 m depth.

Table 10-3. The ^{238}U and ^{232}Th decay series.

	$^{238}_{92}U$			$^{232}_{90}Th$	
α		4.5×10^9 a	α		1.41×10^{10} a
	$^{234}_{90}Th$			$^{228}_{88}Ra$	
β		24.1 d	β		6.7 a
	$^{234m}_{91}Pa$			$^{228}_{89}Ac$	
β		1.18 min	β		6.13 h
	$^{234}_{92}U$			$^{228}_{90}Th$	
α		2.5×10^5 a	α		1.91 a
	$^{230}_{90}Th$			$^{224}_{88}Ra$	
α		8.0×10^4 a	α		3.6 d
	$^{226}_{88}Ra$			$^{220}_{86}Rn$	
α		1.620 a	α		54 s
	$^{222}_{86}Rn$				
α		3.825 d			
	$^{210}_{82}Pb$				
β		22 a			
	$^{206}_{82}Pb$			$^{208}_{82}Pb$	

tent similar to that for the deeper granites. If it had an original U-content similar to that in the deep granite, the $^{230}Th/^{238}U$ ratio would be about 2 for recent uranium loss and the observed $^{230}Th/^{238}U$ ratio shows that the loss must have occurred over a period in excess of 150,000 years. Alternatively, if the uranium leaching is a recent occurrence, the original U-content of this outcrop granite cannot have exceeded 24 µg/g. However, the latter is very unlikely in view of the otherwise uniform radioelement distribution in the granite.

10.2 Uranium and thorium solution by groundwaters

The solution of the natural radioelements in a groundwater is dependent upon its chemical character, that is its pH, redox potential, salinity and the particular dissolved species present. Uranium in solution, for example, is stabilized as carbonate complexes of both U^{IV} and U^{VI}, and the importance of these complexes is dependent upon the pH, Eh and bicarbonate content of the water (Langmuir, 1978). Radioactive equilibrium is established throughout the ^{238}U decay series (Table 10-3) within 1.25 Ma in closed systems containing ^{238}U (rock matrices or solutions). Very frequently, however, the $^{234}U/^{238}U$ activity ratio for uranium dissolved by groundwaters is not in equilibrium, generally being greater than unity. Such disequilibrium may be a consequence of either preferential solution of ^{234}U or of α-recoil induced solution of ^{234}U. Preferential solution of ^{234}U rather than ^{238}U atoms may occur because the former are the decay products of ^{238}U and must, therefore, be present in lattice regions which have suffered recoil damage during the decay process. Such damage involves lattice displacement and is not readily annealed. It is also probable that the ^{234}U atoms are oxidized to the more soluble U^{VI} oxidation state during the recoil process (Rosholt *et al.*, 1963). ^{238}U atoms which decay in the rock surface close to the rock-water interface may result in the ejection of α-recoil ^{234}Th atoms into the solution (Kigoshi, 1971). These short lived ^{234}Th atoms either decay in solution or are deposited on the rock surface where, on decay, the ^{234}U formed may be readily dissolved.

The rate of ^{234}Th recoil solution, $^{234}Th_{rec}$, due to ^{238}U decay at the rock-water interface, is given by:

$$^{234}Th_{rec} = 0.7336[U]_r \cdot 0.235\ \rho R\ min^{-1}/cm^2 \qquad (10.1)$$

where $[U]_r$ is the natural uranium content of the rock, µg/g, ρ is the rock density, g/cm^3, R is the recoil range of ^{234}Th in the rock matrix, cm, 0.235 is the fraction of recoil atoms from within the recoil range of the surface that enter solution, and 0.7336 is the ^{238}U specific activity in natural uranium, $min^{-1}/µg$, which equals the equilibrium specific activity of ^{234}U.

The extent of rock surface, S, in contact with unit volume of a groundwater is given by:

$$S = \frac{\rho s}{\phi} \text{ cm}^2/\text{cm}^3 \text{ of ground water} \qquad (10.2)$$

where ϕ is the fractional porosity of the aquifer and s is the specific internal surface area giving rise to the aquifer porosity. The value of S is very dependent upon the nature of the aquifer porosity but in many cases it is likely to be in the range 1 - 20 cm^{-1} In the case of crystalline rocks which are dominated by flow in tight fractures and especially where the micro-fracture porosity is significant, the value of S may be of order 10^4 cm^{-1}. This parameter is the primary control of the recoil ^{234}Th solution process and it is shown below that, together with the uranium content of the groundwater, it is the most significant control on the $^{234}U/^{238}U$ activity ratio change with time.

The decay rate of ^{234}U which is unsupported by its parent ^{238}U and the rate of ingrowth of ^{234}U in a solution containing ^{234}Th are controlled by the decay constant, $^{234}\lambda$, for ^{234}U. From the standard decay and ingrowth equations it may be shown that a ground water which has acquired an initial natural uranium content of $[U]_s \mu g/g$, will undergo change in the $^{234}U/^{238}U$ activity ratio, AR, of this uranium according to the equation:

$$AR_t = 1 + \frac{(^{234}U_s - {}^{238}U_s)e^{-^{234}\lambda t}}{0.7336[U]_s} + \cdots\cdots$$

$$\cdots\cdots \quad \frac{0.7336[U]_r \; 0.235 \; \rho SR(1 - e^{-^{234}\lambda t})}{0.7336[U]_s} \qquad (10.3)$$

where $^{234}U_s$ and $^{238}U_s$ are the activities of these nuclides in solution, min^{-1}/g. The activity due to ^{238}U in solution is related to the natural uranium content of the solution by the equation:

$$^{238}U_s = 0.7336[U]_s \qquad (10.4)$$

so that equation (10.3) becomes:

$$AR_t = 1 + (AR_i - 1)e^{-^{234}\lambda t} + 0.235 \; \rho SR(1 - e^{-^{234}\lambda t})[U]_r/[U]_s \qquad (10.5)$$

where AR_i is the initial activity ratio of the dissolved uranium in the groundwater (t = 0). An initially enhanced activity ratio may be a consequence of either preferential solution of ^{234}U relative to ^{238}U or of α-recoil induced solution of ^{234}Th. However, the recoil process requires time for subsequent ^{234}U-ingrowth to become significant and enhanced activity ratios for groundwaters close to recharge must generally result from the pre-

ferential ^{234}U-solution process. The recoil process becomes more significant as the residence time of the ground water increases and chemical solution ceases, or uranium deposition occurs, as the ground water evolves towards more reducing conditions. It is evident from equation (10.5) that groundwaters with very low uranium contents are most likely to undergo activity ratio increase due to the α-recoil process. This will tend to counterbalance the decay of any excess ^{234}U which was dissolved by preferential solution closer to recharge. The estimation of groundwater residence times from $^{234}U/^{238}U$ activity ratio changes is, in principle, possible but requires a knowledge of the geochemical processes which occur in different aquifer zones and of its hydrological character. This is only likely to be sufficiently well known in aquifers for which samples can be obtained from various locations. It is unlikely that the uranium geochemistry can be deduced for fluids from a single exploration borehole in an otherwise unknown acquifer.

In contrast with the mobility of uranium in the hydrosphere, thorium is very insoluble and is generally not present above detection limits in natural waters. This is a consequence of its ready hydrolysis to the insoluble hydroxide at the pH values typical of groundwaters. The immediate decay product of ^{232}Th is ^{228}Ra and this may be ejected into solutions from a rock surface by the α-recoil process. The ^{228}Ra (half-life 6.7 years) can then support ^{228}Th (half-life 1.91 years) production in solution although this may be readily hydrolysed and absorbed on any colloidal particles in solution.

10.2.1 Analytical method for U and Th isotopes in solution

Water samples (20-25 kg) were generally filtered through 0.45 μm filters and acidified to pH≤2 by addition of Analar HCl as soons as possible after collection. About 300 mg of Fe^{3+} and 20-40 disintegrations $min.^{-1}$ of ^{232}U were added to each sample. The acidified solution was outgassed with CO_2-free air or nitrogen to remove carbonate which could complex U at high pH. U was coprecipitated with $Fe(OH)_3$ on raising the pH to ~8.5 by addition of NH_4OH solution. The precipitate was recovered dissolved in 6 M HCl, and Fe^{3+} was then extracted into an equal volume of methylisobutyl ketone. The acid solution of U was further purified by anion exchange, first on a Cl^- and then on a NO_3^- column of Dowex-1-X8 100-200 mesh resin. U was finally eluted from the NO_3^- column with 0.1 M HCl and after evaporation to dryness was dissolved in 10 cm^3 1 M $(NH_4)_2SO_4$ solution (acidified to pH 2.4) and transferred to a Teflon electrolysis cell. Electrodeposition of U on a stainless steel plachet was complete after 3 hr. at a current density of 1 A cm^{-2}. The source was counted with a Li-drifted surface barrier alpha-spectrometer.

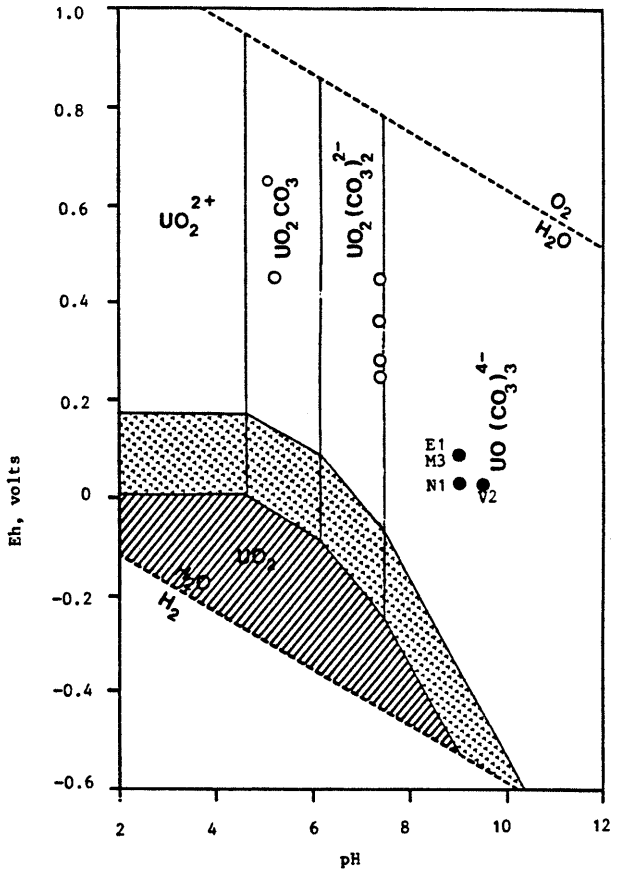

Figure 10-1. The stability of uranyl species in solution as a function of pH and Eh. The minewaters are indicated by full circles and the shallow groundwaters by open circles.

If Th isotopes were to be detemined, they were separated by further anion exchange on the effluent from the Cl^- anion exchange column on which uranium was initially retained. Following separation of Th from other cations, it was electrodeposited on a stainless steel planchet prior to alpha spectrometry.

10.2.2 U-solution and $^{234}U/^{238}U$ activity ratio in the shallow groundwaters

The $^{234}U/^{238}U$ activity ratios of the dissolved uranium in the shallow groundwaters at Stripa (Table 10-4) range from 2.18 to 4.8 and their uranium contents range from less than 1 to almost 100 µg/kg. These are the groundwaters closest to recharge and they have high tritium contents, indicative of their recent origin. Their Eh values show that uranium solution is taking place under oxidising conditions (Figure 10-1). It is possible that preferential etch solution of ^{234}U is the cause of the activity ratio enhancement for the dissolved uranium in these groundwaters. However, laboratory etch experiments on crushed samples of

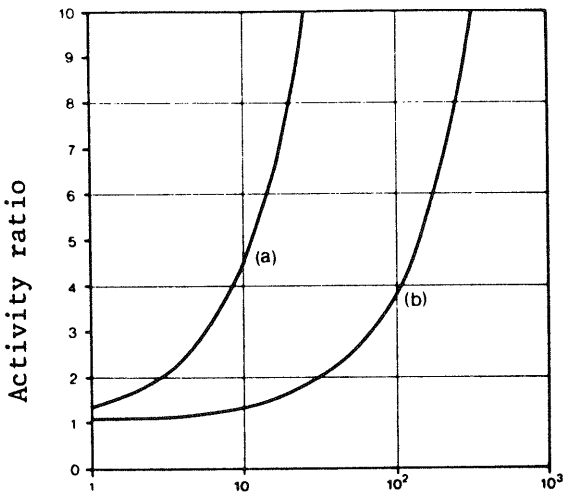

Figure 10-2. $^{234}U/^{238}U$ activity ratio change with age for uranium in groundwater present in the micro-fractures of a granite which has a uranium content of 5000 µg/g in fracture surfaces, calculated from equation 3. The activity ratios are calculated for (a) fracture openings of 0.5 µm (S = 40000 cm^2/cm^3) and (b) fracture openings of 2.0 µm (S = 10000 cm^2/cm^3). In each case the groundwater uranium content is 10 µg/kg.

the Stripa granite resulted in an activity ratio of only 1.15 for the dissolved uranium. The activity ratio for the uranium within a granite sample from outcrop was found to be only 0.72 $\pm$ 0.3. It was only possible to obtain an activity ratio for the dissolved uranium, which was greater than that for the rock matrix, when etch was carried out under very slow and non-oxidising conditions. Preferential etch solution of ^{234}U can probably also occur to some extent under natural conditions of groundwater/rock interaction but ^{234}Th recoil due to the large concentration of uranium in micro-fractures could also be a significant mechanism for generating the observed $^{234}U/^{238}U$ activity ratios in the shallow groundwaters. The increase of this activity ratio with time due to continued ^{234}Th recoil within the micro-fractures is shown in Figure 10-2. The computed changes are shown for 0.5 and 2.0 µm fracture separations, for a uraninite coating on the fracture surfaces equivalent to a surface uranium content of 5,000 µg/g. For a groundwater uranium content of 10 µg/kg, the activity ratio could increase to 4 within 10 years as a result of such ^{234}Th recoil in the micro-fractures. If most of the uranium were present within the ^{234}Th-recoil range of the rock-water interface, the recoil process would eventually establish a $^{234}U/^{238}U$ activity ratio of 0.75 in the uraniferous surface. This is close to the observed ratio in outcrop samples of the granite and suggests that the recoil process is important in

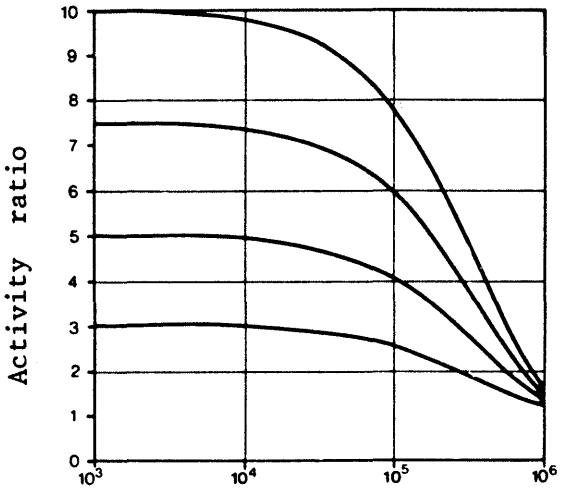

Figure 10-3. $^{234}U/^{238}U$ activity ratio change with age for uranium in groundwater present in a granite with fracture openings of 0.2 cm (S = 10 cm^2/cm^3) and a uniform uranium content of 40 µg/g calculated from equation 3. The activity ratio/age relationship is shown for various initial activity ratios and for a groundwater uranium content of 10 µg/kg.

these groundwaters. The effect of alpha-recoil for fluids contained between fracture walls which have the average U-content of the bulk granite is shown in Figure 10-3. In such situations the $^{234}U/^{238}U$ activity ratio cannot increase with time and enhanced ratios must be due to preferential solution of ^{234}U, following which decay of excess ^{234}U occurs.

10.2.3 Uranium chemistry in the deeper groundwaters

Table 10-4 reports measurements of the U-content and $^{234}U/^{238}U$ activity ratio for dissolved uranium in the groundwaters from 1977 to 1984, and field data for recent measurements are given in Table 10-5. Apart from the increased U-content for the 1981 measurement, both parameters are remarkably constant in the M3 borehole. The activity ratio average is 10.9 with a standard deviation of only $\pm$ 0.2. This may be attributed to the constant flow conditions which existed in this borehole over the period of measurement, so that U-solution and α-recoil effects have been unaffected by variations of the sampled interval or in the flow pattern.

The records for boreholes V1 and V2 are much more variable and this is largely due to the variable sample intervals which were selected and to variations in the flow history of the borehole

Table 10-4. Natural U-contents and $^{234}U/^{238}U$ activity ratios of dissolved uranium in Stripa groundwaters.

Analysis number	Sampling date	Borehole interval, m	Depth below ground, m	U-content µg/kg	$^{234}U/^{238}U$ Activity ratio
Shallow groundwaters					
PW1	18.05.79		60	90.2	3.22
PW1	21.01.81			90.40 ± 1.80	3.23 ± 0.07
PW2	24.10.77		<100	2.84	2.62*
PW2	24.10.77		<100	2.26	2.57
PW3	16.05.79		120	19.47	4.80
PW4	17.05.79		40	7.60	2.74
PW5	4.10.77		40	1.61	3.11*
PW5	15.05.79		40	0.81	2.18
WT2	18.05.79		50	0.85	2.73
Mine Dripwater	16.05.79		157	14.72	2.91
R1	16.05.79	0 - 26	310 - 336	11.69	11.11
R9	16.05.79	0 - 30	336 - 366	10.99	11.75
Borehole M3 :					
	9.09.77	0 - 14	336 - 350	8.25	10.75*
	9.09.77	0 - 14	336 - 350	9.22	10.65*
	6.06.78	0 - 14	336 - 350	8.33	10.70
	16.05.79	0 - 14	336 - 350	11.18	10.68
1452 2F	3.06.81	0 - 14	336 - 350	18.03 ± 0.49	11.24 ± 0.32
1485-83	9.11.83	0 - 14	336 - 350	10.12 ± 0.10	10.97 ± 0.11
1520-84	23.02.84	0 - 14	336 - 350	10.40 ± 0.05	11.09 ± 0.05
Borehole E1					
1455 1F	11.11.81	3 - 300	357 - 385	9.50 ± 0.24	4.71 ± 0.13
1535-84	6.03.84	3 - 300	357 - 385	7.40 ± 0.06	4.16 ± 0.04
Borehole N1					
1454 1F	14.07.81	2 - 300	357 - 401	8.46 ± 0.23	3.22 ± 0.10
1454 3F	6.10.81	3 - 300	357 - 401	1.83 ± 0.08	5.64 ± 0.26
1510-84 I	26.01.84	252 - 300	397 - 401	1.27 ± 0.02	9.00 ± 0.18
1515-84 II	26.01.84	152 - 251	379 - 394	1.24 ± 0.02	9.65 ± 0.20
Borehole V1					
1450 1F	15.01.81	92 - 94	449 - 451	34.76 ± 0.46	2.90 ± 0.04
1450 2F	11.06.81	410 - 506	767 - 863	0.42 ± 0.04	3.96 ± 0.44
1450 3F	17.07.81	409 - 506	766 - 863	0.09 ± 0.13	3.37 ± 0.56
1450 5F	8.09.81	409 - 506	766 - 863	5.35 ± 0.13	3.06 ± 0.08
1450 6F	9.09.81	4 - 506	361 - 863	0.06 ± 0.04	4.91 ± 0.38
1450 7F	16.09.81	4 - 506	361 - 863	0.35 ± 0.05	5.14 ± 0.73
1450 8F	21.09.81	4 - 506	361 - 863	0.36 ± 0.03	4.65 ± 0.49
1450 9F	6.10.81	4 - 506	361 - 863	0.28 ± 0.03	4.52 ± 0.45
1470-83	3.10.83	100 - 505	457 - 862	1.49 ± 0.03	3.20 ± 0.07
1475-83	19.10.83	100 - 505	457 - 862	0.21 ± 0.01	4.81 ± 0.26
1480-83	5.11.83	100 - 505	457 - 862	0.17 ± 0.01	5.41 ± 0.32
1500-84	11.01.84	100 - 505	457 - 862	0.17 ± 0.01	4.55 ± 0.24
1505-84	8.02.84	100 - 505	457 - 862	0.22 ± 0.01	3.70 ± 0.13

Table 10-4. Cont'd.

Analysis number	Sampling date	Borehole interval, m	Depth below ground, m	U-content µg/kg	$^{234}U/^{238}U$ Activity ratio
Borehole V2					
	9.09.77	6 - 50	416 - 460	10.43	5.55*
	10.11.77	0 - 470	410 - 880	6.24	5.87*
	8.09.77	150 - 470	560 - 880	4.56	3.87*
	20.09.77	285 - 470	695 - 880	4.12	4.08*
	29.01.78	376 - 470	786 - 880	1.03	4.02
	16.05.79	401 - 428	811 - 838	0.5	3.74
1453 1F	11.06.81	356 - 470	766 - 880	0.25 ± 0.06	3.98 ± 1.00
1453 2F	19.11.81	356 - 471	766 - 881	0.14 ± 0.03	3.14 ± 0.72
1460F	24.11.82	406 - 510	816 - 920	0.26 ± 0.38	1.97 ± 0.35
1461F	13.12.82	413 - 417	823 - 827	0.48 ± 0.04	3.77 ± 0.35
1462F	19.01.83	490 - 494	900 - 904	0.58 ± 0.19	7.40 ± 0.26
1495-83 I	29.11.83	562 - 822	972 -1232	0.08 ± 0.01	2.54 ± 0.19
1525-84 II	28.02.84	500 - 561	910 - 971	0.13 ± 0.01	6.13 ± 0.29
1530-84 IV	28.02.84	382 - 423	792 - 833	0.25 ± 0.01	4.15 ± 0.14

*Analysed at Florida State University.

(Andrews, 1983). The increase in U-content observed on 8 September, 1981 for V1 followed a shut-in period of no flow. A similar increase was observed on 3 October 1983, when flow was restored after shut-in for several months. The average $^{234}U/^{238}U$ activity ratio for groundwater from this borehole, neglecting the high U-content measurements, is 4.5 ± 0.6. The U-content for V2 shows a marked decline with depth. The activity ratio average is 3.8 ± 0.4 for depths greater than 560 m below surface, neglecting the high ratios found in discrete intervals at 900 - 904 and 910 - 970 m below surface. The lowest activity ratios occur at the greatest depths, where the isotopic composition of the groundwater is also distinctly different. The main features of uranium chemistry in the Stripa groundwaters are summarized in Table 10-6. The U-content is highest in the shallow groundwaters and declines with depth whilst the activity ratio increases to a maximum for groundwaters from about 350 m depth and then declines for deeper groundwaters. The pattern of change is consistent with alpha-recoil enhancement of the $^{234}U/^{238}U$ activity ratio for the shallow groundwaters and a somewhat larger recoil effect around 350 m depth. This could result from U-deposition on fracture surfaces as shallow groundwater migrates downwards. Although the field measurements of Eh/pH for the 350 m groundwaters do not suggest that U-deposition should occur the high ^{222}Rn contents in these groundwaters (10.2.3) are consistent with such deposition. This incursion of meteoric water from outcrop to about 350 m level in the granite is consistent with the expected flow pattern once a hydraulic sink was created by opening the mine galleries to depths of 350 m and, locally, to 410 m.

The decrease in $^{234}U/^{238}U$ activity ratio in the samples from V1 and V2 may be due to any of the following possibilities:

Table 10-5. Physical data for groundwater samples from Stripa for sampling in period October 1983 - March 1984.

Borehole	Interval, m	Flow rate, cm^3/min	Temperature °C	pH	Conductivity µS/cm	Eh mV
M3	0 - 14	75	14.5	9.09	235	+100
E1	3 - 300	400	10.3	8.90	165	+109
N1-I	252 - 300	560	10.5	8.89	200	+ 33
N1-II	152 - 251	555	10.3	8.99	215	+ 39
V1	100 - 505	7-18,000	12.3	9.12	1525	+114
V2 I	562 - 822	11	8.2	9.94	1215	+239
V2 II	500 - 561	252	8.6	10.06	1090	+ 43
V2 III	424 - 499	210	9.0	10.04	1210	+ 46
V2 IV	382 - 423	92	8.0	9.51	1140	+ 26

Relative borehole disposition:

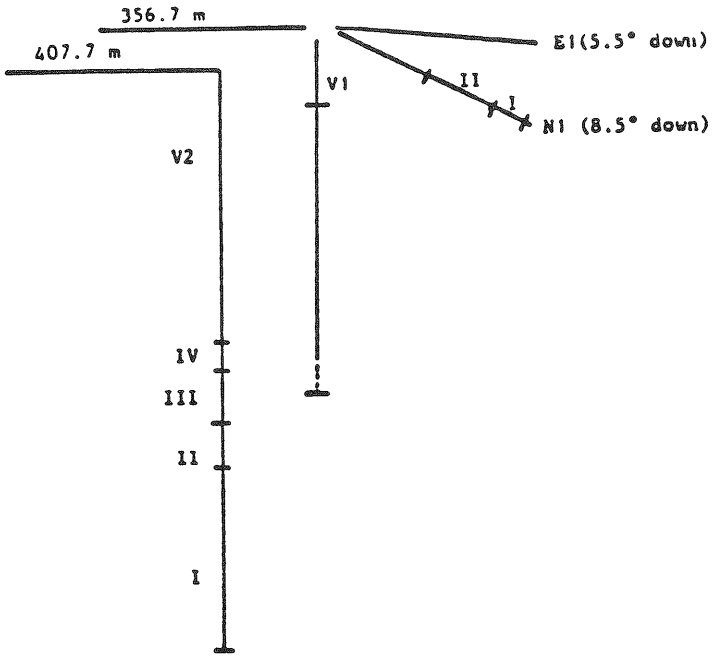

(i) incursion of meteoric water from shallower depths and admixture with stored fluid in the deep fracture system.

(ii) an alternative flow pattern at depth, perhaps involving recharge through the leptite so that the U-chemistry is partially determined within the leptite.

Table 10-6. Summary of the main features of uranium solution chemistry in the Stripa groundwaters.

Groundwater type	Approximate depth below ground, m	^{238}U content µg/kg	$^{234}U/^{238}U$ activity ratio
Shallow	<150	1 - 100	3.0 ± 0.7
Intermediate depth			
Borehole E1	370	7.4 - 9.5	4.4 ± 0.3
Boreholes R1, R9	350	11.3 ± 0.4	11.4 ± 0.3
M3	350	19.6 ± 1.1	10.9 ± 0.2
Borehole N1 (inner)	380	1.25 ± 0.2	9.3 ± 0.3
Deep groundwaters			
Borehole V1		0.2 - 0.4	4.5 ± 0.6
V2		0.1 - 0.5	3.8 ± 0.4
V2, >816 m below surface		0.1 - 0.3	2.0 ± 2.5

(iii) recharge of the deep groundwater occurred through the shallower levels at some time in the past, acquiring a high $^{234}U/^{238}U$ ratio similar to the M3 values and has subsequently decayed to the low levels found at the bottom of V2. This decay would require in excess of 500 ka.

This last possibility can be excluded on the basis of the ^{36}Cl data (Section 9.4) which shows that the deep groundwater residence time is <70 ka. The incursion of a brine into the deep fracture system, probably at a time of lower sea level, is suggested by the isotopic composition of dissolved sulphate (Fontes and Michelot, 1983), and would also explain the ^{36}Cl data. Such a brine would have a low U-content and the $^{234}U/^{238}U$ ratio would probably be close to equilibrium. The first explanation for the present U chemistry in the deep groundwaters, therefore seems the most probable. This is also the most probable explanation on a hydrological basis, as recharge would always have taken place directly through outcrop and would not require long flow-paths through low permeability strata.

10.2.4 Thorium in solution

The first few members of the ^{232}Th decay series are:

$$^{232}Th \xrightarrow{\alpha} {}^{228}Ra \xrightarrow{\beta} {}^{228}Ac \xrightarrow{\beta} {}^{228}Th \xrightarrow{\alpha}$$

1.4×10^{10}a 6.7a 6.13h 1.91a

The isotope ^{230}Th (half-life 8×10^4a) belongs to the ^{238}U decay series and was found to be absent from all of the groundwaters. ^{232}Th and ^{228}Th are present (Table 10-7) and ^{228}Th is generally

Table 10-7. ^{222}Th content, $^{230}Th/^{234}U$ ratio and ^{228}Th content of Stripa groundwaters.

Analysis number	Sampling date	Borehole interval, m	Depth below ground, m	^{232}Th content µg kg^{-1}	$^{230}Th/^{234}U$	^{228}Th dpm kg^{-1}	^{228}Th equiv. ^{232}Th µg kg^{-1}
Borehole H3							
1452-2F	3.06.81	0 - 14	336 - 350	-	-	7.885	32.05
1452-2U	3.06.81	0 - 14	336 - 350	0.113 ± 0.035	0.0013	-	-
Borehole H1							
1454-1	14.07.81	2 - 300	357 - 385	0.232 ± 0.081	0.0012	-	-
Borehole V1							
1450-2F	11.06.81	409 - 506	767 - 863	0.081 ± 0.027	0.0051	-	-
1450-3F	14.07.81	409 - 506	767 - 863	-	-	6.954	28.27
1450-3U	14.07.81	409 - 506	767 - 863	0.274 ± 0.064	0.0319	-	-
Borehole V2							
1453-1F	11.06.81	356 - 470	766 - 880	-	-	6.402	26.02
1453-1U	11.06.81	356 - 470	766 - 880	0.071 ± 0.028	0.0221	-	-

F = 0.45 µm filtered sample
U = unfiltered sample

present in an amount exceeding equilibrium with ^{232}Th. Thorium is generally absent from groundwaters because of the insolubility of its hydroxide. At Stripa, the amounts of ^{232}Th present in the waters are low but significantly above detection limits and a proportion of it may be carried on particulates of colloidal dimensions. ^{228}Th is produced by an α-recoil ejection of ^{228}Ra into solution and this decays to ^{228}Th, transient equilibrium being established after about 35 years. The ^{228}Th content would be indentical to the ^{228}Ra content for a constant ^{228}Ra recoil rate.

The alpha-recoil rate for ^{228}Ra and ^{226}Ra may be estimated from the amount of ^{228}Th in solution. The ^{228}Th activity in solution is equal to that of about 30 µg kg^{-1} of ^{232}Th (Table 10-7), that is, to about 7.4 disintegrations $min^{-1}kg^{-1}$. Provided that the ^{228}Th residence time is greater than a few years, this should equal the ^{228}Ra recoil rate. As the concentrations of U and Th in the Stripa granite are about 40 µg kg^{-1} and 30 µg respectively, the corresponding recoil rate for ^{226}Ra is given by:

Ra recoil rate = ^{238}U series recoil rate

$$= \frac{40 \times 0.7336}{30 \times 0.246} \times 7.4$$

$$= 29.4 \text{ disintegrations } min^{-1}kg^{-1}$$

$$= 13.4 \text{ pCi } kg^{-1}$$

This estimate of the ^{226}Ra recoil rate assumes that both U and Th are uniformly distributed in the rock surface. The very high ^{222}Rn contents in the groundwaters and the ready solution of ^{234}U and ^{238}U indicate that the U concentration in the fracture surfaces may be much greater than that of Th. ^{226}Ra content of the groundwaters exceeds that suggested by the above recoil rate, by a factor of about 10 (Section 10.3). This confirms that U is preferentially concentrated close to fracture surfaces, whilst Th is probably incorporated in accessory minerals to a larger extent than U.

The number of ratio of ^{232}Th to ^{228}Th atoms for radioactive equilibrium is about $10^{10}/1$, so that the mass of ^{228}Th in solution is negligible even though its activity is readily determined. The relatively high activities of ^{228}Th do not exceed solubility limits and this suggests that other high specific activity 4-valent nuclides amongst the actinides could have appreciable mobility in the Stripa groundwaters.

10.3 Radon and radium solution in groundwaters

The dissolution of ^{222}Rn by a groundwater occurs predominantly at the rock-water interface by an α-recoil process (Andrews and Wood, 1972). The ^{222}Rn activity in solution increases with time until it reaches an equilibrium value determined by the decay rate of its parent ^{226}Ra, in the rock surface. This equilibrium is attained when the residence time of the water in the aquifer exceeds 25 days, according to the equation:

$$^{222}A_t = {}^{222}A_e(1 - e^{-{}^{222}\lambda t}) \qquad (10.6)$$

where $^{222}A_t$, $^{222}A_e$ are the ^{222}Rn activities at time, t, and at equilibrium, respectively, and $^{222}\lambda$ is the decay constant for ^{222}Rn.

The equilibrium ^{222}Rn content, [Rn], of a groundwater is related to the uranium content, $[U]_r$ μg/g; bulk density, ρg/cm^3 and fractional porosity, φ, of the aquifer rock by the equation:

$$[Rn] = \frac{F \times 0.7336 \times \rho \times [U]_r \times 10^3}{\phi \times 2.2 \times 10^6} \mu Ci/kg \qquad (10.7)$$

where F is a factor which accounts for the overall efficiency of ^{222}Rn solution due to α-recoil ejection at the rock-water interface and its diffusive movement to the flow porosity. The value of F is generally in the range 0.01 - 0.05.

The diffusion of ^{222}Rn in the x-direction may be represented as:

$$[Rn]_x = [Rn]_o \exp(-x\sqrt{\lambda/D}) \qquad (10.8)$$

where $[Rn]_o$, $[Rn]_x$ are the ^{222}Rn concentrations at x = 0 and x, respectively, and D is the diffusion coefficient for ^{222}Rn. The diffusion coefficient for ^{222}Rn in water is 10^{-5} cm^2/s (Tanner, 1964) and equation (10.8) shows that the ^{222}Rn concentration decreases by a factor of 0.37 for diffusion over a distance equal to $\sqrt{D/\lambda}$ (the diffusion length) which is 2.18 cm in water. Over a distance equal to 10 diffusion lengths the ^{222}Rn concentration is reduced by a factor of 4.5×10^{-5}. In more practical terms this means that ^{222}Rn atoms decay before they can move significant distances by diffusion. In a still fluid the ^{222}Rn concentration decreases to 1% over a distance of 10 cm.

Transport of ^{222}Rn by groundwater movement is, therefore, much more significant than its diffusive movement. For movement by flow in fractures or conduits the ^{222}Rn-content of the water is unsupported by its parent ^{226}Ra in the rock surface and it may decay significantly if transported over long distances. Transport of ^{222}Rn by interstititial flow can maintain the ^{222}Rn-content of the water at its equilibrium value as it is then always supported by ^{222}Rn recoil from the interstitial surfaces.

The following processes are possible for the solution of ^{226}Ra by groundwater:

(1) chemical solution by rock-etch processes,

(2) decay of ^{230}Th in solution,

(3) α-recoil of ^{226}Ra on decay of ^{230}Th

  (a) which was deposited from solution onto the rock surface,

  (b) which was formed by ^{234}U decay in the rock surface.

The chemical solution of ^{226}Ra should increase in importance as the salinity of the groundwater increases, provided that sufficient barium or calcium ions are present in solution. The residence time of ^{226}Ra in solution depends upon the congruent - incongruent solution of barium and calcium as well as upon its half-life (1620 years). The formation of ^{226}Ra due to decay of ^{230}Th in solution is negligible since the ^{230}Th is never present in solution to any significant extent. The activity of ^{226}Ra dissolved by the recoil mechanisms increases with time according to the equation:

$$^{226}A_t = {}^{226}A_e(1 - e^{-226\lambda t}) \qquad (10.9)$$

where $^{226}A_t$ and $^{226}A_e$ are the ^{226}Ra activities at time, t, and at equilibrium, respectively, and $^{226}\lambda$ is the decay constant for ^{226}Ra. The ^{226}Ra activity in solution should, if α-recoil is the dominant mechanism, become constant after about 8000 years.

However, the incongruent solution of calcium carbonate results in the exchange of calcium between solution and rock-carbonate and co-precipitation of ^{226}Ra with calcium may prevent its activity ever attaining the equilibrium value in solution. Nevertheless, relatively high ^{226}Ra contents are generally found in the most evolved groundwaters and as geothermal waters and in oil-field brines.

10.3.1 Analytical method for ^{222}Rn and ^{226}Ra determinations

10.3.1.1 ^{222}Rn

^{222}Rn in 1-litre water samples was determined by outgassing with a stream of radon-free nitrogen and trapping the radon on an activated charcoal trap at -80°C. More than 99 per cent of the equilibrium radon was recovered from the solution by outgassing with ten times its volume of nitrogen at a flow rate of approximately 1.4 l/min. The radon so released was held on the charcoal trap even after prolonged passage of nitrogen, provided that the trap was maintained at -80°C. After radon collection, the charcoal trap was connected to a 50-cm^3 conical flask, the conical walls of which were coated with zinc sulphide scintillator. With the trap maintained at -80°C, the apparatus was evacuated to a pressure less than 1 mbar and the charcoal trap heated to 200°C to desorb the radon. The desorbed radon was transferred to the scintillator flask by admitting a stream of dry air through the trap and into the flask until the pressure equalled atmospheric pressure. After closing the stopcock on the flask, it was placed on the photocathode window of a 3-in diameter photomultiplier (E.M.I. type 9708 KA). The α-particle emission from ^{222}Rn and its daughters was recorded with a pulse amplifier/scaler system.

The counting rate was determined after a delay of 3 h to allow ingrowth of ^{214}Po in the decay sequence:

$$^{222}_{86}Rn \xrightarrow{\alpha} {}^{218}_{84}Po \xrightarrow{\alpha} {}^{214}_{82}Pb \xrightarrow{\beta}$$

3.825 days 3.05 min 26.8 min

$$^{214}_{83}Bi \xrightarrow{\beta} {}^{214}_{84}Po \xrightarrow{\alpha}$$

19.9 min 1.6×10^{-4} sec

The counting rate so obtained was corrected for counter background and for radon decay during the time elapsed since the water sample was collected. Each scintillation flask was periodically calibrated by outgassing radon from a standardized radium solution in which radon-radium equilibrium had been established. The background counting rate for a freshly prepared flask was less

than 0.5 counts/min and increased gradually with use to about 2.5 counts/min. This increase in background is due to the accumulation of the radon decay product ^{210}Pb (half-life 22 years) which has an α-particle emitting daughter, ^{210}Po. The counting efficiency of a scintillator flask was generally about 4 counts/min per pCi of radium.

10.3.1.2 ^{226}Ra

^{226}Ra was determined by estimating the equilibrium ^{222}Rn activity. The ^{222}Rn contents of groundwaters are frequently high, and very much greater than the ^{226}Ra content of the water. This excess radon was removed from the sample by outgassing with nitrogen before the radium determination. The sample was then allowed to stand for ⩾ 20 days to permit ingrowth of ^{222}Rn. The ^{222}Rn then present was determined as described above and the activity was corrected to the equilibrium value by use of the known growth time. The removal of excess radon must be at least 99.9 per cent efficient to avoid errors in the radium determination, and this was achieved by outgassing the water sample with 20 times its volume of nitrogen. After outgassing 99.9 per cent of the radon present in a sample with an excess radon content of 800 pCi/l, 0.8 pCi/l would remain, which after a 20-day decay period, is reduced to 0.02 pCi/l of ^{222}Rn or ^{226}Ra.

10.3.2 ^{222}Rn contents of Stripa groundwaters

The ^{222}Rn contents of the deeper Stripa groundwaters are exceptionally high (Table 10-8). The waters from shallow boreholes (up to 60 m depth) have ^{222}Rn contents of 5 - 20 nCi/kg which is typical of other granitic provinces (Edmunds et al., 1984). For the deep groundwaters, values range from 200 - 2,000 nCi/kg. There are marked temporal variations in the ^{222}Rn content for some of the deep groundwaters. For example, for determinations between October 1983 and February 1984 for V1, there is a large increase in ^{222}Rn content. This suggests that the flow regime in the borehole must have changed during this period. The ^{222}Rn content in this borehole decreased during an earlier shut-in period and was attributed to decay within the borehole and its associated fractures (Andrews, 1983).

The ^{222}Rn content of a groundwater is related to the U-content of the rock, $[U]_r$ ppm, and its porosity, ϕ, by equation (10.7). For the shallow groundwaters, this equation shows that less than 1% of the ^{222}Rn generated within the rock matrix is dissolved in the fracture fluids for a porosity of 1%. The fraction of ^{222}Rn dissolved in the minewaters is much greater and up to 50% release has been observed for M3. These high efficiencies of ^{222}Rn release indicate that the U within the rock matrix must be in close

Table 10-8. ^{222}Rn and ^{226}Ra contents of Stripa groundwaters.

Analysis number	Sampling date	Borehole interval, m	Depth below ground, m	^{222}Rn nCi kg^{-1}	^{226}Ra pCi kg^{-1}
Shallow groundwaters					
PW1	18.05.79		60	6.2	0.57
PW3	16.05.79		120	5.1	0.64
PW4	17.05.79		40	10.3	0.83
PW5	15.05.79		40	8.1	0.41
WT2	18.05.79		50	19.3	0.72
Borehole M3					
	14.02.78	0 - 14	336 - 350	1300.0	34.0
	16.05.79	0 - 14	336 - 350	2010.0	4.59
1452 - 1	2.01.81	0 - 14	336 - 350	1111.8 ± 1.5	6.88 ± 0.04 5.89 ± 0.04
1452 - 2	10.06.81	0 - 14	336 - 350	847.2 ± 3.4 1037.7 ± 4.0	5.24 ± 0.05 5.79 ± 0.05
1485 - 83	9.11.83	0 - 14	336 - 350	1168.3 ± 6.0 1230.4 ± 6.1	4.23 ± 0.11 4.68 ± 0.04
1520 - 84	23.02.84	0 - 14	336 - 350	942.5 ± 4.7 813.9 ± 3.9	4.90 ± 0.12
Borehole E1					
1455 - 1	11.11.81	3 - 300	357 - 385	402.5 ± 1.1 357.0 ± 0.8	5.14 ± 0.04 5.21 ± 0.04
1455 - 2	24.03.82	128 - 130	367 - 369	81.8 ± 0.8 84.1 ± 0.8	- -
1535 - 84	6.03.84	3 - 300	357 - 385	383.7 ± 4.8 351.4 ± 4.5	5.41 ± 0.11
Borehole N1					
1454 - 1	14.07.81	2 - 300	357 - 401	1.7 ± 0 1.9 ± 0	2.28 ± 0.04 2.30 ± 0.02
1454 - 2	19.08.81				2.90 ± 0.03 2.14 ± 0.02 2.47 ± 0.03
1454 - 3	6.10.81	3 - 300	356 - 401	171.7 ± 1.1 173.7 ± 0.8	3.26 ± 0.03 3.67 ± 0.03
1510 - 84	26.01.84	252 - 300	397 - 401	642.0 ± 5.1 639.0 ± 4.5	12.56 ± 0.20 11.74 ± 0.14
1515 - 84	26.01.84	152 - 251	379 - 394	591.4 ± 4.3 480.3 ± 3.7	12.01 ± 0.19 10.25 ± 0.12

Table 10-8. Cont'd.

Analysis number	Sampling date	Borehole interval, m	Depth below ground, m	^{222}Rn nCi kg^{-1}	^{226}Ra pCi kg^{-1}
Borehole V1					
1450 - 2	11.06.81	409 - 506	767 - 863	172.3 ± 1.4 123.4 ± 1.3	112.2 ± 0.22 128.4 ± 0.53
1450 - 3	14.07.81	409 - 506	766 - 863	218.4 ± 0.9 222.7 ± 0.9	134.1 ± 0.33 146.8 ± 1.60
1450 - 4	19.08.81	409 - 506	766 - 863	-	101.9 ± 0.15 106.7 ± 0.24
1450 - 5	8.09.81	409 - 506	766 - 863	11.0 ± 0.1 9.2 ± 0.1	102.1 ± 0.68 95.5 ± 0.85
1450 - 6	9.09.81	4 - 506	361 - 863	178.2 ± 0.8 198.3 ± 0.2	125.6 ± 1.02 103.4 ± 0.71
1450 - 7	16.09.81	4 - 506	361 - 863	209.1 ± 2.8 212.2 ± 1.0	111.2 ± 1.31 104.3 ± 0.92
1450 - 8	21.09.81	4 - 506	361 - 863	182.2 ± 1.5 183.7 ± 0.5	122.5 ± 0.96 120.9 ± 0.36
1450 - 9	6.10.81	4 - 506	361 - 863	170.6 ± 0.7 173.2 ± 0.8	120.1 ± 0.63 109.6 ± 0.91
1470 - 83	3.10.83	100 - 505	457 - 862	99.0 ± 0.3 88.2 ± 0.3	131.3 ± 0.8 141.3 ± 0.8
1475 - 83	19.10.83	100 - 505	457 - 862	125.3 ± 0.6	119.6 ± 0.9 119.3 ± 1.3
1480 - 83	5.11.83	100 - 505	457 - 862	195.2 ± 1.1 200.8 ± 1.2	103.9 ± 0.8 103.2 ± 1.2
1500 - 84	11.01.84	100 - 505	457 - 862	253.1 ± 1.3 242.1 ± 1.5	155.3 ± 2.5 151.3 ± 0.7
1505 - 84	8.02.84	100 - 505	457 - 862	763.6 ± 5.7 609.1 ± 4.5	116.5 ± 0.41 103.5 ± 3.78
Borehole V2					
	14.02.78	0 - 22	416 - 432	360.0	-
	14.02.78	332 - 359	742 - 769	-	-
	14.02.78	376 - 471	786 - 881	560.0	40.0
	16.05.79	401 - 428	811 - 838	810.0	56.0
1453 - 1	11.06.81	356 - 470	766 - 880	224.8 ± 2.0	-
1453 - 2	19.11.81	356 - 471	766 - 881	500.7 ± 0.6	56.6 ± 0.53 56.9 ± 0.66
1453 - 3	22.04.82	6 - 822	416 -1232	471.9 ± 0.5 453.8 ± 0.5	
1460	24.11.82	406 - 410	816 - 920	440.0 ± 0.3 501.0 ± 0.4	71.7 ± 0.41 85.8 ± 0.49
1461	13.12.82	413 - 417	823 - 827	388.0 ± 1.0 434.0 ± 1.0	44.1 ± 0.34 45.9 ± 0.35
1462	19.01.83	490 - 494	900 - 904	574.0 ± 1.0 418.0 ± 1.0	31.2 ± 0.27 33.5 ± 0.29
1463	25.02.83	549 - 553	959 - 963	713.0 ± 1.0 731.0 ± 0.6	42.1 ± 0.33 43.4 ± 0.34
1490 - 83	28.11.83	423 - 499	833 - 909	497.4 ± 4.5 618.5 ± 4.9	45.7 ± 0.3 48.2 ± 0.41
1495 - 83	29.11.83	562 - 822	872 -1232	185.0 ± 2.7 115.3 ± 1.8	56.4 ± 0.8 64.3 ± 0.4
1525 - 84	28.02.84	500 - 461	910 - 971	492.1 ± 2.6 527.9 ± 2.9	75.6 ± 0.35 71.6 ± 0.52
1530 - 84	28.02.84	382 - 423	792 - 833	283.7 ± 2.1 556.7 ± 3.5	96.8 ± 0.46 79.6 ± 0.56

contact with the fracture fluids. The highest ^{222}Rn contents were found in the M3 borehole and this would be consistent with the deposition of uranium in the fracture porosity in the shallower part of the system as suggested in Section 10.2. As only uranium is mobilised by groundwater and ^{230}Th (half-life 80,000 years) requires a long time, such uranium deposition must have occurred naturally before the hydraulic sink was formed by mining operations. Alternatively, as U solution by the shallow groundwaters must also dissolve ^{230}Th, this nuclide may have been transported to depth after adsorption on colloidal matter. The deposition of U on fracture walls is unlikely to be revealed by U-analyses on bulk rock samples.

10.3.3 ^{226}Ra contents of Stripa groundwaters

The ^{226}Ra contents of the Stripa groundwaters (Table 10-8) generally increase with depth to a maximum value between 50-100 pCi kg^{-1} for V2 and up to 150 pCi kg^{-1} for V1. The recent shallow groundwaters all have ^{226}Ra contents <1 pCi kg^{-1} and contents from 2 - 12 pCi kg^{-1} are present in M3, E1 and N1.

As discussed in Section 10.3, ^{226}Ra solution may be strongly influenced by α-recoil following ^{230}Th decay at the rock-water interface. The ^{222}Rn content of the minewaters shows that much ^{226}Ra must also be present at this interface and that it must (for M3) be at least at 50% of equilibrium with the U content of the matrix. It is not possible for ^{226}Ra solution to proceed to the same extent as ^{222}Rn solution since ^{226}Ra would become depleted in the rock surface and it would then be impossible to maintain the ^{222}Rn content of a flowing groundwater. The ratio $^{226}Ra/^{222}Rn$ increases in the sequence: M3 < N1 < V2 < V1, and the values range from 3×10^{-6} (M3) to 2×10^{-4} (V1). These very low ratios suggest that diffusion out of uraninite is a much more significant solution mechanism for ^{222}Rn than direct α-recoil, and this is consistent with the known porosity of uraninite in microfractures to the aqueous phase. In contrast, diffusion of ^{226}Ra is a very slow process and α-recoil must be much more significant. The amount of ^{226}Ra present, however, is greater than that which the ^{230}Th recoil rate (Section 10.2.4) would indicate and it is likely that geochemical factors also influence ^{226}Ra solution.

Barium contents of the Stripa minewaters average about 0.03 mg/l and slight variations from this do not correlate with ^{226}Ra content variations. There is no general correlation between ^{226}Ra content and the Ca-content of the minewaters. Within borehole V2, however, both the Ca^{++} and Ra^{++} contents for water from the 406-410 m interval are approximately 50% higher than those for the 356-470 m interval. In borehole V1, the groundwaters have simi-

lar Ca++ contents to the 406-410 m interval in V2 but the ^{226}Ra-contents are significantly greater than in the latter zone.

The ^{226}Ra content of the waters appears to be specific for particular fracture zones but does not generally correlate with either Ca++ or Ba++ contents.

11 ATMOSPHERIC AND RADIOGENIC GASES IN SOLUTION

11.1 Atmosphere derived gases

A groundwater dissolved atmospheric gases in the unsaturated zone according to Henry's law from which it may be shown that:

$$V_{STP} = K\ P$$

where V_{STP} is the volume of gas dissolved (measured at STP), P is the partial pressure of the gas and K is the Bunsen coefficient for the dissolved gas. The value of the constant, K, varies with temperature, so that the volume of any gas in solution is determined by its partial pressure in the atmosphere and the temperature of equilibration of the groundwater with air. Since the annual average of atmospheric pressure is almost constant, the average temperature during the recharge season is the only other factor which can influence gas solubility. The solubility relationship with temperature for atmospheric gases has been well-established (Morrison and Johnstone, 1954; Benson and Krause, 1976) and it is possible to determine the temperature during recharge from measurements of the amounts of dissolved gases in a groundwater. For example, the recharge temperatures for some palaeo-groundwaters have been related to the palaeo-climatic record by determination of their inert gas contents (Andrews and Lee, 1979).

11.2 Radiogenic helium

The atmospheric gases which were dissolved at groundwater recharge are supplemented by solution of radiogenic gases in the confined zone of the aquifer. The most significant radiogenic gas is ^4He, produced by α-decay of the radioelements uranium and thorium and their daughter nuclides. The amount of dissolved radiogenic ^4He has been shown to increase with groundwater age (Andrews and Lee, 1979; Marine, 1979; Heaton and Vogel, 1981). For an aquifer of porosity, ϕ, in which all the radiogenic ^4He dissolves in the water, the ^4He-content of the water after t years is given by the equation:

$$[He]_t = \rho\phi^{-1}t(1.19 \times 10^{-13}[U] + 2.88 \times 10^{-14}[Th])cm^3STP/cm^3\ H_2O \qquad (11.2)$$

where ρ is the bulk density, g/cm^3; $[U]\mu g/g$ is the natural uranium content and $[Th]$ $\mu g/g$ is the natural thorium content of the rock.

The neutron-induced reaction $^{6}Li(n,\alpha)^{3}H$ followed by decay of ^{3}H produces ^{3}He at very low rates in geological formations. It may be shown that the $^{3}He/^{4}He$ ratio for radiogenic helium is primarily dependent upon the lithium content of the rock and is characteristic of the formation (Andrews, 1983). It is, therefore, possible to use measurements of the $^{3}He/^{4}He$ ratio to determine whether the radiogenic helium in a groundwater is characteristic of the aquifer or has diffused into it from other formations. Changes in the $^{3}He/^{4}He$ ratio as atmospherically derived helium mixes with radiogenic helium may also enable groundwater ages up to about 10^{5} years to be determined for aquifers in which there is no ingress of helium from adjacent formations.

11.3 Radiogenic argon

The $^{40}Ar/^{36}Ar$ isotopic ratio for atmospheric Ar is 295.5. Decay of ^{40}K by K-electron capture in potassic minerals of a rock matrix can provide an additional source of ^{40}Ar which on mixing with dissolved atmospheric Ar can increase its $^{40}Ar/^{36}Ar$ ratio. Alternative mechanisms which enable radiogenic ^{40}Ar to enter solution are:

a) direct ^{40}K decay along rock surfaces in contact with the groundwater. This is unlikely to be a significant cause of ^{40}K generation in times less than 10 million years since considerable ^{40}Ar must be formed by decay to influence the $^{40}Ar/^{36}Ar$ ratio of the relatively large amount of dissolved atmospheric argon.

b) Leakage of radiogenic ^{40}Ar stored in the minerals of the rock (feldspars and micas). Diffusive leakage of ^{40}Ar from these minerals would be aided by elevated temperatures at depth and long groundwater residence times.

It is difficult to estimate the time required for such diffusive argon loss from the rock minerals. The argon diffusion coefficients for ^{40}Ar very over some orders of magnitude for feldspars and are very dependent upon the extent of crystal imperfections and impurities. Argon diffusion is also very temperature-dependent, the rate increasing by a factor of 10^{4} for a 100°C temperature rise. If the maximum temperature encountered by a thermal water in a feldspar dominated system was 200°C, the time required for a 1% argon loss is 10^{7} years using the data of Dalrymple and Lanphere (1969).

11.4 Biogenic gases

Carbon dioxide is first dissolved by a groundwater in the soil zone by equilibration with the soil air in which the partial pressure of CO_2 is enhanced by biological activity. With subsequent groundwater evolution, dissolved CO_2 is controlled by pH and the CO_3^{2-}, HCO_3^-, CO_2 equilibria.

Reduction and thermo-degradation of organic matter can produce significant amounts of dissolved hydrocarbons, particularly CH_4, in deeply circulating, reducing or thermal groundwaters. The amounts of CO_2 and CH_4 present can have a significant influence on the gas solubility in groundwaters and on de-gassing processes.

11.5 Analytical methods

11.5.1 Sampling for inert gas analyses

For inert gas analyses, it is important to adopt procedures which retain the gases in the same state as in the formation. The amounts of gases in solution at formation pressures generally exceed those resulting from air-equilibration at recharge due to (i) solution of entrained air at increased hydrostatic pressures (excess air), (ii) radiogenic gas solution in the formation (He, Ar), and (iii) solution of biogenic gases (CH_4, CO_2) or nitrogen formed by biodegradation. An artersian well which is allowed to flow naturally, is depressurised to atmospheric pressure at the surface. At this pressure the water is supersaturated and gases must be evolved. Degassing occurs in the well to a depth such that the hydrostatic pressure is sufficient to prevent it. This depth depends upon the extent of excess air and additional gases dissolved in the formation and upon the temperature. If the water is to be sampled without gas loss, it must be kept under a pressure corresponding to this minimum depth which prevents degassing. This requires the adoption of either down hole sampling or the pressurisation of the well head.

Down-hole sampling must be carried out at a depth greater than that required to prevent degassing. In this procedure the sample is isolated between automatic shut-off valves once the sampling depth is reached. It is important to ensure that there was adequate flow through the sample tube before these valves are operated. For a pressurised well-head, which is the method adopted in this work, the procedure needs to be carefully controlled to avoid de-pressurisation of the well and to ensure that it is adequately flushed following pressurisation. This requires a complete flushing to a depth at least equal to the degassing depth. Figure 11-1 shows the necessary well head arrangements. Valve A is

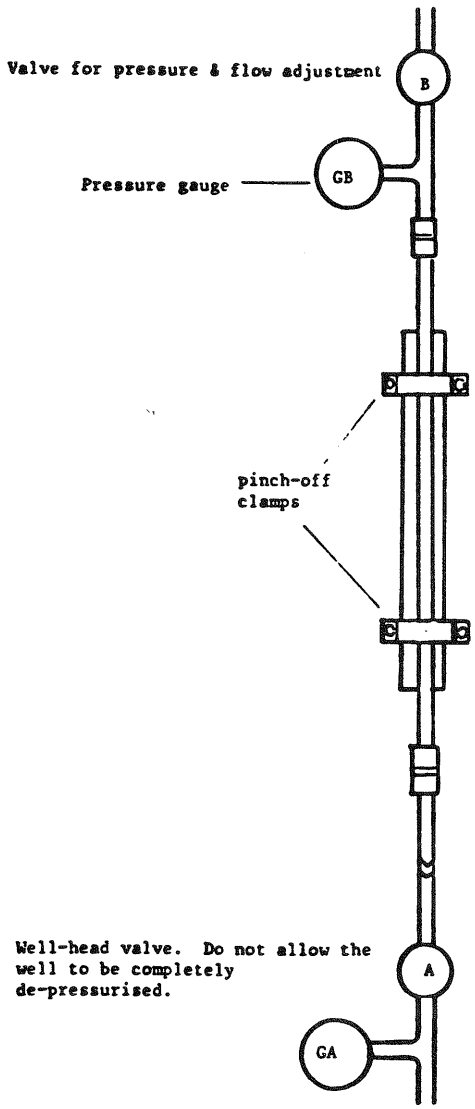

Figure 11-1. Arrangement for sampling groundwater under artesian pressure for dissolved gas analysis.

placed directly on the well head and the pressure of gauge GA adjusted to a minimum pressure equal to the degassing pressure. The well should then be allowed to flow at this pressure to remove water from the degassed zone before sampling. The sampling apparatus consisting of a copper tube with pinch-off clamps, pressure guage GB and valve B is then attached and adjusted to obtain the desired sampling pressure. After adequate flushing at this pressure, the sample is isolated between the pinch-off clamps.

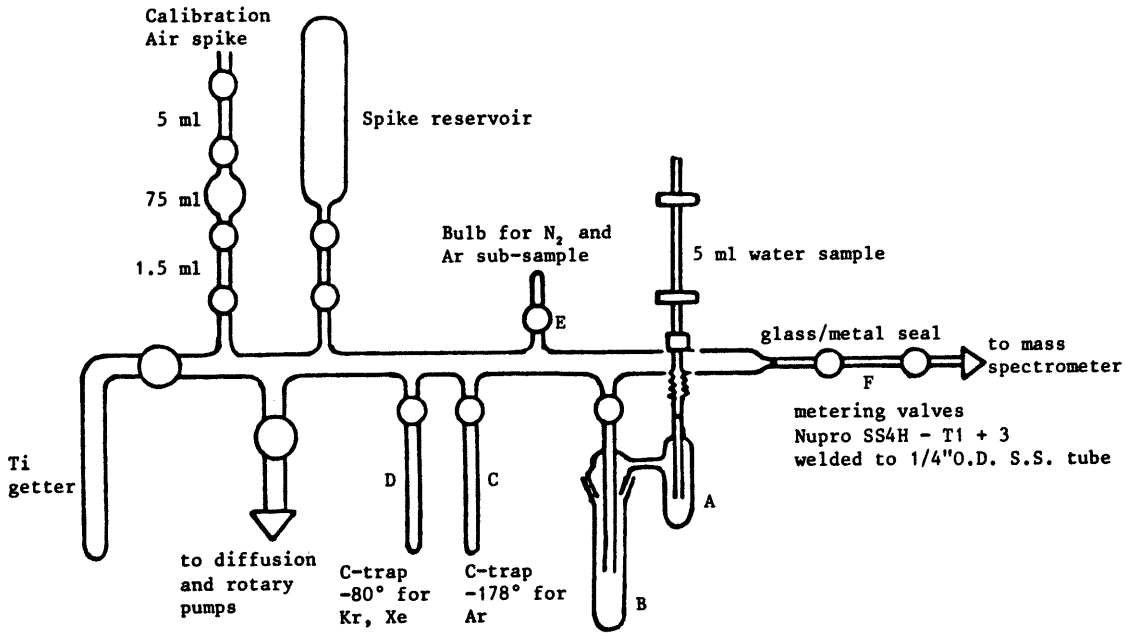

Figure 11-2. Gas extraction line for dissolved inert gas analysis.

11.5.2 Isotope dilution analysis of dissolved inert gases

Samples were initially collected in 1 cm^3 glass sample tubes, isolated between vacuum stopcocks. Later in the programme, samples were collected in 5 cm^3 annealed copper tubes, being isolated between pinch-off clamps which effected a vacuum-tight cold weld of the copper tube. In either case, the fluid was caused to flow through the sample tube to flush it completely free of air.

For analysis, the tube containing the groundwater sample was attached to the gas extraction line (Figure 11-2) with an O-ring seal and the system was then evacuated to better than 10^{-5} mb. A metered volume of isotopically enriched tracers for the inert gases was then admitted to the vacuum system, followed by the water sample. The water was vaporised by warming trap A and the water vapor excluded from the remainder of the system by cooling Trap B with solid CO_2/ethanol. A sub-sample for N_2 and Ar analysis was trapped in bulb E. Nitrogen (and any oxygen) were then removed from the main sample on a titanium getter at 800-900°C. The heavy inert gases, Kr and Xe were then adsorbed on a charcoal trap (D) at -78°C and after this Ar was adsorbed on a second charcoal trap (C) at -196°C. The remaining gases, He and Ne, were then admitted to a 5 cm radium, 180° magnetic deflection mass spectrometer (Kratos, MSIOS) for isotope ratio analysis. After measurement, residual He and Ne in the extraction line was pump-

ed away and the Ar/N_2 sub-sample was admitted for isotope ratio analysis. Residual gases were again pumped from the extraction line and Kr + Xe were then desorbed from trap D by heating it to 200°C. The isotope ratios of these gases were then determined in the mass spectrometer.

The volumes of the inert gases released from the water sample were calculated from the volume of tracer admitted and the change in its isotopic ratios after mixing with the released gases, using the standard relationships for isotopic dilution analysis. The Ne content of water equilibrated with air at 0°C is $2.3 \cdot 10^{-7}$ cm^3 STP/cm^3 H_2O and this is the maximum dissolved Ne content which a groundwater may contain since 0°C is the minimum possible recharge temperature. Samples which contained Ne in excess of this value were considered to contain entrained air in the form of microscopic bubbles. In such cases the inert-gas contents were corrected by subtracting the Ne, Ar, Kr and Xe contents of small volumes of air until as close as possible agreement was obtained between the air equilibration temperatures indicated by the corrected contents of these gases. Since the solubility temperature coefficients for these inert gases are different, this procedure leads to a unique solution for the dissolved inert gases in the sample. The equilibration temperature derived in this way is termed the ´recharge temperature´ of the groundwater.

11.6 Radiogenic helium

All of the Stripa minewaters contain large amounts of radiogenic ^4He (Table 11-1). The groundwater ^4He content generally increases with depth in the granite (Figure 11-3) and the shape of this concentration/depth profile is very similar to those calculated for diffusive loss ^4He from ^4He generating rock with one surface open to the atmosphere (Figure 11-4). This suggests that the ^4He content of the water is due to diffusive equilibration between the rock and water phases. The amount of ^4He generated within a rock of age t years is given by:

$$[He]_{rock} = \rho t \{1.19 \times 10^{-13}[U]_r + 2.88 \times 10^{-14}[Th]_r\} \text{ cm}^3 \text{ STP/cm}^3 \text{ rock} \quad (11.3)$$

The time required to generate the ^4He concentrations observed in the V1/V2 groundwaters for the radioelement contents typical of the Stripa granite is about 200 Ma which may be compared with the pre-Cambrian age of the granite. It is apparent that either the groundwater has not totally equilibrated with the granite or that He has been lost from the rock matrix because of prolonged groundwater flow or by diffusion processes.

The diffusion distance from rock matrix to the water phase in the fracture system is so small that the fracture residence

Table 11-1. Inert gas contents of Stripa Groundwaters (cm^3 STP/cm^3)

Analysis number	Sampling date	Depth interval, m	$^4He \times 10^8$	$Ne \times 10^7$	$Ar \times 10^4$	$Kr \times 10^8$	$Xe \times 10^8$	Estimated Recharge Temperature
Borehole M3								
1452 - 1	12.01.81		20187	2.77	3.71	1.03	-	
			23194	2.69	2.01	-	-	
1452 - 2	4.06.81		81967	6.30	7.90	15.15	1.52	0
			62004	4.85	8.59	17.96	1.91	2.1
			32659	3.24	6.08	13.27	1.48	
			24479	8.28	7.48	17.54	1.87	
1485 - 83	9.11.83		69301	3.84	6.08	12.88	1.83	1.9 - 2.5
			67113	3.56	5.72	12.14	1.67	3.5 - 4.8
1520 - 84	23.02.84		37727	3.46	6.32	12.52	1.74	2.2 - 3.6
			38180	3.78	6.63	13.31	1.79	0.7 - 3.1
			38890	3.58	6.28	13.04	1.64	1.2 - 5.3
						Average (M3)		2.6 ± 1.5
Borehole E1								
1455 - 1	11.11.81	3 - 300	10208	8.87	9.69	-	1.89	5.3
			10759	8.65	9.41	16.62	1.92	4.6
			5488	6.20	7.83	15.54	1.96	2.2
1455 - 2	24.03.82	127 - 130	5281	2.85	5.29	11.73	1.24	3.4
			4374	2.80	5.36	12.01	1.36	2.5
			6780	2.85	5.33	11.43	1.32	4.2
1535 - 84	6.03.84	3 - 300	22451	6.30	7.10	13.92	1.64	3.3
			15297	8.48	8.27	15.23	1.73	3.4
			14730	3.01	5.48	18.44	1.60	5.5
			14236	3.14	5.40	11.80	1.59	3.7 - 5.8
						Average (E1)		4.0 ± 1.1
Borehole N1								
1454 - 1	14.07.81	2 - 300	93614	4.36	6.79	13.06	1.83	2.3 - 2.9
			25267	4.13	6.27	11.89	1.31	
1454 - 2	19.08.81	3 - 300	60917	3.16	5.89	11.47	1.84	1.9 - 4.7
			28679	4.42	6.89	13.45	1.54	1.5 - 7.9
			15923	3.70	6.09	20.71	1.73	3.9
1545 - 84	7.03.84	252 - 300	33223	4.23	7.22	14.35	1.74	4.2
			32221	4.09	7.38	14.15	1.74	4.0
			32434	4.35	7.37	12.31	1.75	4.1 - 4.4
1540 - 84	13.03.84	152 - 251	29104	3.87	6.85	12.84	1.71	2.2 - 4.4
			28361	3.75	6.71	12.78	1.73	2.0 - 4.0
						Average (N1)		3.6 ± 1.5
Borehole V1								
1450 - 1	16.01.81		21987	11.07	9.78	1.33	-	
			21107	11.03	9.20	1.98	0.71	
1450 - 2	4.06.81		387403	5.84	8.91	15.39	2.29	
			335867	2.72	8.60	14.56	1.58	
			103122	3.23	8.62	14.37	3.70	
1450 - 3	14.07.81	409 - 506	168088	3.30	7.86	13.81	1.70	
			133352	2.88	6.96	11.69	1.27	
			91911	3.50	6.00	11.35	1.70	4.3 - 5.7
1450 - 4	19.08.81	409 - 506	371585	4.00	8.33	30.94	-	
			160718	3.40	7.58	12.72	1.81	1.6 - 2.5
			145270	8.19	7.85	37.52	1.66	
1450 - 5	8.09.81	409 - 506	299428	-	8.92	27.00	2.06	
			297042	1.80	8.16	15.64	1.89	
			238288	-	7.68	14.78	1.94	
1450 - 6	9.09.81	4 - 506	89037	6.07	7.74	14.38	1.87	1.6 - 3.5
			168948	-	7.07	13.33	1.77	
			154143	3.38	7.20	14.97	1.46	
			93301	3.22	6.72	11.79	1.66	3.9 - 4.7
1450 - 7	16.09.81	4 - 506	88849	2.71	7.17	13.82	1.79	2.3
			107998	3.10	7.63	14.27	1.79	2.7
			108318	2.66	7.04	14.57	1.63	4.8

Table 11-1. Cont'd.

Analysis number	Sampling date	Depth interval, m	$^4He \times 10^8$	$Ne \times 10^7$	$Ar \times 10^4$	$Kr \times 10^8$	$Xe \times 10^8$	Estimated Recharge Temperature
1450 - 8	21.09.81	4 - 506	96958	3.14	7.40	17.98	1.81	2.3
			111139	2.82	7.12	-	-	
			107574	4.46	8.18	15.43	1.80	3.4
1470 - 83	3.10.83	100 - 505	174350	5.40	7.80	13.61	1.87	2.6 - 3.0
1475 - 83	19.10.83	100 - 505	386026	5.20	7.32	12.43	1.91	2.3 - 5.6
			180658	4.40	7.81	13.13	1.97	0.9 - 2.2
			165920	4.93	8.21	13.80	1.79	1.3 - 3.9
1480 - 83	5.11.83	100 - 505	332374	4.02	7.43	13.18	1.81	1.4 - 2.9
			355070	3.97	7.56	13.29	1.87	1.1 - 2.0
1500 - 84	11.01.84	100 - 505	188887	4.63	8.29	14.55	1.85	2.7
			186824	3.89	8.25	14.52	1.89	1.7
1505 - 84	8.02.84	100 - 505	436887	4.90	8.98	13.99	1.85	0.8 - 2.9
			215006	3.99	7.98	13.34	1.81	1.0 - 2.9
						Average (V1)		2.7 ± 1.3
Borehole V2								
1453 - 1	11.06.81	356 - 471	288818	-	-	-	-	
			257024	-	-	-	-	
			171585	4.31	8.10	13.21	1.88	1.8 - 2.1
			154769	5.76	9.13	13.77	1.71	2.8 - 5.9
			145127	3.83	6.65	-	1.32	
1453 - 2	19.11.81	356 - 471	148241	10.30	10.00	15.85	0.95	
			138565	10.57	9.86	15.54	1.04	
1453 - 3	27.04.82	6 - 822	115410	3.46	6.86	13.32	1.37	0.3
			112454	3.54	7.06	12.63	1.44	2.2
			92278	3.04	6.61	12.35	1.44	1.9
1460	24.11.82	406 - 410	261812	-	8.15	13.77	1.80	
			301004	-	9.14	14.70	1.73	
1461	13.12.82	413 - 417	89740	-	7.25	13.58	1.87	
			104448	-	7.0	12.78	1.75	
1462	19.01.83	490 - 494	223224	-	7.87	13.79	1.79	
			322474	-	7.97	13.41	1.76	
1463	25.02.83	549 - 553	59603	-	3.68	8.01	1.25	
1490 - 83	29.11.83	424 - 499	242680	4.25	7.25	11.19	1.90	1.8
			273270	4.25	7.29	10.82	1.91	1.7
			315015	3.86	7.43	13.48	1.80	0.4 - 2.9
			367993	7.18	8.56	14.37	1.86	3.6 - 4.5
1525 - 84	28.02.84	500 - 561	184450	4.12	7.95	12.67	1.77	3.0 - 3.6
			187679	3.85	7.93	12.91	1.78	1.8 - 3.3
			174819	3.89	7.49	13.89	1.64	5.6
1530 - 84	28.02.84	382 - 423	159697	4.17	8.58	13.90	1.89	1.9
						Average (V2)		2.7 ± 1.5

Notes

1. The analytical data without any corrections are tabulated. The recharge temperatures were estimated from Ne/Kr and Ne/Xe temperature matches where possible.

2. From sample 1460 (November, 1982) onwards, all samples were collected in crimped copper tubes. Earlier samples were collected in glass tubes.

times needed to establish concentration equilibrium between the water and rock, are short. The ^4He flux from a uniform rock matrix which loses He at one surface is given by (Andrews, 1984):

$$F = 2G\left(\frac{Dt}{\pi}\right)^{1/2} \qquad (11.4)$$

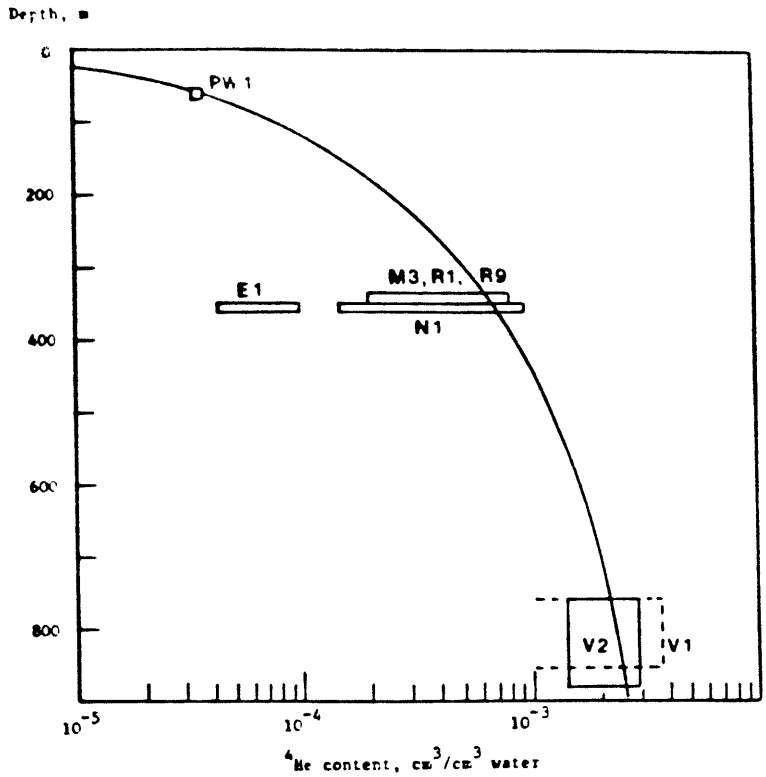

Figure 11-3. The variation of the ^{4}He content of Stripa groundwaters with depth.

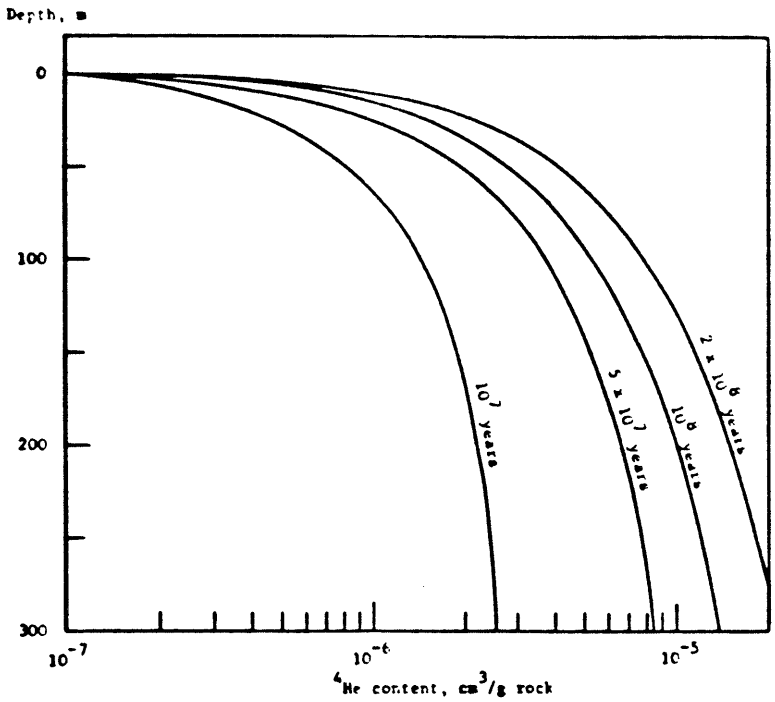

Figure 11-4. The dependence of the radiogenic ^{4}He content on depth and age of rock. (for U = 1.5 ppm, Th = 4.5 ppm and diffusion coefficient = 3.16×10^{-3} m^2a^{-1}.

Table 11-2. $^{3}He/^{4}He$ Ratios of dissolved helium in Stripa groundwaters.

Borehole	Sampling date	$^{3}He/^{4}He$
V1	15.07.81	$5.58 \pm 0.50 \times 10^{-9}$
V1	"	$5.29 \pm 0.53 \times 10^{-9}$
V1	"	$6.28 \pm 0.62 \times 10^{-9}$
	average	$5.72 \pm 0.42 \times 10^{-9}$

where G is the generation rate of He by radioelement decay within the rock, D is the diffusion coefficient for He in the matrix and t is the age of the rock. If this flux of He is dissolved by groundwater within fractures, then the time for the fracture fluid to attain the observed He concentrations may be estimated. This time is dependent upon the values adopted for the diffusion coefficient and for the fracture width but for groundwater movement in 0.1 mm fractures in the Stripa granite, application of equation 11.4 suggests that the maximum observed He-contents in V1 and V2 would require rock-equilibration times of about 150 years. The low He contents found in E1 could diffuse from the rock matrix within 10 years. The E1 borehole has an anomalously low ^{4}He content in its groundwater and this suggests that there is a rapid flow of water from shallower depths in this locality. The high ^{3}H content of this water also suggests that it is of recent origin.

The $^{3}He/^{4}He$ ratio of radiogenic He is principally determined by the Li-content of the rock matrix (Andrews, 1984). The observed $^{3}He/^{4}He$ ratio of dissolved He (Table 11-2) requires a Li-content of 11 ppm in the Stripa granite, on the assumption that the He is entirely radiogenic. This value may be compared with the average analytical Li-content of 8 ppm (Table 2-3).

11.7 $^{40}Ar/^{36}Ar$ ratios

Argon of atmospheric origin has an $^{40}Ar/^{36}Ar$ ratio of 295.5. The waters from borehole E1 clearly contain atmospheric argon and the M3 and N1 waters have only slightly enhanced $^{40}Ar/^{36}Ar$ ratios (Table 11-3). The added radiogenic ^{40}Ar is about 3% of their atmospheric ^{40}Ar content. The $^{40}Ar/^{36}Ar$ ratios for dissolved argon in the V1 and V2 groundwaters are greater than the at-

Table 11-3. $^{40}Ar/^{36}Ar$ ratios of dissolved argon in Stripa groundwaters.

Analysis number	Sampling date	Depth interval, m	$^{40}Ar/^{36}Ar$
Borehole M3			
1485 - 83	9.11.83	0 - 9	301.6 ± 4.4
1520 - 84	23.02.84	0 - 9	316.3 ± 0.5
Borehole E1			
1535 - 84	6.03.84	3 - 300	298.3 ± 3.3
			294.3 ± 0.5
Borehole N1			
1545 - 84 I	7.03.84	252 - 300	305.2 ± 3.7
1540 - 84 II	13.03.84	151 - 251	304.1 ± 3.9
Borehole V1			
1480 - 83	5.11.83	100 - 505	342.6 ± 1.7
1500 - 84	11.01.84	100 - 505	371.5 ± 3.4
			353.1 ± 3.1
1505 - 84	8.02.84	100 - 505	368.1 ± 2.8
Borehole V2			
1460 a	24.11.82		346.8 ± 1.6
1462 c	19.01.83		341.0 ± 1.8
1525 - 84	28.02.84	500 - 561	336.2 ± 1.8

mospheric ratio and correspond to the addition of up to 25% of radiogenic argon. However, diffusive loss of ^{40}Ar from feldspars and micas is generally very slow and at the prevailing ground temperatures would require several million years to proceed to a significant extent. Therefore, mineral alteration would release ^{40}Ar and such Ar-release might be proportional to groundwater salinity. The Cl^- contents of V1 and V2 are approximately 10 times those of M3 and N1, and suggest that the ^{40}Ar release is due to mineral alteration by the migrating fracture fluids. As ^{40}Ar is

produced by ^{40}K decay in the micas and feldspars of the matrix, the release of ^{40}Ar into the groundwaters suggests active alteration of feldspars at depths of at least 1 km. The V1 and V2 groundwaters have enhanced ^{40}Ar contents and higher salinities than those from M3 and N1, suggesting that the former groundwaters have been produced by a longer period of chemical alteration of the granite.

11.8 Recharge temperatures

The inert gas contents of the Stripa groundwaters are reported in Table 11-1. The agreement between replicates is normally better than $\pm 5\%$ for such analyses but much larger variations are observed in the Stripa groundwaters. These variations are attributed to the difficulty of obtaining samples for which the boreholes had been adequately pressurised beforehand. All of the samples have Ne-contents which indicate the presence of considerable amounts of excess air. This may be due to the entrainment of air with the groundwater during recharge or could be caused by sample outgassing in the borehole and consequent incorporation of released gases in the sample.

For the estimation of recharge temperatures, the measured Ar-contents were first corrected for the presence of radiogenic ^{40}Ar as indicated by the $^{40}Ar/^{36}Ar$ ratio determined in other samples from the particular borehole. Excess air corrections were then made by subtracting aliquots of air until the best match was obtained between the recharge temperatures indicated by Ne, Kr and Xe. Normally, the match between Ne and Ar temperatures is the best recharge temperature indicator, but in all cases the Ar contents, even after correction for radiogenic ^{40}Ar, indicated negative recharge temperatures. This suggests that the excess gases present are exsolved gases rather than excess air; which would cause over-correction of Ne contents and undercorrection of Ar contents for recharge temperature estimation. The large ^{4}He contents of the waters also made Ne analysis more difficult, which also effects the precision with which recharge temperatures can be estimated.

The average recharge temperatures for the water from boreholes V1, V2 and M3 are indistinguishable at about $2.6 \pm 1.5^{o}C$ (Table 11-1). For the samples from boreholes N1 and E1, average recharge temperatures are $3.6 \pm 1.5^{o}C$ and $4.0 \pm 1.1^{o}C$ respectively. This trend reflects the changes in the stable isotope composition of the groundwaters.

11.9 N_2/Ar ratios

The N_2/Ar ratio for dissolved gases in a groundwater which has been equilibrated with air is 37.70 for 10°C equilibration and 37.33 for 5°C equilibration. The atmospheric N_2/Ar ratio is 83.54. The N_2/Ar ratios for all of the minewaters are greater than the expected air-equilibration value and indicate that excess air has been incorporated in all of them. The ratio of the total dissolved Ne to the volume of Ne due to air-equilibration has been used as a contamination index. This index was evaluated for samples which were analysed for inert gas contents. The value of the contamination index required to produce the observed N_2/Ar ratio, is compared with the observed values from inert gas analyses in Table 11-4. The high N_2/Ar ratios confirm that

Table 11-4. N_2/Ar ratios of dissolved gases in Stripa groundwaters.

Analysis number	Sampling date	Depth interval, m	N_2/Ar ratio	Contamination Index A	Contamination Index B
Borehole M3					
1485 - 83	9.11.83		55.8	3.40	1.63 - 1.72
1520 - 84	23.02.84		49.0	2.20	1.56 - 1.68
			51.5	2.59	1.56 - 1.68
Borehole E1					
1535 - 84D	6.03.84	3 - 300	48.3	2.10	1.40 - 3.93
1535 - 84E	6.03.84	3 - 300	55.8	3.40	1.40 - 3.93
			53.7	2.97	1.40 - 3.93
Borehole N1					
1540 - 84 II	13.03.84	151 - 251	61.6	5.01	1.69 - 1.75
			57.5	3.80	1.69 - 1.75
1545 - 84 I	7.03.84	252 - 300	59.1	4.22	1.87 - 2.00
			56.9	3.65	1.87 - 2.00
Borehole V1					
1480 - 83	5.11.83	100 - 505	55.6	3.36	1.76 - 1.79
1500 - 84D	11.01.84	100 - 505	47.5	1.99	1.73 - 2.08
			44.7	1.66	1.73 - 2.08
1500 - 84E	11.01.84	100 - 505	50.6	2.44	1.73 - 2.08
			52.8	2.81	1.73 - 2.08
1505 - 84	8.02.84	100 - 505	44.9	1.69	1.80 - 2.18
			46.4	1.86	1.80 - 2.18
Borehole V2					
1525 - 84	28.02.84	500 - 561	41.7	1.35	1.73 - 1.86
			43.0	1.48	1.73 - 1.86

A. To correct N_2/Ar ratio to 37.7 (10°C air equilibration).

B. Observed range for inert gas analyses.

either there is generally excess air entrainment at recharge or that the samples generally contain exsolved gases. There are no N_2/Ar ratios greater than the atmospheric ratio, which would indicate the presence of nitrogen due to degradation of organic matter.

11.10 $^{15}N/^{14}N$ ratios

Seven groundwater samples were collected from boreholes N1, V2, and M3 for isotopic determination of $^{15}N/^{14}N$ ratio at the U.S. Geological Survey. The $\delta^{15}N$ values (relative to air) are given in Table 11-5. These values are identical to atmospheric values for the expected uncertainty in the analyses. Hence, the dissolved nitrogen in the Stripa groundwaters appears to be atmospheric in origin, and there is no clear indication of nitrogenous organic matter being decomposed from these determinations.

Table 11-5. Stable nitrogen isotopes from nitrogen gas extracted from Stripa groundwaters.

Borehole	Interval (m)	$\delta^{15}N$ AIR
N1820830	123-125	-0.15 °/oo
N1820907	203-205	-0.05 °/oo
N1820914	217.1-273.1	-0.35 °/oo
V2820928	4-822	+0.10 °/oo
V2820928	4-822	0.00 °/oo
M3830407	3-10	-0.30 °/oo
M3830407	3-10	-0.25 °/oo

12 CONCLUSIONS

Several important conclusions can be summarized from the investigations carried out during Phase I:

A. Apparent hydraulic connections have been demonstrated between V1 and V2 boreholes and between N1 borehole and the inner part of the Buffer Mass Test area. There is no apparent hydraulic connection between V1 or V2 and N1; neither is there any apparent connection between E1 and N1. The groundwater chemistry between V1 and V2 is very similar, supporting the hydraulic connection. However, the ion ratios of N1 are also very similar to V1 and V2. This suggests that the same geochemical processes are occurring in different parts of the groundwater system regardless of the connectivity of flow paths. In other words, water-rock interactions are general patterns that are not affected by flow path except to control the total amount of dissolved solids. This concept is consistent with the suggestion that geochemical processes are largely governed by processes internal to the bedrock rather than imposed by external sources of solutes.

B. The groundwater chemistry and the total dissolved solids cannot be accounted for by unmodified seawater intrusion. The source of the salt components might be accounted for by residual salts associated with the crystalline bedrock, such as fluid inclusions. Other hypotheses have been considered, such as Holocene seawater intrusion and Permian evaporates transported to this region. If a marine or sedimentary source is postulated for the origin of the dissolved salts, then extreme chemical changes must be invoked to explain the enormous differences in ion ratios between Stripa groundwaters and marine waters. These extreme changes are generally consistent with the high-temperature processes associated with metamorphic reactions whose signature could remain in residual fluid inclusions.

C. The groundwater chemistry and total dissolved solids reflect an irregular increase with depth with distinct heterogeneity in chloride concentrations between water-bearing fracture zones. Although a distinct increase in chloride concentrations occurs below 700 m, the distribution of chloride values is neither gradual nor sharp, but rather irregular.

D. Several water-rock interactions are occurring under present-day conditions, including the dissolution and precipitation of calcite, fluorite, barite, and $Fe(OH)_3$ (ferrihydrite), and the dissolution of feldspars. Carbonate geochemistry, coupled with feldspar dissolution, appears to dominate much of the water chemistry, especially changes in the pH and alkalinity with depth. These processes are likely to be linked to changes in the hydraulic conductivity with depth, and should be generally applicable to other granitic environments in the absence of other influences, such as the intrusion of Holocene (or older) seawater, geothermal activity, and large differences in rock composition and/or hydraulic conductivity profiles.

E. Chemical trends, as expressed by ion ratios, are not unique to Stripa. Other deep groundwaters in Sweden and Finland have very similar ion ratios; some are within Holocene-seawater-intrusion limits, and some are outside. However, whether these groundwaters occur on a large regional scale or not is unknown.

F. Redox processes involving sulfur, iron and carbon species may be important in deep granitic groundwaters. The redox capacity of granitic groundwaters is very low, and may be overwhelmed by introduced radionuclides; nevertheless, evidence does suggest that disequilibrium processes, including sulfate reduction and iron oxidation, are active in certain localized parts of the groundwater system. Iron and sulfide redox species appear to dominate redox processes. Stable isotopes of sulfate and SO_4/Cl ratios suggest that sulfate reduction is more pronounced at intermediate depths and low sulfate concentrations. The stable isotope content of aqueous sulphate is similar to those recorded from sedimentary brines. Further sampling and analysis of iron, sulfur, and carbon species during Phase II investigations will be done to clarify these findings.

G. All groundwaters have a meteoric origin and are unaffected by evaporative, exchange or geothermal processes based on $^{18}O/^{16}O$ and $^{2}H/^{1}H$ data. Deep groundwaters are depleted in the heavy isotopes of H_2O, suggesting that older waters infiltrated under cooler environmental conditions. The lack of correlation between chloride and H_2O stable isotope ratios suggests that the dissolved salts have a different origin than the water itself.

H. The mean residence time of the groundwater based on ^{14}C measurements suggests that the deeper waters are in excess of 20,000 years using the conventional approach; however, several factors could affect these values, such as the presence

of dissolved organic carbon, matrix diffusion, subsurface production, and (least likely) calcite precipitation. Aqueous carbon has a biogenic signature (based on ^{13}C) which could suggest the deep groundwaters infiltrated during an interstadial period or that biological processes are active in the deep groundwaters. The exceptionally low ^{13}C in V2 indicates redox processes. Isotopic signatures of fracture-fill calcite indicates 3 or 4 types of which only those that are modern are similar to those from other Swedish sites, such as Finnsjön and Gideå.

I. High concentrations of tritium at intermediate depths indicate rapid infiltration of meteoric waters. Values of 10-42 T.U. at depths of 330-355 m (in M3, E1, and F2 boreholes) must be due to rapid inflow of surface waters since their residence time is calculated to be less than 60 years. This observation is consistent with the chloride concentration trends in M3 and E1 boreholes; i.e., chloride concentration decreases as tritium concentration increases. The change in these parameters for M3 have occurred in only the last 7 years. The N1 borehole has not yet been affected by the intrusion of young meteoric water because consistently low values of 0.1-0.2 T.U. have been measured, and these values are most likely due to subsurface production or contamination.

J. Values of about 1 T.U. in the deep groundwaters from the V1 and V2 boreholes suggest subsurface production since contamination has been checked and found negligible while young meteoric input seems to be inconsistent with the other isotopic and chemical data. The suggestion of subsurface production is entirely consistent with theoretical calculations and direct measurements of neutron flux in the Stripa granite.

K. The Stripa site is excellent for studying the effect of subsurface production of ^{3}H, ^{14}C, ^{36}Cl and other radioisotopes because the production rate is quite high (300 neutrons/cm^3/yr) or about ten times the average granite. Hence, the Stripa studies can provide some idea of the upper limits of natural radionuclide production for granites.

L. Preliminary ^{36}Cl measurements indicate that it is nearly all produced in the subsurface by neutron flux. Deep groundwaters appear to have significantly less ^{36}Cl than that required for secular equilibrium. It is suggested that these lower values may reflect equilibrium values for the leptite, or alternatively, that chloride with a zero activity infiltrated the bedrock and, during a residence time of less than 200,000 years, acquired the observed values. Further

detailed studies during Phase II should clarify these preliminary findings. Certainly ^{36}Cl promises to be a valuable tool in the elucidation of the origin and evolution of the groundwaters.

M. Uranium concentration and activity ratio measurements in the Stripa groundwaters have shown a general pattern with depth that indicates: oxidizing conditions in the shallow groundwaters (high concentrations and lowactivity ratios), some deposition and effects of α-recoil in the intermediate groundwaters of about 350 m depth (moderately low concentrations and high-activity ratios), and large amounts of uranium deposition (lowest concentrations) with variable activity ratios indicating different degrees of evolution for each flow path in the deep groundwaters. These data again demonstrate that some generalizations can be made assuming evolutionary histories can be related to depth profiles. The data also show little or no mixing between closest neighbor fracture zones, consistent with the chemical data.

N. Although Ra has similar chemical properties to Ba, these two elements do not correlate, and Ra appears to increase with the degree of evolution of the groundwater. A ^{226}Ra recoil-based model suggests residence times of about 8,000 years for V1 groundwater, and about 3,000 years for V2 groundwater. These calculations are not necessarily inconsistent with other radioisotope data, and may simply reflect differences in residence time for each element, as well as uncertain assumptions in the model.

O. Chemical and isotopic composition of the gases have proved valuable in documenting the high production of radiogenic He and Ar, demonstrating rock-water equilibration at depth, indicating diffusive loss of He, indicating an atmospheric origin for non-radiogenic gases, indicating cooler environmental conditions during recharge of deep groundwaters consistent with the ^{18}O and ^{2}H data, and indicating local intrusion of young meteoric water (E1 borehole) consistent with the tritium and chemical data.

P. Finally, it cannot be overemphasized that groundwater age determination based on single-element radioisotope determinations may be entirely misleading for deep groundwaters in crystalline bedrock. In fact, the concept of "groundwater age" may not be meaningful. The results from Stripa indicate that different elements can have different "mean residence times" because they may have different origins and different processes which affect their concentrations during the evolution of the groundwater. The investigations at Stripa

have made considerable progress towards defining what those origins and evolutionary processes are, and how such concepts may be employed towards other investigations in crystalline bedrock.

13 ACKNOWLEDGEMENTS

A program of this scope could not have been possible without the assistance of many individuals who deserve recognition. First and foremost, we are deeply indebted to Hans Carlsson (SKBF/KBS) whose managerial skills and patience allowed a somewhat feisty group of scientists to collaborate on a most exciting and challenging task. We are very appreciative of Henrik Norlander who assisted on the field sampling and who helped to coordinate the scheduling of the various research programs at the Stripa mine.

J.-L. Michelot contributed substantially to the results and interpretations presented in Chapter 7; M. Wolf and M. Forster contributed Sections 9.3 and 9.3.5, respectively. In addition, the following list of individuals are acknowledged for their various contributions to the HAG members and the research at Stripa:

J.W. Ball	- analysis of major and trace elements
J.M. Burchard	- analysis of anions
R.J. Donahoe	- analysis of major and trace elements, preparation and analysis of fluid inclusions
J. Ek	- tabulation of water analyses
A. Frayne	- analysis of uranium-series elements
B.F. Jones	- review of Chapters 4 and 5
J.D. Hem	- review of Chapters 4 and 5
L. Ranhagen	- analysis of major and trace elements
W. Rauert	- isotope analysis and helpful discussions
E. Roedder	- review of Chapters 2, 4 and 5
K. Skagius	- preparation and leaching of granite
W. Stichler	- isotope analysis and helpful discussions
D.O. Whittemore	- analysis of iodide
M.J. Youngman	- analysis of dissolved gases

14 REFERENCES

CHAPTER 1

CARLSSON, L. and OLSSON, T., 1981:
Hydrogeological investigations in boreholes. Summary of defined programs. Stripa Project 81-01, 1-26.

CHAPTER 2

BARKER, F., 1981:
Introduction to special issue on granites and rhyolites: a commentary for the nonspecialist, J. Geophys. Res. 86, 10131-10135.

CARLSSON, L., OLSSON, T. and STEJSKAL, V., 1981: Core-logs of borehole V1 down to 505 m. Stripa Project 81-05, 28 pp.

CARLSSON, L., OLSSON, T. and STEJSKAL, V., 1982: Core-logs of the subhorizontal boreholes N1 and E1. Stripa Project 82-04, 44 pp.

CARLSSON, L., EGERTH, T., OLSSON, T. and WESTLUND, B., 1982: Core-logs of the vertical borehole V2. Stripa Project 82-05, 40 pp.

FRITZ, P., BARKER, J.F. and GALE, J.E., 1979: Geochemistry and isotope hydrology of groundwaters in the Stripa granite. Results and preliminary interpretation. LBL-8285, SAC-12, 105 pp.

FRITZ, P., BARKER, J.F., GALE, J.E., WITHERSPOON, P.A., ANDREWS, J.N., Kay, R.L.F., LEE, D.J., COWART, J.B., OSMOND, J.K. and PAYNE, B.R., 1980: Geochemical and Isotopic investigations at the Stripa test site (Sweden). In: Underground Disposal of Radioactive Wastes, Vol. II, IAEA, Vienna, 341-366.

GALE, J.E., 1982: Hydrogeologic characteristics of the Stripa site. Univ. Waterloo. Res. Inst. Rep. 003C, 60 pp.

GAMBELL, A.W. and FISHER, D.W., 1966: Chemical composition of rainfall in eastern North Carolina and southeastern Virginia, U.S. Geol. Survey Water-Supply Paper 1535-K, 41 pp.

GARRELS, R.M., 1967: Genesis of some groundwaters from igneous rocks, in Researches in Geochemistry, P.H. Abelson, ed., Vol. 2, 405-420.

GEIJER, P., 1938: Stripa odalsfälts geologi. SGU, Ser Ca 28.

HASKIN, L.A., FREY, F.A., SMITT, R.A. and SMITH, R.H., 1966: Meteoritic, solar and terrestrial rare-earth distributions, Phys. Chem. Earth 7, 169-321.

HASKIN, L.A. and HASKIN, M.A., 1968: Rare-earth elements in the Skaergaard intrusion, Geochim. Cosmochim. Acta 32, 433-450.

HEIJER, K.F. and ROGERS, J.J.W., 1963: Radiometric determinations of thorium, uranium and potassium in basalts and in two magmatic differentiations series. Geochim. Cocmochim. Acta, Vol. 27, pp 137-154.

HENDERSON, P., ed. (1984) Rare Earth Element Geochemistry, Elsevier, 510 pp.

JACKS, G., 1978: Groundwater chemistry at depth in granites and gneisses. KBS Tech. Rept. 88, 28 pp.

KOARK, H.J. and LUNDSTRÖM, I., 1979: Berggrundskartan Lindesberg SV. SGU Ser Af 126.

LANDSTRÖM, O., LARSSON, S-Å, LIND, G. and MALMQVIST, O., 1980: Geothermal investigations in the Bohusgranite area in Sweden. Technophysics, (in press).

LINDBLOM, S., 1984: Hydrogeological and hydrogeochemical investigations in boreholes - Fluid inclusion studies in the Stripa granite. Stockholm University, Sweden, Stripa Project. Internal report 84-07, Oct. 1984.

NORDSTROM, D.K., 1983: Preliminary data on the geochemical characteristics of groundwater at Stripa, in Geological Disposal of Radioactive Waste: In Situ Experiments in Granite, OECD/NEA Workshop, 143-153.

OLKIEWICZ, A., HANSSON, K., ALMN, K.-E. and GIDLUND, G., 1978: Geologisk och hydrologisk dokumentation av Stripa försöksstation. SKBF/KBS Tech. Rep. 63, 37 pp.

OLKIEWICZ, A., GALE, J.E., THORPE, R. and PAULSSON, B., 1979: The geology and fracture system at Stripa. LBL-8907, SAC-21.

PAULSRYD, B., 1941: Ore mapping in the Stripa Mine. Ställbergs Grufve AB.

ROEDDER, E. 1958: Technique for the extraction and partial chemical analysis of fluid-filled inclusions from minerals, Econ. Geol. 53, 235-269.

ROEDDER, E., INGRAM, B. and HALL, W.E., 1963: Studies of fluid inclusions III: Extraction and quantitative analysis of inclusions in the milligram range, Econ. Geol. 58, 353-374.

ROEDDER, E., 1972: Composition of fluid inclusions, U.S. Geol. Survey Prof. Paper 440JJ, 164 pp.

ROEDDER, E., 1984: Fluid inclusions, Revs. Mineral. 12, Mineral. Soc. Am., 680 pp.

STRECKEISEN, A.L., 1973: Plutonic rocks: Classification and nomenclature recommended by the IUGS Subcommission on the Systematics of Igneous Rocks, Geotimes, October, 26-30.

STRECKEISEN, A.L., 1976: To each plutonic rock its proper name, Earth Sci. Rev. 12, 1-33.

WELIN, E., 1964: Pitchblende-bearing vein fillings in the Stripa and Blanka iron ores. Transactions Geological Society of Sweden, Vol. 86, pp. 215-270.

WOLLENBERG, H., FLEXSER, S. and ANDERSSON, L., 1982: Petrology and radiogeology of the Stripa pluton, LBL-11654.

CHAPTER 3

CARLSSON, A., 1979: Characteristic features of a superficial rock mass in southern central Sweden. Horizontal and subhorizontal fractures and filling material - Striae. Vol. 11, 79 pp.

CARLSSON, L., and OLSSON, T., 1985a: Hydraulic investigations in boreholes. Hydraulic testing Part 1 - Shut-in tests. Stripa Project, Technical report, In press.

CARLSSON, L., and OLSSON, T., 1985b: Hydraulic investigations in boreholes. Hydraulic testing Part 2 - Injection-recovery tests and interference tests. Stripa Project, Technical report, In press.

CARLSSON, L., and OLSSON, T., 1985c: Hydraulic investigations in boreholes. Final report. Stripa Project, Technical report, In press.

GALE, J.E., 1982: Hydrogeological characteristics of the Stripa site. University of Waterloo, Rep. 003C.

NORTON, D. and KNAPP, R., 1977: Transport phenomena in hydrothermal systems: The nature of porosity. - American Journal of Science. Vol. 277, p. 913-936. New Haven.

OLKIEWICZ, A., GALE, J.E., THORPE, R., PAULSSON, B., 1979: Geology and fracture system at Stripa. - SAC Report 21.

PARSON, M.L., 1972: Determination of hydrogeological properties of fissured rocks. - 24th International Geological Congress. Vol. 11, p. 89-99. Montreal.

SNOW, D.T., 1968: Rock fracture spacings, openings and porosities. - Journal of Soil Mechanics and Foundation Division. Vol. 94, No. 1, p. 73-91.

STRELTSOVA-ADAMS, T.D., 1978: Fluid in naturally fractured reservoirs. - Proceedings of the Second Invitational Well-Testing Symposium, LBL Oct. 1978, pp 71-77.

STRELTSOVA, T.D., McKINLEY, R.M., 1984: Effect of Flow Time Duration on Buildup Pattern for Reservoirs With Heterogeneous Properties. - Soc. Pet. Eng. Jour., June 1984, pp 294-306.

WITHERSPOON, P.A., COOK, N.G., GALE, J.E., 1980: Progress with field investigations at Stripa. - SAC Report 27.

CHAPTER 4

AGERSTRAND, T., HANSSON, G. and JACKS, G., 1981: Effect on groundwater composition of sequential flooding of aquifers with fresh and saline water. In Intruded and relict groundwater of marine origin. Seventh Salt Water Intrusion Mtg., 59-64.

AVOTINS, P. and JENNE, E.A., 1975: The time stability of dissolved mercury in water samples--II. Chemical stabilization. J. Environ. Qual. 4, 515-519.

BARKER, C., and ROBINSON, S.J., 1984: Thermal release of water from natural quartz, Am. Mineral. 69, 1078-1081.

BRINKMANN, R. (1969) Geologic Evolution of Europe, J.E. Sanders, transl. Hafner Publ., 161 pp.

BROTZEN, F. and ASSARSSON, G., 1951: Brines in mesozoic strata, Scania, Sweden. Int. Assoc. Hydrol. Sci., 222-223.

ENGQVIST, P., 1981: Some wells with high content of chloride in central Sweden. In Intruded and relict groundwater of marine origin. Seventh Salt Water Intrusion Mtg., 33-44.

EUGSTER, H.P., 1980: Geochemistry of evaporitic lacustrine deposits. Ann. Rev. Earth Planet. Sci. 8, 35-63.

FRITZ, P., BARKER, J.F. and GALE, J.E., 1979: Geochemistry and isotope hydrology of groundwaters in the Stripa Granite: Results and preliminary interpretation. LBL-8285, SAC-12, 105 pp.

FRITZ, P., BARKER, J.F. and GALE, J.E., 1980: Summary of geochemical activities at the Stripa test site during FY 1979/80. Waterloo Res. Inst. Rept. 803-12.

FRITZ, P., BARKER, J.F. and GALE, J., 1983: Isotope hydrology at the Stripa test site. In Geological disposal of radioactive waste. In situ experiments in granite. OECD/NEA, 133-142.

GIBBS, C.R., 1976: Characterization and application of ferrozine iron reagent as a ferrous iron indicator. Anal. Chem. 48, 1197-1200.

HYYPPÄ, J., 1984: Pohjaveden Kemiallinen Koostumus Suomen Kallioperässä. Nuclear Waste Commission of Finnish Power Companies, Rept. YJT-84-10, 69 pp.

IVES, D.J.G. and JANZ, G.J., eds., 1961: Reference Electrodes Theory and Practice. Academic Press, New York, Publ., 651 pp.

JACKS, G., 1973: Chemistry of some groundwaters in igneous rocks. Nordic Hydrol. 4, 207-236.

JACKS, G., 1978: Groundwater chemistry at depth in granites and gneisses. KBS Tech. Rept. 88, 28 pp.

KREMLING, K., 1969: Untersuchungen über die chemische Zusammensetzung des Meereswassers aus der Ostsee vom Frühjahr 1966. Kieler Meeresforschungen. 25, 104 pp.

KREMLING, K., 1970: Untersuchungen über die chemische Zusammensetzung des Meerwassers aus der Ostsee. II. Frühjahr 1967 - Frühjahr 1968. Kieler Meeresforschungen. 26, 20 pp.

KREMLING, K., 1972: Untersuchungen über die chemische Zusammensetzung des Meerwassers aus der Ostsee. III. Frühjahr 1969 - Herbst 1970. Kieler Meeresforschungen. 28, 99-118.

LINDEWALD, H., 1981: Saline groundwater in Sweden. In Intruded and relict groundwater of marine origin. Seventh Salt Water Intrusion Mtg., 24-32.

MEANS, J.L., 1981: The organic geochemistry of deep groundwaters, ONWI/Battelle Rept., 51 pp.

NORDBERG, L., 1981: Problems in Sweden with intruded and fossil groundwater of marine origin. In Intruded and relict groundwater of marine origin. Seventh Salt Water Intrusion Mtg., 20-23.

NORDSTROM, D.K., 1977: Thermochemical redox equilibria of Zo-Bell's solution. Geochim. Cosmochim. Acta. 41, 1835-1841.

NORDSTROM, D.K., 1982: Recent investigations of the major element, trace element, and isotopic geochemistry of deep granitic groundwaters at the Stripa test site, Sweden. Ann. Mtg., Geol. Soc. Am., New Orleans, LA, p. 577.

NORDSTROM, K., 1983a: Chemical data. In Geochemical and isotope characterization of the Stripa groundwaters - Progress report. Stripa Project Rept. 83-01, 106-115.

NORDSTROM, D.K., 1983b: Preliminary data on the geochemical characteristics of groundwater at Stripa. OECD/NEA, 143-153.

SNELLMAN, M., 1982: Groundwater chemistry in bedrock. Nuclear Waste Commission of Finnish Power Companies, Rept. YJT-82-42, 65 pp.

SUND, B. and BERGMAN, G., 1981: Seawater intrusion in drilled wells. In Intruded and relict groundwater of marine origin. Seventh Salt Water Intrusion Mtg., 45-58.

WHITE, D.E., HEM, J.D. and WARING, G.A., 1963: Chemical composition of subsurface waters. U.S. Geol. Survey Prof. Paper 440-F, 67 pp.

CHAPTER 5

BALL, J.W., JENNE, E.A. and NORDSTROM, D.K., 1979: WATEQ - a computerized chemical model for trace and major element speciation and mineral equilibria of natural waters. In Jenne, E.A., ed., Chemical modelling in aqueous systems. Am. Chem. Soc. Symp. Series 93, 815-836.

BALL, J.W., NORDSTROM, D.K. and JENNE, E.A., 1980: Additional and revised thermochemical data and computer code for WATEQ2--a computerized chemical model for trace and major element speciation and mineral equilibria of natural waters. U.S. Geol. Survey Water Res. Invest. 78-116, 109 pp.

BALL, J.W., JENNE, E.A. and CANTRELL, M.W., 1981: WATEQ3--A geochemical model with uranium added. U.S. Geol. Survey Open-File Rept. 81-1183, 81 pp.

BEHNE, W., 1953: Untersuchungen zur Geochemie des Chlor und Brom. Geochim. Cosmochim. Acta 3, 186-214.

BIRD, D.K. and HELGESON, H.C., 1981: Chemical interaction of aqueous solutions with epidote-feldspar mineral assemblages in geologic systems. II. Equilibrium constraints in metamorphic/geothermal processes. Am. J. Sci. 281, 576-614.

BIRD, D.K., SCHIFFMAN,P., ELDERS, W.A., WILLIAMS, A.E. and McDowell, S.D., 1984: Calc-silicate mineralization in active geothermal systems. Econ. Geol. 79, 671-695.

BISCHOFF, J.L. and DICKSON, F.W., 1975: Seawater-basalt interaction at 200°C and 500 bars: implications for origin of sea-floor hevy-metal deposits and regulation of seawater chemistry. Earth Planet. Sci. Letters 25, 385-397.

BOLES, J.R. and FRANKS, S.G., 1979: Clay diagenesis in Wilcox sandstones of southwest Texas: Implications of smectite diagenesis on sandstones cementation. J. Sediment. Petrol. 49, 55-70.

BRACE, W.F., SILVER, E., HADLEY, K. and GOETZE, C., 1972: Cracks and pores: a closer look. Science 178, 162-164.

DALE, T.N., 1923: The commercial granites of New England. U.S. Geol. Survey Bull. 738, 14-26.

DICKSON, F.W., 1977: The reaction of granite with seawater at 300°C and 1000 bars. Am. Geophys. Union Trans. 58, p. 1251.

DREVER, J.I. (1982) The Geochemistry of Natural Waters, Prentice-Hall, N.J., 388 pp.

DUCE, R.A. and HOFFMAN, EVA J., 1976: Chemical fractionation at the air/sea interface. Ann. Rev. Earth Planet. Sci. 4, 187-228.

EDMUNDS, W.M., KAY, R.L.F. and McCARTNEY, R, 1983: Origin of saline groundwaters in the Carnmenellis granite: nature process and reaction during hot dry rock reservoir circulation. Proc. Fourth Water-Rock Interaction Symp., Japan, 127-131.

EDMUNDS, W.M., ANDREWS, J.N., BURGESS, W.G., KAY, R.L.F. and LEE, D.J., 1984: The evolution of saline and thermal groundwaters in the Carnmenellis granite. Mineral. Mag. 48, 402-424.

ELLIS, A.J. and MAHON, W.A.J., 1967: Natural hydrothermal systems and experimental hot water/rock interactions (Part II). Geochim. Cosmochim. Acta 31, 519-538.

ELLIS, A.J. and MAHON, W.A.J., 1977: Chemistry and geothermal systems. Academic Press, N.Y., 392 pp.

EUGSTER, H.P., 1980: Geochemistry of evaporitic lacustrine deposits. Ann. Rev. Earth Planet. Sci. 8, 35-63.

FABER, H., 1941: On the salt-solutions in microscopic cavities in granites. Dan. Geol. Unders., 44 pp.

FETH, J.H., 1981: Chloride in natural continental water--A review. U.S. Geol. Survey Water-Supply Paper 2176, 30 pp.

FOLK, R.L., 1955: Note on the significance of "turbid" feldspars. Am. Mineral. 40, 356-357.

FOURNIER, R.O. and POTTER, R.W., 1979: Magnesium correction to the Na-K-Ca chemical geothermometer. Geochim. Cosmochim. Acta 43, 1543-1550.

FREEZE, R.A. and CHERRY, J.A., 1979: Groundwater. Prentice-Hall, Inc., Englewood Cliffs, N.J., 604 pp.

FRITZ, P., BARKER, J.F. and GALE, J.E., 1979: Geochemistry and isotope hydrology of groundwaters in the Stripa Granite: Results and preliminary interpretation. LBL-8285, SAC-12, 105 pp.

FRITZ, P., BARKER, J.F. and GALE, J.E., 1980: Summary of geochemical activities at the Stripa test site during FY 1979/80. Waterloo Res. Inst. Rept. 803-12.

FUGE, R., JOHNSON, C.C. and PHILLIPS, W.J., 1978: Iodine in granitic and associated rocks. Chem. Geol. 22, 347-352.

FUGE, R., JOHNSON, C.C. and PHILLIPS, W.J., 1978: Iodine in granitic and associated rocks. Chem. Geol. 22, 347-352.

FUGE, R, 1979: Water-soluble chlorine in granitic rocks. Chem. Geol. 25, 169-174.

GRAUSTEIN, W., 1981: The effects of forest vegetation on solute acquisition and chemical weathering, Ph.D. Thesis, Yale, 695 pp.

HALL, W.E. and FRIEDMAN, I., 1963: Composition of fluid inclusions, Cave-in-Rock fluorite district, Illinois, and Upper Mississippi Valley zinc-lead district. Econ. Geol. 58, 886-911.

HAWKINS, D.B. and ROY, R., 1963: Experimental hydrothermal studies on rock alteration and clay mineral formation. Geochim. Cosmochim. Acta 27, 1047-1054.

HITCHON, B., BILLINGS, G.K. and KLOVAN, J.E., 1971: Geochemistry and origin of formation waters in the western Canada sedimentary basin. III. Factors controlling chemical composition. Geochim. Cosmochim. Acta 35, 567-598.

JACKS, G., 1978: Groundwater chemistry at depth in granites and gneisses. KBS Tech. Rept. 88, 28 pp.

KAY, R.L.F., 1984: Generation of groundwater salinity by low-temperature granite-water interaction: a comparison of results from two British studies. Proc. Intern. Groundwater Symp. Groundwater Resour. Utiliz. Contam. Hydrol., II, Canada, 432-444.

KELLER, W.D., BALGORD, W.D. and REESMAN, A.L., 1963: Dissolved products of artificially pulverized silicate minerals and rocks: Part I. J. Sediment. Petrol. 33, 191-204.

KERRICH, R., 1984: Chronology and ambient temperature/pressure conditions of fluid flow through the Eye-dashwa lakes pluton based on the $^{18}O/^{16}O$ ratio and fluid inclusions. AECL Rept. TR-267, 32 pp.

KHARAKA, Y.K., SPECHT, D.J. and CAROTHERS, W.W., 1985: Low to intermediate subsurface temperatures calculated by chemical geothermometers (abs.). Am. Assoc. Pet. Geol., Ann. Mtg.

KOZLOWSKI, A. and KARWOWSKI, L., 1974: Chlorine/bromine ratio in fluid inclusions. Econ. Geol. 69, 268-271.

LANGMUIR, D., 1971: The geochemistry of some carbonate groundwaters in central Pennsylvania. Geochim. Cosmochim. Acta 35, 1023-1045.

LINDBLOM, S., 1984: Fluid inclusion studies of the Stripa granite. Stripa Project. Internal Report 84-07, Oct. 1984.

McDOWELL, S.D. and ELDERS, W.A., 1983: Allogenic layer silicate minerals in borehole Elmore #1, Salton Sea Geothermal Field, California. Am. Mineral. 68, 1146-1159.

MONTGOMERY, C.W. and BRACE, W.F., 1975: Micropores in plagioclase. Contrib. Mineral. Petrol. 52, 17-28.

MOORE, D.E., MORROW, C.A. and BYERLEE, J.D., 1983: Chemical reactions accompanying fluid flow through granite held in a temperature gradient. Geochim. Cosmochim. Acta 47, 445-454.

MOTTL, M.J. and HOLLAND, H.D., 1978: Chemical exchange during hydrothermal alteration of basalt by seawater. I. Experimental results for major and minor components of seawater. Geochim. Cosmochim. Acta 42, 1103-1115.

NORDSTROM, D.K., JENNE, E.A. and BALL, J.W., 1979: Redox equilibria of iron in acid mine waters. In Chemical Modelling in Aqueous Systems: Speciation, Sorption, Solubility and Kinetics, Jenne, E.A., ed. Am. Chem. Soc. Symp. Series 93, 51-79.

NORDSTROM, D.K., 1983a: Chemical data. In Geochemical and isotope characterization of the Stripa groundwaters - Progress report. Stripa Project Rept. 83-01, 106-115.

NORDSTROM, D.K., 1983b: Preliminary data on the geochemical characteristics of groundwater at Stripa. OECD/NEA, 143-153.

NUR, A. and SIMMONS, G., 1970: The origin of small cracks in igneous rocks. Int. J. Rock Mech. Min. Sci. 7, 307-314.

PLUMMER, L.N. and BUSENBERG, E., 1982: The solubilities of calcite, aragonite and vaterite in CO_2-H_2O solutions between 0 and 90°C, and an evaluation of the aqueous model for the system $CaCO_3$-CO_2-H_2O. Geochim. Cosmochim. Acta 1011-1040.

ROEDDER, E., INGRAM, B. and HALL, W.E., 1963: Studies of fluid inclusions III: Extraction and quantitative analysis of inclusions in the milligram range. Econ. Geol. 58, 353-374.

ROEDDER, E. and SKINNER, B.J., 1968: Experimental evidence that fluid inclusions do not leak. Econ. Geol. 63, 715-730.

ROEDDER, E., 1972: Chapter JJ. Composition of fluid inclusions. In Data of Geochemistry, M. Fleischer Tech., ed. U.S. Geol. Survey Prof. Paper 440-JJ, 164 pp.

ROEDDER, E., 1984: Fluid inclusions. Revs. Mineral. 12, Min. Soc. Am., 680 pp.

RYZHENKO, B.N., MEL´NIKOVA, G.L. and SHVAROV, YU. V., 1981: Computer modelling of formation of the chemical composition of natural solutions during interaction in the water-rock system. Geochem. Intern. 18, 94-108.

SCHIFFMAN, P., ELDERS, W.A., WILLIAMS, A.E., McDOWELL, S.D. and BIRD, D.K., 1984: Active metasomatism in the Cerro Prieto geothermal system, Baja California, Mexico: a telescoped low-pressure low-temperature metamorphic facies series. Geology 12, 12-15.

SCHWERTMANN, U. and TAYLOR, R.M., 1977: Iron oxides. In Minerals in soil environments, J.B. Dixon and S.B. Weed, eds. Soil Sci. Am., 145-180.

SCHWERTMANN, U., 1979: Is there amorphous iron oxide in soils? (abs.). Soil Sci. Soc. Am., Ann. Mtg.

SELLA, C. and DEICHA, G., 1962a: Etude au microscope electronique des pores intergranularies des gangues et des roches. Compt. Rend. Acad. Sci. Paris 254, 2796-2798.

SELLA, C. and DEICHA, G., 1962b: Lacunes de cristallisation et pores intergranulaires du quartz (abs.). In Electron Microscopy, S. Breese, Jr., ed. Academic Press.

SELLA, C. and DEICHA, G., 1963: Importance des cavites intra et intercristallines dans l'architecture des mineraux et des roches. J. Microscopie 2, 283-296.

SEYFRIED, W.E., Jr. and BISCHOFF, J.L., 1979: Low temperture basalt alteration by seawater: an experimental study at 70°C and 150°C. Geochim. Cosmochim. Acta 43, 1937-1947.

SEYFRIED, W.E., Jr. and MOTTL, M.J., 1982: Hydrothermal alteration of basalt by seawater under seawater-dominated conditions. Geochim. Cosmochim. Acta 46, 985-1002.

SPRUNT, E.S. and BRACE, W.F., 1974: Direct observation of microcavities in crystalline rocks. Int. J. Rock Mech. Min. Sci. Geomech. Abstr. 11, 139-150.

TAPPONNIER, P. and BRACE, W.F., 1976: Development of stress-induced microcracks in Westerly granite. Int. J. Rock Mech. Min. Sci. Geomech. Abstr. 13, 103-112.

TRUESDELL, A.H., THOMPSON, J.M., COPLEN, T.B., NEHRING, N.L. and JANIK, C.J., 1981: The origin of the Cerro Prieto geothermal brine. Geothermics 10, 225-238.

TULLBORG, E.-L. and LARSON, S.A., 1982: Fissure fillings from Finnsjön and Studsvik, Sweden. SKBF/KBS Tech. Rept. 82-20, 76 pp.

VINOGRADOV, A.P., 1944: Geochemistry of dissolved elements in Moscow waters, Uspekhi Khimii 13, 3-34.

WHITE, D.E., 1970: Geochemistry applied to the discovery, evaluation, and exploitation of geothermal energy resources. Geothermics, special issue, 2, 58-80.

WISE, D.U., 1964: Microjointing in basement, middle rocky mountains of Montana and Wyoming. Geol. Soc. Am. Bull. 75, 287-306.

ZEN, E-An and THOMPSON, A.B., 1974: Low grade regional metamorphism: mineral equilibrium relations. Ann. Rev. Earth Planet. Sci. 2, 179-212.

CHAPTER 6

ANDREWS, J.N., BALDERER, W., BATH, A.H., CLAUSEN, H.B., EVANS, G.V., FLORKOWSKI, T, GOLDBRUNNER, J., ZOJER, H., IVANOVICH, M. and LOOSLI, H.H., 1984: Environmental isotope studies in two aquifer systems: A comparison of groundwater dating methods. IAEA (Vienna), Symp. 270. In press.

BATH, A.H., EDMUNDS, W.M. and ANDREWS, J.N., 1979: Paleoclimatic trends deduced from hydrochemistry of a triassic sandstone aquifer, U.K. In: Isotope Hydrology 1978. IAEA (Vienna) Symp. Proc. 545-568.

BURGMAN, J.O., ERIKSSON, E., KOSTROV, L. and WESTMAN, F., 1981: Oxygen-18 variation in monthly precipitation over Sweden. Avdelning för Hydrologi, Univ. of Uppsala, Sweden. Dec. 1981, 39 pp.

CRAIG, H., 1961: Isotopic variations in meteoric waters. Science, 133, 1702-1703.

DANSGAARD, W., 1964: Stable isotopes in precipitation. Tellus, 16, 436-468.

EICHINGER, L, RAUERT, W., STICHLER, W., BERTLEFF, B., EGGER, R., 1984: Comparative study of different aquifer types in central Europe using environmental isotopes. IAEA, (Vienna), Symp. 270, Sept. 1983. In press.

FONTES, J.-C., 1981: Paleowaters. In: Stable Isotope Hydrology. IAEA Tech. Rep. No 210, 273-302.

FRITZ, P. and FRAPE, S.K., 1982: Saline groundwaters in the Canadian Shield, a first overview. Chem. Geol. 36, 179-190.

FRITZ, P, BARKER, J.F. and GALE, J., 1983: Isotope Hydrology at the Stripa Test Site. IN: Geological Disposal of Radioactive Waste, in situ Experiments in Granite. OECD and KBS, Paris 1983, 133-142.

FRITZ, P., BARKER, J.F. and GALE, J.E., 1979: "Geochemistry and Isotope Hydrology of Groundwaters in the Stripa Granite," Univ. of California, Lawrence Berkeley Laboratories, Berkeley, CA, Rep. LBL-8285, pp. 107.

FRITZ, P., BARKER, J.F., GALE, J.E., ANDREWS, J.N., KAY, R.L.F., LEE, D.J., COWART, J.B., OSMOND, J.K., PAYNE, B.R. and WITHERSPOON, P.K., 1980: "Geochemical and Isotopic Investigation at the Stripa Test Site (Sweden), "Proc. Symp. Underground Disposal of Radioactive Wastes, IAEA, Otaniemi, Finland, July 1979, Symp. 243/6, 341-365.

FRITZ, P., DRIMMIE, R.J. and O'SHEA, K. Deuterium, tritium and ^{18}O in precipitations over Canada. In preparation.

GAT, J.R. and CARMI, I., 1970. Evolution of the isotopic composition of atmospheric waters in the Mediterranean Sea. J. Geophys. Res., 75, 3039-3048.

CONFIANTINI, R., CONRAD, G., FONTES, J.C., SANZAY, G. and PAYNE, B.R., 1974: Etude isotopique de la nappe du Continental Intercalaire et de ses relations avec les autres nappes du Sahara septentrional. Isotope Techniques in Hydrology 1974. Proc. Symp. Vienna, 1974, Vol. I, 227-241.

HÖTZL, H., JOB, C., MOSER, H., RAUERT, W., STICHLER, W. and ZÖTL, J.G.: 1980. Isotope methods as a tool for Quaternary studies in Saudi Arabia. In: Arid Zone Hydrology. IAEA (Vienna), Panel Proc. 1980, 215-235.

IAEA. 1981: Stable Isotope Hydrology. Deuterium and oxygen-18 in the water cycle. IAEA, (Vienna). Tech. Rep. No 210.

IAEA. 1983a: Guidebook on Nuclear Techniques in Hydrology. IAEA (Vienna), Techn. Rep. 91.

IAEA. 1983b: Isotope techniques in the Hydrogeological Assessment of Potential Sites for the Disposal of High-Level Radioactive Wastes. IAEA (Vienna), Techn. Rep. 228.

MERLIVAT, L. and JOUZEL, J., 1979: Global climatic interpretation of the deuterium-oxygen-18 in the water cycle. J Geophys. Res., 34, 18, 5029-5033.

MOSER, H., STICHLER, W. and TRIMBORN, P., 1983: Stable isotope studies on paleowaters. In: Paleoclimatic and paleowaters. IAEA, Vienna, 1983, 201-204.

SAVIN, S.M., 1980: Oxygen and hydrogen isotope effects in low--temperature mineral water interactions. In: Handbook of Environmental Isotope Geochemistry, P. Fritz and I.C. Fontes. Edts. Elsevier, Publ. Co., Amsterdam. Vol. 1, 283-328.

TRUESDELL, A.H. and HULSTON, J.R.: 1980: Isotopic evidence on environments of geothermal systems. In: Handbook of Environmental Isotope Geochemistry, P. Fritz and J.C. Fontes Eds. Elsevier Publ. Co., Amsterdam, Vol. 1, 179-226.

YURTSEVER, Y. and GAT, J.R., 1981: Atmospheric waters. In Stable Isotope Hydrology. IAEA, Vienna, Technical Rep. No. 210, 103-142.

CHAPTER 7

CLAYPOOL, G.E., HOLSER, W.T., KAPLAN, I.R., SAKAI, H. and ZAK, I., 1980: The age curve of sulfur and oxygen isotope in marine sulfate and their mutual interpretations. Chem. Geology, 28:199-260.

CORTECCI, G. and LONGINELLI, A., 1970: Isotopic composition of sulphate in rainwater. Pisa, Italy. Earth Planet. Sci. Lett., 8:36-40.

CORTECCI, G., 1973: Oxygen-isotope variation in sulfate ions in the water of some Italian lakes. Geochim. Cosmochim. Acta, 37:1531-1542.

FONTES, J.CH. and MICHELOT, J.L., 1983: Stable isotopes geochemistry in groundwater systems from Stripa site. Report 83-01 (Chap. 4) SKBF-KBS. Stockholm.

FONTES, J.CH. and GUENDOUZ, A., 1984: Deutérium, oxygène 18, carbone 13, carbone 14, soufre 34 dans les eaux, le carbonate et le sulfate dissous des nappes profondes du Sahara. Proc. Symp. Etude des ressources en eaux du Sahara. IAEA. Vienna (to be published).

FRIEDMAN, I. and O'NEIL, J.R., 1977: Compilation of stable isotope fractionation factors of geochemical interest. In: M. Fleischer (Ed). Data of Geochemistry. U.S. Geol. Sur., Prof. Paper, 440-KK:1-12 (6th ed).

FRITZ, P., BARKER, J.F., GALE, J.E., WITHERSPOON, P.A., ANDREWS, J.N., KAY, R.L.F., LEE, D.J., COWART, J.B., OSMOND, J.K. and PAYNE, B.R., 1980: Geochemical and isotopic investigations at the Stripa test site (Sweden). In: Underground Disposal of Radioactive Wastes, vol. II, IAEA, Vienna: 341-366.

FRITZ, P., BARKER, J.F. and GALE, J.E., 1980b: Summary of Geochemical Activities at the Stripa Test Site during FY 1979/80. Submitted to LBL.

FRITZ, P. and FONTES, J.CH., 1980: Handbook of Environmental Isotope Geochemistry. Vol. I, Elsevier, Amsterdam.

FRITZ, P., BARKER, J.F. and GALE, J.E., 1983: Isotope hydrology at the Stripa test site. Proc. Symp. Geological Disposal of Radioactive Waste. In Situ Experiments in Granite. OECD/NEA. Paris. 133-142.

FRITZ, P., 1983: The isotopic composition of sulphur compounds in the hydrosphere (in prep.).

GIKELSON, R.H., PERRY, E.C. and CARTWRIGHT, K., 1981: Isotopic and geologic studies to identify the sources of sulfate in groundwater containing high barium concentrations. Report 81-01165. University of Illinois, Water Res. Cent.

KAMINENI, D.C., 1983: Sulphur-isotope geochemistry of fracture-filling gypsum in an archean granite near Atikokan, Ontario, Canada. Chem. Geol., 39: 263-272.

KANKAINEN, T. and HYYPPÄ, J., 1984: Isotopic analyses of groundwater from the Rapakivi granite, Southern Finland, for the management of radioactive waste. Proc. Int. Symp. Isotope Hydrology in Water Resources Development. IAEA, Vienna, 801-803.

KAPLAN, I.R. and RITTENBERG, S.C., 1964: Microbiological fractionation of sulfur isotopes. J. Gen. Microbiol., 34:195-212.

KROOPNICK, P.M. and CRAIG, H., 1972: Atmospheric oxygen: Isotopic composition and solubility fractionation. Science, 175:54-55.

KROOPNICK, P.M. and CRAIG, H., 1976: Oxygen isotope fractionation in dissolved oxygen in the deep sea. Earth Planet. Sci. Lett., 32:375-385.

KROUSE, H.R., 1980: Sulphur isotopes in our environment. In: P. Fritz and J.Ch. Fontes (Eds). Handbook of Environmental Isotope Geochemistry. Vol. I, Elsevier, Amsterdam: 435-471.

LLOYD, R.M., 1967: Oxygen 18 composition of oceanic sulfate. Science, 156:1228-1231.

LLOYD, R.M., 1968: Oxygen isotope behaviour in the sulphate-water system. Jour. Geoph. Res., 73:6099-6110.

LONGINELLI, A. and CRAIG, H., 1967: Oxygen 18 variations in sulfate ions in seawater and saline lakes. Science, 156:56-59.

MICHELOT, J.L., BENTLEY, H.W., BRISSAUD, I., ELMORE, D. and FONTES, J.CH., 1984: Progress in environmental isotope studies (^{36}Cl, ^{34}S, ^{18}O) at the Stripa site. Proc. Int. Symp. Isotope Hydrology in Water Resource Development. IAEA. Vienna, 207-229.

MIZUTANI, Y. and RAFTER, R.A., 1969a: Oxygen isotopic composition of sulfates. 3. Oxygen isotopic fractionation in the bisulfate-water system. N.Z.J. Sci., 12:54-59.

MIZUTANI, Y. and RAFTER, R.A., 1969b: Oxygen isotopic composition of sulphates. 4. Bacterial sulphate and the oxidation of sulphur. N.Z.J. Sci., 12:60-68.

MIZUTANI, Y. and RAFTER, R.A., 1969c: Oxygen isotopic composition of sulphates. 5. Isotopic composition of sulfate in rainwater, Gracefield, New Zealand. N.Z.J. Sci., 12:69-80.

NIELSEN, H. and RICKE, W., 1964: Schwefel-Isotopenverhältnisse von Evaporiten aus Deutschland; ein Beitwag zur Kenntnis von $\delta^{34}S$ in Meerwasser-Sulfat. Geochim. Cosmochim. Acta, 28:577-591.

NORDSTROM, K., 1983: Conceptual framework for the chemical processes in the Stripa groundwaters. Rep. 83-01 (Chap. 5) SKBF-KBS. Stockholm.

PEARSON, F.J., Jr., RIGHTMIRE, C.T., 1980: Sulphur and oxygen isotopes in aqueous sulphur compounds. In: P. Fritz and J.Ch. Fontes (Eds). Handbook of Environmental Isotope Geochemistry. Vol. I, Elsevier, Amsterdam: 227-258.

PIERRE, C., 1982: Teneurs en isotopes stables (^{18}O, ^{2}H, ^{13}C, ^{34}S) et conditions de genèse des évaporites marines: applications à quelques milieux actuels et au Messinien de la Méditerranée. Thèse Doct. Sc. Nat. Université Paris-Sud, Orsay, 266 p.

RAFTER, R.A. and MIZUTANI, Y., 1967: Oxygen isotope composition of sulfates. 2. Preliminary results on oxygen isotopic variation in sulfates and relationship of their environment and to their $\delta^{34}S$ values. N.Z.J. Sci., 10:816.

RIGHTMIRE, C.T., PEARSON, F.J., Jr., BACK, W., RYE, R.O. and HANDSHAW, B.B., 1974: Distribution of sulphur isotopes of sulphates in groundwaters from the principal artersian aquifer of Florida and the Edwards aquifer of Texas. U.S.A. In: Isotope Techniques in Groundwater Hydrology. Vol. 2, IAEA, Vienna: 191-207.

THODE, H.G. and MONSTER, J., 1965: Sulfur-isotope geochemistry of petroleum evaporites and ancient seas. In: A. Young and J.E. Galley (Eds). Fluids in Subsurface Environments. Am. Assoc. Petr. Geol. Mem., 4:367-377.

TREMBACZOWSKI, A. and HALAS, S., 1984: Oxygen and sulfur isotope ratio in sulfate from atmospheric precipitation, Lublin, Poland. Proc. Int. symp. Isotope Hydrology in Water Resources Development. IAEA, Vienna, 819-820.

ZAK, I., SAKAI, H. and KAPLAN, I.R., 1980: Factors controlling the $^{18}O/^{16}O$ and $^{34}S/^{32}S$ isotopes ratios of ocean sulfates, evaporites and interstitial sulfates from modern deep sea sediment In: Isotope Marine Chemistry. Uchida Rokakuho, tokyo: 339-373.

ZIEGLER, P.A., 1982: Paleogeography of western and central Europe. Elsevier, Amsterdam.

CHAPTER 8

CARLSSON, L. and OLSSON, T., 1983: Geological and hydrogeological characterization of the Stripa granite. SKBF/KBS. Internal Report 83-01.

FONTES, J.C. and GARNIER, J.M., 1979: Determination of the initial C-14 activity of the total dissolved carbon, a review of the existing models and a new approach. Water Resour. Res. 15, pp 399-413.

FRITZ, P., BARKER, J.F. and GALE, J.E., 1979: Geochemistry and isotope hydrology of groundwaters in the Stripa granite. LBL-8285, SAC-REPORT 12, 105 pp.

FRITZ, P., BARKER, J.F. and GALE, J.E., 1980: Summary of Geochemical Activities at the Stripa Test Site during F.Y. 1979/1980. Waterloo Research Inst., Rep. 803-12, 1980.

GEYH, M.A., 1972: On the determination of the dilution factor of groundwater. Proc. 8th Int. Conf. Radiocarbon Dating, New Zealand, pp 369-380.

MOZETO, A.A., FRITZ, P. and PEARSON, E.J., 1984: Experimental observations on carbon isotope exchange in carbonate-water systems. Geochim. Cosmochim. Acta, 48, pp 495-504.

NERETNIEKS, I., 1980: Diffusion in the rock matrix, an important factor in radionuclide retardation? J. Geophys. Res. 85, B8, 4379-81.

PLUMMER, L.N., JONES, B.F. and TRUESDELL, A.H., 1976: WATEQF, a FORTRAN IV version of WATEQ, a computer programme for calculating chemical equilibrium of natural waters. U.S. Geol. Survey, Water Resour. Invest. 76-13.

REIMER, J., 1980: In Fritz et. al., 1980.

REARDON, E.J. and FRITZ, P., 1978: Computer modelling of ground water C-13 and C-14 isotope compositions. Jour. Hydrol. 36, pp 201-224.

TULLBORG, E.L. and LARSON, S.A., 1982: Fissure fillings from Finnsjön and Studsvik, Sweden. Identification, chemistry and dating. SKBF/KBS Techn. Report 82-20.

TULLBORG, E.L. and LARSON, S.A., 1983: Fissure filling from Gideå, Central Sweden. SKBF/KBS Techn. Report 83-74.

WIGLEY, T.M.C., PLUMMER, L.N. and PEARSON, F.J. Jr., 1978: Mass transfer and carbon isotope evolution in natural water systems. Geochim. Cosmochim. Acta, 42, pp 1117-1139.

ZITO, R, DONAHUE, D.J., DAVIS, S., BENTLY, H. and FRITZ, P., 1980: Possible subsurface production of C-14. Geophys. Res. Lett. 74, pp 235-238.

CHAPTER 9

AIREY, P.L., BENTLEY, H., CALF, G.E., DAVIS, S.N., HABERMEHL, M.A., PHILLIPS, F., SMITH, J., TORGERSEN, T., ELMORE, D. and GROVE, H., 1983: Isotope hydrology of the great artesian basin. Proc. Int. Conf. Groundwater and Man. December 1983. Sydney (to be published).

ANDREWS, J.N., 1983: Radioelements and inert gases in the Stripa groundwaters. Report 83-01 (Chap. 3). SKBF-KBS. Stockholm.

ANDREWS, J.N.L. and KAY, R.L.F., 1982: Natural production of tritium in permeable rocks. Nature 298, 361-363.

BENTLEY, H.W., 1978: Some comments on the use of chlorine-36 for dating very old groundwater: Proc. Symp. Dating of Very Old Groundwater. Tucson, Arizona. 102.

BENTLEY, H.W., PHILLIPS, F.M., DAVIS, S.N., GIFFORD, S., ELMORE, D., TUBBS, L. and GOVE, H.E., 1982: The fallout of thermonuclear ^{36}Cl. Nature, 300, 737.

BENTLEY, H.W., PHILLIPS, F.M., DAVIS, S.N., 1984: Chlorine-36 in the terrestrial environment. In Handbook of Environmental Isotope Geochemistry (FRITZ, P. and FONTES, J.Ch., eds). Elsevier, Amsterdam (in press).

BRERETON, N.R., 1970: Corrections for interfering isotopes in the $^{40}Ar/^{39}Ar$ dating method, Earth Planet. Sci. Letters 8, 427-433.

CARLSSON, L., OLSSON, T., 1982: Stripa hydrogeochemistry - compilation of analysing results, Internal Report Stripa Project, Stockholm, pp. 10.

CLARKE, W.B., JENKINS, W.J., TOP, Z., 1976: Determination of tritium by mass spectrometric measurement of ^{3}He, Int. J. Appl. Rad. Isot. 27, 515-522.

EICHINGER, L., FORSTER, M., RAST, H., RAUERT, W., WOLF, M., 1981: Experience gathered in low-level measurement of tritium in water. - In: Low-Level Tritium Measurement, IAEA-TECDOC-246, Vienna, 43-64.

ELMORE, D., TUBBS, L.E., NEWMAN, D., MA, X.Z., FINKEL, R., NISHIIZUMI, K., BEER, J., OESCHGER, H. and ANDREE, M., 1982: ^{36}Cl bomb pulse measured in a shallow ice core from Dye 3, Greenland. Nature, 300, 735-737.

FEIGE, Y., OLTMANN, B.G., KASTNER, J., 1968: Production rates of neutrons in soils due to natural radioactivity, J. Geophys. Res. 73, 3135-3142.

FLORKOWSKI, T., 1984: personal communication.

FONTES, J-Ch., BRISSAUD, I. and MICHELOT, J.L., 1984: Hydrogeological implications of deep production of chlorine-36. Proc. 3rd Int. Symp. Accelerator Mass Spectrometry. Nuclear Inst. Met., B5, 303-307.

FONTES, J-Ch. and MICHELOT, J.L., 1983: Stable isotope geochemistry of groundwater systems from Stripa. Report 83-01 (Chap. 4). SKBF-KBS. Stockholm.

FRITZ, P., 1983: personal communication.

FRITZ, P., BARKER, J.F., GALE, J.E., 1979: Geochemistry and isotope hydrology of groundwaters in the Stripa granite, Univ. of California, Lawrence Berkeley Laboratories, Berkeley, CA. Rep. LBL-8285, pp 107.

LAL, D. and PETERS, S., 1967: Cosmic ray produced radioactivity on the earth. In: Handbuch der Physik, 46/2 (SITTE, K., ed.). Springer-Verlag, Berlin. 551.

LOOSLI, H., FORSTER, M., 1982: Ein Beitrag zum Vergleich von ^{39}Ar- und ^{14}C-Konzentrationen im Grundwasser. - In: Beiträge über hydrologische Tracermethoden und ihre Anwendungen, GSF-Bericht R 290, Munich/Neuherberg, 133-138.

MICHELOT, J.L., BENTLEY, H.W., BRISSAUD, I., ELMORE, D. and FONTES, J-Ch., 1984: Progress in environmental isotope studies (^{36}Cl, ^{34}S, ^{18}O) at the Stripa site. Proc. Int. Symp. Isotope Hydrology in Water Resources Development. IAEA, Vienna, 207-229.

MOSER, H., RAUERT, W., 1983: Determination of groundwater movement by means of environmental isotopes - State of the art. IAHS-Symposium "Relation of Groundwater Quantity and Quality", Hamburg, IAHS Publ. (in print).

NERETNIEKS, I., 1981: Age dating of groundwater in fissured rock: Influence of water volume in micropores, Wat. Resourc. Res. 17, 421-422.

ROETHER, W., 1967: Tritium im Wasserkreislauf, Thesis Univ. Heidelberg.

WEISS, W., BULLACHER, J., ROETHER, W., 1979: Evidence of pulsed discharges of tritium from nuclear energy installations in Central European precipitation. - In: Behaviour of Tritium in the Environment, IAEA, Vienna, 17-30.

WEISS, W., ROETHER, W., 1975: Der Tritiumabfluss des Rheins 1961 - 1973, Deutsche Gewässerkundliche Mitteilungen 19, 1-5.

WEISS, W., ROETHER, W., BADER, G., 1976: Determination of blanks in low-level tritium measurement, Int. J. Appl. Rad. Isot. 27, 217-225.

WOLF, M., RAUERT, W., WEIGEL, F., 1981: Low-level measurement of tritium by hydrogenation of propadiene and gas counting of propane, Int. J. Appl. Rad. Isot. 32, 919-928.

WOLLENBERG, H., FLEXSER, S. and ANDERSON, L., 1980: Petrology and radiogeology of the Stripa pluton. Laurence Berkeley Laboratory rep. 11654 Berkeley, California.

ZIEGLER, P.A., 1982: Paleogeography of Western and Central Europe. Elsevier, Amsterdam.

CHAPTER 10

ANDREWS, J.N., 1983: "Radioelements and inert gases in the Stripa groundwaters". SKBF/KBS report 83-01, Stockolm.

ANDREWS, J.N., GILES, I.S., KAY, R.L.F., LEE, D.J., OSMOND, J.K., COWART, J.B., FRITZ, P., BARKER, J.F. and GALE, J., 1982: "Radioelements, radiogenic helium and age relationships for groundwaters from the granites at Stripa, Sweden". Geochim. Cosmochim. Acta, 46, 1533-1543.

ANDREWS, J.N. and WOOD, D.F., 1972: "Mechanism of radon release in rock matrices and entry into groundwaters". Inst. Min. Metall. Trans., Sect. B81, 198.

EDMUNDS, W.M., ANDREWS, J.N., BURGESS, W.G., KAY, R.L.F. and LEE, D.J., 1984: "The evolution of saline and thermal groundwaters in the Carnmenellis granite". Min. Mag., 48 407-4274.

FONTES, J.C. and MICHELOT, J.L., 1983: "Stable isotope geochemistry in groundwater systems from Stripa". SKBF/KBS report 83-01, Stockholm.

KIGOSHI, K., 1971: "Alpha-recoil ^{234}Th: dissolution into water and the $^{234}U/^{238}U$ disequilibrium in nature". Science 173 47-48.

LANGMUIR, D., 1978: "Uranium solution - mineral equilibria at low temperatures with applications to sedimentary ore deposits. Geochim. Cosmochim. Acta 42 547-569.

NELSON, P., PAULSSON, B., RACHIELE, R., ANDERSSON, L., SCHRAUF, T., HUSTRULID, W., DURAN, D. and MAGNUSSON, K.A., 1979: "Preliminary report on the geophysical and mechanical borehole measurements at Stripa". Report LBL-8280, Lawrence Berkeley Lab., Univ. California.

ROSHOLT, J.N., SHIELDS, W.R. and GARNER, E.L., 1963: "Isotopic fractionation of uranium in sandstone". Science 139 224-226.

TANNER, A.B., 1964: "Radon migration in the ground: a review". In The Natural Radiation Environment, (eds. J.A.S. Adams and W.M. Lowder), Chicago University Press, Chicago.

CHAPTER 11

ANDREWS, J.N., 1984: "The isotopic composition of radiogenic helium and its use to study groundwater movement in confined aquifers". Chem. Geol. in press.

ANDREWS, J.N., 1983: "The isotopic composition of helium and its use to study groundwater movement". Proc. 4th Int. Symp. Water-Rock Interaction, Misasa, Japan, 17-21.

ANDREWS, J.N. and LEE, D.J., 1979: "Inert gases in groundwater from the Bunter Sandstone of England as indicators of age and palaeoclimatic trends". J. Hydrol. 41 233-252.

BENSON, B.B. and KRAUSE, D., 1976: "Empirical laws for dilute aqueous solutions of non-polar gases". J. Chem. Phys., 64 639.

DALRYMPLE, G.B. and LANPHERE, M.A., 1969: "Potassium-Argon Dating". W.H. Freeman and Company, San Fransisco.

HEATON, T.H.E., and VOGEL, J.C., 1981: "Excess air in groundwater". J. Hydrol. 50 201-216.

MARINE, I.W., 1979: "The use of naturally occurring helium to estimate groundwater velocities for studies of geologic storage of radioactive waste." Water Resour. Res. 15 1130.

MORRISON, T.J. and JOHNSTONE, N.B., 1954: "Solubilities of inert gases in water". J. Chem. Soc., p. 3441.